IMPACT OF RECLAIMED ASPHALT PAVEMENTS ON PAVEMENT SUSTAINABILITY

BY

QAZI AURANGZEB

DISSERTATION

Submitted in partial fulfillment of the requirements
for the degree of Doctor of Philosophy in Civil Engineering
in the Graduate College of the
University of Illinois at Urbana-Champaign, 2014

Urbana, Illinois

Doctoral Committee:

Professor Imad L. Al-Qadi, Chair
Professor Harry H Hilton
Professor William G Buttlar
Mr. Gerry Huber, Heritage Research Group
Research Assistant Professor Hasan Ozer

Abstract

Highway pavements are one of the main building blocks of the United States infrastructure and economy. Asphalt concrete is the most common material to construct highway pavements. Billions of dollars are spent every year to maintain and rehabilitate two-million-mile the U.S. highway network. Asphalt pavement recycling is one of the few ways to reduce the amount of dollars spent on maintenance and new pavements construction. Reclaimed asphalt pavements (RAP), being a source of aggregates and asphalt binder, is the most recycled material in the U.S. However, incorporating high amount of RAP in asphalt mixtures can pose significant mix design issue and could compromise the pavement performance. Technical complications aside, for RAP to be considered a sustainable material, it is essential for it to be cost effective and socially and environmentally beneficial. The main objective of this study is to evaluate the feasibility of using high RAP in base-course asphalt mixtures. A holistic approach is taken to achieve the objective of the study; mixtures with high RAP contents are not only designed and characterized, their economic and environmental impacts have also been evaluated.

The asphalt mixtures with high RAP content (up to 50%) are designed with desired and similar volumetrics as those of asphalt mixtures prepared with virgin materials, setting a great precedent for any future study conducted on high RAP content. The effect of RAP content as well as the effect of binder-grade bumping on the laboratory performance of asphalt mixtures was evaluated. Results showed that the asphalt mixtures with RAP can perform equal to the mixtures produced with virgin aggregate provided they are designed properly. The asphalt binder-grade bumping is found effective in helping to retain the original properties of the virgin mixture.

An in-depth multiaxial viscoelastic characterization of the recycled mixtures is conducted by implementing a novel analytical approach. The new approach bypasses the controversial viscoelastic Poisson's ratios and measures Young's, shear, and bulk moduli directly in time domain. It has been shown that incorrect assumption of constant PRs for

viscoelastic materials can lead to significant errors in estimating the moduli values. Use of Poisson's ratios should be completely avoided in characterizing the asphalt concrete.

The outcome of life cycle cost analysis (LCCA) and life-cycle assessment (LCA) conducted in this study showed viability of using high RAP content in asphalt mixtures. Significant reduction in cost as well as in energy consumption and global warming potential (GWP) have been observed. The economic and environmental LCA conducted under various performance scenarios highlighted the importance of achieving equivalent field performance for recycled mixtures to that of the virgin mixtures. The actual field performance of these mixtures would eventually dictate their net benefits over the virgin mixtures.

To my mother, wife, and daughter
Razia, Hina, and Layaan.

Acknowledgements

I thank everyone who has supported, encouraged, and guided me throughout my PhD studies.

I am among the few privileged people who have had the opportunity to have Professor Imad L. Al-Qadi as advisor. I am greatly indebted to him for the consistent encouragement, guidance, motivation, and unconditional support he provided during my PhD studies. He has helped me immensely in my personal, professional, and intellectual growth. I am in awe of the dedication and enthusiasm he has always shown for his profession and his research.

I am especially thankful to Professor Harry H Hilton for the time he spent discussing the intricacy of viscoelastic materials. It has always been a pleasure and an enlightening experience to talk to him about Poisson's ratio—the topic dearest to him. I am also grateful to Hasan Ozer for his support, encouragement, mentoring, and guidance. Whether my question was about an intriguing concept, an experimental glitch, or a mathematical problem, he always provided satisfactory answers. I shall always be indebted to him for lending a helping hand, patient ears, and words of encouragement and wisdom whenever I was in need. I am also grateful to my other PhD committee members, Gerry Huber and William G. Buttlar for their valuable input on my dissertation. I would also like to acknowledge Bill Pine from Heritage Research Group, whose continuing support helped me immensely in understanding asphalt mixtures.

I would also like to thank the friends and colleagues at work who helped me throughout my PhD in one way or the other. Thanks to Sarfraz, Shih-Hsien, Behzad, Valentina, Baek, Hao, Zhen, Alejandro, Songsu, Jaime, Pengcheng, Angeli, Seung-gu, Rebekah, Khaled, Guillermo, Ahmad, Saleh, Heena, Stefano, and Ibrahim for making my stay at ATREL a memorable one. I am especially thankful to Ibrahim for helping me on my project while I was away for my wedding. Special thanks to ICT staff members Jim Meister, Jeff Kern, and Aaron Coenen for their technical support during my research project and PhD.

I spent some of the best days of my life in Chambana, mostly because of the wonderful people surrounding me. I would like to thank my friends Azeem Sarwar, Osman Sarood, Ahmed Qadir, Syed Usman, Salman Noshear, Sarfraz Ahmed, Abdul Qudoos, Kamran Akhter, Manzoor Hussain, Adeel Zafar, Atif Irfan, Ibrahim Pasha, Riaz Ahmed, Numair Ahmed, Zeeshan Fazal, Ahmed Sadeque, Haris Chaudry, Asma Faiz, Shehla Saleem, Shaista Babar, Salman Qureshi, Zeeshan Fazal, Shahzad Bhatti, Aneel Kumar, Ahmed Sadeque, Aizaz Syed, Asfand Waqar, Usman Tariq, Ibrahim Abuawad, Randa Ibrahim, Bilal Mehdi, Rakesh Kumar, Rashid Tahir, Talha Zafar, Kashif Nawaz, Adeel Ahmad, Ammar Bhutta, and others for their camaraderie. I would also like to thank Dr. Irfan Ahmed for his guidance and mentorship in several social and community-related activities. I am likewise grateful to Dr. Zeeshan Ahmed for his help, support, and kindness.

I don't think I can find sufficient words to express the level of gratitude I have for my parents, Qazi Muhammad Yousaf and Razia Yousaf. Their relentless support, unconditional love, and dedicated prayers are the precious assets of my life; it is impossible to pay my parents back for their kindnesses. I am forever indebted to them for the sacrifices they have made during their lives to ensure my well-being. I am also very thankful to my wonderful sisters, Gulrukh Qazi, Mahrukh Arshad, Shehla Zahidullah, and Bushra Fayaz and their husbands; they have been a constant source of love, encouragement, and care for me. Qazi Jehanzeb, my twin and my buddy since the time in our mother's womb, has been a huge support for me throughout my stay at the University of Illinois. I am thankful to him and his wife, Saima Jehanzeb, for their advice, encouragement, and love for me. I would also like to express my gratitude to my parents-in-law, Tahira and Syed Hakeemshah, for their support to me.

I dedicate this dissertation to my wife, Hina Syed. She has been extraordinarily supportive, understanding, and encouraging throughout the three years we been together. It's tough to be the wife of a PhD student; she will always have my deepest appreciation and respect for walking by my side during the most demanding of times. I also owe my deepest gratitude to her for being a wonderful mother to our precious daughter, Layaan, to whom I promise to give ample time from now on.

Finally, I express my humble gratitude to Allah (the most gracious and the most

merciful) for giving me the opportunity and strength to undertake the daunting task of completing my PhD. I am grateful to Him for all the blessings He has bestowed on me. Alhamd-o-Lillah-e-Rab-il-Aa'lameen (All praises to Allah, the Lord of all the worlds).

Table of Contents

List of Tables

List of Figures

CHAPTER 1

INTRODUCTION

1.1 Introduction

Sustainable practices in the pavement industry target increased use of recycled materials and encouraging innovations in the design and construction of asphaltic mixtures. Asphalt recycling is a step forward in the direction of building sustainable pavement systems. The impetus to recycle old pavement is fueled by environmental awareness and proven cost savings. The percentage of reclaimed asphalt pavements (RAP) in conventional asphaltic mixture design seldom increases above 20% to 25% (Copeland 2011). A major reason for limited use of RAP in asphalt mixtures is that it introduces variability in aggregate gradation. In addition, the high percentages of fines with RAP, the increased stiffness of aged asphalt, and the need for overheating virgin aggregates in asphalt plants all pose challenges to mixture design and production. A major challenge with increased use of RAP in asphaltic mixtures is the potential for an increase, or a decrease, in the voids in mineral aggregates (VMA) caused by changes in gradation, shape, texture, and strength of the RAP aggregates.

The VMA mixture parameter plays an important role in the performance of flexible pavements. The thickness of asphalt film around aggregate particles is approximated by the aggregate gradation and volume of asphalt binder. Loss of durability and stability are two asphaltic mixture problems caused by low and high VMA, respectively. AASHTO M323-04 includes a warning that asphalt mixtures prepared with VMA values greater than 2.0% above the specified minimum VMA might be prone to rutting and flushing.

Apart from introducing complexities in mix designs, use of a high amount of RAP content has the potential to impact durability and structural performance of the pavements. Asphalt mix designs with low RAP percentages (up to 15%) are not significantly affected by RAP variability; however, higher percentages of RAP may considerably change the overall performance of asphalt mixtures (Aurangzeb et al. 2012).

RAP is usually acquired from an old weathered pavement. The asphalt binder introduced by RAP is aged and stiffer, which affects the asphalt mixtures in multiple ways. It causes a decrease in the rutting potential of the asphalt mixture, and it is also known to induce early fracture and fatigue cracking (Shu et al. 2008 and Li et al. 2008).

Asphalt concrete is a viscoelastic material; the relationship between stress and strain depends on time, loading, and temperature. Asphalt concrete, owing to the presence of asphalt binder, exhibits viscous-like characteristics at high temperatures and exhibits a more elastic-like behavior at low temperatures. The current practice of characterizing asphalt concrete involves measuring the uniaxial dynamic modulus, E, and determining material properties such as bulk (K) and shear moduli (G), assuming a constant value for Poisson's ratio. The assumption of a constant Poisson's ratio is the most common feature encountered while attempting to model the viscoelastic behavior of asphalt mixtures. Moreover, the relaxation functions for different moduli are also considered similar. Such simplified assumptions in characterizing a complex viscoelastic material may make the long path leading to sustainable pavement systems even more challenging.

The core elements of sustainability are the economy, the environment, and society. Unless a product is cost effective—and socially and environmentally beneficial—it is difficult for a product to be considered sustainable. While reducing use of virgin material and reducing the amount of waste in landfill, have their own economic and environmental benefits, it is important to assess the total economic and environmental impact of using RAP material over the entire lifespan of the pavement. Impact elements include the required amount of reprocessing of RAP material, transportation requirements, and the RAP material's effects on the new pavement's life. Two useful tools available to assess the environmental and economic impact of a product or process are life-cycle assessment (LCA) and life-cycle cost analysis (LCCA).

1.2 Problem Statement

To gain full advantage of the abundant supply of RAP, the amount of RAP to be incorporated in plant-produced asphalt mixtures must be increased. However, achieving acceptable volumetrics for asphalt mixtures with a high amount of RAP is a challenge. Incorporating higher amount of RAP can pose significant design and performance issues.

Although long-term performance of mixtures with high RAP content can be monitored in the field and compared with mixtures with no RAP, the mixtures' behavior under traffic and environmental loading can be simulated using laboratory tests in conjunction with numerical modeling. Ironically, the value of Poisson's ratio is incorrectly assumed to be constant while modeling viscoelastic asphalt concrete. The viscoelastic Poisson's ratio is time, stress, and stress history dependent and does not represent a unique viscoelastic material property. The addition of high RAP content complicates the issue even further. Hence, there is a need to bypass Poisson's ratio and characterize the asphalt concrete in terms of fundamental properties such as relaxation, bulk, and shear moduli.

Moreover, the prepared mixtures must achieve the desired performance and design volumetrics while addressing economic and environmental concerns. Incorporating high amounts of RAP in asphalt mixtures will be feasible only if a thorough analysis of its economic and environmental impact is conducted before field use.

1.3 Research Objective and Scope

The objective of this research is to evaluate the feasibility of using high RAP in binder-course asphalt mixtures. To achieve this objective, this thesis undertakes the following research tasks:

1. Laboratory protocols are developed to design asphalt mixtures containing high RAP contents with acceptable volumetrics.
2. High-quality prepared asphalt mixtures are first characterized using state-of-the-practice testing protocols. This task explores moisture susceptibility, fracture, fatigue, and permanent deformation behavior of the prepared mixtures.
3. A laboratory testing protocol is developed for implementation of a novel analytical approach to determine the multiaxial viscoelastic characteristics of asphalt mixtures without the use of Poisson's ratio. This task involves development and verification of a program code and proposing a testing protocol to directly measure the Young's, bulk, and shear moduli of asphalt mixtures.
4. The economic and environmental impact of using RAP in asphalt mixtures is

quantified. This task involves collection of vast data to perform LCCA and LCA. The analysis is conducted under different performance scenarios. Breakeven performance levels for the mixtures with different RAP contents have been identified.

1.4 Research Contribution

Contributions of this research ranges from improved laboratory protocols for designing the asphalt mixtures with high RAP content to direct determination of bulk and shear relaxation moduli using a novel protocol. Contributions of this research work include the following:

1. Designing asphalt mixtures, that include high amounts of RAP, with acceptable volumetrics. Being able to reproduce these volumetrics in the field is a function of several factors, including but not limited to (a) accuracy of the original mix design, (b) similarities or dissimilarities between the design and the asphalt plant materials (aggregate specific gravities, gradation, shape, texture, strength, etc.), (c) consistency of the plant material, and (d) change in volumetrics of the plant mix resulting from alterations in shape and texture of aggregates during the plant operation.
2. The outcome of laboratory performance of the asphalt mixtures with high RAP may help instill confidence among highway agency experts regarding the use of high RAP content in asphalt mixtures.
3. Currently, viscoelastic characterization of asphalt concrete include determining uniaxial modulus and relaxation and derivation of bulk and shear relaxation functions assuming a constant (time-independent) Poisson's ratio. This assumption may not be acceptable for asphalt concrete, which also exhibits viscoelastic characteristics at a wider temperature range. Two relaxation components of the linear isotropic viscoelastic model—bulk and shear relaxation functions—exhibit distinct relaxation characteristics for most of the viscoelastic materials. The difference in the two relaxation functions also lends itself to a time-dependent Poisson's ratio. A practical application of a novel approach to determine viscoelastic moduli and compliances without using the controversial

Poisson's ratio is proposed. The proposed approach may prove to be a significant milestone toward enrichment of experimental characterization of asphalt concrete's linear viscoelastic behavior with multiaxial deformation measurements. Independently acquired relaxation functions can also be used as input in numerical models such as the finite element (FE) method.

4. A thorough LCCA based on detailed real-time energy and fuel consumption data during plant production of asphalt could provide a clearer picture of RAP's utility as a sustainable material and offer a better way of determining the most cost-effective alternative.
5. Sustainable pavement systems require materials and technologies that are economically sound but also are environmentally beneficial to current and future generations. Proponents of using high RAP content in asphalt mixtures claim the benefits of resource conservation and waste reduction; however, it is necessary to quantify such claims. Applying LCA will allow quantifying the environmental benefits of using high RAP content.

1.5 Dissertation Organization

This research dissertation is organized into nine chapters. Chapter 1 introduces the research statement, objectives, and the research scope to accomplish the objectives.

Chapter 2 summarizes the literature related to use of RAP in asphalt mixtures. The issues related to designing asphalt mixtures with high RAP and their laboratory characterization are reviewed.

Chapter 3 presents in depth material characterization, mix design procedure, and laboratory protocols to handle RAP. Susceptibility of the designed mixtures to moisture is analyzed as well.

Chapter 4 deals with characterizing and evaluating the stability and durability characteristics of the prepared recycled mixtures. The results of laboratory tests such as the dynamic modulus test, beam fatigue test, wheel tracking test, and semi-circular bending (SCB) test are discussed. Likewise, the effect of stiffer RAP binder on performance properties of the asphalt mixtures is presented.

Chapter 5 is first of two chapters that address problems associated with assuming a constant Poisson's ratio and similar moduli relaxation times for asphalt concrete. The chapter presents findings on the inapplicability of the elastic-viscoelastic correspondence principle for Poisson's ratios. Numerical analysis were conducted to establish time and stress dependency of viscoelastic Poisson's ratios. Chapter 6 then details the analytical algorithm followed to determine the bulk and shear moduli of the asphalt mixtures with and without RAP. The specifics involving code development, implementation, and verification are presented. The laboratory experimental protocol developed for multiaxial characterization is described as well.

Chapter 7 presents the economic appraisal of using a high amount of RAP in binder course mixtures. An LCCA was conducted to compare the agency and user costs associated with different mixture alternatives. The LCCA was conducted under different performance scenarios of mixtures with RAP. The breakeven performance level for each mixture with RAP is discussed.

Chapter 8 presents results of the LCA conducted to assess the environmental impact of using a high amount of RAP in asphalt binder mixtures. Energy and carbon footprints of the asphalt mixtures with and without RAP are compared. Similar to economic analysis, the LCA was conducted under different performance scenarios. The breakeven performance levels based on LCA are presented.

Chapter 9 summarizes the research work conducted for this thesis. Conclusions drawn from this study are presented and recommendations for future work are offered.

It is important to note that from this point onward in this thesis, asphalt mixtures with and without RAP are referred to as *recycled mixtures* and *control/virgin mixtures*, respectively. An asphalt mixture with 50% RAP is termed a *50% recycled mix*. Both English and SI units are used throughout the document; whenever possible, both units are provided.

CHAPTER 2
LITERATURE REVIEW

2.1 Introduction

When asphalt pavements reach the end of their service lives, the pavement materials can be salvaged and used to construct new pavements. For the past four decades, the material obtained from old pavements, known as reclaimed asphalt pavement (RAP), has been recycled to produce new asphalt pavements. RAP is commonly mixed with various percentages of new aggregates and asphalt binders to produce fresh asphalt mixture pavements. It can also be used in the lower pavement layers (i.e., binder and base layers) to provide improved layer support for traffic loads. Apart from reducing the cost of the new asphalt pavement, asphalt recycling is also an environmentally sound option for pavement rehabilitation.

In the United States, interest in asphalt mixture recycling began in the 1970s, when the nation experienced an oil embargo. Before that time, the cost involved in removing and crushing the existing pavement section was more than the cost of using virgin material. However, the development of advanced milling machinery changed the economic balance in favor of recycling. Since then, a number of studies have reported that pavements incorporating RAP performed almost similar to or even better than pavements made without RAP (Epps et al. 1997; Kandhal et al. 1995).

Many states have had good experiences with using RAP, but there are still many issues that need to be resolved before deciding to use high percentages of RAP in asphalt concrete. Some of the major barriers and technical issues that prevent various states from using high percentages of RAP are stockpile management, availability of RAP, and binder and mix issues. Binder issues are related primarily to bumping grades and properties of the final blend. Mix issues can be further divided into mix design issues and mix performance issues. The contribution of asphalt binder from RAP (i.e., the amount of blending), the volumetrics of asphalt mixture containing RAP, and requirements of any additional testing to predict performance of RAP mixes are the key problems that need

further investigation.

Asphalt is a viscoelastic material. It behaves like an elastic material at very low temperatures and like a viscous material at high temperatures. At service temperatures, it exhibits characteristics of both materials, which makes it a more complicated material to understand. As asphalt binder ages, it becomes harder and stiffer. Although this stiffening increases the resistance of asphalt mixture to deformation, it also becomes prone to thermal and fatigue cracking from increased brittleness. Roberts et al. (1996) described six major mechanisms that contribute to asphalt aging and hardening during its construction and service. These factors include oxidation, volatilization, polymerization, thixotropy, syneresis, and separation.

Asphalt binder properties have a significant influence on asphalt mixture properties. Binder viscosity needs to be sufficiently low at high temperatures to allow the material to be moved through the asphalt mixture plant. It also needs to be sufficiently stiff at the average maximum high in-service temperature so that load-induced deformation (rutting) is minimized. At the same time, the binder needs to be flexible (ductile) at cold temperatures so that thermal cracking is minimized by the material's ability to dissipate stresses through deformation. Incorporation of RAP into asphalt mixtures contributes to the complexity of the mixture because of the RAP aged binder.

An extensive amount of work has been published describing methods and strategies of asphalt recycling, including mixture laboratory and field performances, and binder and mix properties. This literature review focuses on issues related to mix design and performance testing of asphalt mixture incorporating high percentage of RAP. The literature review is divided into two sections; the first section addresses the incorporation of RAP into asphalt mixture design, and the second section focuses on laboratory performance testing of RAP mixes.

2.2 Asphalt Mix Design Using Reclaimed Asphalt Pavement

An asphalt mixture with RAP poses significant challenges in the design procedure. These challenges arise from the variability of asphalt mixture mixes, aged binder, unknown amount of working binder, and other factors. Though high percentages of RAP have been used with in-place asphalt recycling, there are limits to the percentage of RAP that should

be used with in-plant recycling. Except for in-place asphalt recycling on small/country roads, high percentages of RAP are not commonly used in practice because of the variability in RAP.

This variability not only arises from asphalt binder aging but also from finer gradation of RAP aggregates. During the milling process or ripping and crushing, the coarse aggregate is broken and results in an increase in fine material. The gradation of RAP material is determined by conducting a sieve analysis on the recovered RAP aggregate after binder extraction. When RAP in its original form is added to virgin material, it does not release all of its asphalt binders and fine aggregate. Fine aggregate may remain attached to the coarse aggregate and may not contribute to the mix properly. This uncertainty of the amount of binder and fine aggregate released by RAP creates considerable problems in determining the precise volumetrics of asphalt mixture.

The potentially adverse effects of the milling operation can present a problem in meeting SuperPave™ fine graduation requirements. A large amount of fines is detrimental because it can result in insufficient asphalt film thickness, which has been associated with poor mixture durability. The size reduction of the larger aggregate also increases mixture susceptibility to rutting and decreases fatigue life. Currently, this problem is addressed by placing restrictions on the maximum amount of RAP that may be used in the mixture and by blending with virgin aggregate.

It has been suggested by Gardiner and Wagner (1999) that RAP could be split into coarse and fine fractions to keep a large amount of the dust fraction out of the mix, thereby allowing a higher percentage of RAP to be used. In that study, the finer RAP fraction was used in an above-the-restricted zone, 12.5-mm SuperPave gradation. RAP from two sources (Georgia and Minnesota) was split on a 1.2-mm (No. 16) sieve. Two 12.5-mm SuperPave gradations were selected: One below and the other above the restricted zone. It was observed that screening the RAP allowed up to 40% of the coarse RAP fraction to be used while still meeting the restricted zone SuperPave gradation requirements. This was primarily due to the significant reduction in the finer aggregate fractions, especially the minus 0.075-mm (sieve #200) material. The addition of coarser fraction reduced the virgin asphalt requirement by approximately 18% to 33% at different RAP content levels. Although the use of minus 1.19-mm (No. 16) sieve reduced the

virgin asphalt requirement by about 25% for minimum RAP content (15%), it can only be used in limited percentages to produce SuperPave gradation. A maximum of 15% of the fine RAP fraction was used to produce an acceptable above-the-restricted-zone SuperPave gradation.

According to many researchers (Bukowski 1997; Huang et al. 2005; Shah et al. 2007), asphalt mixture designs with low RAP percentages (up to 15%) are not significantly affected by RAP variability; however, higher percentages of RAP can considerably change the overall performance of the asphalt mixture.

Solaimanian and Tahmoressi (1996) identified the variability in different stockpiles of RAP material and the variability in plant-produced asphalt mixture containing 20% to 50% RAP. Different tests, such as the Hveem stability test, asphalt content determination (Abson recovery and nuclear gauges), gradation of RAP material, density of field cores, theoretical maximum gravity, and asphalt binder viscosity and penetration were conducted. The asphalt mixture projects with a high percentage of RAP studied in that research exhibited a larger variation in asphalt content, gradation, air voids, and stabilities compared with typical asphalt mixture projects without RAP material. The use of a high percentage of RAP did not influence densities as much as it influenced the asphalt content of the plant mix. Projects with higher variation in RAP asphalt binder content also had higher variation in asphalt binder content of plant mix. Similarly, projects with higher variability in stiffness of RAP asphalt binder also showed higher variability in stiffness of plant mix asphalt binder. The RAP binder with a higher coefficient of variation in penetration also resulted in a higher coefficient of variation in penetration of plant mix binder. In general, production aggregate gradation was finer than the job mix formula target aggregate gradation, possibly because of aggregate crushing during the milling operation. It was recommended that high RAP not be used in asphalt mix designs unless variability is controlled.

One of the shortcomings of the SuperPave mix design method was that it did not specifically provide for the use of RAP in mix design. In 1997, Kandhal and Foo developed a procedure for selecting the performance grade (PG) of virgin asphalt binder to be used in recycled mixtures. They recommended using specific-grade blending charts instead of temperature-sweep blending charts. The information necessary to construct a

specific-grade blending chart is the $G^*/\sin\delta$ of both the aged asphalt binder and the virgin asphalt binder at the high pavement service temperature.

In 1997, based on past experiences, the Federal Highway Administration's (FHWA) RAP expert task force developed interim guidelines for the design of SuperPave asphalt mixture containing RAP (Bukowski 1997). The developed methodology was based on a tiered approach to determine the level of testing required in the design of asphalt mixture containing RAP. For RAP content less than 15%, there was no adjustment in the virgin binder grade to compensate for the RAP binder's stiffness. For RAP content ranging from 16% to 25%, FHWA suggested using a virgin binder one grade lower (for both high- and low-temperature grades) than the required binder grade. For RAP content greater than 25%, it was recommended that blending charts be used to select the appropriate binder grade. It was also suggested that RAP be handled as aggregate and that RAP binder be considered part of the blended binder. In 1989, the Asphalt Institute developed blending charts for incorporating RAP in asphalt mixture design. The FHWA guidelines are supported by the findings of NCHRP Project 9-12 (McDaniel et al. 2000), which was undertaken to develop guidelines to incorporate RAP in SuperPave mix design. The RAP binder evaluation and mix design using the Superpave system according to this project (McDaniel and Anderson 2001) is detailed next.

2.2.1 SuperPave Mix Design Method

Under the recommended guidelines for using RAP in SuperPave mixtures are three tiers of RAP usage. Table 2.1 presents the recommended tiers for SuperPave RAP mixtures and the appropriate changes to the binder grade. The limits of these tiers depend on the RAP binder grade. With softer RAP binders, higher percentages of RAP can be used. The first tier establishes the maximum amount of RAP that can be used without changing the virgin binder grade. The second tier shows the percentages of RAP that can be used when the virgin grade is decreased by one grade (a 6-degree increment) on both the high- and low-temperature grades. The third tier is for higher RAP contents. For these higher contents, it is necessary to extract, recover, and test the RAP binder and to construct a blending chart (McDaniel and Anderson 2001).

Table 2.1. Binder Selection Guidelines for RAP Mixtures (McDaniel and Anderson 2001)

	RAP Percentage Recovered RAP Grade		
Recommended virgin asphalt binder grade	PG xx-22 or lower	PG xx-16	PG xx-10 or higher
No change in binder selection	< 20%	< 15%	< 10%
Select virgin binder one grade softer than normal (e.g., select a PG 58-28 if a PG-64-22 would normally be used)	20%–30%	15%–25%	10–15%
Follow recommendations from blending charts	> 30%	> 25%	> 15%

The desired final binder grade, the physical properties (and critical temperatures) of the recovered RAP binder, and the physical properties (and critical temperatures) of the virgin binder, or the percentage of RAP in the mixture are needed to construct a blending chart.

Once the RAP binder has been extracted and recovered, it must be tested in the dynamic shear rheometer (DSR) at a high temperature as if it were an original, unaged binder. This results in a critical high temperature (T_c) at which $G^*/\sin\delta$ is equal to 1.00 kPa:

$$T_c(High) = \left(\frac{log(1.0) - log(G_1)}{a} \right) + T_1 \qquad (2.1)$$

where,

$G_1 = G^*/\sin\delta$ at temperature T_1; and

a = slope of the stiffness-temperature curve as $\Delta \log (G^*/\sin\delta)/\Delta T$.

Then the remaining RAP binder is aged in the rolling thin film oven (RTFO) and is tested in the DSR and bending beam rheometer (BBR). RTFO aged binder is again tested in the DSR to obtain $T_c(High)$ at which $G^*/\sin\delta$ is equal to 2.2 kPa:

$$T_c(High) = \left(\frac{log(2.2) - log(G_1)}{a} \right) + T_1 \quad (2.2)$$

The high-temperature performance grade of the recovered RAP binder is then determined based on this single critical high temperature. The critical high temperature of the recovered RAP binder is the lower of the original DSR and RTFO DSR critical temperatures. The RTFO+pressure aging vessel (PAV) aged binder is used in determining the critical intermediate temperature $T_c(Int)$ at which $G^* \sin\delta$ is equal to 5000 kPa:

$$T_c(Int) = \left(\frac{\log(5000) - \log(G_1)}{a} \right) + T_1 \quad (2.3)$$

where

$G_1 = G^*\sin\delta$ at temperature T_1; and

a = slope of the stiffness–temperature curve as $\Delta log\ (G^*\sin\delta)/\Delta T$.

The RTFO+PAV aged binder is then tested in the BBR to determine the critical low temperature, $T_c(S)$ or $T_c(m)$, based on BBR stiffness or m-value.

$$T_c(S) = \left(\frac{log(300) - log(S_1)}{a} \right) + T_1 \quad (2.4)$$

$$T_c(m) = \left(\frac{0.300 - m_1}{a} \right) + T_1 \quad (2.5)$$

where

S_1 = S-value at temperature T_1;

m_1 = m-value at temperature T_1; and

a = slope of the stiffness-temperature curve as $\Delta log\ (S)/\Delta T$.

The higher of the two low critical temperatures $T_c(S)$ and $T_c(m)$ is selected to represent the low critical temperature for the recovered asphalt binder, $T_c(Low)$. The low-temperature performance grade of the recovered RAP binder is determined based on this single critical low temperature.

Once the physical properties and critical temperatures of the recovered RAP binder are known, two blending approaches may be used. In the first approach, the percentage of RAP that will be used in an asphalt mixture is known, but the appropriate virgin asphalt binder grade for blending must be determined. In the second approach, the maximum percentage of RAP that can be used in an asphalt mixture while still using the same virgin asphalt binder grade must be determined. These two approaches are explained briefly in the following subsections (McDaniel and Anderson 2001).

2.2.1.1 Blending with a Known RAP Percentage (Virgin Binder Grade Unknown)

If the final blended binder grade, percentage of RAP, and recovered RAP properties are known, then the properties of an appropriate virgin asphalt binder grade can be determined. Using the following equation for the high, intermediate, and low critical temperatures separately, the properties of the virgin asphalt binder necessary to satisfy the assumptions can be determined.

$$T_{Virgin} = \frac{T_{Blend} - (\%RAP \times T_{RAP})}{(1 - \%RAP)} \tag{2.6}$$

where

T_{Virgin} = critical temperature of the virgin asphalt binder;

T_{Blend} = critical temperature of the blended asphalt binder (final desired);

$\%RAP$ = percentage of RAP expressed as a decimal (i.e., 0.30 for 30%); and

T_{RAP} = critical temperature of recovered RAP binder.

A blending chart, shown as Figure 2.1, can be used instead of Equation 2.6.

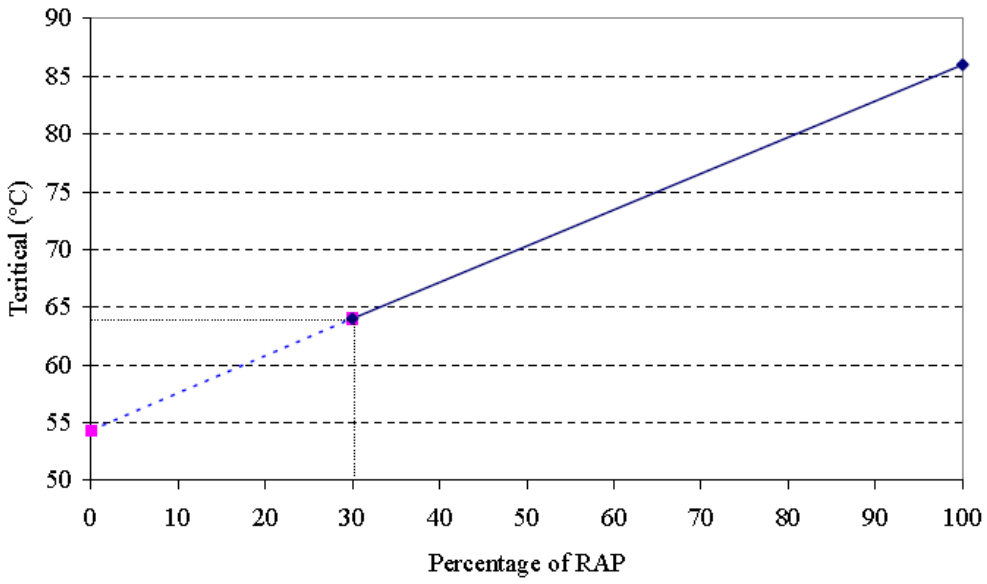

Figure 2.1. High-temperature blending chart (RAP percentage known) (McDaniel et al. 2000).

2.2.1.2 Blending with a Known Virgin Binder Grade (RAP Percentage Unknown)

If the binder grade is fixed based on economics and availability or on the specifications for a given project, it is necessary to determine the maximum amount of RAP that can be used with the specific virgin binder grade and still meet the final blended binder properties. The construction of a blending chart to determine RAP content is described next.

If the final blended binder grade, virgin asphalt binder grade, and recovered RAP properties are known, then the appropriate amount of RAP to use can be determined. Using Equation 2.7 for the high, intermediate, and low critical temperatures separately, the percentage of RAP required to satisfy the assumptions can be determined.

$$\%RAP = \frac{T_{Blend} - T_{Virgin}}{T_{RAP} - T_{Virgin}} \tag{2.7}$$

where all terms are as previously defined.

Figure 2.2 shows the graphical method for determining the RAP percentage to be used in asphalt mixture mix.

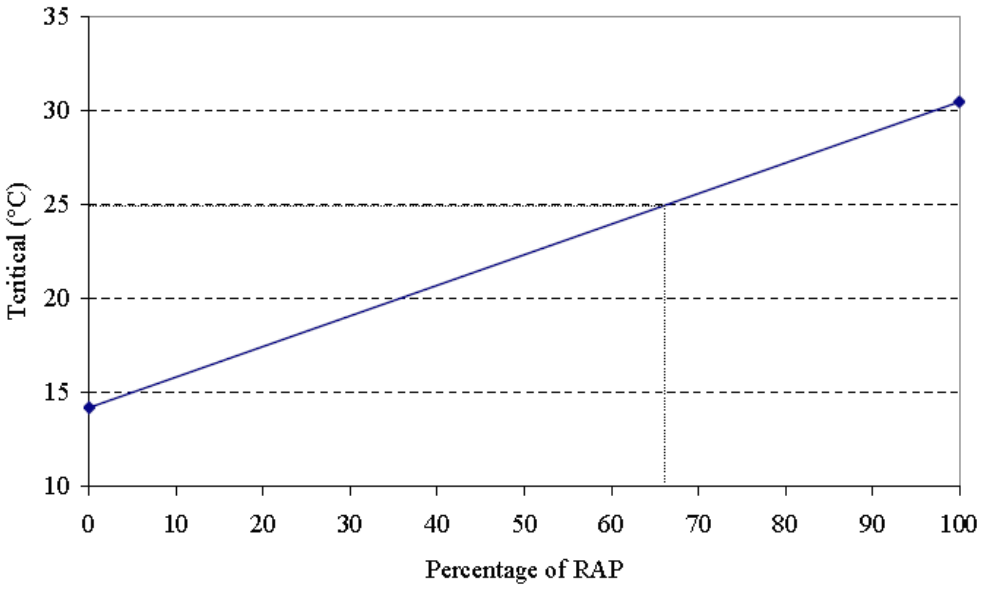

Figure 2.2. Intermediate temperature blending chart (RAP percentage unknown) (McDaniel et al. 2000).

2.2.2 Developing the Mix Design

The amount of RAP to be included in the new asphalt mixture may be limited by two main factors: Material-related and production-related factors. These factors include specification limits for mix type; plant type; gradation; aggregate consensus properties; binder properties; heating, drying, and exhaust capacity of the plant; moisture content of the RAP and virgin aggregates; temperature to which the virgin aggregate must be superheated; ambient temperature of the RAP; and virgin aggregate (McDaniel and Anderson 2001).

Overall, however, the process of using RAP in SuperPave mixtures is similar to that of using RAP in Marshall or Hveem mixtures. The blend of materials has to meet certain properties, and the plant must be capable of drying and heating the materials. Many of the techniques used to evaluate the RAP are similar to previous techniques. A detailed procedure for developing mix design involving RAP, along with examples, is described in NCHRP Report 452 (McDaniel and Anderson 2001).

To account for the presence of binder in the RAP material, the weight of RAP aggregate is calculated as follows (McDaniel and Anderson 2001):

$$\frac{M_{RAP(Agg)}}{(100 - P_b)} \times 100 \tag{2.8}$$

where

$M_{dry(RAP)}$ = mass of dry RAP;

$M_{RAP(Agg)}$ = mass of RAP aggregate (including RAP binder); and

P_b = RAP binder content.

Equation 2.8 is used when the amount (percentage) of RAP used in a mix is taken as the amount of RAP aggregate instead of the RAP (including binder) itself. It is important to note that in the study, IDOT's method of incorporating RAP was adopted (i.e., the percentage of RAP represents the actual RAP, including binder, not the RAP aggregate). For example, if 15% RAP is used with a particular asphalt content, then the actual aggregate contribution by RAP to the total aggregate blend will be less than 15%.

2.2.3 Issues with Specific Gravities and VMA

The bulk specific gravity of each aggregate stockpile, including the RAP aggregate, must be determined in order to calculate the bulk specific gravity of the combined aggregates. It is difficult to precisely measure the bulk specific gravity G_{sb} of the extracted RAP aggregate because of changes in aggregate gradation and properties due to the extraction process. NCHRP Report 452 (McDaniel and Anderson 2001) noted that few states used RAP effective specific gravity (G_{se}) instead of G_{sb}. G_{se} is determined using following equation:

$$G_{se} = \frac{100 - P_b}{\frac{100}{G_{mm}} - \frac{P_b(RAP)}{G_b(RAP)}} \tag{2.9}$$

where

$G_{b(RAP)}$ = specific gravity of RAP binder; and

$P_{b(RAP)}$ = RAP binder content.

The methodology recommended in NCHRP Report 452 (McDaniel and Anderson

2001) consists of assuming a value for absorption of the RAP aggregate. Some states estimate this value quite accurately based on past experience. The G_{sb} of the RAP aggregate can be calculated based on this assumed absorption using Equation 2.10. The G_{sb} value can then be used to estimate the combined aggregate bulk specific gravity and to calculate VMA.

$$G_{sb} = \frac{G_{se}}{\left(\frac{P_{ba} G_{se}}{100 G_b} + 1\right)} \tag{2.10}$$

where

P_{ba} = absorbed binder, percentage by weight of aggregate.

Recently, Hajj et al. (2008) concluded that using G_{se} instead of G_{sb} resulted in overestimating both the combined aggregate bulk specific gravity and the VMA, since for a given aggregate G_{sb} is always smaller than G_{se}. For instance, when the G_{se} of RAP is used in lieu of G_{sb}, the calculated VMA value will often change by 0.3% per 10% of RAP used, a one-tenth reduction in the optimum binder content, leading to dry mixes when designing to minimum VMA. This introduced error will be greater when higher percentages of RAP are used. For this reason, some states that allow the use of G_{se} for the RAP aggregate also increase their minimum VMA requirements to account for this error. Kvasnak et al. (2010) also recommended determining RAP G_{sb} by using the maximum theoretical specific gravity (G_{mm}) method when a known regional absorption is available. If a regional absorption is not available, then the RAP G_{sb} should be determined from extracted aggregate.

The following is a summary of a test method for measuring the bulk specific gravity of RAP aggregates. The method is used by IDOT and was introduced by Anderson and Murphy (2004).

After determining the P_b of the RAP material according to AASHTO T164, the G_{mm} of a RAP sample is determined after mixing with a 1% virgin asphalt binder by dry weight of RAP. The 1% asphalt binder is added to the RAP mixture to ensure a uniform coating of all particles. Then the adjusted P_b of the RAP mixture is calculated to account for the 1% virgin asphalt binder added. The G_{se} of the RAP aggregate is calculated using

Equation 2.11.

$$G_{se}(RAP) = \frac{100 - Adjusted\ P_b}{\frac{100}{G_{mm}} - \frac{AdjustedP_b}{1.040}} \quad (2.11)$$

The G_{sb} of the RAP aggregate is then calculated using Equation 2.12.

$$G_{sb}(RAP) = G_{se}(RAP) - 0.100 \quad (2.12)$$

Hajj et al. (2008) recommended that if the test method proposed by Murphy Pavement Technology is used, then the proposed equation that correlates G_{sb} to G_{se} (Equation 2.12) must first be validated since it will be most likely influenced by aggregate absorption and geological formations within each region/state.

Al-Qadi et al. (2009) investigated the effect of the amount of RAP on the volumetric and mechanical properties of asphalt concrete. Six different job mix formulae (JMFs) were designed with two materials to investigate the effect of RAP variation on asphalt mixtures. It was observed that optimum asphalt content for mix designs with different percentages of RAP was not significantly changed. VMA at optimum asphalt content had opposite trends for two materials. For one material, VMA decreased with an increase in RAP percentage, but it showed an opposite trend for the other material. In another study, by West et al. (2009), VMA showed a decreasing trend with an increase of RAP percentage. The optimum asphalt contents of the mixtures were also decreased by 1% with an increase in RAP from 0% to 45%. Kim et al. (2009) also demonstrated the similar results (i.e., a decrease in optimum asphalt content and VMA with an increase in RAP amount). The study by Mogawer et al. (2009) showed the same trend.

Daniel and Lachance (2005) observed some contrary results; they observed that the VMA and VFA of the RAP mixtures increased at 25% and 40% levels. They hypothesized that the difference between VMA values was due to the extent of blending of the RAP material with the virgin materials. They observed that there is an optimum heating time for the RAP material to allow for the greatest extent of blending between the virgin and RAP materials. The influence of pre-heating time of asphalt mixture with RAP on the volumetric properties of mixes was also evaluated. The VMA decreases by 0.5% when the heating time increases from 2 to 3.5 hrs and then increases by almost 3% with a

heating time of 8 hrs.

At the shorter heating time, the RAP is not heated enough to allow RAP particles to break up into smaller pieces and blend with the virgin materials. With the longer heating time, the RAP has likely aged further, its particles have hardened, and even fewer of them are able to break down and blend with the virgin material. They concluded that a RAP mixture may not meet the SuperPave VMA requirements when the RAP is heated for a particular amount of time; but the mixture may meet the requirements if the RAP is heated for a different amount of time. Hajj et al. (2008) also observed similar increasing trends in VMA and VFA with an increase in RAP percentages.

The purpose of the above discussion was to highlight asphalt mix design problems. Conflicting results from different studies show that emphasis should be put on studying the variation in volumetrics when using RAP in an asphalt mixture.

2.3 Laboratory Evaluation and Performance Testing of RAP Mixtures

To determine the potential benefits and adverse effects of RAP, researchers looked at various performance measures of RAP mixtures, such as rutting and cracking. Asphalt concrete pavements are designed to resist traffic and environmental loading for a specific period of time. Traffic loading as well as aging of the asphalt binder lead to deterioration of pavement and significantly affect pavement performance. After pavement is removed from the field, RAP materials age even further during the stockpiling process due to the exposure to air. Moreover, when RAP is added to asphalt concrete, the aged binder in the RAP mixes to some unknown degree with the virgin binder. This produces a composite effective binder system with unknown material properties and, hence, unpredictable pavement performance.

Huang et al. (2005) investigated the uncertainties caused by the unknown degree of blending of RAP binder with virgin binder. A lab study was conducted in which the blending process of RAP with virgin mixture was analyzed through controlled experiments. One type of screened RAP was blended with virgin (new) coarse aggregate at different percentages. A blended mixture containing 20% of screened RAP was subjected to staged extraction and recovery. The results from this experiment indicated that only a small portion of aged asphalt in RAP actually participated in the remixing

process; other portions formed a stiff coating around RAP aggregates and RAP functionally acted as "composite black rock." The resulting composite layered structure was desirable in improving the performance of the asphalt mixture.

Numerous studies on RAP have indicated that addition of RAP to an asphalt mixture changes the physical behavior of the mix. The increased stiffness of the RAP binder is believed to be the cause of increased modulus of asphalt mixtures. Similarly, it also affects the fatigue behavior and low-temperature cracking of the mixes. The effect of added RAP on asphalt mixture laboratory performance has been studied by many researchers. Gardiner and Wagner (1999) tested RAP mixture low-temperature properties using the SuperPave indirect tensile creep test at 0ºC (32ºF), –10ºC (14ºF), and –20ºC (-4ºF). The rutting potential was determined with an Asphalt Pavement Analyzer (APA). They also used a resilient modulus test to evaluate temperature susceptibility of the mixes at three temperatures (4ºC, 25ºC, and 40ºC). They found that inclusion of RAP decreased rutting potential and temperature susceptibility and increased the potential for low-temperature cracking. The addition of RAP approximately doubled the stiffness at warmer temperatures, but this increase was minimal at lower temperatures. They observed that the increase in RAP was also accompanied by an increase in tensile strength ratio (TSR).

Tam et al. (1992) looked into the thermal cracking of plant and lab recycled asphalt mixtures and confirmed that they are less resistant than nonrecycled mixes to thermal cracking. The thermal cracking properties of laboratory and field mixes were analyzed using McLeod's limiting stiffness criteria and the pavement fracture temperature (FT) method. When the induced stress or strain, because of temperature drop, exceeds the failure stress or strain, cracking is expected to occur. The corresponding temperature is called the FT. The higher the FT of a material, the lower its resistance to thermal cracking. Tam et al. (1992) came up with a few suggestions to minimize thermal cracking and more accurately predict fracture temperature. They suggested limiting recycling ratios to 50:50 and selecting an appropriate virgin asphalt binder for a desirable recovered mix penetration.

To compare mixtures compacted with only virgin materials to those compacted with varying amounts of RAP, Sondag et al. (2002) measured the resilient modulus for 18

different mix designs. These mixtures incorporated three different asphalt binders and two sources of RAP at varying levels. The RAP from one source (District 6) was coarser than the other (District 8). The study showed that at 25ºC, adding 40% District 6 RAP to a PG 58-28 control mixture resulted in a 74% increase in stiffness and a 164% increase with a PG 46-40 control mixture. A similar increase was observed with the addition of District 8 RAP. Therefore, the addition of RAP increased the resilient modulus. The RAP source also affected the resilient modulus results. The District 8 RAP binder had a higher PG grade than the District 6 RAP, and accordingly yielded a higher resilient modulus.

McDaniel and Shah (2003) and McDaniel at el. (2002) conducted a laboratory study to determine if the tiered approach of the FHWA and SuperPave RAP specifications are applicable to Midwestern materials obtained from Indiana, Michigan, and Missouri. The experimental program consisted of first comparing laboratory mixtures to plant-produced mixes containing the same RAP content and source, virgin aggregates, and binder. Additional samples were prepared in the laboratory with a RAP content of up to 50% to determine the effect of recycled materials on the mix performance. Prepared mixes were tested using the SuperPave Shear Tester (SST). Results of this study indicated that plant-produced mixes were similar in stiffness to laboratory mixtures at the same RAP content for the Michigan and the Missouri samples. The plant-produced mixes from Indiana were significantly stiffer than the lab mixes. Analysis of the SST data also indicated an increase in stiffness and decrease in shear deformation as the RAP content increased, but it also increased the potential for fatigue and thermal cracking. This indicates that higher RAP content mixtures (with no change in binder grade) would exhibit more resistance to rutting, provided that the aggregates are of acceptable quality.

Testing conducted for the NCHRP 9-12 study confirmed that recycled mixtures with RAP content greater than 20% had a lower fatigue life than virgin mixtures (McDaniel et al. 2000). Decreasing the virgin binder grade may be an option to improve the mixture fatigue performance, especially at high RAP content. The authors also emphasized that designing mixtures that conform to SuperPave specifications may not be feasible at a RAP content greater than 40% to 50% due to the high fine content in RAP materials.

Pereira et al. (2004) performed the repeated simple shear test at constant height

(RSST-CH) and four-point bending fatigue test to determine the rutting and fatigue behavior, respectively, of 50% RAP mix and a control mix (no RAP). The RSST-CH tests were conducted at 50ºC. Of the three asphalt contents (4.5%, 5%, and 5.5%), the mixture with RAP having 4.5% binder content exhibited the maximum resistance to permanent deformation. Generally, all the recycled mixes showed better behavior than the control mix without RAP. The authors observed improvement in fatigue resistance of RAP mixtures with 5% asphalt content compared to 4.5% asphalt content, but no further improvement was noticed with asphalt content of 5.5%. Thus, it was concluded that an increase in binder content did not significantly increase fatigue resistance.

Huang et al. (2004) evaluated fatigue resistance of asphalt concrete containing No. 4 sieve-screened (4.75 mm) RAP. A typical surface mixture commonly used in Tennessee was evaluated at 0%, 10%, 20%, and 30% RAP content. Fatigue characteristics of mixtures were evaluated with the indirect tensile strength test, semi-circular bending (SCB) test, semi-circular fatigue test, and semi-circular notched specimen fracture test. They found that long-term aging influenced the ranking of fatigue characteristics for mixtures containing different percentages of RAP. Generally, long-term aged mixtures more closely resembled the properties of field mixtures that had been in service for several years. Also, inclusion of RAP into the limestone surface mixture generally increased tensile strength, reduced post-failure tenacity, increased the mixture's modulus (stiffness), and reduced viscosity characteristics. In the study, total dissipated energy to failure at 20% of SCB tensile strength also indicated that inclusion of RAP generally increased fatigue life for unaged mixtures, whereas for long-term aged mixtures, dissipated energy increased with inclusion of 20% RAP and dropped to the - same level as the mix without RAP. The inclusion of RAP in the mixtures improved the mixtures' resistance to fracture failure. The inclusion of less than 20% of RAP material had very limited influence on mixture stiffness and indirect tensile strength characteristics.

Focusing on the same objective to determine the effect of adding RAP on the volumetric and mechanistic properties of asphalt concrete, Daniel and Lachance (2005) conducted a study on different asphalt concretes with RAP. They used a 19-mm SuperPave mixture containing no RAP as a control mix for evaluating properties of

mixes containing 15%, 25%, and 40% RAP. Testing included complex modulus in tension and compression, creep compliance in compression, and creep flow in compression. The complex modulus of the processed RAP mixtures increased from the control to the 15% RAP level. Unexpectedly, however, the 25% and 40% RAP mixtures had complex modulus curves similar to the control mixture in both tension and compression. The creep compliance curves showed similar trends. A combination of gradation, asphalt content, and volumetric properties was identified as the cause of these unexpected trends.

To assess the feasibility of utilizing a high RAP content in asphalt mixture, Widyatmoko (2008) prepared wearing and base course mixes with 10%, 30%, and 50% RAP. One of the asphalt mixture properties measured was deformation resistance, for which two tests were carried out. The repeated load axial test (RLAT) was carried out at 40ºC (104ºF) in the Nottingham Asphalt Tester (NAT). The wheel track test (WTT) was carried out under a wheel load of magnitude 520 N (117 lb) at 60ºC (140ºF). Contrary to norm, it was found that mixtures containing RAP show lower resistance to permanent deformation (i.e., greater WTT rut depth, WTT rut rate, and/or RLAT strain) compared with equivalent mixtures without RAP. They also noticed a reduction in stiffness with an increase in RAP content. This behavior was explained by the fact that with an increase of RAP percentage, more rejuvenators or softer binder are added to the mix—resulting in a softer mix. For same reasons, the RAP mixes showed at least similar or better fatigue resistance than mixes without RAP. It was also concluded that these mixes with RAP were not susceptible to moisture damage (stiffness ratio > 0.8).

Chehab and Daniel (2006) studied the sensitivity of the predicted performance of RAP mixtures to the assumed binder. This was accomplished with Mechanistic-Empirical Pavement Design Guide (MEPDG) software to predict performance of a specific flexible pavement structure with a RAP-modified asphalt mixture surface layer. In the study, RAP content and effective binder PG grade were the main variables. They found that alligator cracking was not significant in the analysis, possibly due to a thick test section and low truck traffic. The RAP mixes showed a lower predicted amount of longitudinal cracking after 10 yrs than the asphalt mixture mix, but none reached the failure limit. The amount of cracking was higher for 40% RAP than for the other two RAP mixes. It was predicted

that increasing the amount of RAP would result in more transverse cracking. The authors observed a slight increase in rutting with an increase in RAP content from 15% to 25%, which may be due to the higher asphalt content in the 25% RAP mixture, which offset the increase in stiffness. For the mix with 40% RAP, the amount of rutting was lowest, as expected. The authors also concluded that the assumed PG binder grade, particularly the high temperature grade, for the RAP mixtures had a significant influence on the predicted amount of thermal cracking and rutting performances. The results emphasized the importance of determining the effective binder grade of RAP mixtures.

Shah et al. (2007) conducted a study to investigate the effects of RAP content on virgin binder grade and to determine the properties of plant-produced mixtures. RAP was added at 15%, 25%, and 40% levels to an asphalt mixture with PG 64-22 and at 25% and 40% levels to an asphalt mixture with PG 58-28 binder. In addition, control mixture samples with PG 64-22 and no RAP were collected and tested for comparison. The results from complex modulus ($|E^*|$) testing showed no increase in stiffness with the addition of 15% RAP compared with the control mixture. However, the addition of 25% and 40% RAP resulted in an increase in the modulus. No significant change in stiffness was observed from a change in binder grade at higher RAP levels except for a slight lowering in moduli with respect to the control mixture at higher frequencies. Indirect tensile strength results showed that mixes with higher strength also generally showed higher stiffness values. The mix with the highest RAP content had the highest strength and stiffness, and, hence, the highest critical temperature. It was also observed that the stiffness of the binder changed only 3%, not the 40% (RAP added), which showed that combined properties of the binder did not change linearly based on the proportion of old and new binders as claimed earlier (McDaniel et al. 2000).

Carter and Gardiner (2007) developed a simple indirect tension stress relaxation test method and analysis approach for assessing binder-related asphalt mixture properties. The objective was to evaluate the effect of adding RAP to asphalt concrete on relaxation modulus and rate of relaxation. A total of 160 different asphalt mixture (combinations of binders, aggregates, and RAP) were compacted and tested using indirect tension stress relaxation at 5ºC and 22ºC. Two experiments were conducted. The first experiment was developed to compare binder stress relaxation modulus to the asphalt mixture indirect

tension (IDT) stress relaxation modulus. Constant strain parallel plate testing was used to develop stress relaxation master curves for the virgin binders (PG 64-22 and PG 76-22). The asphalt mixture stress relaxation modulus was determined using a test method developed for the study. The binder relaxation master curves were compared to those for the asphalt concrete. The second experiment was designed to determine if the asphalt mixture indirect tension stress relaxation approach (developed and refined during the first experiment) was sensitive to changes in the mix binder, such as those anticipated with increasing percentages of RAP.

Two relaxation characteristics from a power law fit through the data were used to define the effect of RAP on properties related to asphalt mixture binder: the initial modulus at 1s (regression constant) and the curvature coefficient (regression exponent). The results showed a nonlinear relationship between both the initial modulus and the curvature coefficient and the percentage of RAP from 0% to 100% RAP. A linear relationship could be obtained only between the properties and the percentage of RAP between 0% and 50%. There is little change in either the initial modulus or curvature coefficient for asphalt mixture mixes with 50% or more RAP.

Li et al. (2008) investigated the effect of RAP percentage and sources on the properties of asphalt concrete by performing complex modulus and semi-circular beam (SCB) tests. Ten laboratory-prepared asphalt mixtures were studied using three RAP percentages (0%, 20%, and 40%). The mixes were fabricated using two RAP sources and two asphalt binders (PG 58-28 and PG 58-34). One of the RAPs had a single source; the other consisted of RAP collected from different pavements and blended in a single pile at the mixing plant. The authors observed that the asphalt mixtures containing RAP had higher complex modulus values than the control mixtures containing no RAP. At high temperatures, the asphalt mixtures containing 40% RAP were found to have higher or similar complex moduli as mixtures with 20% RAP. On the contrary, most mixtures containing 20% RAP were observed to have the highest complex modulus at lower temperatures or high frequencies. The authors hypothesized that the aged and brittle binder in the RAP resulted in the formation of microcracks. The stiffer asphalt binder was found to result in a higher complex modulus for both the control and the RAP-modified mixtures. Experimental data also showed that the RAP source was not a significant factor

for complex modulus values at low temperatures, though it significantly affected the complex modulus values at high temperatures. The fracture resistance was significantly affected by the testing temperature and the percentage of RAP in the mixtures. Fracture testing results indicated that 20% RAP-modified mixtures exhibited similar fracture resistance abilities to the control mixtures, which had the highest fracture energies. The addition of 40% RAP significantly decreased low-temperature fracture resistance. At low temperatures, RAP source did not significantly affect fracture resistance of the asphalt concrete. As would be expected, no significant statistical relationship between complex modulus and fracture energy was found.

To evaluate and compare fatigue performance of asphalt concrete with RAP, Shu et al. (2008) prepared four asphalt mixtures consisting of 0%, 10%, 20%, and 30% RAP with one source of aggregate (limestone) and one type of binder (PG 64-22). The mixture characterization included indirect tensile strength (ITS), failure strain, toughness index (TI), resilient modulus, dissipated creep strain energy ($DCSE_f$), energy ratio, plateau value, and load cycles to failure. They observed that inclusions of RAP into asphalt mixtures generally increased tensile strength and reduced post-failure tenacity in indirect tensile strength tests. The inclusion of RAP also generally decreased the $DCSE_f$ threshold and energy ratio calculated from IDT tests, which may result in the short fatigue life of asphalt concrete. Lower $DCSE_f$ values mean that the energy required to fracture the asphalt mix mixtures decreased as RAP percentage increased.

The energy ratio concept was found more reasonable than $DCSE_f$ for characterizing the cracking resistance of asphalt concrete because it takes into account both the energy required to fracture asphalt concrete and the dissipated energy accumulation in asphalt concrete under certain loading conditions. Based on the failure criterion of 50% reduction in stiffness (obtained from the beam fatigue test), incorporation of RAP increased the fatigue life of asphalt concrete, whereas based on plateau values from the beam fatigue test, inclusion of RAP would turn more input energy into damage, which may result in the shorter fatigue life. The plateau value failure criterion appeared more reasonable in evaluating fatigue performance of asphalt concrete. It was concluded that both SuperPave IDT and beam fatigue test results agreed in ranking fatigue resistance of mixtures when proper procedures were followed.

One of the primary concerns about using RAP is its effect on mixture durability. Moisture susceptibility is regarded as the main cause of poor mixture durability. Moisture susceptibility can be evaluated by performing stability, resilient modulus, or tensile strength tests on unconditioned and moisture conditioned samples. Gardiner and Wagner (1999) used the tensile strength ratio (TSR), ratio of unconditioned tensile strength and moisture-conditioned tensile strength, to evaluate moisture sensitivity. They showed that the inclusion of coarse RAP decreased moisture susceptibility. Sondag et al (2002) used the TSR to evaluate the moisture sensitivity for 18 different mix designs incorporating three different asphalt binders, two sources of RAP and varying amounts of RAP. They found that the addition of RAP to a mixture had no positive or negative influence on the mixture moisture susceptibility. The properties of aged binder are also affected by the level of moisture damage on the existing pavement prior to recycling. In principle, stripped asphalt mixture should not be recycled due to the probability of reoccurrence of this distress in the new asphalt mixture (Karlsson and Isacsson 2006). However, when a small percentage of RAP is used (15 to 20%) together with an anti-strip agent, samples with moisture-damaged asphalt mixture provided a comparable strength and moisture resistance to samples made with virgin materials (Amirkhanian and Williams 1993).

2.4 Life-cycle Assessment

Life-cycle assessment (LCA) is an environmental management technique to assess the environmental burden associated with any product or process though its life cycle. Environmental burdens include the materials and energy resources required to create the product, as well as the wastes and emissions generated during the process. For pavements, the term “life cycle” refers to the major activities throughout the pavement’s life span, from its materials acquirement, construction, use, and maintenance to its final disposal. Pavement LCA is a technique that assess the potential environmental impact associated with the various pavement life phases. ISO (2006a) described the four components of LCA process as follows:

- Goal Definition and Scoping – The goal of the LCA should be clearly defined and described. Scope of the LCA should comprise of the processes to be considered, the functional unit to be used, the boundaries of the product system, and

assumptions if any.

- Inventory Analysis – This components deals with data collection and making an inventory of the energy and materials usage and environmental releases (e.g., air emissions, solid waste disposal, waste water discharges). Since data collection can be a resource-intensive process, particle constraints on data collection should be considered while defining the scope of the LCA (ISO 2006a).
- Impact Assessment – The life-cycle inventory needs to be associated with some specific environmental impacts. Impact Assessment component of LCA evaluates the significance of potential environmental impacts of energy, water, and material usage and the environmental releases identified in the inventory analysis.
- Interpretation – The findings of inventory analysis and/or impact assessment phases are used to reach conclusions of the LCA. The conclusion and recommendations are made within the scope of the study.

There are two basic approaches to conduct LCA: process-based LCA and economic input-output (EIO) LCA. In a process-based LCA, the inputs (materials and energy resources) and the outputs (emissions and wastes to the environment) are itemized for a given step in producing a product. So, for an asphalt pavement, aggregates and binder can be itemized as material inputs, whereas, electricity, natural gas, fuel for operating the asphalt plant, transportation vehicles, and construction equipment to construct the pavement as energy inputs. For the output, greenhouse gases (GHG) and wastes released during the material manufacturing process may be listed as outputs. The process-based LCA gives a lot of attention to details and the results are very process/product specific. The extensive data required to conduct such a detailed analysis usually limits the scope of the process-based LCA. Process-based LCA has to ignore a number of upstream processes and are usually limited to an arbitrary system boundary which can cause some truncation errors (Santero et al. 2010).

EIO-LCA, on the other hand, is based on the work of Wassily Leontief who developed the idea of input-output models of the U.S. economy in 1930s. *EIO-LCA* uses information about purchases of materials by one industry from other industries, and the information about direct environmental emissions of industries, to estimate the total emissions throughout the supply chain (Hendrickson et al. 2006 and CMUGDI 2013).

EIO-LCA "estimates the materials and energy resources required for, and the environmental emissions resulting from, activities in our economy" (Hendrickson et al. 2006). Table 2.2 shows the structure of input-output model. Each entry, X_{ij} represents input to sector *j* from sector *I* in the production process. The output of each sector (X_i) is the sum across the rows of the output supplied to final demands. Within the input-output table, the column sum represent the total amount of input to each sector from other sectors (Hendrickson et al. 2006).

Table 2.2. Structure of an economic input-output table (CMUGDI 2013).

	Input to sectors (*j*)				Intermediate output *O*	Final demand *D*	Total Output *X*
Output from sectors (*i*)	1	2	3	*n*			
1	X_{11}	X_{12}	X_{13}	X_{1n}	O_1	D_1	X_1
2	X_{21}	X_{22}	X_{23}	X_{2n}	O_2	D_2	X_2
3	X_{31}	X_{32}	X_{33}	X_{3n}	O_{3n}	D_3	X_3
n	X_{n1}	X_{n2}	X_{n3}	X_{nn}	O_n	D_n	X_n
Intermediate input *I*	I_1	I_2	I_3	I_n			
Value added *V*	V_1	V_2	V_3	V_n		*GDP*	
Total Input *X*	X_1	X_2	X_3	X_n			

A matrix A can be defined showing the proportional inputs from each sector for a single dollar of output (*Xij/Xi*). The matrix A with entries ranging from 0 to 1 shows the requirements of other sectors required to produce a dollar of output for each sector. Algebraically, the required economic purchase in 480 sectors of the U.S. economy required to make a vector of desired output y can be calculated as follows:

$$x = (I + A + A \times A + A \times A \times A + ...)y = (I - A)^{-1} y \qquad (2.13)$$

where *x* is the vector (or list) of required inputs, *I* is the identity matrix, *A* is the input-output direct requirements matrix (with row representing the required input from all other sectors to make a unit of output for that row's sector), and *y* is the vector of desired output. In *EIO-LCA* model, the vector of required outputs is multiplied by the average of

these individual environmental impact or resource requirement for each sector, and the aggregation of these individual impacts represents the total supply chain impact of a purchase.

Both process-based and EIO LCAs have their own strengths and weaknesses, however, in hybrid LCA, both LCAs can be used to complement each other by filling the gaps of the other. In a hybrid LCA, process-based LCA can be used to analyze the main, direct process, while using the *EIO-LCA* for indirect, upstream processes.

2.5 Life Cycle Cost Analysis

Life cycle cost analysis (LCCA) is an engineering economic analysis tool to determine the most cost-effective option among different competing alternatives to do a project, when each is equally appropriate to be implemented on technical grounds. For a highway pavement, apart from the initial cost, LCCA considers all the user costs, (e.g., reduced capacity at work zones) as well as agency costs related to future activities, including periodic maintenance and rehabilitation. LCCA goes beyond a simple cost comparison and offers a sophisticated approach to evaluate and demonstrate the economic merits of the alternatives under consideration in an analytical manner (FHWA 2013a). LCCA methodology can be break down into the following steps:

- Establish alternative design strategies – the LCCA process starts with identifying different product/process alternatives to complete a project. The analysis period, a common period of time to assess cost differences between the alternatives, is defined.
- Determine activity timing – The project alternative may be differentiated from each other based on initial construction and subsequent maintenance and rehabilitation activities. An activity schedule is then developed/adopted to run the analysis. It is important to be accurate in determining the timing and frequency of these activities as a considerable portion of total life-cycle cost is constituted of expenses associated with these activities.
- Estimate agency and use costs – All the agency and user costs that are not common to each alternative are compared. Agency costs include initial construction costs, maintenance and rehabilitation costs, and the value of any

alternative at the end of analysis period (in terms of a salvage value or remaining service life value).

- Determine life-cycle cost – The amount of money spent at different times have different present values. Therefore, all the future costs are converted to present money value so that the lifetime costs of different alternatives can be directly compared (FHWA 2002). Either probabilistic or deterministic analysis are conducted to carry out the LCCA.
- Analyze the results – Once all the results are available present value cost of different alternative can be compared. Procedure to analyze deterministic and probabilistic analysis are slightly different. In case of deterministic analysis, a sensitivity analysis is conducted to see effect of a particular factor (e.g. interest rate) on LCCA. Probabilistic approach usually gives a full range of possible NPV outputs.

  In this study, both agency and user costs will be determined for each alternative.

CHAPTER 3

MATERIAL PROCESSING AND ASPHALT MIX DESIGNS

3.1 Introduction

The use of recycled material is a key component of sustainable practices in the pavement industry. Although recycling asphalt has been practiced in the US for the past 40 years, the percentage of RAP used in asphalt mixes seldom increases above 20-25%. Several downsides have hindered the use of high percentages of RAP in asphalt pavements, including high percentages of fines, aged asphalt binder, and variability in aggregate gradation. The two most important characteristics to be considered when designing asphalt mixtures are the stability and durability of asphalt pavements. The variation in voids in mineral aggregates (VMA) affects the stability and durability of asphalt mixtures. The major challenge with increased use of RAP in asphaltic mixtures is the potential for an increase or decrease in the VMA due to the changes in aggregate packing. The aggregate packing is influenced by gradation, shape, surface texture, and type and amount of compactive effort (Vavrik et al. 2002).

Ozer et al. (2009) investigated the effects of the amount of RAP (up to 40%) on the volumetric and mechanical properties of asphaltic mixtures. They observed that the optimum asphalt content for the mix designs with different percentages of RAP was not significantly changed. VMA at optimum asphalt content had opposite trends for two materials. While for one material, VMA decreased with an increase in RAP percentage, it increased for the other material. In another study by West et al. (2009), VMA showed a decreasing trend with increasing RAP percentage. The optimum asphalt contents of the mixtures also decreased by 1% with an increase in RAP from 0 to 45%. Kim et al. (2009) and Mogawer et al. (2009) also demonstrated similar results, i.e., decrease in optimum asphalt content and VMA with an increase in RAP amount. In another study, Daniel and Lachance (2005) observed results which were contrary to the above mentioned studies. They observed that the VMA and VFA of the mixtures with RAP increased at 25% and

40% levels. According to the authors, the difference between the VMA values was due to the extent the RAP material was blended with the virgin materials. A similar trend of increasing VMA and VFA with increasing RAP percentages was found in another study (Hajj et al. 2008). Keeping in perspective the earlier unsuccessful efforts for controlling the volumetrics of mixtures with RAP, this chapter aims at designing asphaltic base-course mixtures containing high RAP content with acceptable volumetrics. This chapter lends itself to describing the materials used and the laboratory protocols followed to process them. The efforts to achieve acceptable volumetrics for asphalt mixtures with a high percentage of RAP is described in detail.

3.2 Material Processing

The virgin aggregate and RAP for this study were obtained from two source locations, District 1 and District 5, Illinois. District 1 material was collected from Gallagher Asphalt Co. in Thornton, Illinois. Five aggregate gradations were collected from District 1: CM11, CM16, FM20, FM22, and mineral filler (baghouse fines). FM22 was obtained from Hanson Material Services in Thornton. Two gradations of 3/4-in. (19-mm) nominal maximum aggregate size (NMAS) RAP [+3/8 and –3/8 in. (9.5 mm)] were also obtained from the same source. Table 3.1 shows the stockpile gradation for District 1 aggregates.

Table 3.1. Stockpile aggregate gradation (District 1).

Sieve	CM11	CM16	FM20	FM22	Mineral Filler	+3/8-in. RAP[1]	–3/8-in. RAP[1]
1 in.	100.0	100.0	100.0	100.0	100.0	100.0	100.0
3/4 in.	90.9	100.0	100.0	100.0	100.0	96.9	100.0
1/2 in.	43.5	100.0	100.0	100.0	100.0	81.5	100.0
3/8 in.	18.8	98.4	100.0	99.6	100.0	64.8	98.9
No. 4	5.6	27.8	99.7	60.0	100.0	43.0	69.4
No. 8	4.2	5.2	81.0	14.0	100.0	31.4	47.0
No. 16	3.6	3.7	49.4	5.4	100.0	24.6	34.3
No. 30	3.3	3.2	31.0	4.2	100.0	19.8	26.2
No. 50	3.1	3.1	17.4	3.8	100.0	14.5	19.7
No. 100	3.0	3.0	10.3	3.6	95.0	9.3	12.9
No. 200	2.7	2.8	5.6	3.4	90.0	7.0	9.6
Binder Content (%)	—	—	—	—	—	4.2	5.1

[1]Extracted gradation

District 5 material was collected from Open Road Paving in Urbana, Illinois. The source of the virgin aggregate was Vulcan in Kankakee. The material collected from

District 5 was CM11, CM16, and FM20. The same FM22 used for District 1 mix designs was used for District 5 mix designs. Table 3.2 shows the stockpile gradation for District 5 aggregates. Open Road Paving also provided two gradations of 1/2-in. NMAS RAP, +3/8 and –3/8 in.

Table 3.2. Stockpile Aggregate Gradations (District 5).

Sieve	CM11	CM16	FM20	FM22	Mineral Filler	+3/8-in RAP[1]	–3/8-in RAP[1]
1 in.	100.0	100.0	100.0	100.0	100.0	100.0	100.0
3/4 in.	82.1	100.0	100.0	100.0	100.0	99.3	100.0
1/2 in.	39.1	100.0	100.0	100.0	100.0	90.8	100.0
3/8 in.	19.0	97.3	100.0	99.6	100.0	78.6	99.3
No. 4	3.9	36.7	98.6	60.0	100.0	39.0	71.7
No. 8	2.7	6.8	74.6	14.0	100.0	26.5	48.6
No. 16	2.4	3.1	43.9	5.4	100.0	19.1	32.6
No. 30	2.2	2.3	24.6	4.2	100.0	14.8	24.2
No. 50	2.1	2.2	14.5	3.8	100.0	10.7	17.2
No. 100	2.1	2.1	9.7	3.6	95.0	7.7	12.7
No. 200	2.0	2.0	7.1	3.4	90.0	6.0	10.1
Binder Content (%)	—	—	—	—	—	3.9	5.5

[1]Extracted gradation

For all mixes, asphalt binders PG 64-22 and PG 58-22 were obtained from Emulsicoat Inc., Champaign, Illinois, and asphalt binder PG 58-28 was procured from Indiana. The true PGs for all binders, including the RAP binder, were determined in the lab, Table 3.3.

Table 3.3. PG grades for virgin and RAP binders.

Binder Type	True grades	PG grades
District 1 PG 64-22	66.7–24.2	64-22
District 5 PG 64-22	67.0–22.9	64-22
PG 58-22	62.3–22.4	58-22
PG 58-28*	61.4–27.4	58-22
District 1 RAP	82.4–13.7	82-10
District 5 RAP	89.3–14.9	88-10

*Not a true PG 58-28

Aggregate bulk specific gravities (G_{sb}) were determined for each RAP by IDOT's

Bureau of Materials and Physical Research (BMPR). The theoretical maximum specific gravity (G_{mm}) was used to determine the RAP material's G_{se}. In this study, G_{sb} of the RAP aggregates was calculated using an empirical relationship, Equation 3.1. IDOT. 0.1 is usually used as a reduction factor for slag RAP to determine G_{sb} of RAP aggregates. However, this study involved natural aggregate, so the value of 0.075 was used.

$$G_{sb}(RAP) = G_{se}(RAP) - 0.075 \quad (3.1)$$

3.3 Asphalt Mix Designs

Eight asphalt mix designs were prepared for the study; four mix designs were prepared for each district. The asphalt mixtures designed were binder course 3/4-in. (19-mm) N90 mixtures with an air void content of 4.0%, minimum VMA of 13.0%, and VFA of 65% to 75%. For each source of material, a control mix design (0% RAP) and three mix designs with 30%, 40%, and 50% RAP, respectively, were developed. The Bailey method (Vavrik et al. 2002) was used to develop all mix designs. That method, based on the aggregate packing theory, is an efficient approach that can be used in asphalt mix design. The Bailey method not only reduces the number of trials to achieve the target volumetrics but also provides useful insight into the aggregate packing effect on asphalt mixture volumetrics.

3.3.1 District 1 Asphalt Mix Designs

All virgin and RAP aggregates were fractionated in different sieve sizes and blended back to required average stockpile gradation listed for RAP in the mix design. Prior to fractionation, the RAP material was dried by heating it to 132ºF (50ºC) for 36 to 48 hrs. The gradation obtained from fractionating the RAP ("apparent gradation") was then used to batch the samples for asphalt extraction and G_{mm} samples.

The gradation of the extracted aggregate was determined and then used in the asphalt mix design to determine the final blends. A step-by-step procedure to determine apparent gradation is described elsewhere (Al-Qadi et al. 2008). The apparent and extracted gradations for the District 1 RAP material are presented in Table 3.4.

As previously explained, the Bailey method was used to determine all asphalt mix designs. The unit weights of virgin aggregates—which take into account the effects of

aggregate gradation, texture, shape and size, and compaction effort— were determined as part of the Bailey method. The unit weight test was not performed on RAP and mineral filler. Detailed information about the mix design is provided in the following sections.

Table 3.4. Apparent and extracted gradations of District 1 RAP aggregate.

Sieve	Retained on each sieve (%) Apparent Gradation		Passing (%) Extracted/Actual Gradation	
	+3/8-in. RAP	–3/8-in. RAP	+3/8-in. RAP	–3/8-in. RAP
3/4 in.	3.0	—	100.0	100.0
1/2 in.	33.1	—	96.9	100.0
3/8 in.	27.2	—	81.5	100.0
No. 4	17.9	43.3	64.8	98.9
No. 8	8.7	24.8	43.0	69.4
No. 16	—	15.2	31.4	47.0
No. 30	5.9	9.1	24.6	34.3
No. 50	—	—	19.8	26.2
No. 100	—	—	14.5	19.7
No. 200	—	—	9.3	12.9
Pan	4.3	7.6	7.0	9.6
Binder Content (%)	—	—	4.2	5.1

3.3.1.1 Aggregate Blend and Gradation

At the start of the study, a control (0% RAP) mix design was provided by IDOT, but due to the relative high specific gravities of procured virgin aggregate, the target blend was modified to achieve acceptable volumetrics, including air void contents and VMA. The aggregate blend for the control mix is presented in Table 3.5.

After designing the control asphalt mix, various percentages of RAP were added. The aggregate percentages, after including RAP, were altered such that the new blends containing RAP had the same percentage passing through the primary control sieve (PCS) as the control mix. The primary control sieve is defined as the closest sieve size to the product of 0.22 × NMAS. For example, for a 3/4-in. (19-mm) NMAS mixture, the PCS is a No. 4 (4.75-mm) sieve.

To maintain the desired split of coarse and fine aggregate, the percentage that passed through the PCS were kept approximately the same for virgin and RAP blends. Moreover, coarse aggregate (CA) ratio values were kept the same because there were two

coarse aggregates in virgin and RAP blends. In addition, the blend by mass of virgin fine aggregates in the virgin and RAP blends was the same [See Vavrik et al. (2002) for details about PCS and the Bailey method]. Initially, keeping the passing #200 material constant for all mix designs was considered, but the idea was dropped because of the presence of high amounts of fines (minus #200) in RAP. The asphalt mix blends with RAP were finalized such that similar volumetrics were achieved for all mixtures. Table 3.5 shows design aggregate blends, and Table 3.6 shows aggregate stockpile percentages for the District 1 mixtures with 0% (control), 30%, 40%, and 50% RAP.

Table 3.5. Design aggregate blend for District 1 asphalt mix designs.

Sieve Size	Control	30% RAP	40% RAP	50% RAP
1 in.	100.0	100.0	100.0	100.0
3/4 in.	96.1	96.1	96.4	96.6
1/2 in.	75.6	75.9	77.8	79.1
3/8 in.	64.5	63.7	65.6	66.6
No. 4	39.5	38.0	37.9	37.3
No. 8	27.5	23.2	22.5	21.7
No. 16	17.8	16.2	16.3	16.2
No. 30	12.3	12.4	12.8	13.1
No. 50	8.3	9.4	9.9	10.1
No. 100	6.2	6.8	7.1	7.2
No. 200	4.6	5.4	5.7	5.8

3.3.1.2 Mix Design and Volumetrics

As described in the literature review, researchers have faced considerable difficulties in achieving the required VMA values with RAP mixes. Changes in VMA are the result of variation in RAP aggregate gradation and characteristics (i.e., shape, texture, and angularity). By adopting a stringent approach for aggregate and RAP processing and using the Bailey estimation process, similar VMA values were achieved for all mixes, including the ones with various RAP contents. Therefore, any variation in mixture performance is independent of VMA. Table 3.6 shows the volumetrics, including VMA, for all District 1 mixes. Detailed volumetrics for each mix are provided in Appendix A.

Table 3.6. Stockpile percentages and volumetrics of District 1 asphalt mix designs.

	Control	30% RAP	40% RAP	50% RAP
CM11 (%)	43.2	37.7	31.0	25.5
CM16 (%)	27.1	12.5	13.3	14.0
FM20 (%)	28.5	8.5	4.0	0.0
FM22 (%)	—	10.5	11.0	10.0
+3/8-in. RAP (%)	—	15.0	25.0	35.0
–3/8-in. RAP (%)	—	15.0	15.0	15.0
Mineral Filler (%)	1.2	0.8	0.7	0.5
Binder Content (%)	4.9	4.9	5.1	5.0
Air Voids (%)	4.0	4.0	4.0	4.0
VMA (%)	13.7	13.6	13.7	13.7
VFA (%)	70.8	70.6	70.8	70.8

Table 3.7 presents a comparison between the design mix formula (DMF) and the extracted aggregate gradation of G_{mm} samples of 30%, 40%, and 50% recycled mixtures. Stringent specimen preparation and RAP processing protocols helped ensure that gradation variability was insignificant.

Optimum binder content was obtained by determining the volumetrics of mixtures at three different binder contents (at estimated optimum binder content, optimum + 0.5%, and optimum – 0.5%). In this study, asphalt mix designs with RAP were created assuming a 100% contribution of asphalt binder from RAP. In addition, IDOT's method of incorporating RAP was adopted—that is, the RAP percentages represents the actual

RAP (including binder) not the RAP aggregate. For example, if 15% RAP is used with particular binder content, then the actual aggregate contribution by RAP to total aggregate blend will be less than 15%, based on the RAP binder content. Table 3.8 illustrates the actual percentages of virgin and aged RAP binders and aggregate contributed by RAP for various mixtures.

Table 3.7. Comparison between target and achieved aggregate gradations for District 1 mixtures.

Sieve	30% RAP		40% RAP		50% RAP	
	DMF	Extracted	DMF	Extracted	DMF	Extracted
1 in.	100.0	99.5	100.0	100.0	100.0	100.0
3/4 in.	96.1	95.9	96.4	96.2	96.6	97.4
1/2 in.	75.9	76.3	77.8	77.9	79.1	79.7
3/8 in.	63.7	64.8	65.6	65.8	66.6	67.4
No. 4	38.0	38.4	37.9	38.4	37.3	37.8
No. 8	23.2	23.4	22.5	22.7	21.7	22.0
No. 16	16.2	16.3	16.3	16.5	16.2	16.3
No. 30	12.4	12.6	12.8	13.1	13.1	13.4
No. 50	9.4	9.6	9.9	10.1	10.1	10.5
No. 100	6.8	7.0	7.1	7.5	7.2	7.6
No. 200	5.4	5.7	5.7	6.0	5.8	6.2

Table 3.8. Asphalt binder and aggregate contribution from RAP for District 1 mixtures.

Mix Type	Binder Contribution (%)			Aggregate Contribution (%)		
	Virgin Binder	RAP Binder	Total	New Aggregate	RAP Aggregate	Total
Control Mix	100.0	0.0	100.0	100.0	0.0	100.0
30% RAP Mix	72.4	27.6	100.0	71.0	29.0	100.0
40% RAP Mix	65.4	34.6	100.0	61.1	38.9	100.0
50% RAP Mix	56.3	43.7	100.0	51.1	48.9	100.0

3.3.1.3 Moisture Susceptibility Test

IDOT's moisture susceptibility test (Illinois Modified AASHTO T 283-07; IDOT 2011) was conducted using PG 64-22 as part of the mix design evaluation. Six samples

were compacted at 7 ± 0.5% air void content. The specimens prepared were 6 in. (150 mm) diameter and 3.75 in. (95 mm) height. The ITS test was performed on three dry specimens and three conditioned specimens. Visual stripping inspection was conducted after the ITS test. Figures 3.1 and 3.2 show the ITS and TSRs for each of the control and RAP mixtures, respectively. Detailed results are tabulated in Appendix B.

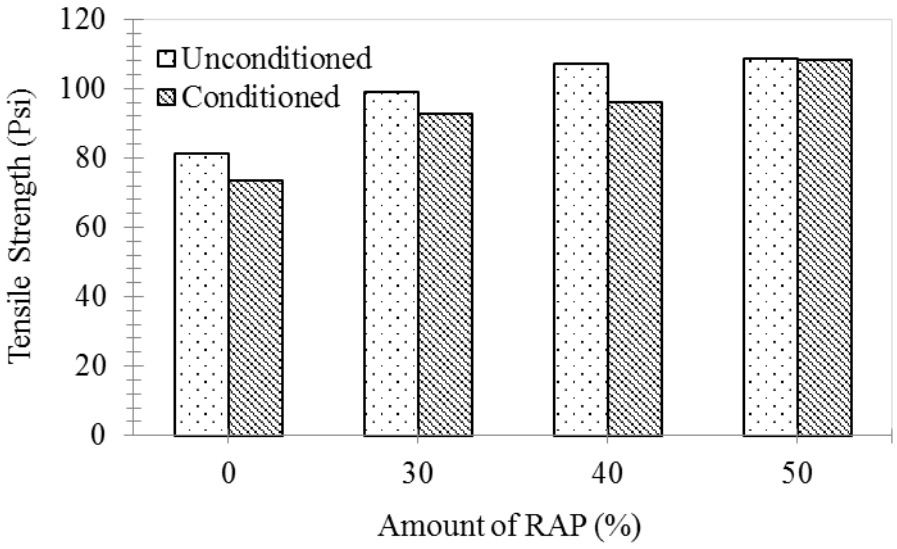

Figure 3.1. Tensile strengths of District 1 conditioned and unconditioned specimens.

All the tested specimens passed IDOT's minimum requirement of 85% TSR. With the exception of 40% recycled mixtures, TSRs increased with an increase in RAP content. This observation was similar to the trend noted in an earlier study by Al-Qadi et al. (2009). One of the factors contributing to the strength increase could be the presence of the aged binder because ITS is a test that is relatively more dependent on asphalt binder.

Visual inspection was carried out on split TSR specimens. The specimens revealed that the stripping susceptibility of mixtures with RAP remained similar to that of the control mixture (0% RAP), with the exception of specimens with 50% RAP—which showed the least resistance to stripping for the coarse aggregate.

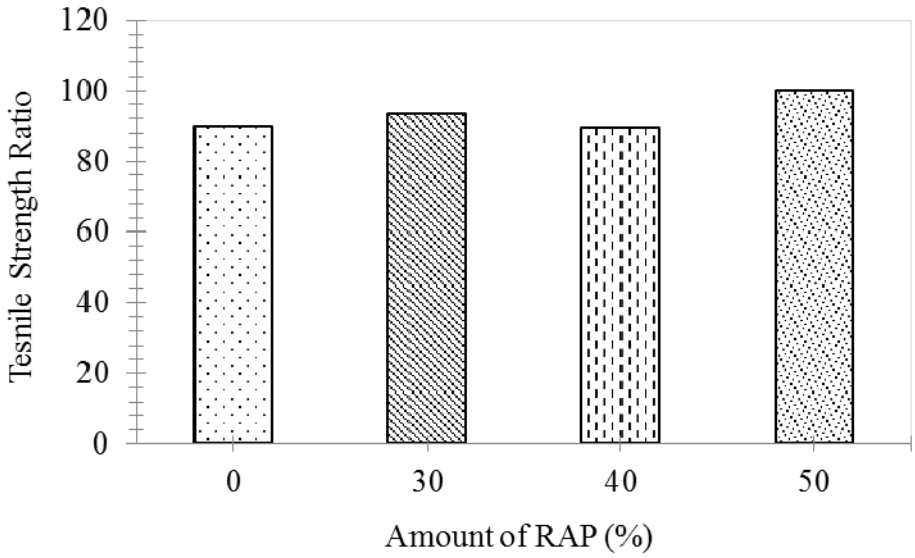

Figure 3.2. Tensile strength ratios (TSRs) for District 1 control and mixtures with RAP.

Table 3.9 shows the stripping rating for mixtures. A rating of 1 indicates no stripping, 2 indicates moderate stripping, and 3 indicates severe stripping. If a RAP used in the asphalt mixture wasn't exposed to moisture damage during its service life, it could strip during a moisture sensitivity test after being recoated with new asphalt binder. On the other hand, if it has been in the field for a long time without moisture damage, it most probably would not strip during the moisture sensitivity test.

Table 3.9. Stripping rating for District 1 control and recycled mixtures.

RAP (%)	0	30	40	50
Dry (coarse/fine)	1/1	1/1	1/1	1/1
Wet (coarse/fine)	2/2	2/2	2/2	3/2

3.3.2 District 5 Asphalt Mix Designs

3.3.2.1 Aggregate Blend and Gradation

Apparent gradations obtained after fractionating the District 5 RAP are shown in Table 3.10. The batches for extraction and G_{mm} were made using the apparent gradation. The specimens were extracted at IDOT's facility in Springfield, and the values obtained were used to determine the G_{sb} of the RAP aggregates, utilizing Equation 3.1.

Table 3.10. Apparent and actual gradations of District 5 RAP aggregate.

Sieve	Retained on each sieve (%)		Passing (%)	
	Apparent Gradation		Extracted/Actual Gradation	
	+3/8-in. RAP	–3/8-in. RAP	+3/8-in. RAP	–3/8-in. RAP
3/4 in.	3.4	—	99.3	100.0
1/2 in.	17.6	—	90.8	100.0
3/8 in.	22.0	1.5	78.6	99.3
No. 4	37.4	33.2	39.0	71.7
No. 8	9.7	29.4	26.5	48.6
No. 16	—	—	19.1	32.6
No. 30	6.1	28.7	14.8	24.2
No. 50	—		10.7	17.2
No. 100	—		7.7	12.7
No. 200	—		6.0	10.1
Pan	3.9	7.2	—	—
Binder content (%)	—	—	3.9	5.5

The extracted RAP aggregate gradations are also shown in Table 3.10. As discussed previously, the apparent gradation was used throughout the study for batching the samples in order to determine the extracted gradations shown in Table 3.10. Table 3.11 shows the design aggregate blend for District 5 control mix and for mixtures with RAP.

Table 3.11. Design aggregate blend for District 5 asphalt mix designs.

Sieve	Control	30% RAP	40% RAP	50% RAP
1 in.	100.0	100.0	100.0	100.0
3/4 in.	93.1	93.7	94.4	95.2
1/2 in.	76.6	77.6	79.3	81.2
3/8 in.	67.8	68.3	69.7	71.4
No. 4	38.7	39.5	39.3	39.9
No. 8	21.7	22.4	22.3	23.3
No. 16	13.6	14.6	14.8	15.6
No. 30	9.0	10.6	11.0	11.7
No. 50	6.8	7.9	8.2	8.6
No. 100	5.6	6.3	6.4	6.6
No. 200	4.9	5.3	5.4	5.4

3.3.2.2 Mix Design and Volumetrics

The District 5 control mix and RAP mixes were developed using PG 64-22, in accordance with IDOT specifications and using the Bailey method of aggregate packing. The District 5 control mix has already been used in the field. Slight modifications were applied to achieve the required volumetrics in the laboratory. The stockpile percentages and volumetrics of all District 5 mix designs are shown in Table 3.12. Again, it is important to note that similar VMA has been achieved for all the mix designs. Since shape, texture, and strength of the RAP aggregates are usually different than those for virgin aggregates, matching the aggregate gradation of the RAP mixes to that of the control mixture does not provide the desired VMA. The targeted VMA were achieved by slightly modifying the gradation of the trial fractionated RAP blends. The Bailey method was used, which reduced the number of trials to reach the desired volumetrics (detailed volumetrics of the final trial for each mix design are presented in Appendix A).

Table 3.12. Stockpile percentages and volumetrics of District 5 asphalt mix designs.

	Control	30% RAP	40% RAP	50% RAP
CM11 (%)	38.5	34.5	31.2	25.6
CM16 (%)	37.9	15.5	12.5	9.5
FM20 (%)	21.6	9.0	6.5	4.8
FM22 (%)	—	10.0	9.0	9.6
+3/8-in. RAP (%)	—	15.0	25.0	35.0
–3/8-in. RAP (%)	—	15.0	15.0	15.0
Mineral Filler (%)	2.0	1.0	0.8	0.2
Binder Content (%)	5.2	5.2	5.2	5.2
Air Voids (%)	4.0	4.0	4.0	4.0
VMA (%)	13.8	13.8	13.6	13.5
VFA (%)	71.0	71.0	70.8	70.4

Table 3.13 presents the design mix formula (DMF) and the extracted aggregate gradation of G_{mm} or separate extraction samples for 30%, 40%, and 50% recycled mixtures. Table 3.14 shows the actual percentages of virgin and RAP asphalt binders and new and RAP aggregates for various asphalt mixtures.

Table 3.13. Comparison between target and actual aggregate gradations for District 5 mixtures.

Sieve	30% RAP		40% RAP		50% RAP	
	DMF	Extracted	DMF	Extracted	DMF	Extracted
1 in.	100	100.0	100.0	100	100.0	100.0
3/4 in.	93.7	94.9	94.4	93.8	95.2	95.5
1/2 in.	77.6	78.4	79.3	78.4	81.2	80.9
3/8 in.	68.3	68.0	69.7	69.1	71.4	71.5
No. 4	39.5	39.4	39.3	39.2	39.9	40.1
No. 8	22.4	22.2	22.3	22.4	23.3	23.2
No. 16	14.6	15.1	14.8	14.8	15.6	15.4
No. 30	10.6	10.5	11.0	11.0	11.7	11.7
No. 50	7.9	7.7	8.2	7.9	8.6	8.6
No. 100	6.3	6.3	6.4	6.3	6.6	6.7
No. 200	5.3	5.3	5.4	5.3	5.4	5.6

Table 3.14. Asphalt binder and aggregate contributions from RAP for District 5 mixtures.

Mix Type	Binder Contribution (%)			Aggregate Contribution (%)		
	Virgin Binder	RAP Binder	Total	New Aggregate	RAP Aggregate	Total
Control Mix	100.0	0.0	100.0	100.0	0.0	100.0
30% RAP Mix	73.9	26.1	100.0	71.0	29.0	100.0
40% RAP Mix	66.6	33.4	100.0	61.1	38.9	100.0
50% RAP Mix	59.2	40.8	100.0	51.1	48.9	100.0

3.3.2.3 Moisture Susceptibility Test

The moisture susceptibility of District 5 RAP mixtures was also evaluated. Figures 3.3 and 3.4 depict the ITS and TSRs of tested mixtures (detailed results are tabulated in Appendix B). An increase in tensile strength with an increase in RAP content was found for both conditioned and unconditioned specimens.

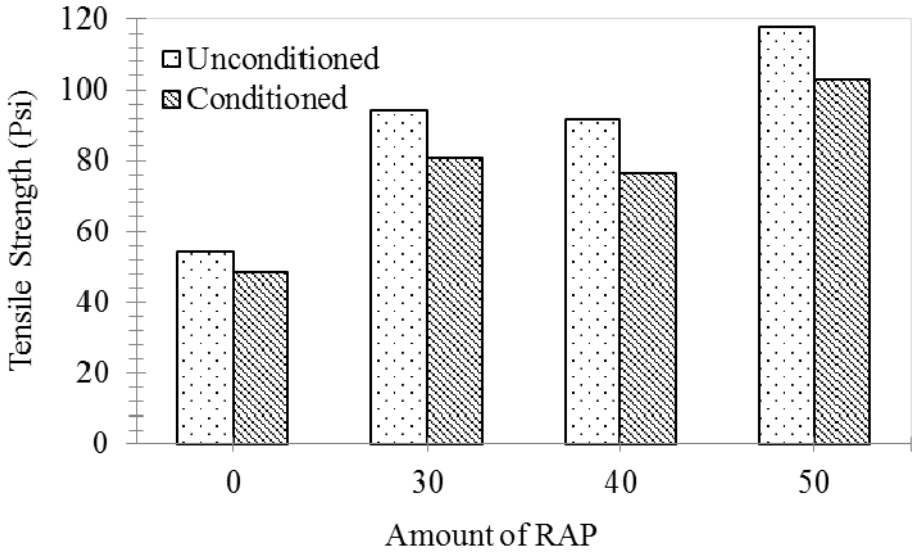

Figure 3.3. Tensile strengths of District 5 conditioned and unconditioned specimens.

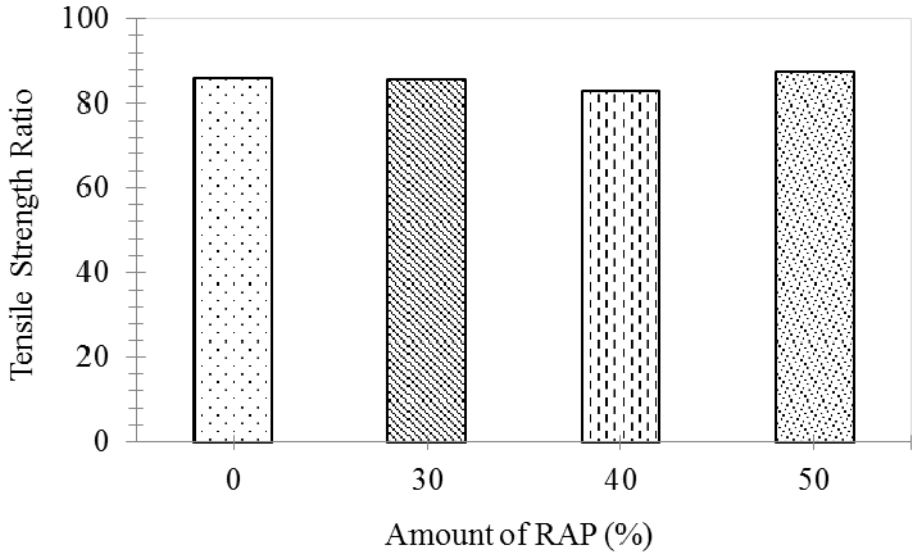

Figure 3.4. Tensile strength ratios (TSRs) for District 5 control and mixtures with RAP.

District 5 mixtures exhibited reductions in TSR values. The visual evaluation did not show any significant stripping, however. Table 3.15 presents the stripping ratings for District 5 mixtures. With the exception of the mixture with 40% RAP, all other mixtures passed IDOT's minimum criterion of 85% TSR. It is important to note that the District 5

control mixture is known to be moisture susceptible (tensile strength less than 60 psi (413.7 kPa), minimum threshold set by IDOT), which is evident in mixtures with RAP as well. Unlike the District 1 mixes, the addition of RAP did not bring any improvement in the TSR values, although an increase in the tensile strength was observed.

Table 3.15. Stripping rating for District 5 control and mixtures with RAP.

RAP (%)	0	30	40	50
Dry (coarse/fine)	1/1	1/1	1/1	1/1
Wet (coarse/fine)	1/2	2/2	2/1	2/2

3.4 Summary and Remarks

Eight 3/4-in. (19-mm) NMAS binder mix designs (N_{des} = 90) were developed for both material sources. The mix designs included a control mix with 0% RAP and mixtures with 30%, 40%, and 50% RAP for each district. The Bailey method of aggregate packing was used to design all the asphalt job mix formulae. Very similar and acceptable volumetrics were achieved for all District 1 and District 5 mix designs. The key reason behind achieving similar volumetrics was to gain control over gradation, which was accomplished by fractionating the RAP material similar to virgin aggregate. The number of trials required to achieve the required VMA was greatly reduced with the help of Bailey estimation procedure. Apart from a few exceptions, tensile strengths and TSRs of the asphalt mixtures increased as RAP increased. Almost all of the control and RAP mixtures passed IDOT's minimum TSR criterion of 85%. Only District 5's control mix and mix with 40% RAP failed to pass the minimum tensile strength and minimum TSR criteria, respectively. It is worth mentioning here that G_{sb} value was used for each of the RAPs, not a G_{se} value, to determine VMA.

Based on the findings of this chapter, it can be concluded with confidence that it is possible to design high-quality, asphalt mixtures with high RAP that meet the desired volumetrics. It is important to show in the laboratory that good volumetrics are achievable with RAP materials. Being able to reproduce these volumetrics in the field is a function of several factors, including but not limited to: a) accuracy of the original mix design, b) the similarities or dissimilarities between the design and the asphalt plant materials (e.g. specific gravities, gradation, shape, texture, etc.), c) consistency of the plant material, and d) change in volumetrics of the plant mix due to shape and texture

change in aggregates during the plant operation.

Next chapter details the performance tests conducted on the prepared mixtures.

CHAPTER 4

LABORATORY PERFORMANCE OF RECYCLED ASPHALT MIXTURES

4.1 Introduction

Traffic loading as well as aging of the asphalt binder lead to deterioration of pavement and significantly affect pavement performance. After pavement is removed from the field, RAP materials age even further during the stockpiling process due to the exposure to air. Moreover, when RAP is added to asphalt concrete, the aged binder in the RAP mixes to some unknown degree with the virgin binder. This produces a composite effective binder system with unknown material properties and, hence, unpredictable pavement performance.

As Chapter 2 described in detail, the effect of adding RAP on asphalt concrete laboratory performance has been studied by many researchers. It has been shown that asphalt mixtures with RAP show higher resistance to permanent deformation; whereas, the most common downside of using RAP is an increased vulnerability of asphalt mixtures to thermal cracking. As discussed in Chapter 3, however, achieving volumetrics for the designed asphalt mixtures makes the current study stand out among contemporary studies on RAP. Excluding the variable of the mixture's volumetrics from the equation ensured that laboratory performance of mixtures with high RAP content is based solely on their mechanical properties. The laboratory testing suite used in this study emphasized characterizing and evaluating the stability and durability characteristics of the prepared recycled mixtures. The following sections in this chapter describe the tests conducted. The results are analyzed and discussed in this chapter.

4.2 Dynamic (Complex) Modulus Test

Complex modulus (E^*) describes the modulus characteristics of asphalt concrete as a function of sinusoidal loading frequency and temperature. E^* is a fundamental linear viscoelastic material property (in compression) and is used in the *Mechanistic Empirical*

Pavement Design Guide (MEPDG) as a primary material input for pavement asphalt concrete layer thickness design. The so-called dynamic modulus is the amplitude of the E^* and is determined by calculating the ratio of peak stress to strain amplitudes from the cyclic test. In viscoelastic materials, strain lags stress by a phase lag, known as phase angle (δ). Purely viscous materials have a phase angle of 90 degrees, whereas, in purely elastic materials, strains and stresses are in phase and have a phase angle of 0 degree.

The E^* test was conducted on specimens from both material sources. Sixty test specimens were fabricated based on the eight asphalt mix designs (i.e., mixes with 0%, 30%, 40%, and 50% RAP for both District 1 and District 5). Three binder types (PG 64-22, PG 58-22, and PG 58-28) were used. Specimens were compacted in the SuperPave Gyratory Compactor (SGC) to obtain 7.0 ± 0.5% air void content level. SGC samples were then cored and cut to obtain specimens for E^* tests. The tests were conducted at various frequencies and temperatures in accordance with AASHTO TP 62 specifications. Dynamic loading was adjusted to obtain an axial deformation of 50 microstrains. The matrix for the E^* tests is presented in Table 4.1.

Table 4.1. E^* testing matrix for each material source.

Temperatures (ºC /ºF)	RAP (%)				Total
	0	30	40	50	
–10 / 14	3[1]	9[2]	9	9	30
4 / 39	3	9	9	9	30
21 / 70	3	9	9	9	30
38 / 100	3	9	9	9	30
54 / 129	3	9	9	9	30
Total	15	45	45	45	150

[1]The same three samples were tested at all temperatures and at the following frequencies: 0.1, 1, 5, 10, 25 Hz
[2]Three test sets (no binder bump, single bump, double bump)

The complex modulus test results are presented in master curves, which were constructed using the time–temperature superposition principle at a temperature of 70ºF (21ºC). The master curves shown in Figure 4.1a illustrate the effect of adding RAP to mixes prepared with a base binder (PG 64-22). An increase in the modulus values was observed when RAP was added. Given that stringent quality control for aggregate gradation and volumetrics was imposed throughout the study, the increase in modulus

values can only be attributed to stiffer RAP binder.

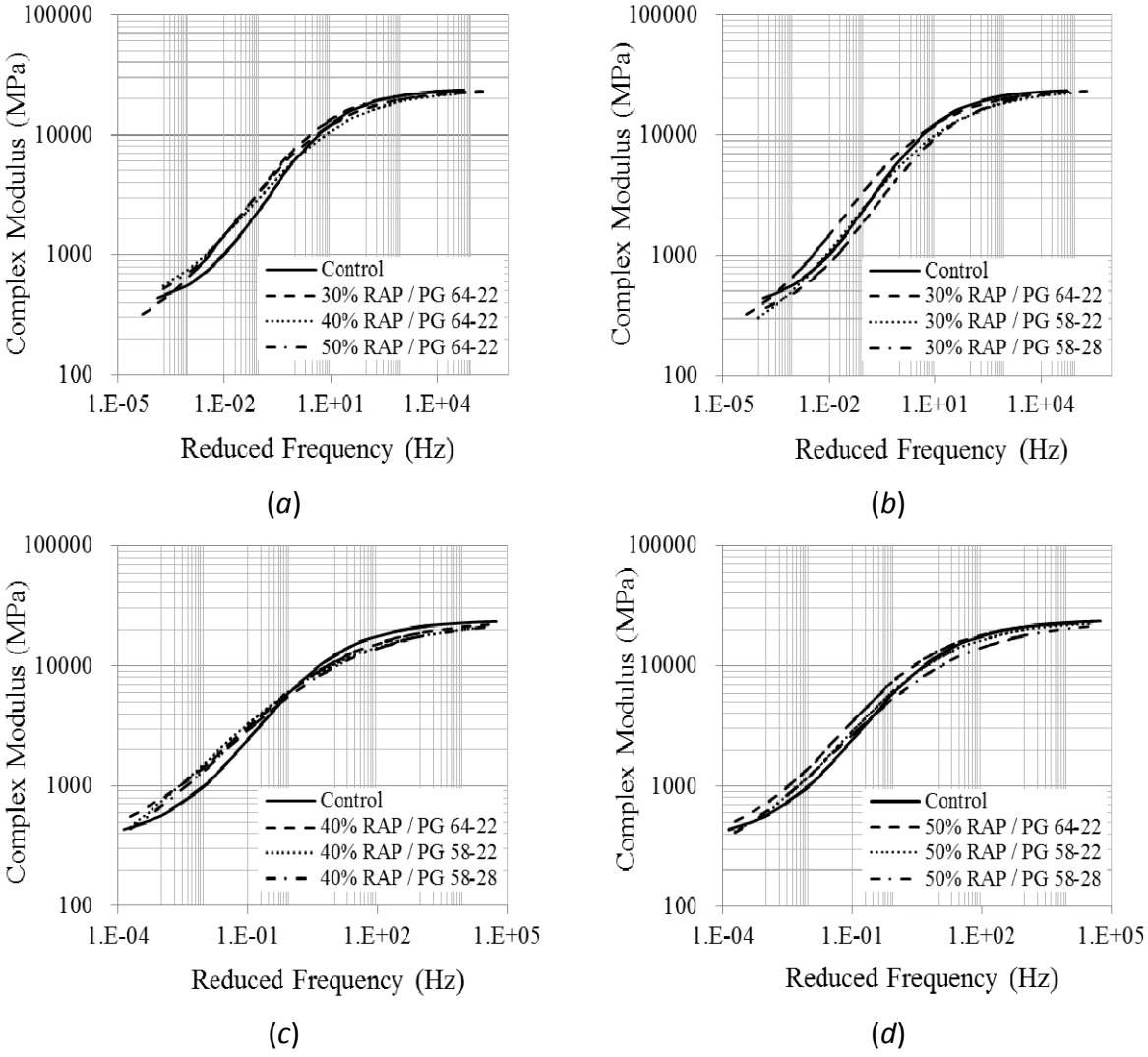

Figure 4.1. Master curves for District 1 asphalt mixtures: (a) RAP effect; (b) binder grade bumping effect on 30% RAP mix; (c) binder grade bumping effect on 40% RAP mix; and (d) binder grade effect on 50% RAP mix.

The control blend (0% RAP) had the lowest complex modulus over the reduced frequency. The 30% recycled mix showed an increase in the stiffness at both high and low frequencies. The 40% RAP showed inconsistent behavior: a higher modulus at a low frequency (high temperature) and a lower modulus at a high frequency (low temperature). The 50% RAP mixes consistently showed higher modulus values throughout the frequency spectrum.

The effect of softer binders was evaluated for the recycled mixtures. Figure 4.1b

shows that 30% RAP with the base binder PG 64-22 had a slightly higher modulus than the control mixture. While the complex modulus of the 30% RAP mix with PG 58-22 decreased to or below the modulus of the control mixtures, the lowest modulus values were obtained when double-bumped binder (PG 58-28) was used.

The 40% recycled mix showed some erratic behavior, as illustrated in Figure 4.1c. The control mix (0% RAP) had the lowest modulus at a low frequency (high temperature) but had the highest modulus at a high frequency. Although the modulus at a low frequency followed the expected trend, it showed an opposite trend on the other end of the curve. Figure 4.1d shows a considerable decrease in modulus for 50% recycled mix using PG 58-22 but no significant effect resulted from the use of double-grade bumping. The binder-grade bumping was found to be effective in reducing the moduli of mixtures with RAP to the moduli of the control mixtures; and in some cases lower.

Overall, it is evident from the complex modulus test results that RAP increases the modulus values of the asphalt concrete due to the use of aged binder, especially at high temperatures. Although, the effect of single and double binder-grade bumping was visible from the master curves, statistical analyses were conducted on complex modulus data to evaluate whether the tested mixtures were statistically different from each other.

A multiple-comparison procedure, Tukey's W procedure, was performed in conjunction with analysis of variance (ANOVA) to determine which means are significantly different from each other. Two population means are declared different if the difference between their sample means is greater than W, where W is dependent on the number of observations in each sample, degrees of freedom, and q, which is the upper-tail critical value of the Studentized range distribution (Ott and Longnecker 2010). All the analyses were completed using Statistical Analysis Software (SAS) v9.2. An example of an output file is presented at the end of Appendix B.

Different asphalt mixtures and asphalt binder combinations were grouped and analyzed at two frequency levels (0.1 and 10 Hz) and three temperatures –10ºC (14ºF), 21ºC (70ºF), and 54ºC (129.2ºF) for District 1 and District 5 mixtures. The alpha value used was 0.05. The following are the findings for District 1:

- When all the mixtures made with the base binder (PG 64-22) were grouped, none of the modulus values of recycled mixtures were significantly different

from the control mixture at any combination of frequency and temperature. This implies that the stiffening effect of RAP on District 1 asphalt mixture is not evident from *E** results.

- To quantify the effect of binder-grade bumping, the control and 30% recycled mixtures were grouped. None of the 30% recycled mixtures using different binders was significantly different from the control mixture. The 30% recycled mix and PG 58-28 was significantly different (softer) compared to 30% recycled mixtures using PG 64-22 at 0.1 Hz and 21ºC (70ºF). At 10 Hz and 54ºC (129.2ºF), the mixtures with PG 58-22 and PG 58-28 were significantly different (softer) than the 30% recycled mix and PG 64-22. This clearly shows the effect of binder-grade bumping. At –10ºC (14ºF), all mixtures behaved similarly, and no mix was significantly different from any other mix. It was noted that the effect of double bumping the binder was evident at intermediate temperatures, while at a high temperature, which is influenced by the high PG limit, the effect is similar to when a single-bump grade binder was used.
- The effect of binder-grade bumping on 40% recycled mix was analyzed. None of the 40% recycled mixtures with different binders was significantly different from the control mixture. The mixtures with PG 58-28, though, were significantly different from the mixtures with PG 58-22 only at 10 Hz and 54ºC (129.2ºF).
- When control and 50% recycled mixtures were grouped together, none of the mixtures was significantly different from others at any temperature and frequency combination.

In summary, District 1 mixtures with RAP performed on par with the control mixture, based on *E** test results. Although adding RAP stiffens asphalt mixtures at high temperatures and improves complex modulus, steps should be taken to avoid possible block cracking due to increased asphalt binder stiffness. On the other hand, this test is insensitive at low temperatures because specimens are loaded in compression, while thermal cracking occurs in tension.

The E^* master curves were also generated for District 5 mixtures. At low frequencies (or high temperatures), mixtures with RAP exhibited stiffer behavior (i.e., higher moduli) compared to the control mix. However, it is difficult to differentiate the mixtures with RAP from each other. As shown by the master curves in Figure 4.2a, mixtures with 30%, 40%, and 50% RAP showed similar behaviors. The 30% recycled mix (the master curves in Figure 4.2b) showed a decrease in moduli values with softer binder grades.

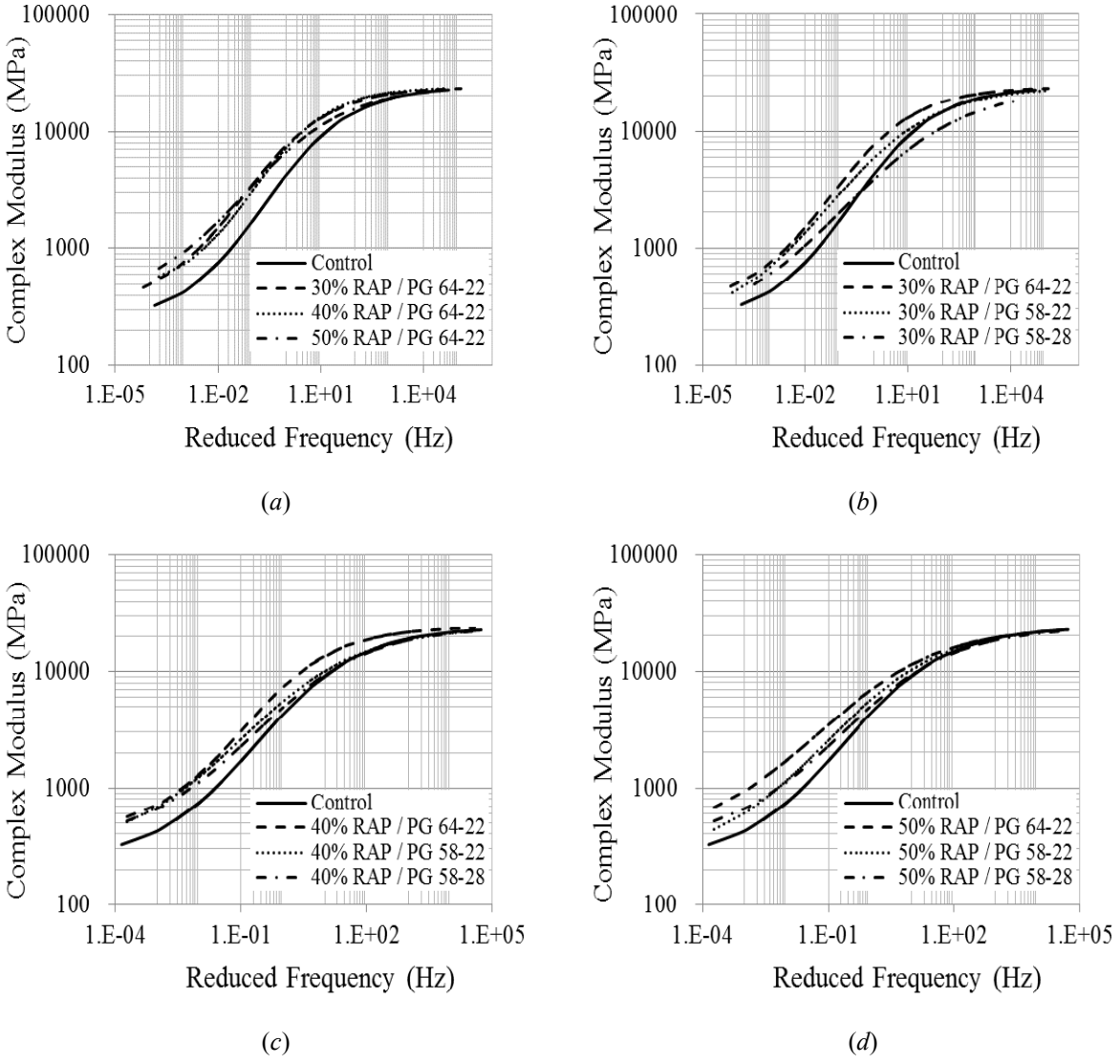

Figure 4.2. Master curves for District 5 asphalt mixtures: (a) RAP effect; (b) binder grade bumping effect on 30% RAP mix; (c) binder grade bumping effect on 40% RAP mix; and (d) binder grade effect on 50% RAP mix.

For 40% recycled mixtures, no significant effect of binder-grade bumping was observed on moduli, as shown in Figure 4.2c. For 50% recycled mixtures, single and double binder-grade bumping showed similar amount of reduction in the moduli (Figure 4.2d).

To cover a wide range of temperatures and frequencies, statistical analyses were performed on District 5 complex modulus data at 0.1 and 10 Hz at temperatures of –10ºC (14ºF), 21ºC (70ºF), and 54ºC (129.2ºF). The findings from the statistical analyses were as follows:

- At 0.1 Hz and 21ºC (70ºF) and 10 Hz and 54ºC (129.2ºF), all recycled mixtures with the base binder were significantly different from the control mixture, whereas no difference was found among the recycled mixtures. At 10 Hz and 21ºC (70ºF), the control mixture was significantly different from the 30% and 40% recycled mixtures. No significant difference between the recycled mixtures and the control mixture was found at –10ºC (14ºF).
- The effect of binder bumping was analyzed by grouping the control mix with all of the 30% recycled mixtures:
  - At 0.1 Hz and 21ºC (70ºF), the control mix was significantly different (softer) than the 30% recycled mix with PG 64-22 and PG 58-22. The double-bumped mixture (30% RAP with PG 58-28) was not significantly different from the control mix. The 30% recycled mix with PG 58-28 was significantly different from the 30% recycled mix with PG 64-22.
  - At –10ºC (14ºF), at both 0.1 and 10 Hz, mixture with PG 58-28 were significantly different (softer) than the control mix and 30% recycled mix with PG 64-22, indicating that double bumping reduced the modulus and made those mixtures softer than the control mix.
  - At 10 Hz and 21ºC (70ºF), both the control and the 30% recycled mix and PG 58-28 were significantly different from the 30% recycled mix and PG 64-22.
  - At 10 Hz and 54ºC (129.2ºF), the control was significantly different from the 30% recycled mixtures with PG 64-22.

- For 40% recycled mix, the control mix was significantly different from the rest of the mixes at 0.1 Hz and 21ºC (70ºF). At 10 Hz at both 21ºC (70ºF) and 54ºC (129.2ºF), the control mix was significantly different from 40% recycled mix with PG 64-22. The effect of binder bumping is prominent at higher temperatures, but at –10ºC (14ºF), none of the mixtures was significantly different from others.
- For 50% recycled mix, at 0.1 Hz and 21ºC (70ºF), the control mix was significantly different (softer) from the rest of the mixes. At 0.1 Hz and 54ºC (129.2ºF), the control mix was significantly different from 50% recycled mix. At 10 Hz, the only significant difference between the control and the 50% recycled mix using PG 64-22 was shown at 54ºC (129.2ºF). Since the 50% recycled mix with PG 58-22 and PG 58-28 were not significantly different from the control mix, it was concluded that binder-grade bumping was effective to soften the mix. At –10ºC (14ºF), none of the mixtures was significantly different than others. This could be related to testing temperature; testing at further low temperature could distinguish between them.

4.3 Flow Number (FN) Test

Flow number test is used as a performance indicator for permanent deformation resistance of asphalt mixtures. It simulates different loading conditions by placing repetitive loading on a cylindrical sample. Higher flow number indicates higher resistance to permanent deformation (rutting). The flow number test was performed at 58ºC (136ºF), a total deviator stress of 200 kPa (29 psi) and a frequency of 10 Hz. The test was conducted until the completion of 10,000 cycles or 5% permanent strain, whichever occurred first. The flow number is usually considered at the cycle number where the strain rate starts increasing with loading cycle. A specimen at the end of the test is shown in Figure 4.3.

Figure 4.3. A specimen at the conclusion of a flow number test.

Figure 4.4 shows the average of three tests for each mix and binder type combination. The results reveal a consistent trend of increase in the flow number with an increase in RAP amount used in the asphalt mixture. Since a higher flow number implies higher resistance to permanent deformation, 50% recycled mix showed the highest resistance to rutting, followed by the mixtures with 40% and 30% RAP and the control mix.

The effect of grade bumping is also evident in Figure 4.4. Although the effect of softer binder is obvious and consistent in the flow number of the mixtures with RAP, the effect diminishes with an increase in RAP percentage in the mix. While the flow number of 30% recycled mix having PG 58-28 is 57.5% less than that with 30% RAP and PG 64-22, there is only an 11% reduction in the flow number of 50% recycled mix due to double-binder-grade bumping. Tukey's W procedure was performed on the flow data, and the main findings are as follows:

- To identify the effect of RAP addition, the control and mixtures with RAP using base binder PG 64-22 were grouped. It was found that 30% and 40% recycled mixtures behaved similarly to the control mixture. The control mixture was found to be significantly different from 50% recycled mix.

- When data for the control mixture and 30% recycled mixtures were grouped in order to see the effect of binder-grade bumping, no mix was found to be significantly different from another.
- For 40% recycled mixtures, the control mixture was significantly different (softer) from 40% recycled mixtures with PG 64-22. When 40% recycled mix and different binder types were grouped with the control mixture, the effect of binder-grade bumping was evident. The control mixture was not significantly different from 40% recycled mix prepared with PG 58-22 and PG 58-28.
- When data for the control mixture and 50% recycled mix were grouped, the control mixture was significantly different from all mixtures with RAP, irrespective of the binder used.

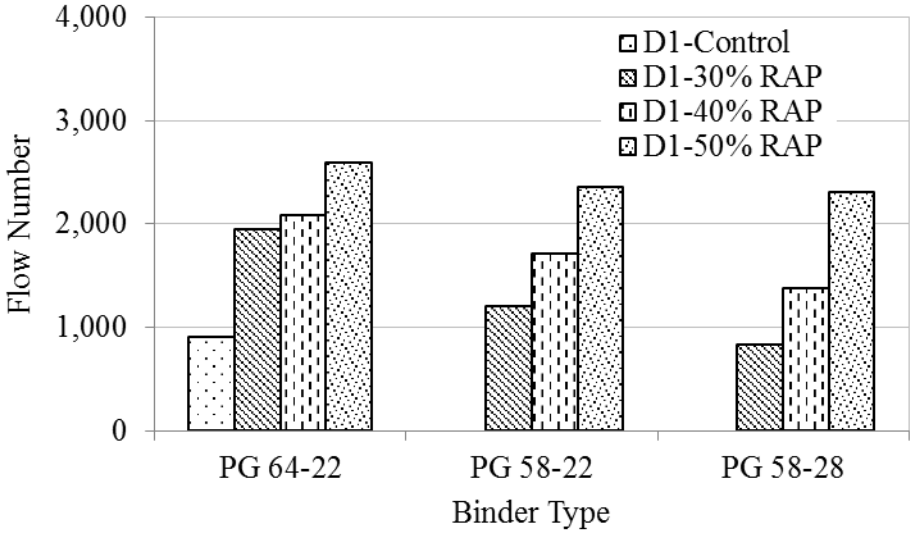

Figure 4.4. Flow number test results, District 1.

Flow number results for District 5 mixtures are shown in Figure 4.5. The effect of increasing RAP is obvious in mixes using the base binder grade (PG 64-22). An increase in the flow number was observed as RAP content in asphalt mixture increased. When softer binder was used in mixtures with RAP, the F_N was reduced. The reduction in the flow number of mixtures with RAP was more pronounced when double-bumped binder was used. Overall, the trends are clear and consistent enough to show the effect of RAP and binder bumping.

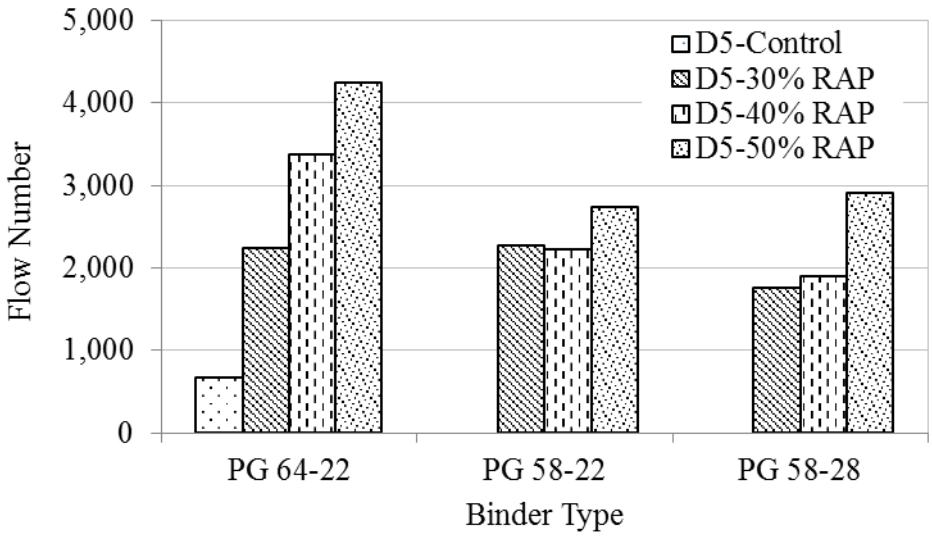

Figure 4.5. Flow number test results, District 5.

Statistical analyses were performed on District 5 flow number data, and the key findings are as follows:

- When the control and the recycled mixtures having the base binder (PG 64-22) were grouped to evaluate the effect of RAP on flow number, the control mix was significantly different than 40% and 50% recycled mixtures.
- With regard to the binder-bumping effect on 30% recycled mix, when the control and the 30% recycled mix data were grouped, no mix was significantly different than another.
- When the control and the 40% RAP data were grouped, the control mix was significantly different (softer) than 40% recycled mix using the base binder. The control mix was not different from 40% recycled mix when using PG 58-22 or PG 58-28, thereby indicating the effect of binder bumping.
- When the control and the 50% recycled mix were grouped, the control mix was significantly different than all the RAP mixtures, irrespective of the binder used.

In summary, as RAP content increases, the flow number increases because the asphalt mixture becomes stiffer. The single-bump binder grade worked as expected and reduced the stiffness of the asphalt mixture. The stiffness could be reduced further when

using a binder with a lower high PG limit. Double bumping the binder grade can further soften the asphalt mixture; however, it would be limited in this case because the test was conducted at a high temperature, 136.4ºF (58ºC).

4.4 Fatigue Testing

4.4.1 Beam Fatigue Test

The flexural beam fatigue test is used to characterize the fatigue behavior of asphalt mixture at intermediate pavement operating temperatures. The test is believed to simulate the fatigue life of asphalt pavements as a result of vehicular loading. In this study, a strain-controlled four-point beam fatigue test was conducted at 68ºF (20ºC) at levels of 1000, 800, 700, 500, 400, and 300 microstrains. A total of 120 beams were tested utilizing the eight mixtures from the two material and RAP sources (Districts 1 and 5) and three different asphalt binders. The failure criterion used in the study was the traditional 50% reduction in initial stiffness (i.e., the initial stiffness is the stiffness at the 50th load cycle).

A rolling wheel compactor was used to compact the asphalt mixture beams to 14.8 in × 4.956 in × 2.953 in (376 mm × 125.9 mm ×75 mm). The weight of the mixtures was adjusted to achieve 7% air void content. Each compacted beam was cut into two smaller fatigue beams of 14.8 in × 2.48 in × 1.968 in (376 mm × 63 mm × 50 mm). Table 4.2 presents the beam fatigue test matrix for this study.

Table 4.2. Beam fatigue testing matrix for each material source.

Strain Level (μ-strains)	Control	30% RAP	40% RAP	50% RAP
1000	1	3*	3	3
800	1	3	3	3
700	1	3	3	3
500	1	3	3	3
400	1	3	3	3
300	1	3	3	3
Total	6	18	18	18

*Three beams (no binder bump, single bump, double bump)

Equation 4.1 shows a typical relationship between the tensile strain at the bottom of the asphalt concrete layer (ε_o) and the number of load applications to crack appearance

in the pavement (N_f).

$$N_f = K_1\left(\frac{1}{\varepsilon_0}\right)^{K_2} \tag{4.1}$$

where K_1 and K_2 are the intercept and slope of a fatigue curve, respectively, and are dependent on the composition and properties of the asphalt mixture. The higher the absolute value of K_2, the better the fatigue behavior of the mix. Typical fatigue curves for District 1 asphalt mixture are shown in Figure 4.6. The values of flexural stiffness and K_2, obtained from the District 1 asphalt mixture fatigue testing, are presented in Table 4.3. In general, asphalt mixture flexure stiffness increased as RAP content in the mixture increased. The typical average K_2 value for Illinois asphalt mixtures is 4.5 (Carpenter 2006), but IDOT uses a K_2 value of 3.5 for design purposes. Although the District 1 control mixture apparently performed acceptably, its fatigue behavior is at the lower end. Detailed results are presented in Appendix B.

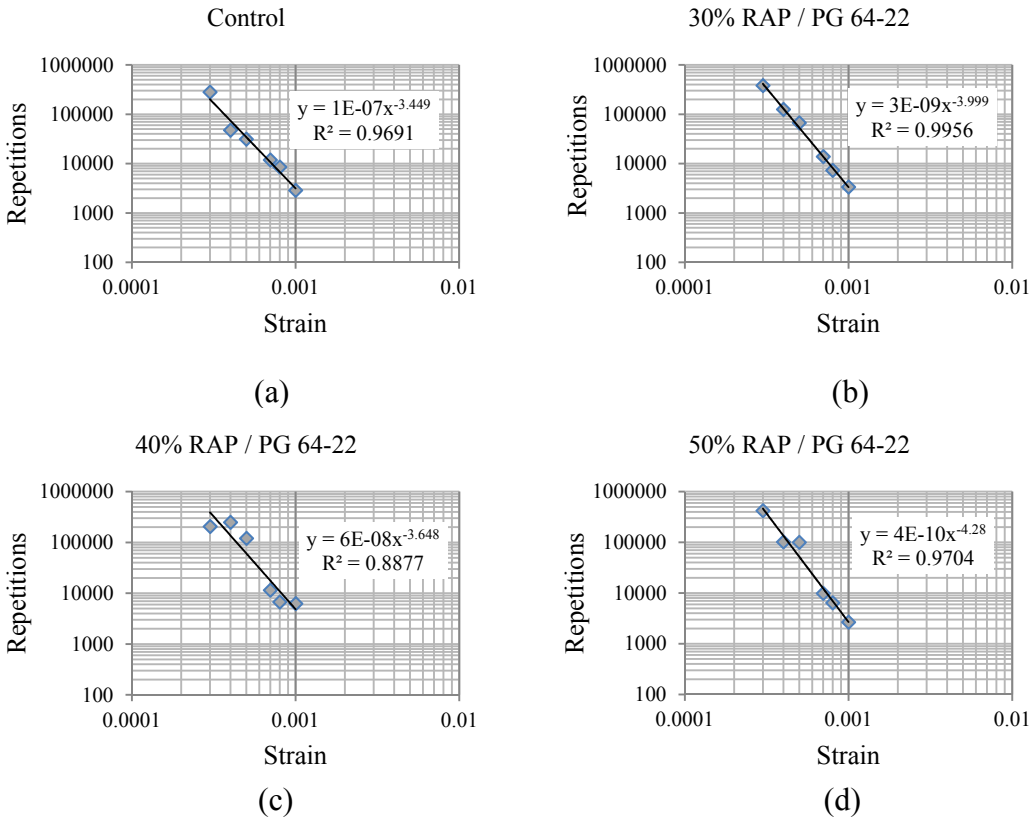

Figure 4.6. Fatigue curves for District 1: (a) control mix; (b) 30% recycled mix; (c) 40% recycled mix; and (d) 50% recycled mix.

The effect of RAP content was evaluated for asphalt mixture with each binder type. For PG 64-22, it was observed that 40% recycled mix showed insignificant changes in K_2. However, the mixtures with 30% and 50% RAP had an improved K_2 value. The flexural modulus (E_f) values showed an increase of approximately 22% when the RAP content increased from 0% to 30%. However, the flexural modulus did not change as the RAP content increased from 30% to 50%. Examining the effect of RAP when PG 58-22 binder was used, it was noted that the 30% recycled mix showed a significant increase in K_2 over the control mixture, while the 40% RAP showed moderate improvement. The 50% recycled mix had the most significant improvement In addition, the flexural modulus showed an increase as RAP content increased from 30% to 50%.

The effect of RAP content on asphalt mixture with PG 58-28 was also examined relative to the control mix. The effect of RAP on mixtures' flexural modulus was evident as it proportionally increased with RAP. For 30% recycled mix, the K_2 value was significantly improved, possibly due to the significantly lower flexural modulus (at constant strain, low modulus improves fatigue resistance). However, for mixtures with RAP contents of 40% and 50%, K_2 values dropped significantly relative to single bumping yet remained greater than the control mix value. This finding indicates that a double-grade binder bump does not provide improvement over a single bump, but it does provide slight improvement over the control mixture.

Table 4.3. Fatigue beam test results for District 1 mixtures.

Sample	E_f(MPa)	K_2	E^*[1] (MPa)	(E_f/E^*)
0% RAP-PG 64-22	3,500	3.45	10,902	0.3
30% RAP-PG 64-22	4,305	4.00	10,802	0.4
30% RAP-PG 58-22	4,042	4.42	9,160	0.4
30% RAP-PG 58-28	2,892	4.34	8,000	0.4
40% RAP-PG 64-22	3,492	3.65	9,010	0.4
40% RAP-PG 58-22	4,285	3.84	9,813	0.4
40% RAP-PG 58-28	3,683	3.56	7,490	0.5
50% RAP-PG 64-22	4,256	4.28	11,477	0.4
50% RAP-PG 58-22	4,495	4.98	9,635	0.5
50% RAP-PG 58-28	3,775	3.89	8,870	0.4

[1] Complex Modulus values at 10 Hz and 21°C

The effect of binder bumping on fatigue life of asphalt mixture with the same amount of RAP was evaluated. For 30% recycled mix, binder bumping improved the K_2 values, primarily due to reduction in the modulus. For 40% recycled mix, the double bump appeared to lower the fatigue behavior compared to a single bump. For 50% recycled mix, it was evident that a single bump results in the best fatigue behavior. Although the double bump in binder grade significantly lowered fatigue behavior compared to the single bump, it was still an improvement over the control mixture. This reduction in K_2 value was observed in spite of a significantly lower modulus when the double-bumped binder was used, compared to asphalt mixture with PG 64-22 or PG 58-22. Again, fatigue life is a function of material stiffness (modulus and geometry) and level of strain applied.

Examining the District 5 fatigue data revealed that, similar to District 1 mixtures, a positive effect was observed in fatigue trends when adding RAP. As shown in Table 4.4, K_2 for PG 64-22 values increased as RAP increased up to 40%; the mix with 50% RAP showed a slight decrease in the K_2 value but was still higher than the mix with 30% RAP. Analysis of the effect of RAP on fatigue behavior for the mixtures with the bumped binders (PG 58-22 and PG 58-28) showed that all mixtures with RAP had significant improvement in fatigue behavior. The E_f and K_2 values increased as RAP content increased.

The effect of binder-grade bumping was also evaluated; for single-bumped binder (PG 58-22), the behavior of 30% recycled mix remained approximately the same as that of the mixtures with PG 64-22. The 40% and 50% recycled mixtures, however, showed significant (20%) improvement. Again, the double-bumped binder (PG 58-28) showed a decrease in fatigue behavior relative to the single-bumped binder; the K_2 value for the asphalt mixture with 30% RAP was below the assumed design value (3.5) of typical Illinois mixtures (Carpenter 2006). The double-bumping effect was not that pronounced for 40% and 50% recycled mixtures; there was still a reduction in K_2 values compared to the single bumping results. It is important to note that binder bumping is very effective in restoring the flexural modulus to that of the control mix values. In addition, fatigue testing is performed at normal temperatures, whereas the effect of double bumping is

more pronounced at low temperature.

Tables 4.3 and 4.4 show that the average ratio of flexural to complex modulus values was 0.40 for both District 1 and District 5 materials, which is within the range of the tested materials in Illinois. This indicates that all the mixtures prepared in the study had a good structural mix and consistent composition and were not different from normal virgin mixtures. The tensile behavior, which potentially could be the most negatively impacted by high RAP content, did not show significant difference with respect to normal mixes. These mixes were of similar quality as a virgin mix, and adding RAP did not have a negative impact.

Table 4.4. Fatigue beam test results for District 5 mixtures.

Sample	E_f (MPa)	K_2	E^*[1] (MPa)	(E_f/E^*)
0% RAP-PG 64-22	3,314	3.64	7,477	0.4
30% RAP-PG 64-22	4,327	3.88	11,390	0.4
30% RAP-PG 58-22	3,579	3.80	9,549	0.4
30% RAP-PG 58-28	3,322	3.31	7,222	0.5
40% RAP-PG 64-22	4,864	4.55	11,579	0.4
40% RAP-PG 58-22	4,158	4.42	9,410	0.4
40% RAP-PG 58-28	3,695	4.24	8,964	0.4
50% RAP-PG 64-22	5,089	3.98	9,903	0.5
50% RAP-PG 58-22	4,175	4.78	8,929	0.5
50% RAP-PG 58-28	4,224	4.50	10,071	0.4

[1] Complex Modulus values at 10 Hz and 21°C

Apart from conventional analysis of the fatigue data, which showed dominance of mixtures with RAP over the control mixture, a few more fatigue analysis methods and tests were explored. A relatively newer concept of energy dissipation for determining the fatigue life of asphalt mixtures was proposed by Ghuzlan and Carpenter (2000), Carpenter et al. (2003), and Shen and Carpenter (2005). A ratio of change in dissipated energy between two consecutive loading cycles divided by the dissipated energy of first cycle is termed as ratio of dissipated energy change (RDEC). Plateau value (PV), an almost constant value of RDEC, describes a period where there is a constant percentage of input energy dissipated due to damage accumulation in the specimen (Shihui 2006). The damage in the specimen can be realized as microcrack evolution due to applied loads. Eventually these microcracks coalesce to form a macrocrack identifying the failure

of the specimen, which can be easily recognized in RDEC plots (Figure 4.7).

For a strain-controlled test, the lower the PV, the longer the fatigue life for a specific asphalt mixture (Shen and Carpenter, 2005). Herein, the PV concept was used to characterize the fatigue behavior of asphalt mixtures with RAP. To find PV, first a power law relationship, Ax^s, was used to fit the dissipated energy-Load cycles (DE-LC) curve. The average RDEC and PV per 100 cycles were then calculated using Equations 4.2 and 4.3 (Shihui 2006).

$$RDEC_a = \frac{1-\left(1+\frac{100}{a}\right)^s}{100} \tag{4.2}$$

$$PV = \frac{1-\left(1+\frac{100}{N_{f50}}\right)^s}{100} \tag{4.3}$$

where,

a = load cycle,

N_{f50} = load cycle corresponding to 50% stiffness reduction, and

s = the exponential slope of the power equation for the regressed DE-LC curve.

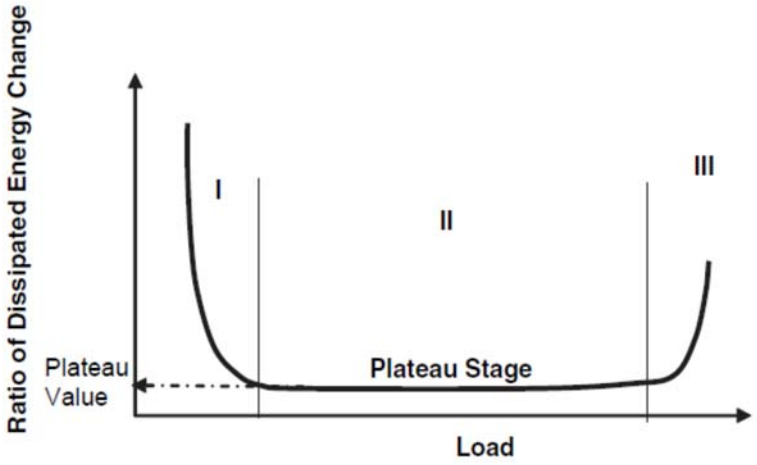

Figure 4.7. Typical dissipated energy plot (Ghuzlan, 2001).

Keeping in mind that strain levels at the bottom of the asphalt layer hover at around 150 to 300 microstrains, a level of 300 microstrains was selected to compare the mixtures. For District 1, PV results followed similar trends to those shown in the

traditional analysis of fatigue data. Apart from the mixture with 40% RAP, which has the highest PV, mixtures with RAP showed lower PVs (i.e., better fatigue behavior than the control mix). The binder grade bumping showed a positive effect on fatigue behavior as well: mixtures with single-bumped binder (PG 58-22) still showed a slight edge over the ones with double-bumped binder (PG 58-28). The double-bumped binder may show its effect at a very low temperature, which was not considered in this study.

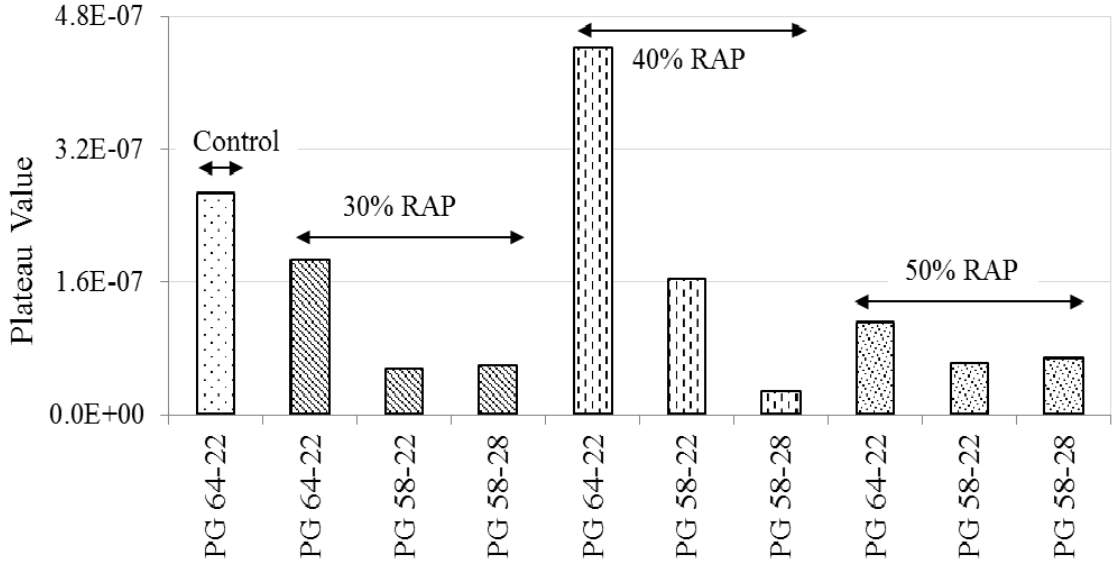

Figure 4.8. Plateau values for District 1 mixtures at 300 microstrains.

For District 5, asphalt mixtures with higher RAP content, with exception of 40% RAP, exhibited an increase in the PV which indicates reduction in their expected fatigue life (Figure 4.9). Although, this prediction contradicts the aforementioned observations using the traditional strain versus N_f approach; it is more intuitive to expect worse fatigue behavior from stiffer asphalt mixtures. The positive effect of binder single bumping is also apparent in Figure 4.9 as shown with the reduction in PVs for mixtures with PG 58-22 as compared to those prepared with PG 64-22. For the mixtures with double-bumped binder (PG 58-28), same trend of reduction in fatigue life was observed relative to the single-bumped binder mixtures. Mixtures with 40% RAP again showed same anomalous results having the least PVs.

Energy based PV method of determining the fatigue behavior showed contrasting results for the two materials. While the fatigue performance improved for District 1

mixtures, it decreased for District 5 mixtures with addition of RAP. Intuitively, a mixture with RAP (stiffer/brittle mixture) should perform worse than a virgin mixture (softer/flexible) in a strain-controlled test; a contrary behavior was observed though from the analysis of the beam fatigue test data for both the material sources using traditional fatigue curve approach and for District 5 material using PV approach. In addition to questions on performing the test under strain control, it can be hypothesized that despite a constant applied actuator strain, on-specimen strains may not remain constant throughout the test. It rather increase with passage of time. So the strain-controlled test run in this study may not be considered a "truly" strain controlled test. For future beam fatigue testing, it is important to collect the on-specimen strain data apart from the actuator strain.

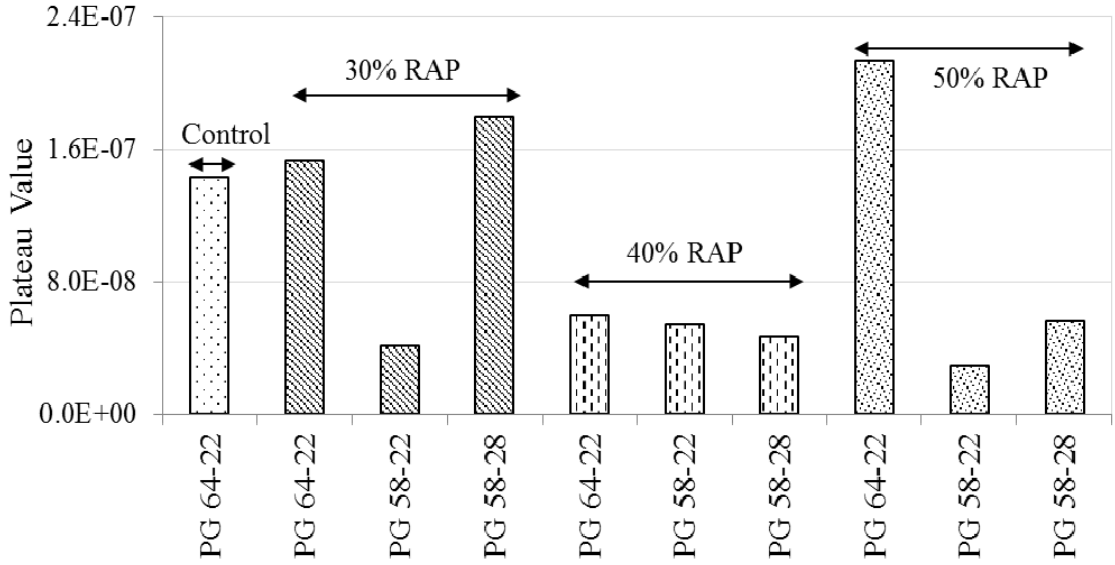

Figure 4.9. Plateau values for District 5 mixtures at 300 microstrains.

4.4.2 Push-Pull Fatigue Test

Push-pull (compression-tension) fatigue test assess the fatigue characteristics of asphalt mixtures using viscoelastic continuum damage (VECD) theories. The test is conducted under cyclic pure tensile and compressive stress states using gyratory compacted cores, similar to the ones used for complex modulus test. Uniform tensile and compression stresses can be generated on a relatively larger surface area than classical beam fatigue tests. This might be particularly useful for mixes with high percentages of RAP. This test

becomes more relevant when used for large aggregate asphalt mixtures avoiding local aggregate effects. Researchers have used the VECD theory to study the fatigue response of asphalt mixtures *(*Kim et al. 1997, Lee et al. 2000, Chehab 2002, Daniel 2001, Lundstrom and Isacsson 2003, and Kutay et al. 2008). The concept of "pseudo-strain" can be used, according to the theory, to solve the problem of time-dependent viscoelasticity through linear elastic solutions. Internal state variables are used for characterizing nonlinear behaviors caused by microcracks. These variables define the damage growth within the specimen *(*Schapery 1984*)*.

The cyclic push-pull (compression-tension) test was conducted in strain-controlled testing mode. The effect of various percentages of RAP in asphalt mixture on their fatigue properties was evaluated; only material from District 5 were testes under push-pull setup. The test was conducted at 10 Hz and two strain levels of 300 microstrains and 200 microstrains at 20ºC (68ºF) and 15ºC (59ºF), respectively. The test was terminated when the specimen reached failure criterion of 50% reduction in pseudostiffness (C), which is equivalent to 50% reduction in the initial stiffness defined by dynamic modulus $|E^*|$. It is worth mentioning that during the test, the actuator strain levels were controlled instead of the three axial extensometers mounted on the specimen. Hence, a machine compliance factor was used to achieve target strains on the specimens. A fingerprint test was performed prior to the fatigue testing to determine the machine compliance factor and dynamic modulus ratio (DMR). DMR is the specimen variability compensation parameter and it usually has a value between 0.9 and 1.1 (Kutay et al. 2008). DMR is ratio between average representative dynamic modulus of the sample and dynamic modulus obtained in the fingerprint test. Figure 4.10 shows the experimental setup used for push-pull fatigue tests.

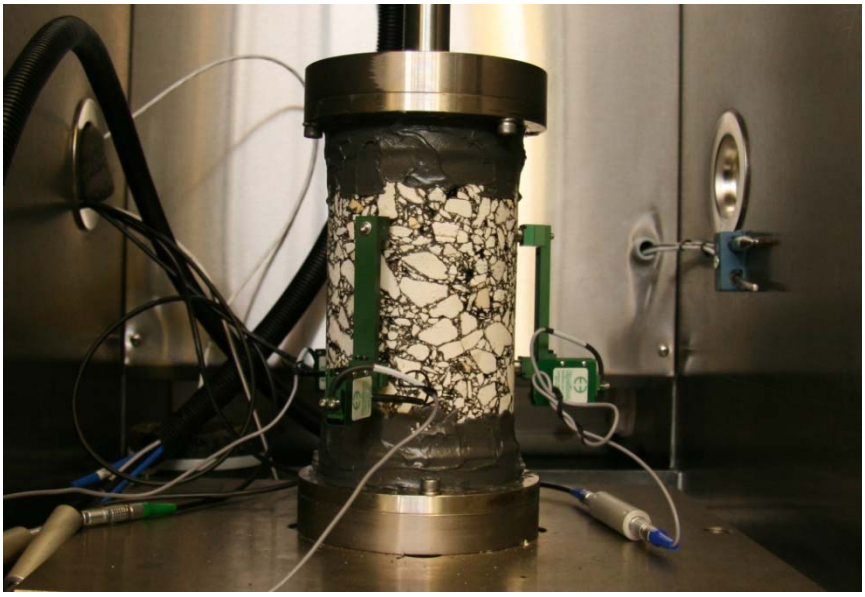

Figure 4.10. Push-pull test setup.

According to the viscoelastic continuum damage theories, damage in asphalt concrete is defined by a damage parameter (*S*) and pseudostiffness (*C*). The relationship between *S* and *C* was determined and expressed as damage characteristic curve using PP-VECD v0.1 software (Kutay 2013). The damage curve (*C* vs. *S*) in Figure 4.11 illustrates stiffness reduction with increasing damage in the specimens. According to the continuum damage theories, damage can be interpreted as evolution of voids and/or microcracks as loading progresses. As damage increases, the specimen's load carrying capacity decreases; hence, the stiffness. A decrease in performance with an increase in the RAP content is evident in this figure. Figure 4.11 is plotted by fitting an exponential curve to *C* versus *S* data.

Slope of the characteristic damage curve can be used to develop fatigue curves for each mixture. The number of cycles to failure (N_f) given in Equation 4.4 can be approximately calculated by using the discrete formulation given in Equation 4.5 (Kutay at al 2009):

$$N_f = \int_{S=1}^{S_f} \left[-\frac{\varepsilon^{R^2}}{2} \frac{dC}{dS} \right]^{-\alpha} f dS \qquad (4.4)$$

$$N_f = \sum_{S=1}^{S_f} \left[-\frac{\varepsilon_0^2 \left|E^*\right|_{LVE}^2}{2} \frac{dC}{dS}\bigg|_{at\ S} \right]^{-\alpha} f\Delta S_s \tag{4.5}$$

where,

$\frac{dC}{dS}$ = slope of damage characteristic curve,

ε^R = Pseudostrain computed using $\varepsilon_o \times E^*_{LVE}$,

E^*_{LVE} = Linear viscoelastic modulus at testing temperature and frequency,

ε_o = Applied strains,

S_f = value of damage paramter corresponding to C at failure i.e. 50% reduction in E^*,

α = relaxation parameter = $\frac{1}{m}$, and

m = slope of the master relaxation curve.

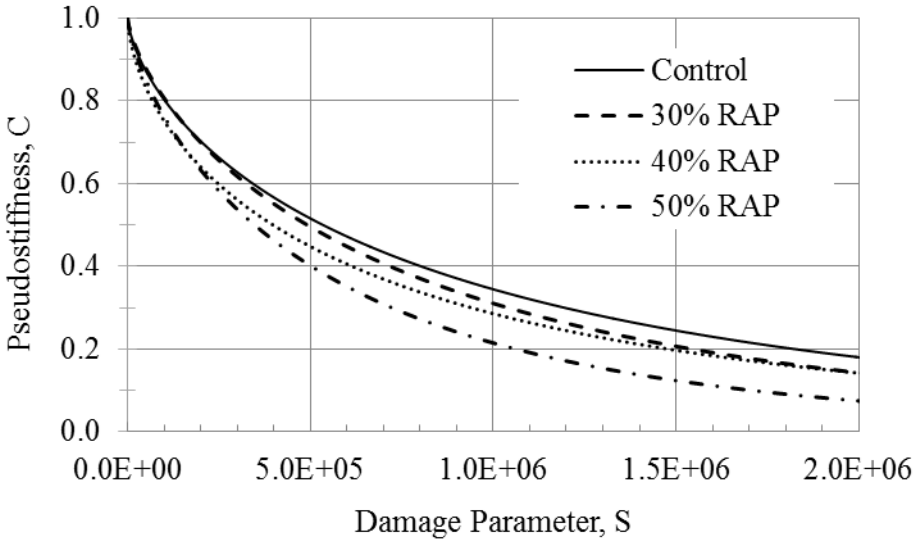

Figure 4.11. Pseudostiffness (C) vs. damage parameter (S) for District 5 asphalt mixtures.

The PP-VECD software (Kutay 2013) then calculates N_f by dividing the C-versus-S curve into small intervals up to the selected failure point (S_f). The parameters dC/dS and ΔS are calculated at each interval, plugged into the Equation 4.5, and summed to calculate N_f. The simulations were conducted at strain levels ranging from 100 to 500

microstrains at an interval of 20 microstrains, temperature of 10 to 30ºC (50-86ºF) at interval of 4ºC (39ºF) and at a frequency of 10 Hz. Figure 4.12 shows the fatigue curves for all the mix designs at 22ºC (71.6ºF).

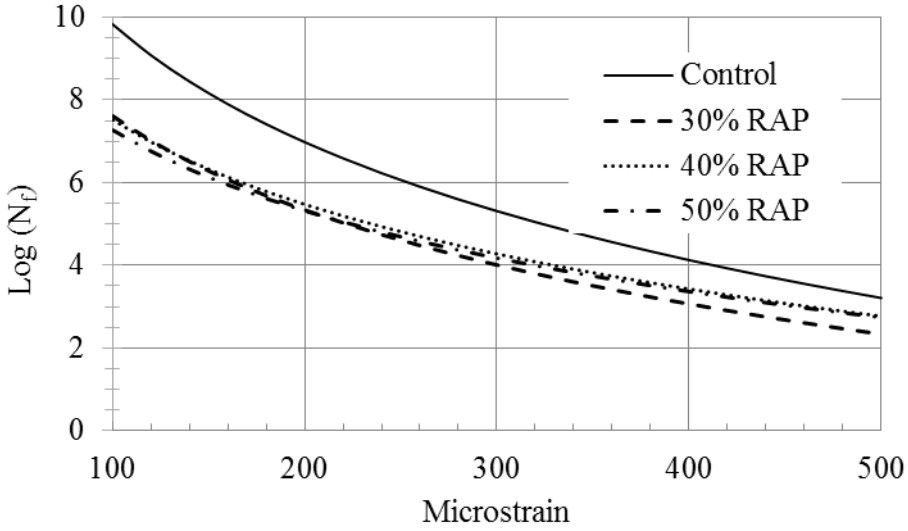

Figure 4.12. Fatigue curves obtained using VECD method.

The fatigue curves clearly indicate a reduction in the number of cycles to failure with the introduction of RAP in the mixtures; however, mixtures with different RAP contents showed similar N_f.

Fatigue is a crucial performance characteristic of asphalt concrete pavements. The fatigue tests and analyses conducted in this study showed slightly different results for the asphalt mixture with different RAP sources. For District 1, only the beam fatigue test was conducted, and recycled mixture performed better than the virgin mixture based on both traditional fatigue analysis and the PV method. District 5 mixtures, however, showed contrasting results when different tests and analysis were conducted. While traditional analysis of beam fatigue test results showed better performance of asphalt mixture with RAP, PV analysis of the fatigue test and VECD-based analysis of the push-pull fatigue test showed opposite trends. The performance of these mixtures in the field will ultimately establish the potential of these tests and analysis techniques to predict performance. Again, if actual traffic loading in the field is considered to be stress-controlled, asphalt mixtures with higher stiffness may well perform better than softer ones.

4.5 Wheel Tracking Test

Wheel tracking test (a torture test) was conducted to evaluate the rutting potential of the control mix and the mixtures with various RAP contents. SGC specimens were compacted to 7.0% ± 1% air void content to create the test specimens. Although control mix (0% RAP) specimens were fabricated using only the base PG binder (PG 64-22), mixtures with RAP were tested with base, single-bumped (PG 58-22), and double-bumped (PG 58-28) binders. The wheel tracking test was performed on wet-conditioned (submerged in water) specimens at 50ºC (122ºF) for 20,000 passes of 150 lb (222 N) of steel wheel or until 12.5 mm (0.5 in.) of deformation. The test matrix for the wheel tracking test is shown in Table 4.5.

Table 4.5. Wheel tracking testing matrix for each material source.

Condition	RAP (%)				Total
	0	30	40	50	
Wet	3[1]	9[2]	9	9	30
Total	6	18	18	18	60

[1]Three replicates
[2]Three replicates × three binder types

Three replicates were tested for each asphalt mixture. None of the District 1 mixtures reached the 12.5-mm (0.5-in.) criterion of failure. Figure 4.13a shows the effect of RAP on mixture's permanent deformation. An improvement in rutting resistance was observed as RAP content increased from 0% to 40%. However, 50% recycled mix showed rutting resistance similar to that of 40% recycled mix.

The binder-grade bump effect on 30% recycled mix was evaluated, as presented in Figure 4.13b. The rut depths of the 30% recycled mix increased when the virgin binder was softened. For 40% recycled mix (Figure 4.13c), the effect of single- and double-grade binder bumping was similar, but it significantly increased rut depth compared to mixtures with PG 64-22. The rut depths remained less than those of the control mixture, even with using double-bumped binder.

Figure 4.13d shows rut depth for 50% recycled mix. While single-grade bump did not affect rut depths, double bumping increased rut depth slightly—but still less than with the control mixture. Overall, wheel tracking data showed improvement in permanent deformation with an increase in RAP content. The single- and double-bumped binders

were effective in reducing the stiffness increase induced by the addition of aged RAP binder. Figure 4.14 shows average rut depths for all combinations of District 1 mixtures.

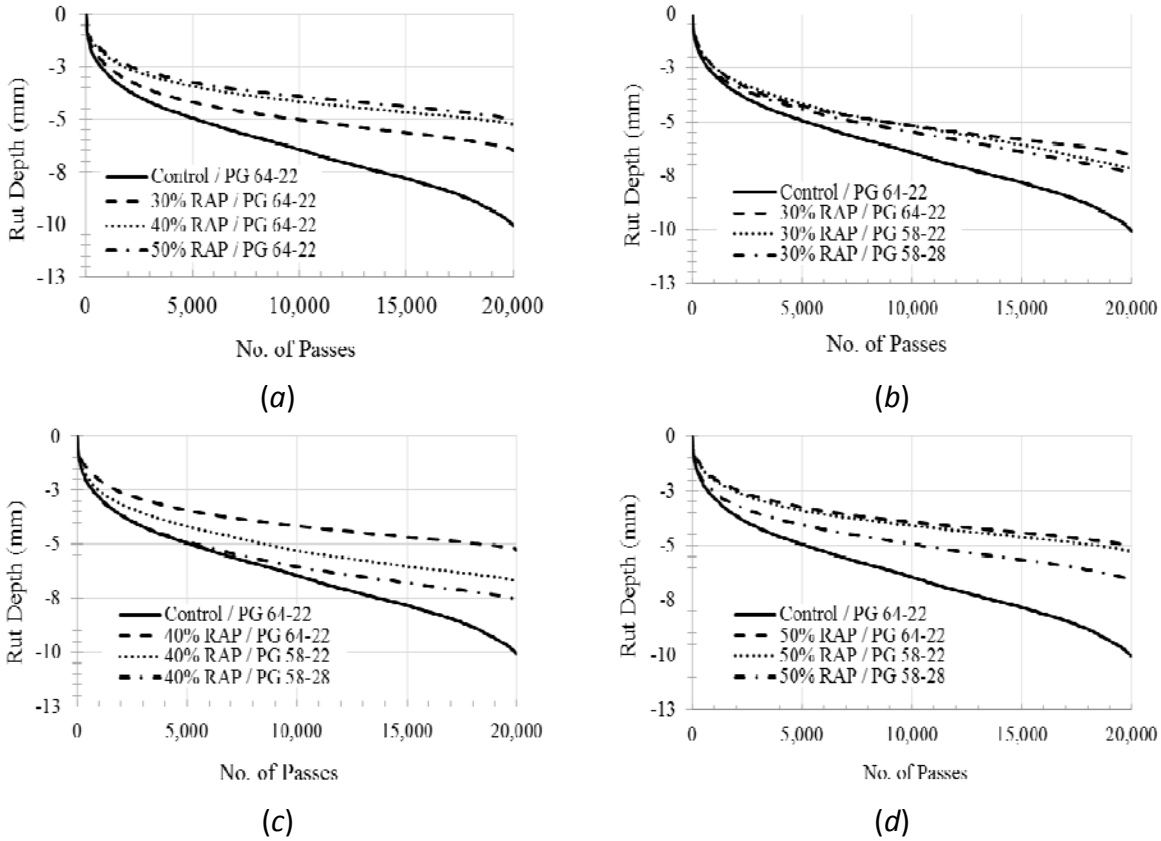

Figure 4.13. Average rut depths for District 1 asphalt mixtures: (a) RAP effect; (b) binder grade bumping effect on 30% RAP mix; (c) binder grade bumping effect on 40% RAP mix; and (d) binder grade effect on 50% RAP mix.

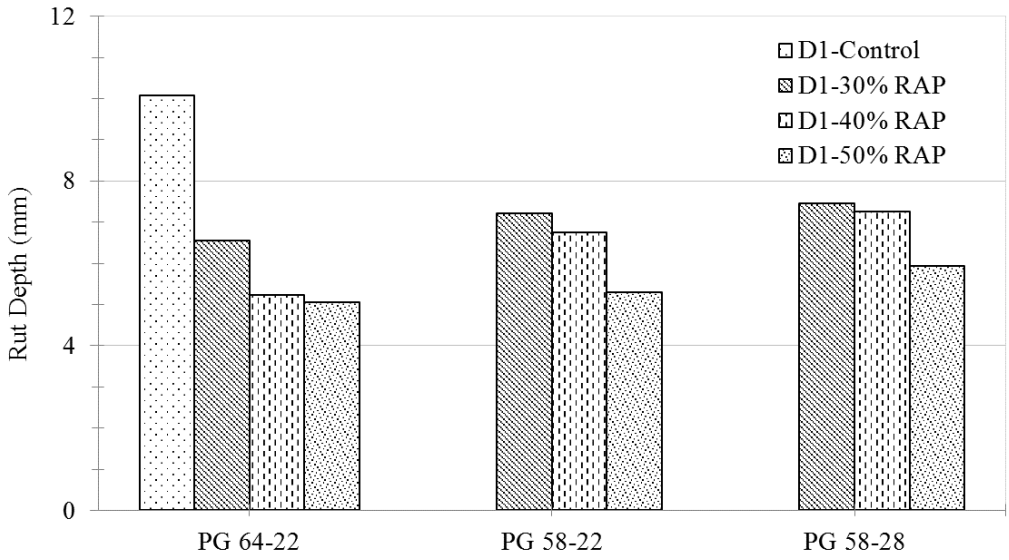

Figure 4.14. Average rut depths for all District 1 mixtures.

Tukey's W statistical analysis was performed on the rutting data. The following conclusions can be made:

- When the control and all RAP mixtures with PG 64-22 were grouped, the control mixture results were significantly different from all RAP mixtures. The 30% recycled mix was also significantly different (softer) than 50% recycled mix.
- When data for the control and 30% recycled mix were grouped, no mix differed significantly from another. It shows that binder bumping is effective to bring 30% recycled mixtures' properties near to the control mixture. Moreover, binder bumping has no significant effect on increasing potential rutting.
- When data for the control and 40% recycled mix were grouped, the control mixture was found to be significantly different (softer) from the asphalt mixture, regardless of the binder used. Binder-grade bumping appears to increase rutting potential, but those mixes still performed better than the control.
- The 50% recycled mix showed similar behavior as the 40% recycled mix. The control mixture was significantly different (less rut resistant) from all 50% recycled mixtures, irrespective of the binder grade used.

In general, as RAP content increased, the amount of virgin binder decreased. Therefore, binder-grade bumping becomes more important as RAP content increases.

For District 5, Figure 4.15a shows that the control mix had very high potential for rutting and exceeded the failure criterion threshold of 12.5 mm (0.5 in). Introduction of RAP increased rutting resistance remarkably. For the base binder (PG 64-22), the 30% recycled mix appeared to improve rutting resistance. The asphalt mixture with higher RAP (i.e., 40% and 50%) behaved almost similarly to the asphalt mixture with 30% RAP having PG 64-22. For softer grades (PG 58-22 and PG 58-28), an increase in rutting resistance was observed with an increase in RAP content.

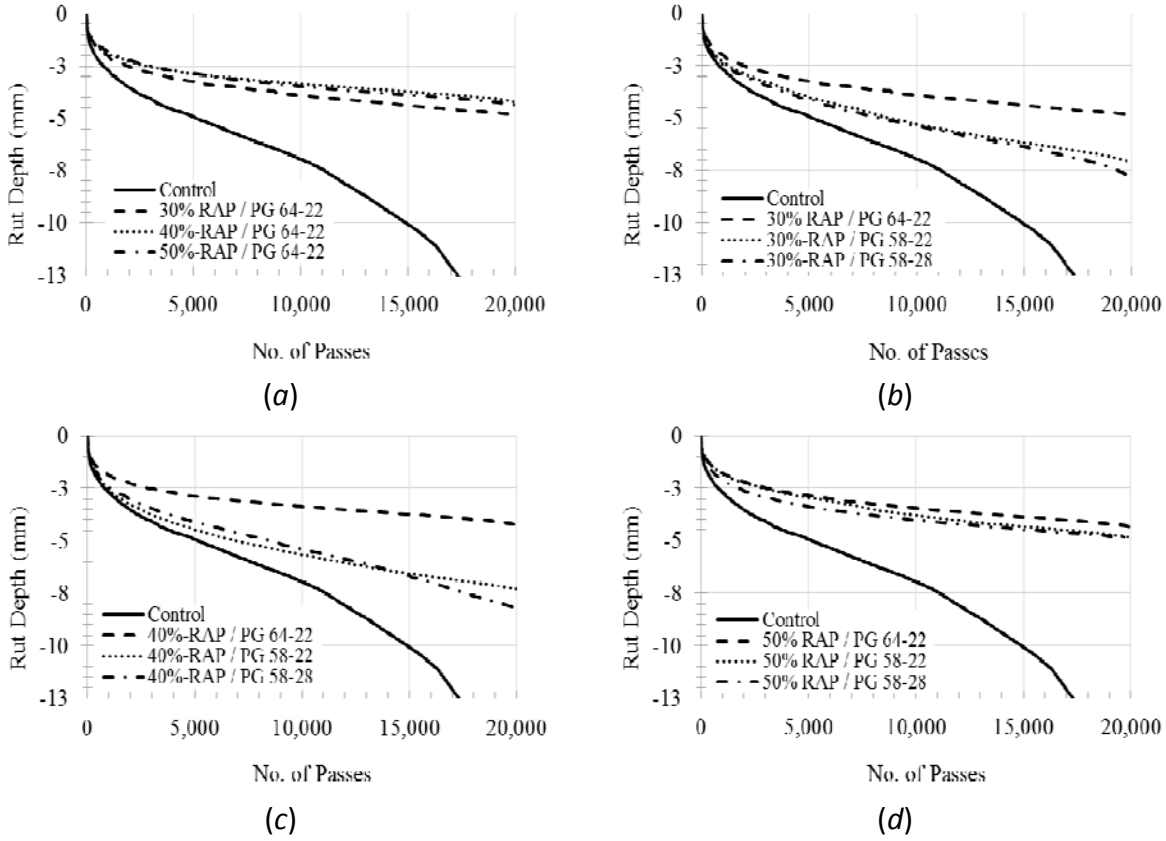

Figure 4.15. Average rut depths for District 5 asphalt mixtures: (a) RAP effect; (b) binder grade bumping effect on 30% RAP mix; (c) binder grade bumping effect on 40% RAP mix; and (d) binder grade effect on 50% RAP mix.

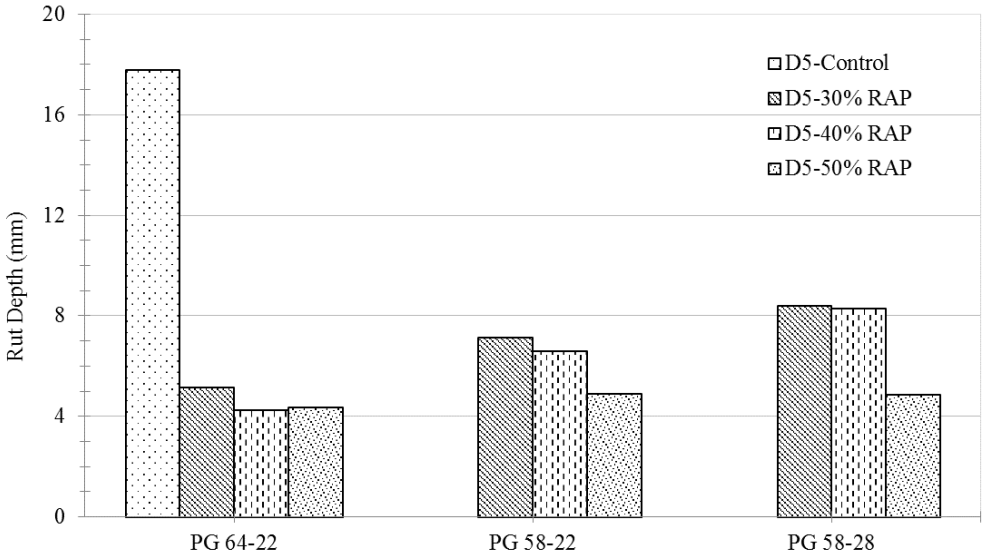

Figure 4.16. Average rut depths of all District 5 mixtures.

Analyzing the effect of binder-grade bumping, it appears that softer binders affect the mixtures with lower RAP content the most. For all District 5 mixtures with RAP, single and double bumping did not appear to produce different results. For 30% and 40% RAP, as shown in Figures 4.15b and 4.15c, respectively, rutting resistance decreased with single-grade binder bumping, but double bumping did not decrease it further.

For 50% recycled mix, there was a minimal effect of binder bumping, as shown in Figure 4.15d. In short, with an increase in RAP content, the binder effect was reduced slightly. This is similar to the trend observed for District 1 mixtures and may be attributed to the fact that less virgin binder is added as the RAP content increases. Figure 4.16 summarizes the test data that explains the effect of RAP as well as that of binder bumping. Overall, the addition of RAP increased rutting resistance of the District 5 mixtures, and the performance was not compromised by using softer binder grades.

The findings of the statistical analysis on wheel tracking data for District 5 are as follows:

- When data for the control and all recycled mixtures using base binder PG 64-22 were grouped, the control was significantly different (softer) than all mixtures with RAP.

- When data for the control and each of 30%, 40%, and 50% recycled mixtures were grouped, the control was significantly different (softer) than each of the 30%, 40%, and 50% recycled mixtures.

4.6 Semi-Circular Bending Fracture Test

Low-temperature fracture properties of the mixtures were determined using a semi-circular bending (SCB) test. The test setup is shown in Figure 4.17. A specimen 2 in. (50 mm) thick was used instead of a 1-in. (25-mm) specimen because of larger aggregates size [3/4-in (19-mm) NMAS] used in the study. To fabricate an SCB test specimen, a 2-in (50-mm) slice was cut from the middle of a 4.5-in (115-mm) gyratory specimen compacted at 7% air void content. The slice was cut into two halves, making semi-circular specimens of 2.91 in (74 mm) in radius, 5.9 in (150 mm) long, and 1.97 in (50 mm) thick.

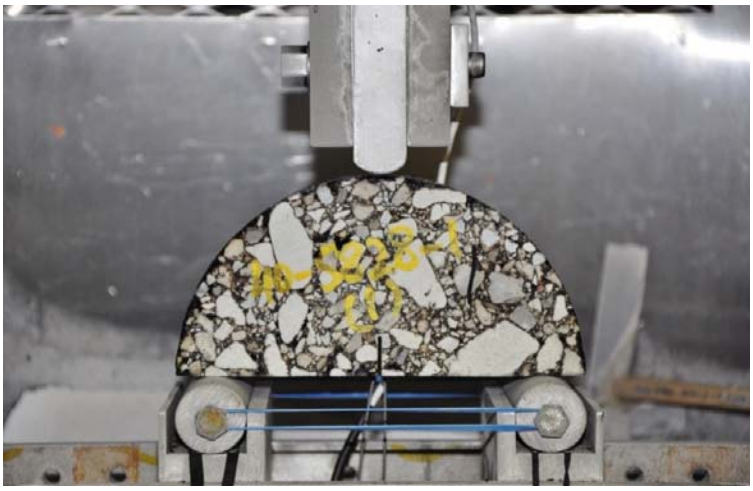

Figure 4.17. Semi-circular bending (SCB) test setup.

The test was conducted at two temperatures: 2ºC (35.6ºF) below and (10ºC) 50ºF above the lower limit of the base PG (64-22) grade. The two testing temperatures were –24ºC (-11.2ºF) and –12ºC (10.4ºF) for the base PG grade, in accordance with a draft AASHTO test protocol. Table 4.6 presents the SCB test matrix for each material source.

A contact load of 0.1 kN (22.5 lb) was applied before starting the test. The test was controlled using the crack mouth opening displacement (CMOD) rate of 0.1 mm/min (0.003937 in/min). The test was stopped when the load level dropped to 0.1 kN (22.5 lb).

Table 4.6. Semi-circular bending (SCB) test matrix for each material source.

Temperatures (ºC)	RAP (%)				Total
	0	30	40	50	
2ºC below Lower PG Grade (–24ºC)[1]	3	9[2]	9	9	30
10ºC above Lower PG Grade (–12ºC)	3	9	9	9	30
Total	6	18	18	18	60

[1]Base PG grade: PG 64-22
[2]Three test sets (base binder, single bump, double bump)

The parameter used to determine the fracture properties of the asphalt mixture was fracture energy (G_f); it is equal to the energy absorbed when the unit sectional area is fractured. Fracture energy is obtained by dividing fracture work by ligament area. (Fracture work is the area under the load-CMOD curve; ligament area is the product of ligament length and thickness of the specimen):

$$G_f = \frac{W_f}{A_{lig}} \tag{3.2}$$

where,

W_f = fracture work and

A_{lig} = area of a ligament.

To better understand thermal cracking, glassy transition temperatures (T_g) were measured for four binders—that is, base binders (PG 64-22) and extracted RAP binders for both Districts 1 and 5. The T_g were measured with a differential scanning calorimeter (DSC). The binder samples were cooled to –70ºC (–94ºF) from 0ºC (32ºF) at a rate of 10 ºC/min (18 ºF/min). The T_g for the binders are presented in Table 4.7.

As explained in Chapter 3, the semi-circular bending (SCB) test was performed at two temperatures: 10.4ºF (–12ºC) and –11.2ºF (–24ºC). Figures 4.18 and 4.19 show the effect of RAP content and virgin binder grade on asphalt mixture fracture energy at –12ºC (10.4ºF) and -24ºC (-11.2ºF), respectively. Detailed results are presented in Appendix B. Higher fracture energy suggests that more energy is required to create a unit surface area of a crack. Therefore, the lower the fracture energy, the greater the potential for thermal cracking.

Table 4.7. Glassy transition temperatures (T_g).

Sample No.	Binder	T_g (ºC)	
		Onset*	Peak
1	District 1, PG 64-22	–9.9	–16.3
2	District 1, extracted RAP Binder	–12.1	–14.5
3	District 5, PG 64-22	–11.8	–16.1
4	District 5, extracted RAP binder	–10.2	–14.7
5	PG 58-22	–16.1	–18.3
6	PG 58-28	–17.2	–18.2

[1]The temperature at the onset of the spike; 1ºF = 1.8 × Temperature (ºC) + 32

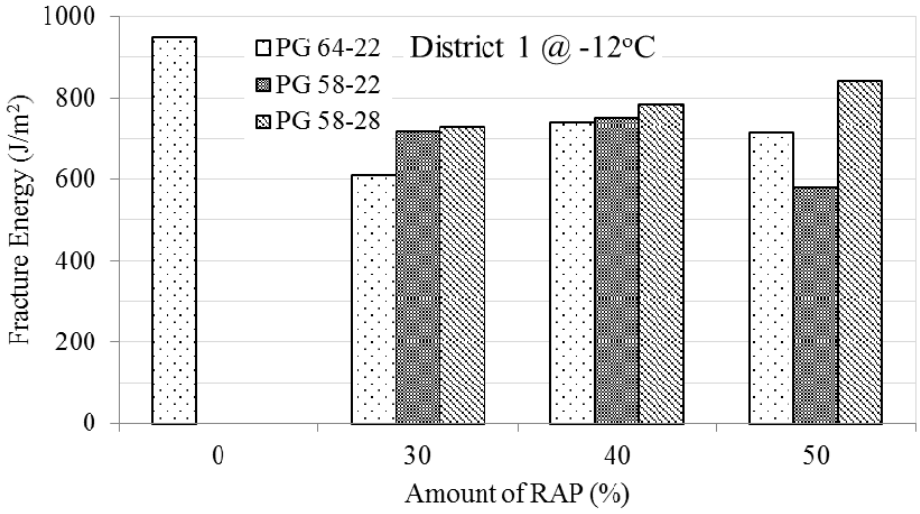

Figure 4.18. Fracture energy for District 1 mixtures at -12°C.

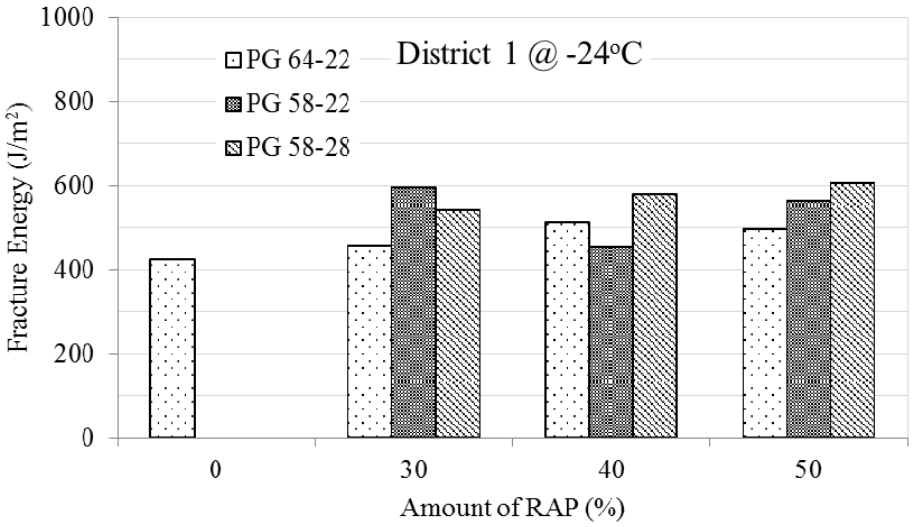

Figure 4.19. Fracture energy for District 1 mixtures at -24ºC.

First, the effect of RAP on fracture energy was analyzed for asphalt mixtures prepared with the base binder (PG 64-22). Apart from the control mixture, recycled mixtures showed a similar trend at both temperatures: At –24ºC (–11.2ºF), the fracture energy of the mixture increased from 30% to 40%; however, the fracture energy for 50% recycled mix slightly decreased. At –12ºC (10.4ºF), the control mixture showed the highest fracture energy. Fracture energy sharply plummeted for the 30% recycled mix. The mixtures with RAP showed a similar trend as that seen at –12ºC (10.4ºF). Fracture energies were greater at 10.4ºF (–12ºC) compared to –24ºC (–11.2ºF), possibly because the asphalt binder is relatively ductile and still within the viscoelastic range as shown by the T_g values. Hence, the creep effect was more pronounced, which consequently required more energy to initiate and propagate a crack. In addition, at relatively low temperatures, the crack tended to propagate in a straight path irrespective of the presence of aggregate and mastic, whereas at higher temperatures, the cracks were more likely to circumnavigate the aggregate particles and propagate through the softer mastic.

Regarding the effect of binder-grade bumping, the fracture energy of 30% recycled mixtures increased at both temperatures, when PG 58-22 was used. Whereas double bumping the binder grade (PG 58-28) resulted in no difference from that of mixtures with PG 58-22. However, the double bump showed improved fracture energy over the control mixture. For 40% recycled mixtures, with the exception of 40% recycled

mixtures with PG 58-22 at –24ºC (–11.2ºF), fracture energy increased when the binder became softer. This increase in fracture energy is expected because the binder becomes more ductile and resistant to cracking when it is softer. For mixtures with 50% RAP, at –24ºC (–11.2ºF), a steady increase in fracture energy was observed when the binder changed from no bumping to double bumping. At –12ºC (10.4ºF), the fracture energy decreased when single bumping was applied and then increased when double bumping was used. This is expected because single bumping affects binder behavior at a higher temperature range. The variation in fracture behavior between binders at –12ºC (10.4ºF) and –11.2ºF (–24ºC) is primarily due to the change in binder phase, as indicated by the measured T_g values.

In general, the stiffening effect of RAP aged binder and softening effect of bumped binder is more pronounced at 10.4ºF (–12ºC) than at –24ºC (–11.2ºF). The softening effect when using single and double binder-grade bumping did not appear to be significant most of the times at –24ºC (–11.2ºF). The fracture energy test results at –24ºC (–11.2ºF) appeared to be unable to capture the effect of aged and softer binders, maybe because new and aged binders behave similarly at that temperature, which is well below the T_g. At –12ºC (10.4ºF), on the other hand, fracture energy was significantly reduced by the addition of RAP with respect to the control mix, which can be improved by using a softer binder.

For District 5, SCB test results showed that fracture energies are similar at both temperatures, as shown in Figures 4.20 and 4.21 (detailed results are tabulated in Appendix B). Also, the effect of high RAP content on fracture behavior was not manifested from the data. At –24ºC (–11.2ºF), fracture energy slightly increased with addition of 30% RAP, whereas it decreased for the 40% recycled mix. The data showed an increase in fracture energy of 50% RAP relative to 40% RAP. At –12ºC (10.4ºF) though, a slight decreasing trend was exhibited as the RAP content increased.

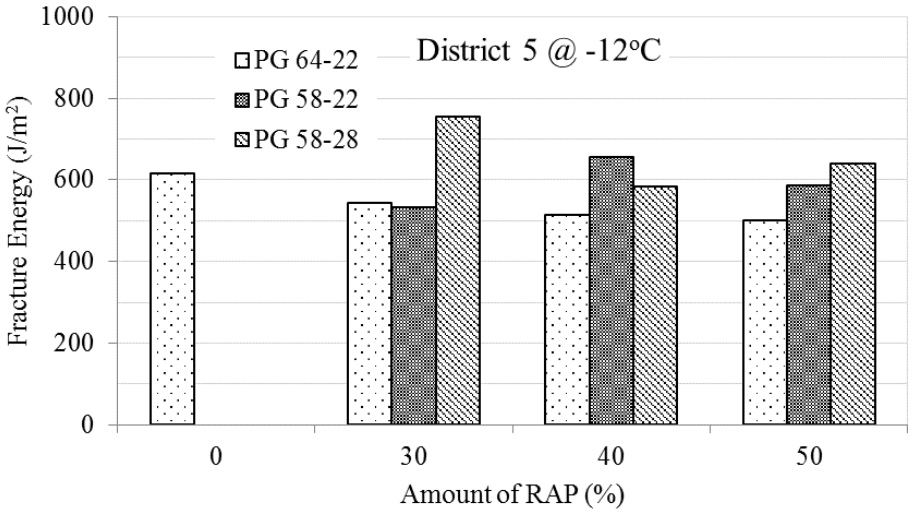

Figure 4.20. Fracture energy for District 5 mixtures at -12ºC.

For 30% recycled mix, fracture energy decreased with single bumping at both temperatures. The double bumping did not affect the fracture energy at –24ºC (–11.2ºF), whereas a sharp increase was observed at –12ºC (10.4ºF). As noted for the test results obtained on District 1 mixtures, testing below transition temperature (T_g) could not manifest the effect of adding aged binder.

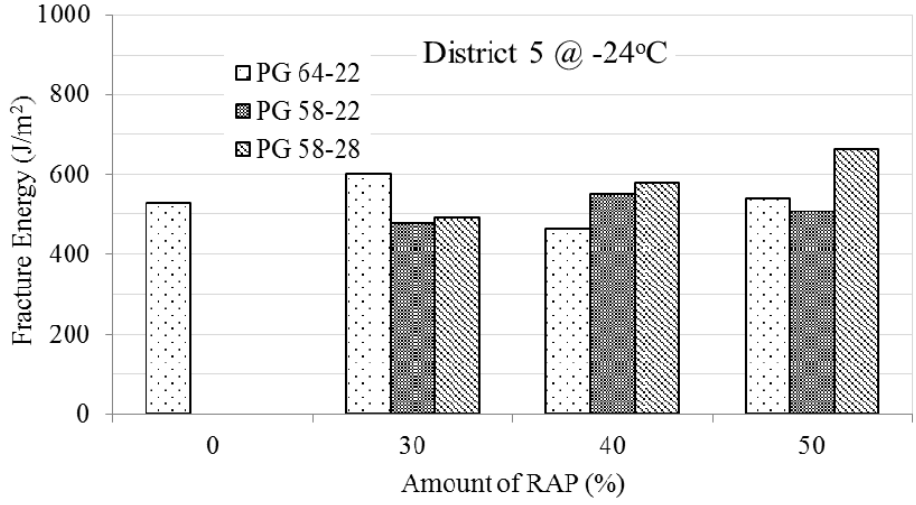

Figure 4.21. Fracture energy for District 1 mixtures at -24ºC.

For 40% recycled mix, fracture energy increased with single bumping at both temperatures. For double binder-grade bumping, the mixtures showed an increase in fracture energy at –24ºC (–11.2ºF), whereas, little change was observed at –12ºC

(10.4ºF). The 50% recycled mix did not result in considerable difference in the fracture energies for no bumping, single bumping, and double bumping, although double binder-grade bumping resulted in the highest fracture energy. This could be expected as double-bumped binder affects low temperature performance.

It appears that the aggregate skeleton of these 19-mm NMAS mixtures had a strong effect on fracture behavior. It may be hypothesized that, with 30% or more RAP, the fracture behavior of asphalt mixtures is predominantly governed by RAP binder properties. So irrespective of the amount of RAP used beyond 30% RAP, the fracture energy remained almost unaffected. However, it was clear that the double-bumped binder would increase the fracture energy.

4.7 Summary and Remarks

The main objective of this chapter was to characterize and evaluate the stability and durability characteristics of mixtures with up to 50% RAP. The effect of RAP content as well as the effect of binder-grade bumping on the laboratory performance of asphalt mixtures was evaluated. The effectiveness of single and double binder-grade bumping was also assessed to determine what level of binder-grade bumping is necessary at various amounts of RAP to maintain virgin mix characteristics.

The complex modulus (E^*) data for District 1 asphalt mixtures showed a nominal increase as RAP content increased, whereas for District 5 mixtures, the increase in the complex moduli was more pronounced with the increase in RAP content. The wheel tracking test and flow number test results for both mixture types were in agreement; the results clearly showed a reduction in rutting potential as RAP content increased for all mixes. Based on the traditional fatigue curve slope analysis of the beam fatigue test, fatigue life of the mixtures slightly improved with addition of RAP for both materials. For District 1 mixtures, the energy-based PV method showed the same trends. However, for District 5 mixtures, worse fatigue behavior was observed in recycled mixtures when results were analyzed using the PV method for the beam fatigue test and the VECD for the push-pull fatigue test. It was evident that RAP addition would increase the potential for thermal cracking (fracture energy was decreased); it occurred in both mixture types when 30% RAP was added. Additional RAP (above 30%) did not show any significant

difference in fracture behavior with respect to the 30% recycled mix, but the fracture energy remained lower than those of the control mix. Single and double bumping of virgin binders fulfilled their intended function to an extent; the softer binders diminished the negative effects of stiffer aged RAP binder. However, it is recommended that use of softer binder grades such as PG 58-34, 52-28, or 52-34 be explored and that use of softening or rejuvenating agents be explored as an alternative.

Based on the results of fracture and fatigue tests performed in this study, it is recommended that new tests be developed to characterize fracture and fatigue behavior of mixtures with high RAP contents. It is important to simulate actual field traffic loading and environmental conditions in the lab. For instance, fatigue tests should be conducted under a stress-controlled setup. Similarly, either the existing fracture tests or the testing temperatures should be modified in a way that can differentiate fracture properties of asphalt mixtures with different RAP contents. The next two chapters provide an in-depth discussion of the viscoelastic characterization of asphalt concrete with and without RAP.

CHAPTER 5

VISCOELASTIC CHARACTERIZATION OF ASPHALT CONCRETE

As already shown in Chapter 4, addition of reclaimed asphalt pavement (RAP) can induce some complexities to material characterization of the asphalt concrete. As would be shown in the subsequent chapters, the economic and environmental advantage of RAP can be realized only when pavements included RAP perform better or equal to the pavements made of virgin materials. An accurate characterization of asphalt concrete would result in enhanced understanding of the material and its behavior under different loading and temperature conditions. This would result in a reduction in maintenance and rehabilitation costs of the asphalt pavements and warranty a long-lasting sustainable pavement system.

This chapter starts with a literature review for common practices of characterization asphalt concrete using time-independent and time-dependent Poisson's ratio (PR). A brief review of the literature for linear viscoelastic characterization is presented next. Time dependency of material constants commonly used in characterization of linear viscoelastic materials is introduced herein. An analytical evaluation of PR is conducted and its variability with respect to time and stress has been verified. Inapplicability of EVCP on PRs is also proved.

5.1 Introduction

Asphalt concrete is commonly characterized as a viscoelastic material where the relationship between stress and strain of asphalt concrete depends on time, loading, and temperature. Asphalt concrete, due to presence of asphalt binder, exhibit viscous-like characteristics at high temperatures and exhibits a more elastic like behavior at low temperatures. The parameters that are usually used to characterize elastic and viscoelastic materials are Young's *(E)*, shear *(G)*, and bulk *(K)* moduli, Lame constant (λ), corresponding compliances (C), and PRs (v). These are linear elastic and viscoelastic

material constants. It is important to note that asphalt concrete's linear viscoelastic material characterization is limited to small strains.

Linear viscoelastic constitutive relationship is expressed in terms of convolution integrals indicating history dependence of the material at the current time.

$$\sigma_{ij}(t) = \int_0^t E_{ijkl}(t-t') \frac{\partial \varepsilon_{kl}(t')}{\partial t'} dt' \tag{5.1}$$

$$\varepsilon_{ij}(t) = \int_0^t C_{ijkl}(t-t') \frac{\partial \sigma_{kl}(t')}{\partial t'} \partial t' \tag{5.2}$$

where, *E(t)* and *C(t)* are viscoelastic modulus and compliance, and σ and ε are stresses and strains. Constitutive relationships for linear elastic materials can be expressed in terms of any two of the modulus parameters. Experimental characterization of elastic and viscoelastic materials is designed to measure one of the modulus parameter (mostly uniaxial modulus) and PR. Once two of these material constants are determined, linear elastic characterization is completed for isotropic materials. However, extension of uniaxial modulus to isotropic viscoelastic characterization (including the terms with shear and bulk modulus) is not a trivial task.

Linear isotropic viscoelastic material characterization can be expressed as follows:

$$\sigma_{ij}(t) = \int_0^t 2G(t-t') \frac{\partial \varepsilon_{ij}^d(t')}{\partial t'} dt' + \delta_{ij} \int_0^t K(t-t') \frac{\partial \varepsilon_v}{\partial t'} dt' \tag{5.3}$$

where *G(t)* and *K(t)* are shear and bulk relaxation functions, respectively and ε_{ij}^d and ε_v are deviatoric and volumetric components of total strains. *G(t)* and *K(t)* can be expressed in terms of Prony series based on a mechanical analog (spring-dashpot model known as the Generalized Maxwell Model):

$$G(t) = G_\infty + \sum_{n=1}^{N^G} G_n \exp\left(-\frac{t}{\tau_n^G}\right) \tag{5.4}$$

$$K(t) = K_\infty + \sum_{j=1}^{N^K} K_j \exp\left(-\frac{t}{\tau_j^K}\right) \tag{5.5}$$

and

$$E(t) = E_\infty + \sum_{j=1}^{N^E} E_j \exp\left(-\frac{t}{\tau_j^E}\right) \tag{5.6}$$

Prony coefficients, E_i, where i indicates the number of spring/dashpot parameters used in the Prony series, are usually normalized by E_0. The ratio $\alpha_i = E_i / E_0$ is then used to determine Prony coefficients for bulk and shear moduli i.e. $K_i = \alpha_i \times K_0$ and $G_i = \alpha_i \times G_0$.

The implementation of viscoelasticity follows from the linear isotropic definition of viscoelastic characterization given by Equation 5.3. According to this definition, two time dependent material constants, *G(t)* and *K(t),* are needed. Experimental characterization of these constants for materials like asphalt concrete is usually very difficult and requires specialized equipment. Therefore, instead of direct measurement of these constants, we predict them using uniaxial Young's modulus *E(t)*. Uniaxial test is relatively a very easy test to conduct and its outcome (axial stresses and strains) can yield *E(t)* directly. This is sufficient for 1-D characterization of materials and modeling applications. In order to translate this characterization to three-dimensional framework, another coefficient is needed. Poisson's ratio is often used to fill this gap between 1-D and 3-D characterization. The Equations 5.7 and 5.8 indicate the relationship between elastic material constants. The range of Poisson's ratio is also predictable for most of the linear elastic materials.

$$K(t) = \frac{E(t)}{(1-2v)} \tag{5.7}$$

$$G(t) = \frac{E(t)}{2(1-2v)} \tag{5.8}$$

Therefore, Poisson's ratio for elastic materials is a very useful material constant to expand the findings of a simple uniaxial test to three-dimensional characterization. When a material is compressed/expanded in one direction, it expands/shrinks in the other two directions perpendicular to the direction of applied load. This phenomenon is called the Poisson effect. In linear elastic materials, PR can be defined as negative ratio of two orthogonal normal strains.

$$\nu_{ji} = -\frac{\varepsilon_{jj}}{\varepsilon_{ii}} \qquad i \neq j \tag{5.9}$$

where,

ν_{ji} = elastic PR,

ε_{ii} = strains in axial/longitudinal direction, and

ε_{jj} = strains in transverse direction.

For homogenous, isotropic, linear elastic materials, PR is a constant and ranges from 0.5 to -1. When a constant (time-independent) load is applied in one direction, all normal strains are also constant resulting in a constant PR. In case of application of a time-dependent strain, the strains in other directions will respond with the same time function, resulting in a constant PR.

A similar approach was also commonly practiced for viscoelastic materials to obtain linear isotropic material functions. This approach involves constant PR assumption and using Equations 5.7 and 5.8 in the characterization of complete linear isotropic viscoelastic behavior of asphalt mixtures. When such characterization with constant PR is used, *K(t)* and *G(t)* inherently assume same relaxation times for *E(t)*, *K(t)*, and *G(t)*. Moduli, compliances, and also PRs for elastic materials are constant coefficients and they are invariant to time and stress path. Whereas, for linear viscoelastic materials, moduli and compliances are time-dependent but still remains independent of stress and loading history. Whereas, PR for viscoelastic materials are proven to be not only time dependent but also stress and stress history (path) dependent (Hilton and Yi 1998, Hilton 2001, 2009, and 2011, and Khan and Hilton 2010). Moreover, elastic-viscoelastic correspondence principle (EVCP), explained later in this chapter, is not applicable to the common definition of PRs being used in asphalt concrete research (Hilton 2001, 2009, and 2011, Micheali et al. 2012 and 2013). Inapplicability of EVCP and time/stress-dependency of the viscoelastic PR will be discussed in the subsequent sections of this chapter. In this chapter, the problems associated with assuming constant PRs and similar moduli relaxation times for a viscoelastic material like asphalt concrete will be discussed. This will be achieved through:

1. Reviewing the literature regarding the current use of PRs with regards to asphalt concrete characterization in specific and viscoelastic material in general.
2. Showing the inapplicability of EVCP for PRs.
3. Conducting numerical analysis to show time and stress dependence of viscoelastic PRs.

5.2 Use of Poisson's Ratio for Asphalt Concrete Characterization

In a linear viscoelastic case, the elastic PR, as defined in Equation 5.9 becomes

$$\nu_{ji}(t) = \nu_{ji}^{I}(t) = -\frac{\varepsilon_{jj}(t)}{\varepsilon_{ii}(t)} = -\frac{\int_0^t C_{jjkl}(t-t')\frac{\partial \sigma_{kl}(t')}{\partial t'}\partial t'}{\int_0^t C_{iikl}(t-t')\frac{\partial \sigma_{kl}(t')}{\partial t'}\partial t'} \qquad i \neq j \qquad (5.10)$$

where *C(t)* = uniaxial viscoelastic compliances; Hilton (2001) defined it as Class I PR. As discussed in section 5.1, PRs are often assumed to be constant while characterizing the asphalt concrete. Hill and Heukelom (1969), two of the early researchers who studied the PRs of asphalt concrete, called ratio between lateral and longitudinal strain as strain ratio (instead of Poisson's ratio) based on the fact that asphalt binder and asphalt mixture are viscoelastic materials rather than elastic. The study explored the effect of air voids and binder stiffness on strain ratios. Irony is that, even today PRs are taken as constant for asphalt concrete just for the matter of convenience. Table 5.1 shows a partial list of otherwise excellent studies related to asphalt concrete characterization and modeling studies that assumed a constant PR for their analysis. The typical PR values used in these studies ranged from 0.25-0.35.

For the past few years though, there has been realization in asphalt modeling community about the inappropriate use of constant PRs for asphalt concrete. In 2007, Benedetto et al., recognizing the dependence of PR on frequency and temperature, introduced a master curve for PRs similar to that of the complex modulus using the same shift factor for both. A sinusoidal loading was applied on cylindrical specimen of asphalt binders, mastics, and asphalt mixtures. Small axial strain amplitudes (less than 10^{-4} m/m) were applied ensuring the behavior to remain inside the linear domain. They found that PR is not a constant as generally considered for binders, mastics, and mixtures. The

values of PR ranged from 0.5 (at low frequencies and/or high temperatures) to about 0.35 (at high frequencies and/or low temperatures) for asphalt binder.

Table 5.1. Asphalt studies related to use of Poisson's ratio.

Authors (year)	Type of Study	PR used
Gonza´lez et al. (2006)	Viscoelastic constitutive model development for simula ting the response of a real flexible pavement structure	Constant (0.3)
Kai and Fang (2011)	3-D FE model to conduct applied mechanics analysis o f asphalt overlays	Constant (0.25)
Ameri et al. (2011)	Top-down cracking using 3-D FE analysis	Constant (0.35)
Darabi et al. (2011)	Permanent deformation of asphalt materials	Constant
Heinicke and Vinson (1988)	2- and 3-D FE models for Resilient modulus of asphalt concrete	Constant (0.35)
Huang et al. (2007)	Nonlinear viscoelastic analysis of asphalt mixtures und er shear loading	Constant
Huang et al. (2006)	FE analysis for 3-layered asphalt mixture	Constant (0.35)
You et al. (2012)	3-D microstructure modeling of asphalt concrete	Constant
Wang and Al-Qadi (2009)	FE analysis related to moving wheel load and 3-D cont act stresses	Constant
Collop et al. (2003)	Stress-dependent elastoviscoplastic constitutive model with damage	Constant (0.3)
Benedetto et al. (2007)	Master curves of PRs. Whereas PRs defined as ratio of normal strains.	Time- and frequenc y- dependent PRs
Maher and Bennert (2008)	Sensitivity analysis of constant and time-dependent PR s on predicted pavement distresses.	time-dependent PR
Lee and Kim (2009)	Measuring compliances and time- and frequency-depen dent (complex) PRs from complex modulus and creep compliance tests in indirect tension testing mode.	Time- and frequenc y- dependent PRs

In the mechanistic empirical pavement design guide (MEPDG, 2004), it is recommended to determine PR for the asphalt concrete either using Equation 5.8 with user entered values of a and b (or with typical values of a = -1.63 and b = $3.84*10^{-6}$), or using the values given in Table 5.2.

$$v_{AC}^{I} = 0.15 + \frac{0.35}{1 + e^{(a+bE_{AC})}} \tag{5.9}$$

The variation with respect to temperature (or indirectly modulus) is an incomplete description of viscoelastic PR. In viscoelastic materials, moduli are just time-dependent, whereas, PRs are also dependent on stress and stress/loading history.

Table 5.2. Typical PRs at different input levels for dense graded mixes (MEPDG 2004).

Temperature ^{o}C (^{o}F)	Level 2C[1]	Level 3[1]
< -18 (0)	< 0.15	0.15
-18 (0) – 4.5 (40)	0.15 – 0.20	0.20
4.5 (40) – 21 (70)	0.20 – 0.30	0.25
21 (70) – 38 (100)	0.30 – 0.40	0.35
38 (100) – 149 (300)	0.40 – 0.48	0.45
> 149 (300)	0.45 – 0.48	0.48

[1] Hierarchical levels of design inputs

In a study conducted at Rutgers University, Maher and Bennert (2008) determined the PRs (negative ratios of time-dependent axial and transverse strains) using a radial LVDT system and found consistent lower PR values relative to the ones determined using the MEPDG's equation. The sensitivity analysis conducted in the study showed discrepancies between the predicted pavement distresses by the authors and the MEPDG; they attributed the difference in predicted distresses to variation in PRs used by the study and the MEPDG.

Lee and Kim (2009) presented a methodology to determine time- and frequency-dependent Poisson's ratio and creep compliance of asphalt mixtures using indirect tension (IDT) test. They found that the PRs can be accurately determined using both creep compliance and complex modulus tests in indirect tension mode. They found that complex PRs in frequency domains from complex modulus test matched well with PRs obtained from the creep test. The sensitivity analysis conducted in the study showed that creep compliances determined from a constant PR value of 0.35 agreed well with those determined from the IDT tests. In another paper related to same study, Kim at al. (2010) developed formulation to determine time-dependent shear and bulk moduli using IDT test. Finite element (FE) analyses showed that creep strains estimated using shear and bulk moduli obtained from time-dependent PRs showed excellent agreement with the measured strains. The creep strains indicated that a suitable assumption of PR could result in reasonably accurate creep compliance close to what could be obtained using the time-dependent approach.

Recently, Kassem et al. (2013) used another PR-like parameter (termed as

viscoelastic PR in that study) which is independent of stress history of the material but was not equivalent to elastic PR. The PRs were first defined incorrectly (by applying correspondence principle on PR elastic equations) as a material property in terms of bulk and shear moduli (Equation 5.11) and then related back as ratio of measured strains as shown in Equations 5.12. Stresses are ignored in the derivation of following equations for PR:

$$v^{111}(t) = L^{-1}\left\{ \frac{K(s) - 2G(s)}{2[K(s) + G(s)]} \Big/ s \right\} \tag{5.11}$$

$$s\bar{v}^{III}(s) = -\frac{\bar{\varepsilon}_{22}(s)}{\bar{\varepsilon}_{11}(s)} \tag{5.12}$$

where $\bar{v}^{III}(s)$ is viscoelastic PR in Carson-transformed domain as defined by the authors. Hilton (2001) refers to this PR (as defined in Equation 5.12) in Fourier or Laplace domain as Class III PR. Here, we use s-multiplied Laplace transforms (Carson transforms) since we derive stress-strain relationship using modulus or compliance functions and partial derivatives of stress or strain excitations. Such integral form of viscoelastic stress-strain relationship results in s-multiplied terms in the transformation domain. The transformation variable "s" would disappear if convolution integral form without partial derivatives is used to describe stress-strain relationship. Class III PR is the only class of PRs that works with correspondence principle but it is artificially defined as ratio of transforms rather than the transform of ratios. Equation 5.12 can be written as

$$s\bar{v}^{III}(s) = -\frac{\bar{C}_{2211}(s)\bar{\sigma}_{11}(s)}{\bar{C}_{1111}(s)\bar{\sigma}_{11}(s)} \tag{5.13}$$

For 1-D loading case, axial stress will cancel out resulting in

$$s\bar{v}^{III}(s) = -\frac{\bar{C}_{2211}(s)}{\bar{C}_{1111}(s)} \tag{5.14}$$

Transforming Equation 5.14 to time domain results in stress-independent PRs which might be wrong for stress state is not purely uniaxial. Therefore, Equation 5.12 must be used for transforming to time domain for general multi-axial stress states. This can be clearly observed in the case of 2-D loading where stresses are not canceled out as shown

in Equation 5.15 and results in completely different PRs in time domain.

$$s\bar{v}^{III}(s) = -\frac{\bar{C}_{2211}(s)\bar{\sigma}_{11}(s) + \bar{C}_{2222}\bar{\sigma}_{22}(s)}{\bar{C}_{1111}(s)\bar{\sigma}_{11}(s) + \bar{C}_{1122}(s)\bar{\sigma}_{22}(s)} \tag{5.15}$$

Moreover, Class III PR in time domain does not have any physical meaning and comes with a double (nested) time integral; conducting a finite element analysis (FEA) can cost a huge amount of central processing unit (CPU) time, making them very prohibitive.

5.3 Viscoelastic Poisson's Ratio Discussion

Hilton (2001) provides a comprehensive literature review on the use of viscoelastic PRs. Outside the realm of asphalt research, extensive work has been conducted on PRs and their applicability to viscoelastic materials, Lakes and Wineman 2006, Tschoegl et al. 2002, Hilton and Yi 1998, Lakes and Alan 2006, Hilton 2001 and 2011, Hilton and Fouly 2007, to mention but a few.

Tschoegl et al (2002) developed a linear theory of the time- or frequency-dependent Poisson's ratio, and reviewed work on its experimental determination. The paper also reported on attempts to measure the PR of a viscoelastic material as a function of temperature. Lakes and Wineman (2006) discussed the difference in time-dependence of Poisson's ratio under various test configurations/modalities. They showed an insignificant difference between the PRs obtained using a tensile creep and tensile relaxation test for moderate degree of viscoelasticity. Correspondence principles were developed for relaxation type PRs in the time domain and complex PRs in the frequency domain. They also showed that PRs need not increase with time and need not be monotonic in time which is in contrast with what Tschoegl et al. (2002) suggested.

On the other hand, there are some studies proving experimentally and analytically that PR is not a fundamental property of materials and should be completely avoided during material characterization (Hilton and Yi 1998, Hilton 2001, Hilton et al. 2008, Hilton 2009, Khan and Hilton 2009, Hilton 2011, Michaeli et al. 2011, 2012, and 2013, and Shtark et al. 2012). Hilton (2001) provided a detailed account of issues associated with assumption of time-independent PRs and the conditions under which constant PRs

can exist. Hilton and co-workers showed five forms/classes of viscoelastic PRs that have been used by different researchers in the past.

To fully characterize an isotropic material, two independent material properties are required. Due to non-linear nature of viscoelastic PRs and complexities surrounding their values and definitions, Hilton (2001, 2011), Hilton and Fouly (2007), and Shtark et al. (2012) recommended characterizing viscoelastic materials in terms of relaxation or creep functions.

Although possible, performing shear and bulk modulus tests are quite complex and costly. To address this problem, an alternative protocol was formulated by Hilton and Fouly (2007) for determination of bulk, shear, and Young's moduli from 1-D tests without using PRs. The protocol has been explained by Shtark et al. (2012). The alternative algorithm is based on the fact that two material functions (two moduli or two compliances) are needed to be determined instead of one modulus and PR. The procedure consists of collecting experimental data like axial stress and resulting stains in axial and transverse directions. Deformations are measured using photogrammetric techniques. A stress loading function $\sigma(t)$ is established by least square fit or Fourier series. Compliances are then calculated using the relations involving the compliances and hereditary integral for a uniaxial stress. The set of equations obtained can be solved using LSQ or other methods. The relaxation times and compliance coefficients are determined in such a way so that the calculated strains are matched to the experimental strains. The isotropic shear modulus $G(t)$, Young's modulus $E(t)$ and bulk modulus $K(t)$ are then calculated by taking Laplace or Fourier transforms of the compliances and then inverting the equations below to time domain.

$$G(x,t) = L^{-1}\left\{\int_{-\infty}^{\infty} \frac{\exp(-st)ds}{2[\overline{C}_{1111(x,s)} - \overline{C}_{2211(x,s)}]}\right\} \tag{5.16}$$

$$K(x,t) = L^{-1}\left\{\int_{-\infty}^{\infty} \frac{\exp(-st)ds}{2[\overline{C}_{1111(x,s)} + 2\overline{C}_{2211(x,s)}]}\right\} \tag{5.17}$$

$$E(x,t) = L^{-1}\left\{\int_{-\infty}^{\infty} \frac{\exp(-st)ds}{2[\overline{C}_{1111(x,s)}]}\right\} \tag{5.18}$$

Recently, Michaeli et al. (2013) provided a solution to the problem directly in real time

space without the use of integral transforms. The solution includes the complete history of loading and of displacements including their build ups. The analytical approach adopted by Michaeli et al. (2013) is adopted in this study to characterize asphalt mixtures with and without RAP. The details of this analytical approach are provided in Chapter 6.

5.4 Correspondence Principle for Viscoelastic Poisson's Ratio

The EVCP (Read 1950) is an important and unique method for allowing utilization of elastic solutions for viscoelastic materials. Tschoegl (1989) defined it as "*if an elastic solution to a boundary value problem (stress analysis problem) is known, substitution of the appropriate Fourier or Laplace transforms for the quantities employed in the elastic analysis furnishes the viscoelastic solution in the transformed plane*." In simple words, an elastic material has the following constitutive equation:

$$\varepsilon(t) = C^{elastic}\sigma(t) \tag{5.19}$$

whose viscoelastic counterpart is defined by Equation 5.1.

For the integral transform analogy or correspondence principle EVCP to be applicable, there must be one-to-one replacement of elastic solutions of elastic moduli with corresponding viscoelastic complex moduli (Hilton 2009). That is, the transformed (Laplace or Fourier) form of Equation 5.1 should be of the same algebraic form as that of elastic case (Equation 5.19), such that

$$\bar{\varepsilon}(s) = \overline{sC}(s)\bar{\sigma}(s) \tag{5.20}$$

where overbars represent transformed parameters. One of the common examples of utilizing EVCP in asphalt research is determining the stiffness modulus in a bending beam rheometer test; the elastic beam theory in conjunction of EVCP is used to determine compliances and stiffness of an asphalt binder beam. In order to show the inapplicability of correspondence principle on PRs, its applicability on a general constitutive equation is shown first.

For a Linear viscoelastic, homogenous isotropic material, Equation 5.21 shows general forms of viscoelastic constitution equation, which can also be written as

$$\varepsilon_{ij}(t) = \int_0^t C_{ijkl}(t-t')\frac{\partial \sigma_{kl}(t')}{\partial t'}\partial t' \tag{5.21}$$

where C_{ijkl} = Compliance, and stresses and strain are related to each other through convolution integral. Convolution (f*g) is a mathematical operation on two functions f and g such that

$$(f * g)(t) = \int_0^{\infty} f(t-t')g(t')\partial t' \tag{5.22}$$

$$\varepsilon_{ij}(t) = \int_0^t \overbrace{C_{ijkl}(t-t')}^{f} \underbrace{\frac{\partial \sigma_{kl}(t')}{\partial t'}}_{g} \partial t' = (C_{ijkl} * \frac{\partial \sigma_{kl}}{\partial t})(t) \tag{5.23}$$

Convolution theorem states that Laplace transform (LT) of a convolution equals product of the transformed function such as

$$LT\{f*g\} = F(s)G(s) \tag{5.24}$$

Applying convolution theorem on right hand side (RHS) of Equation 5.23 results in

$$\varepsilon(s) = sC(s)\sigma(s) \tag{5.25}$$

where s occurs due to time derivative in the convolution integral, i.e.

$$LT\{f'(t)\} = sF(s) - f(0) \tag{5.26}$$

It can be seen that the Equation 5.25 has the similar algebraic form to that of Equation 5.19. Considering the viscoelastic PR as defined in Equation 5.9, it is obvious that PR is a ratio of two strains and not in a form of convolution integral. Therefore, the convolution theorem cannot be applied in this case. Applying LT on Equation 5.9:

$$\overline{\nu}^{I}(s) = -\int_0^{\infty} \left\{ \frac{\int_0^t C_{jjkl}(t-t')\frac{\partial \sigma_{kl}(t')}{\partial t'}\partial t'}{\int_0^t C_{iikl}(t-t')\frac{\partial \sigma_{kl}(t')}{\partial t'}\partial t'} \right\} e^{-st} dt \tag{5.27}$$

resulting in:

$$\overline{\nu}^{I}(s) = -\left[\frac{\overline{\varepsilon_{jj}(s)}}{\varepsilon_{ii}(s)}\right] \neq -\frac{\overline{\varepsilon_{jj}}(s)}{\overline{\varepsilon_{ii}}(s)} = -\frac{L\left\{\int_0^t C_{jjkl}(t-t')\frac{\partial \sigma_{kl}(t')}{\partial t'}\partial t'\right\}}{L\left\{\int_0^t C_{iikl}(t-t')\frac{\partial \sigma_{kl}(t')}{\partial t'}\partial t'\right\}} = \overline{\nu}^{III}(s) \tag{5.28}$$

where overbars show the transformed parameters. Equation 5.28 shows that transformed viscoelastic PR is the *transform of strain ratios* not the *ratio of strain transforms* (which would have been algebraically similar to elastic PR). It shows that, unlike constitutive

equations, PRs do not contribute to EVCP and their use in viscoelastic material characterization is inappropriate.

5.5 Numerical simulations for Time Dependence of Viscoelastic Poisson's Ratios

Bulk modulus *K(t)* is an important material property which expresses the response of material to changes in size under an isotropic pressure. Actual determination of *K(t)* is a difficult task and involves measuring volumetric changes under an isotropic pressure. As mentioned earlier, for the sake of convenience, two assumptions are usually made with regards to *K(t)*. The first, and the most common one, is assuming same relaxation time for *E(t)*, *G(t)*, and *K(t)*. The second one, on the other extreme, is to assume *K(t)* constant (no relaxation) over the entire time range of *G(t)* (i.e. from G_0 to G_∞). Real materials do have bulk moduli which relax at a rate which are orders of magnitude larger than the shear and Young's moduli (Hilton, 2001), but assuming them to be constant can have some serious repercussions. In this study, few numerical simulations were conducted to explore the following:

- Effect of different initial Poisson's ratios and bulk relaxation times τ^K on long-term Poisson ratios
- Effect of different K_0 values on PRs.
- Effect of different τ^K on the relaxation modulus components E_{1111} and E_{1122} (defined later in this chapter).

5.5.1 Effect of Initial PR and τ^K on Long-term PR

It is important to note the definition of bulk modulus *K(t)* adopted in this study. Viscoelastic constitutive equation for volumetric deformations can be written as follows:

$$\sigma(x,t) = \int_0^t K(t-t') \frac{\partial \varepsilon_v(x,t')}{\partial t'} dt' \qquad (5.29)$$

where

$$\sigma(x,t) = \frac{\sigma_{ii}(x,t)}{3} \text{ and } \varepsilon_v(x,t) = \frac{\varepsilon_{ii}(x,t)}{3}$$

are volumetric stress and volumetric strain respectively.

Shear modulus *G(t)* was first obtained using a three-parameter model

$$G(t) = G_\infty + \sum_{j=1}^{N_G} G_j \exp\left(-\frac{t}{\tau_j^G}\right) \tag{5.30}$$

where j = 1 to simplify the simulation, relaxation time τ_1^G = 1000 seconds, G_0 = 10,000 MPa, $G_1 = \alpha * G_0$, where $\alpha = G_1/G_0$, and $G_\infty = G_0 - G_1$. Different values of K_0 was determined from G_0 value based on assumed initial PR (0.25, 0.3, 0.35, 0.4, and 0.45). Corresponding K_1 value was obtained based on α value; i.e. $K_1 = \alpha * K_0$. Long time (infinity) bulk modulus then becomes $K_\infty = K_0 - K_1$. Bulk relaxation time τ_1^K was varied to have different relaxation time ratios (τ^K/τ^G). Bulk modulus, *K(t)*, was obtained using the following model:

$$K(t) = K_\infty + \sum_{j=1}^{N_K} K_j \exp\left(-\frac{t}{\tau_j^K}\right) \tag{5.31}$$

Strains were first found in Carson domain and then transformed to time domain using inverse transforms as

$$\varepsilon_{11}(t) = L^{-1}\left\{\frac{1+G(s)/K(s)}{3G(s)}\sigma_{11}(s)\Big/s\right\} \tag{5.32}$$

$$\varepsilon_{22}(t) = L^{-1}\left\{\frac{2G(s)/K(s)-1}{6G(s)}\sigma_{11}(s)\Big/s\right\} \tag{5.33}$$

$$v^I(t) = -\frac{\varepsilon_{22}(t)}{\varepsilon_{11}(t)} = -\frac{L^{-1}\left\{\frac{2G(s)/K(s)-1}{6G(s)}\sigma_{11}(s)\Big/s\right\}}{L^{-1}\left\{\frac{1+G(s)/K(s)}{3G(s)}\sigma_{11}(s)\Big/s\right\}} \tag{5.34}$$

Dependence of PRs on time is clearly shown in Figures 5.1 and 5.2, time plots of viscoelastic PRs when they are incorrectly assumed as constants. PR variation seems to be strongly influenced by the initial PR value chosen; lower the initial PR value, greater the variation of viscoelastic PR with time. It may be possible that mixtures with RAP, that are usually stiffer than virgin asphalt mixtures, have lower instantaneous PR values, making their time-dependent PRs more sensitive at longer times.

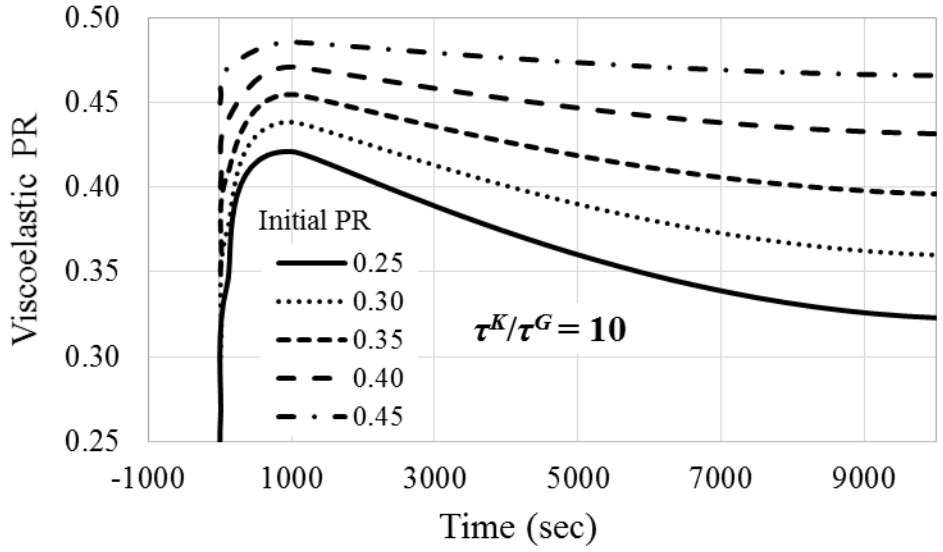

Figure 5.1. Time-dependence of Poisson's ratios based on varying initial PR for relaxation time ratio τ^K/τ^G=10.

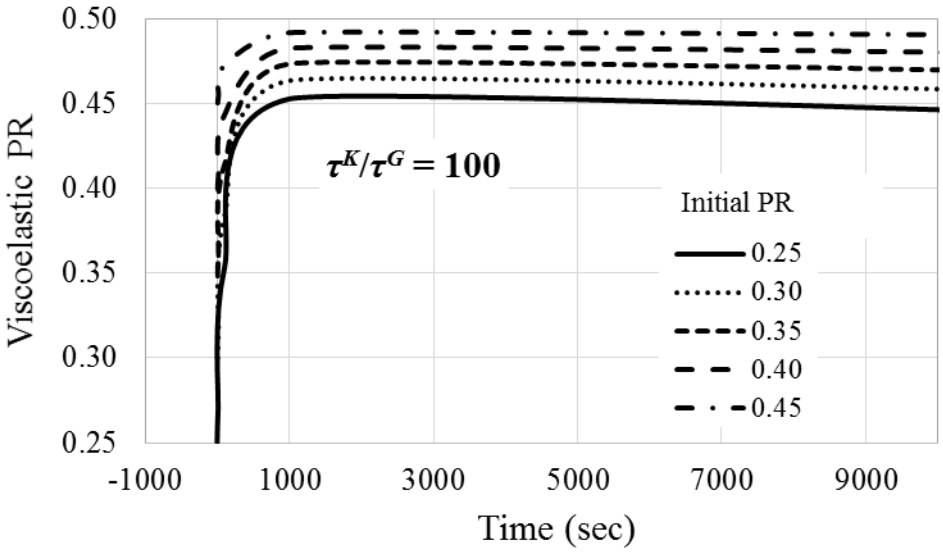

Figure 5.2. Time-dependence of Poisson's ratios based on varying initial PR for relaxation time ratio τ^K/τ^G=100.

Moreover, the effect of assuming similar relaxation times for *G(t)* and *K(t)*, a normal practice, is demonstrated from Figure 5.3.

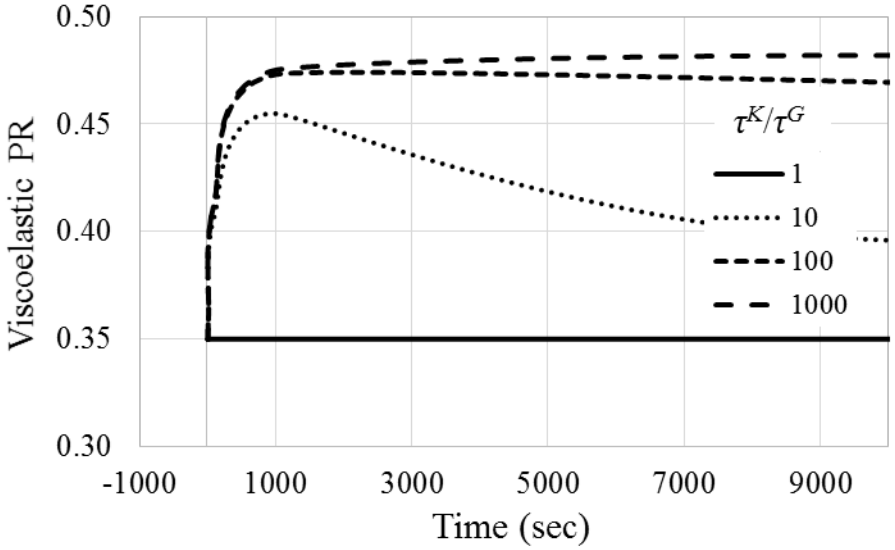

Figure 5.3. Poisson's ratios for various relaxation time ratios between bulk modulus and shear modulus.

Class I (Equation 5.34) and Class III (Equation 5.11) PRs are compared; it has been observed that even for constant stress case, both the cases give different results as shown in the Figure 5.4. Figure 5.5 shows that both PRs match only either at very initial time ($t \approx 0$) or very long times.

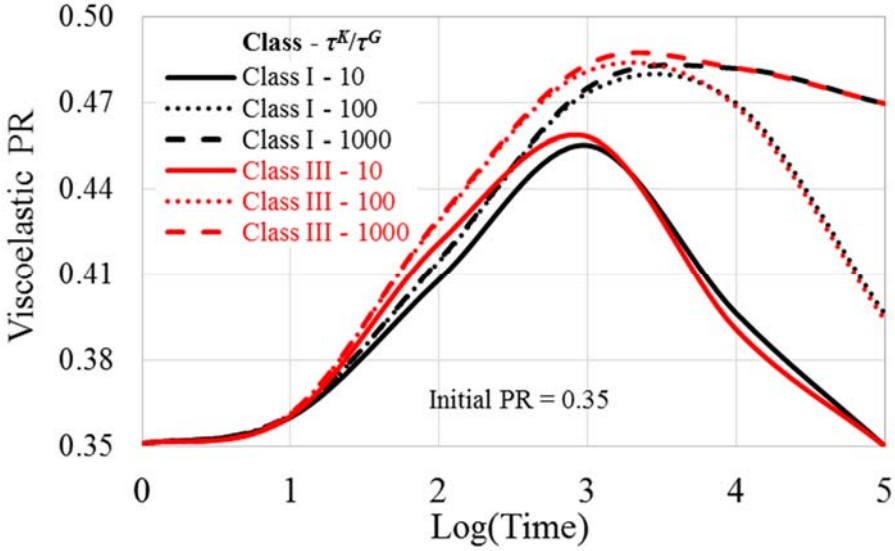

Figure 5.4. A comparison of class I and class III Poisson's ratios for various relaxation time ratios.

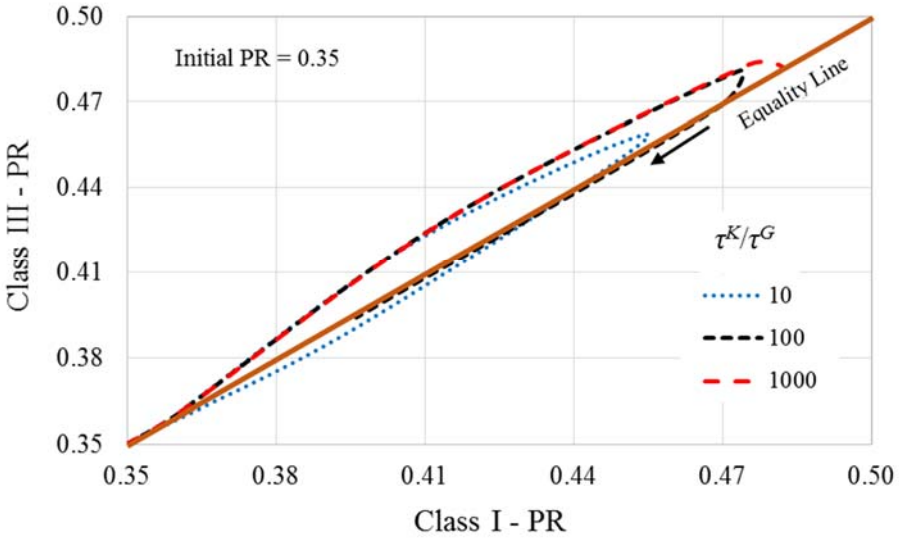

Figure 5.5. Inequality between Poisson's ratios from two different definitions.

5.5.2 Effect of Instantaneous Bulk Modulus on Poisson's Ratio

Constant PR assumption lead to selection of false K_0 and G_0 based on E_0 obtained from a uniaxial test. Therefore, influence of different moduli ratios (i.e. K_0/G_0 and K_0/E_0) was explored. It can be deduced from the Figure 5.6 and Figure 5.7 that sensitivity of the PRs is strongly influenced by the moduli ratios. Lower the moduli ratios, greater the sensitive of PRs with time. Larger the ratios K_0/G_0 and K_0/E_0, lower the PRs sensitivity and closer to the material incompressibility ($K_0 = \infty$) i.e. $v^I(t) = 0.5$. The typical assigned PR value of 0.35 to asphalt concrete corresponds to K_0 / E_0 and K_0/G_0 values of 3.33 and 9, respectively.

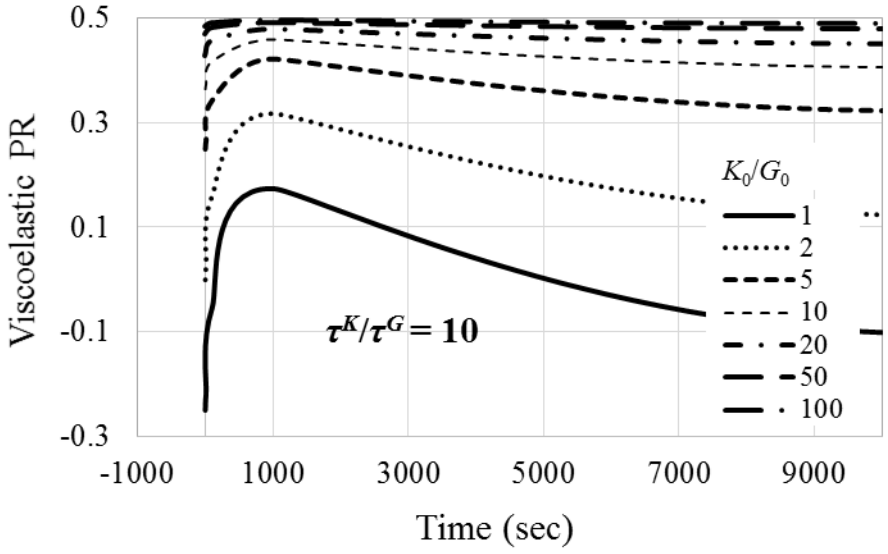

Figure 5.6. Poisson's ratios at different moduli ratios (K_0/G_0).

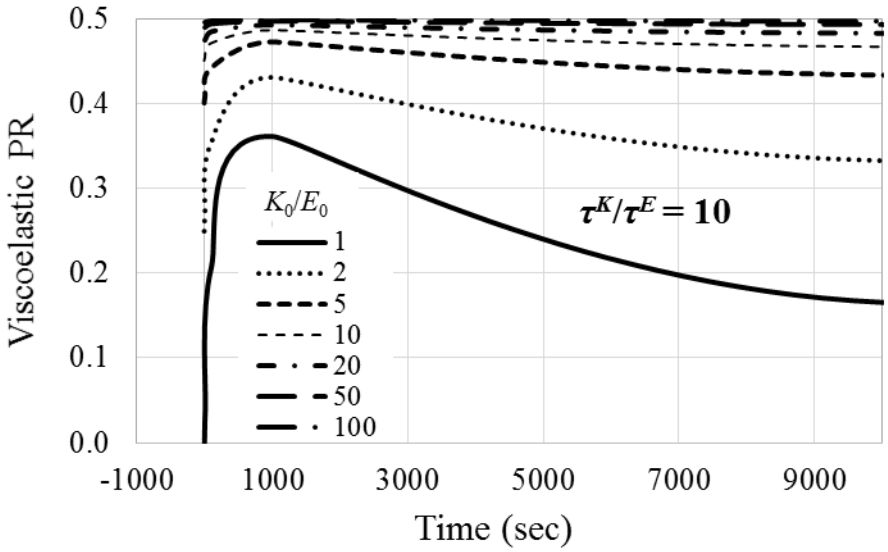

Figure 5.7. Poisson's ratios at different moduli ratios (K_0/E_0).

5.5.3 Effect of Time-Dependent Poisson's Ratio on E_{1111} and E_{1122}

The ultimate goal of material characterization is to provide modulus or compliance functions or coefficients to characterize stress-strain relationship accurately for generalized stress states. This chapter deals with various approaches for viscoelastic characterization and sensitivity of Poisson's ratio to time, stress state, and modulus ratios.

Based on the results presented in this chapter and elsewhere in the literature (Hilton 2001 and 2011), it is concluded that PRs cannot be used as a fundamental material property.

It is important to quantify the magnitude of error in the ultimate material properties such as relaxation modulus or compliance functions for various Poisson's ratio assumptions. Minor errors in PRs and relaxation time may lead to significant fluctuations in modulus and their time responses. The relaxation modulus components E_{1111} and E_{1122}, shown in Figure 5.8, for different relaxation times ratios were calculated using Equation 5.35 and 5.36, respectively. An error term was introduced to quantify the impact of time-dependent PR. The percent difference in E_{1111} and E_{1122} for different relaxation time ratios τ_K/τ_G relative to a relaxation time ratio $\tau_K/\tau_G=1$ were calculated using Equation 5.37. Here, the case with relaxation time ratio $\tau_K/\tau_G=1$ is considered to be the reference state, where PR becomes constant.

$$E_{1111} = E_{11} = \frac{4G(t) + K(t)}{3} \tag{5.35}$$

and

$$E_{1122} = E_{12} = \frac{-4G(t) + 2K(t)}{3} \tag{5.36}$$

$$\text{Difference (\%)} = \frac{E_{11}^{\tau^K/\tau^G=1} - E_{11}^{\tau^K/\tau^G=10,100,1000}}{E_{11}^{\tau^K/\tau^G=1}} \times 100 \tag{5.37}$$

The solid blue and red curves show the usual practice, i.e. assuming same relaxation times for all moduli. It can be seen that values of the moduli and their time responses change immensely with change in relaxation ratios. Figure 5.9 demonstrates that a single- to triple-decade time shift between bulk and shear moduli produces significant differences in E_{1111} and E_{1122}. It is evident form the above simulations that the assumptions of constant PRs and similar relaxation time lead to errors in relaxation moduli determination that results in incorrect stress and strain analyses.

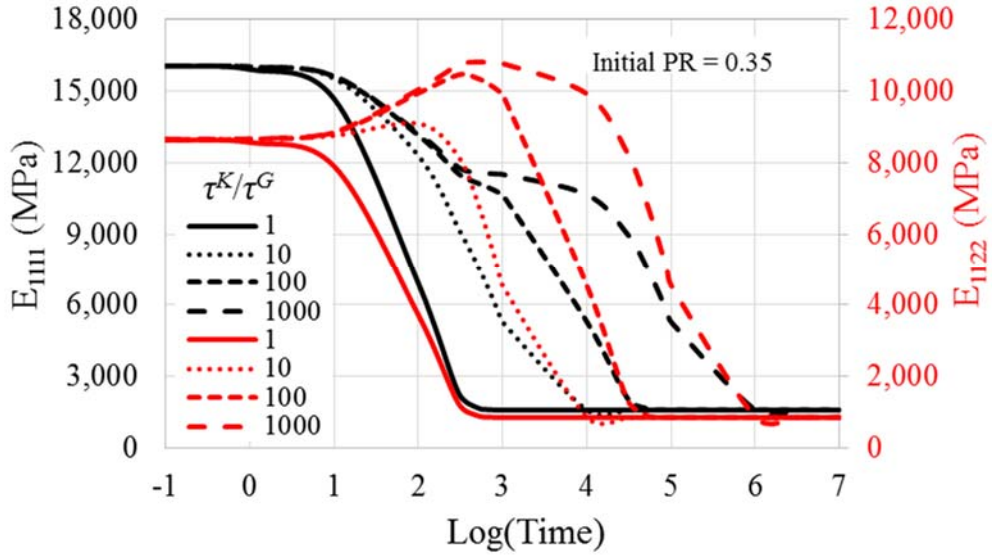

Figure 5.8. Relaxation moduli, E_{1111} and E_{1122}.

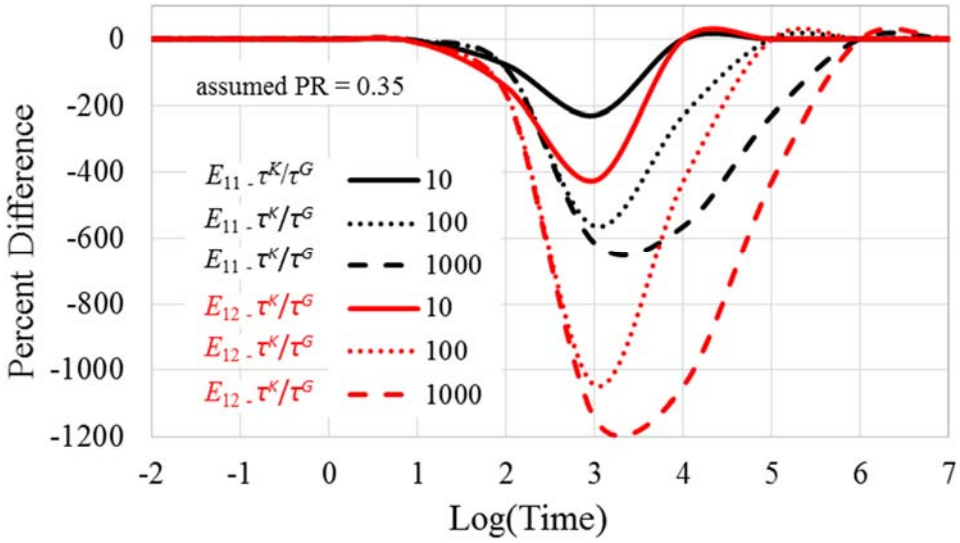

Figure 5.9. Differences in relaxation moduli relative to τ^K/τ^G=1.

5.6 Numerical simulations for Stress Dependence of Viscoelastic Poisson's Ratios

The classical PR definition (Equation 5.10) for viscoelastic materials under uniaxial load with stress $\sigma_{11} \neq 0$ and all other stresses $\sigma_{ij} = 0$ can be rewritten as

$$\nu_{ij}^{I}(t) = -\frac{\varepsilon_{\underline{jj}}(x,t)}{\varepsilon_{\underline{ii}}(x,t)} = -\frac{\int_{-\infty}^{t} C_{\underline{jj}11}(x,t-t')\sigma_{11}(x,t')dt'}{\int_{-\infty}^{t} C_{\underline{ii}11}(x,t-t')\sigma_{11}(x,t')dt'} \qquad i \neq j \qquad (5.38)$$

Equation 5.38 clearly shows that viscoelastic PR is stress and stress history dependent and is therefore, unlike moduli and compliances, not a unique material property. All five classes of PRs, as defined by Hilton (2001), are dependent on time and loading histories. Hilton (2001, 2009, and 2011) gives detailed account of very restricted scenarios and conditions when PRs do in fact can be called as a material property. The EVCP is applicable only on the PRs obtained using a relaxation test (ε_{11} = constant), also suggested by Tschoegl (1989 and 2002), but those PRs are still path and history dependent and do not represent a general definition for viscoelastic PRs. It is important to note that it is physically impossible to apply a constant stress or strain (in a creep and relaxation test, respectively). A constant stress or strain can never be applied instantaneously i.e. in time $t = 0$; there is always some path through which the stresses or strains pass to reach a steady state.

To visualize the stress dependency of the PRs, the Class 1 PRs (Equation 5.34) were determined under different axial stress modes and magnitudes. As before, value of G_0 was assumed and K_0 was obtained using constant PR of 0.35. Figure 5.10 shows the effect of different stress configurations on PRs. It was observed though that PRs are independent of the stress magnitude, e.g. a in $\sigma_{11} = at$ or the magnitude of constant stress in a creep test will not cause any variation in PR; but the function itself will.

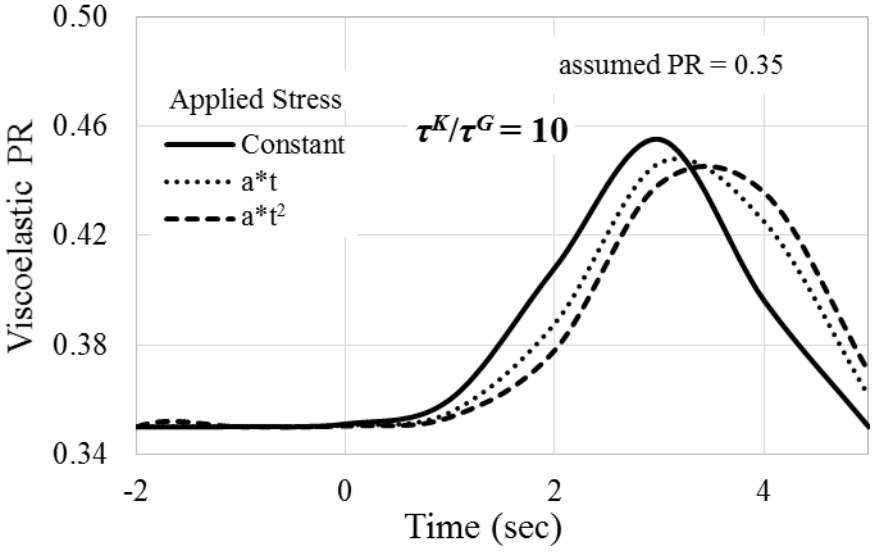

Figure 5.10. Stress dependence of viscoelastic Poisson's ratios.

5.7 Summary and Remarks

This chapter identifies the problems associated with assuming constant PRs and similar moduli relaxation times for viscoelastic materials in general and asphalt concrete in specific. A brief literature review was conducted emphasizing the state-of-the-practice of using PR for viscoelastic materials including asphalt concrete. Majority of the reviewed studies used an assumption of constant PR value of 0.35. It is evident from the literature search, analytical derivations and examples presented in this chapter that PR is a derived material property that depends on time, stress, and stress history, should not be used to characterize viscoelastic materials. Alternative protocols were recommended to bypass the PRs to avoid the complexities associated with their use.

Inapplicability of correspondence principle on viscoelastic PRs is presented. In order to realize the time- and stress-dependence of viscoelastic PRs, few simulations are conducted. The effect of varying moduli ratios (K_0/G_0 and K_0/E_0) on PRs is also studied. It is evident from the simulations that the assumptions of constant PRs and similar relaxation time lead to some serious errors in characterization of viscoelastic materials. Hence, use of PRs should be avoided in characterizing the asphalt concrete. Next chapter deals with introduction and implementation of a novel numerical technique to determine the viscoelastic properties of asphalt concrete bypassing the PRs.

CHAPTER 6

ALTERNATE PROTOCOL FOR MULTI-AXIAL CHARACTERIZATION OF ASPHALT MIXTURES

6.1 Introduction

The previous chapter discussed in detail the inefficacy of Poisson's ratios (PR) to properly characterize the viscoelastic materials. Assumption of a time- and stress-independent PR along with equal moduli relaxation times cause significant errors in estimating the three dimensional constitutive relationship of viscoelastic materials. Similar arguments can also be made for linear viscoelastic characterization of asphalt concrete. In addition, the introduction of recycled materials (such as reclaimed asphalt pavements (RAP), recycled asphalt shingles (RAS), and steel slag) and other innovative materials like bio-asphalts and technologies like warm mix asphalt have made the asphalt concrete characterization more challenging than before.

Realistic characterization of materials used in pavements is critical to accurately predict its response under complex traffic and environmental loading conditions. Pavements are subjected to repeated applications of traffic loadings (higher frequency) and thermal loads (lower frequency) which result in three-dimensional stress and strain fields. Complexity of loading is higher on or near-surface of pavements due to three-dimensional and non-uniform contact stresses, higher temperature and moisture gradients. Accurate response prediction of pavements under these conditions requires three dimensional characterization of asphalt concrete and sub layers.

The proper way of characterizing the isotropic viscoelastic material is to experimentally determine directly and simultaneously any two of the three fundamental material properties; Young's modulus $E(t)$, shear modulus $G(t)$, and bulk modulus $K(t)$. These properties can be determined in separate tests; but it is not always possible based on availability of required equipment in laboratories, which is very expensive and

complicated system.

An alternative approach, in the absence of separate shear and bulk modulus tests, is through a uniaxial modulus test along with an assumption of PR. The two of the material functions (in this case *E(t)* and PR) can be sufficient to characterize an isotropic elastic material whose properties are not dependent on stress-state (confining pressure). Elastic materials (bound and some of the unbound layers in the pavements) can be characterized with this approach successfully. Poisson's ratio can be predicted with sufficient accuracy for such materials and it can be safely assumed that it is time and stress independent.

However, viscoelastic materials present some challenges for its three-dimensional characterization. As discussed in Chapter 5, PR is time, stress, and path dependent. In addition, many of the well-known and commonly applied formulations for calculation of PR are shown to be theoretically incorrect. Therefore, three-dimensional characterization of viscoelastic materials using *E(t)* and PR couple can introduce significant errors to the constants of constitutive relationship of viscoelastic materials.

An alternative way of multi-axial characterization bypasses PR and takes advantage of existing uniaxial tests with minor modification. This alternative protocol was first introduced by Hilton and his colleagues (Hilton and Fouly 2007). This chapter deals with developing an experimental protocol to implement numerical procedures to determine the viscoelastic properties of asphalt concrete without a need for the PRs. Details of the algorithm and formulations are presented in this chapter. The alternative protocols are implemented for characterization of the asphalt mixtures with and without RAP

A laboratory experimental protocol was developed to conduct multi-axial characterization of the designed virgin and recycled asphalt mixtures without the use of PR. Following tasks have been conducted:

1. Detailed description of the algorithm followed.
2. Code development and verification
3. Development of laboratory experimental protocol
4. Determination of *E(t)*, *G(t)*, and *K(t)*

6.2 Determination of Bulk and Shear Relaxation Moduli in Time Domain

Uniaxial quasi-static tests like complex modulus (AASHTO TP 62) test is commonly conducted for asphalt material characterization mainly because of the convenient moduli determination based on measured harmonic stresses and strains. The outcome of this test is complex Young's modulus and phase angle. This information is translated to three dimensional characterization using an assumed and constant PR.

Hilton and his colleagues formulated alternative protocols for determination of three dimensional material properties (*K(t)*, *G(t)*, and *E(t)*) from uniaxial tests without using PRs (Hilton and Fouly 2007). The protocol was further explained and utilized experimentally by Shtark et al. (2012). Lately, Michaeli et al. (2013) provided a solution to the problem directly in real time space without the use of integral transforms. The solution includes the complete history of loading and of displacements including their build ups. In this study, Michaeli's approach is adopted to characterize asphalt mixtures with and without RAP.

The viscoelastic constitutive equations defining *K(t)* and *G(t)* can be written as

$$\sigma(x,t) = \int_0^t K(t-t') \frac{\partial \varepsilon_v(x,t')}{\partial t'} dt' \tag{6.1}$$

where $\sigma(x,t) = \frac{\sigma_{ii}(x,t)}{3}$ = dilatational stress and $\varepsilon_v(x,t) = \frac{\varepsilon_{ii}(x,t)}{3}$ = dilatational strain, and

$$S_{ij} = \sigma_{ij}(x,t) - \delta_{ij}\sigma(x,t) = 2\int_0^t G(t-t') \frac{\partial \varepsilon_{ij}^d}{\partial t'} dt' \tag{6.2}$$

where S_{ij} is stress deviator, $\varepsilon_{ij}^d = \varepsilon_{ij}(x,t') - \delta_{ij}\varepsilon(x,t')$ is strain deviator and δ_{ij} is Kronecker delta; *t* is the present time and *t'* is some previous (historical) time. Considering a specific example of 1-D test conducted under following boundary conditions.

$$\sigma_{11} = \sigma_{11}(\mathrm{t}), \text{ and } \sigma_{22} = \sigma_{33} = 0 \tag{6.3}$$

$$\frac{\partial \varepsilon_{11}(x,t)}{\partial t} = \begin{Bmatrix} f_{1\varepsilon}(t) & 0 \le t \le t_1 \\ \dot{\varepsilon}_{11}^c & \mathrm{t} \ge \mathrm{t}_1 \end{Bmatrix} \tag{6.4}$$

$$\frac{\partial \varepsilon_{22}(x,t)}{\partial t} = \frac{\partial \varepsilon_{33}(x,t)}{\partial t} = \begin{Bmatrix} f_{2\varepsilon}(t) & 0 \le t \le t_1 \\ f_{3\varepsilon}(t) & \mathrm{t} \ge \mathrm{t}_1 \end{Bmatrix} \tag{6.5}$$

where t is present time and t_1 is end time of the loading phase, for example in a creep test, t_1 would be the time to reach from no load condition (t = 0) to target creep load. It is noteworthy that this protocol is equally applicable to other 1-D loading such as constant strain (relaxation), constant load (creep), etc. The stresses and strains from Equations 6.3 to 6.5 results into

$$S_{ij} = \sigma_{ij}(x,t) - \delta_{ij}\sigma(x,t) \Rightarrow S_{11} = \sigma_{11}(x,t) - \frac{\sigma_{11}(x,t)}{3} = \frac{2}{3}\sigma_{11}(x,t)$$

$$\varepsilon_{ij}^{d}(x,t') = \varepsilon_{ij}(x,t') - \delta_{ij}\varepsilon(x,t') \Rightarrow \varepsilon_{11}^{d} = \frac{2}{3}\left[\varepsilon_{11}(x,t') - \varepsilon_{22}(x,t')\right]$$

$$\sigma(x,t) = \frac{\sigma_{11}(x,t)}{3} \text{ and } \frac{\varepsilon_{11}(x,t') + 2\varepsilon_{22}(x,t')}{3} = \varepsilon(x,t')$$

Substituting into equation 6.1 and 6.2 yields,

$$\sigma_{11}(x,t) = \int_0^t K(t-t')\frac{\partial}{\partial t'}\left[\varepsilon_{11}(x,t') + 2\varepsilon_{22}(x,t')\right]\, dt' \tag{6.6}$$

and

$$\sigma_{11}(x,t) = 2\int_0^t G(t-t')\frac{\partial}{\partial t'}\left[\varepsilon_{11}(x,t') - \varepsilon_{22}(x,t')\right]\, dt' \tag{6.7}$$

Since $G(t)$ and $K(t)$ can be represented by Prony series,

$$K(t) = K_\infty + \sum_{j=1}^{N^K} K_j \exp\left(-\frac{t}{\tau_j^K}\right) \tag{6.8}$$

and

$$G(t) = G_\infty + \sum_{n=1}^{N^G} G_n \exp\left(-\frac{t}{\tau_n^G}\right) \tag{6.9}$$

with $K_0 = K_\infty + \sum_{j=1}^{N^K} K_j$ and $G_0 = G_\infty + \sum_{j=1}^{N^G} G_j$ respectively. Substitution of these series and integration by part transform Equations 6.6 and 6.7 into

$$\sigma_{11}(t) = \left(K_\infty + \sum_{j=1}^{N^K} K_j\right)\left[\varepsilon_{11}(t) + 2\varepsilon_{22}(t)\right] - \sum_{j=1}^{N^K}\left[\frac{K_j}{\tau_j^K}\int_0^t \exp\left(-\frac{t-t'}{\tau_j^K}\right)\left[\varepsilon_{11}(t') + 2\varepsilon_{22}(t')\right]dt'\right] \tag{6.10}$$

$$\sigma_{11}(t) = 2\left(G_\infty + \sum_{j=1}^{N^G} G_j \right)\left[\varepsilon_{11}(t) - \varepsilon_{22}(t)\right] - 2\sum_{j=1}^{N^G}\left[\frac{G_j}{\tau_j^G}\int_0^t \exp\left(-\frac{t-t'}{\tau_j^G}\right)\left[\varepsilon_{11}(t') - \varepsilon_{22}(t')\right]dt' \right] \tag{6.11}$$

and, similarly

$$\sigma_{11}(t) = \left(E_\infty + \sum_{j=1}^{N^G} E_j \right)\varepsilon_{11}(t) - \sum_{j=1}^{N^E}\left[\frac{E_j}{\tau_j^E}\int_0^t \exp\left(-\frac{t-t'}{\tau_j^E}\right)\varepsilon_{11}(t')\,dt' \right] \tag{6.12}$$

Strain function developed in Equations 6.4 and 6.5 can be inserted above to define RHS in an analytical form. Following the definition of strain function, the Equations 6.10 to 6.12 are now defined for loading phases i.e. $0 \le t \le t_1$ and for steady-state phase i.e. $t \ge t_1$. Partition of RHS in two phases is needed since the response of the material usually exhibits a sharp gradient at time $t = t_1$ and it is difficult to fit a continuous function to such a function. The solution of Equations 6.10 to 6.12 through a non-linear optimization procedure yield material moduli *E(t)*, *G(t)* and *K(t)* and their corresponding relaxation times independently.

The number of Prony series parameters N^G and N^K may or may not be equal. Similarly, values of each set of τ's are calculated separately for each modulus.

Alternatively, substituting Equation 6.1 into 6.2 gives (Michaeli et al. 2013),

$$\sigma_{11}(x,t) = \int_0^t \underbrace{\frac{4G(t-t') + K(t-t')}{3}}_{=E_{1111}(t-t')} \frac{\partial \varepsilon_{11}(x,t')}{\partial t'}\,dt' + \int_0^t \underbrace{\frac{-4G(t-t') + 2K(t-t')}{3}}_{=E_{1122}(t-t')} \frac{\partial \varepsilon_{22}(x,t')}{\partial t'}\,dt' \tag{6.13}$$

$$0 = \int_0^t \underbrace{\frac{-2G(t-t') + K(t-t')}{3}}_{=E_{2211}(t-t')/2=E_{1122}(t-t')/2} \frac{\partial \varepsilon_{11}(x,t')}{\partial t'}\,dt' + \int_0^t \underbrace{\frac{2G(t-t') + 2K(t-t')}{3}}_{=E_{1111}(t-t')+E_{1122}(t-t')/2} \frac{\partial \varepsilon_{22}(x,t')}{\partial t'}\,dt' \tag{6.14}$$

which are isotropic constitutive relations for $\varepsilon_{22} = \varepsilon_{33}$ and define E_{ijkl} in real time space. As an alternative to Equations 6.10 to 6.12, Equations 6.13 and 6.14 can be solved as two simultaneous equations with two unknowns.

The protocol defined herein provides an alternative approach for 3-D linear

viscoelastic characterization. It uses the existing framework of uniaxial tests with only an addition of strain measurements in the radial or secondary direction. This allows determination of linear viscoelastic coefficients (relaxation modulus and times) independently for bulk, shear, and Young's moduli.

6.3 The Development of Multi-Axial Linear Viscoelastic Characterization Algorithm and Verification

A MATLAB code was developed to take the test data file as input and provide *G(t)*, *K(t)*, and *E(t)* as output. The step-by-step algorithm to obtain the moduli is as follows:

1. Collecting uniaxial test data for axial stress σ_{11}, axial strain ε_{11}, and transverse strain ε_{22}, during the entire test time. If possible, collect the data at very high rate during initial transient loading phase $(0 \le t \le t_1)$ to collect sufficient data points.
2. Fitting polynomial functions to ε_{11} and ε_{22} by least square fits. Fit ε_{11} and ε_{22} during transient and steady state loading separately.
3. Keeping the stress σ_{11} as target function, non-linear optimization is used to obtain Prony coefficients (G_j, K_j, and E_j and their respective relaxation times τ^G, τ^K, τ^E) from Equations 6.12 to 6.14. Relaxation times (τ) for each moduli are first estimated, the final values are determined through optimization process.
4. Constraints on instantaneous and long-time (infinity) moduli can be applied if appropriate estimates can be made. Repercussions of not applying constraints will be evaluated later in this chapter. It is important to note here that the relaxation times and coefficients may lose their physical meaning; however, the key parameters are the entire functions *G(t)*, *K(t)*, and *E(t)* and not their individual components.

In order to verify the proper functioning of the developed code, test simulations were conducted. The test simulations are designed for the uniaxial conditions with imposed axial strains in such a way that an analytical and exact expression can be obtained for the target function axial stresses. The objective here is to recover relaxation function using the code developed with the input relaxation function. First, a monotonically increasing vertical axial strain ε_{11} with a constant strain rate $\frac{d\varepsilon_{11}}{dt}$ is imposed. Corresponding axial stresses can be calculated using the hereditary equation for

this case as follows:

$$\sigma_{11}(t) = \int_0^t E(t-t')\frac{\partial \varepsilon_{11}(t')}{\partial t'}dt' \tag{6.15}$$

The stress σ_{11} becomes

$$\sigma_{11}(t) = \frac{d\varepsilon_{11}(t)}{dt}\int_0^t E(t-t')dt' \tag{6.16}$$

where $E(t)$ can be represented by Prony coefficients as

$$E(t) = E_\infty + \sum_{j=1}^{N^E} E_j \exp\left(-\frac{t}{\tau_j^E}\right) \tag{6.17}$$

where $E_\infty = E_0 + \sum_{n=1}^{N^E} E_n$. To keep the calculations simple, just one spring and one dashpot was considered, i.e. j=1. That resulted in

$$\sigma_{11}(t) = \frac{d\varepsilon_{11}(t)}{dt} \times \left(tE_\infty - E_1\tau_1(\exp\left(-\frac{t}{\tau_1}\right) - 1)\right) \tag{6.18}$$

Values of E_0 = 800, E_∞ = 50, E_1 = 750, and τ_1 = 60 were assumed to produce input for stress function. Figure 6.1 shows the comparison of the $E(t)$ obtained using the algorithm and the input.

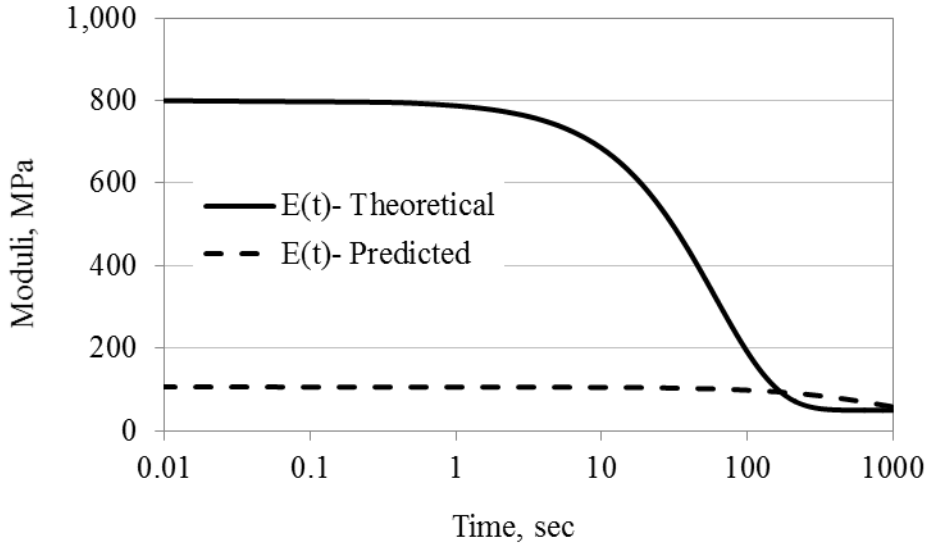

Figure 6.1. A comparison of input relaxation modulus and algorithm solution for large time interval.

As seen in the Figure 6.1, the algorithm was unable to recover the same *E(t)*. Probing the code revealed that results could be improved by decreasing the time interval between the two data points. Analysis with data having smaller time increments (1/1000 sec) provided a good fit between the theoretical and analytical methods (Figure 6.2).

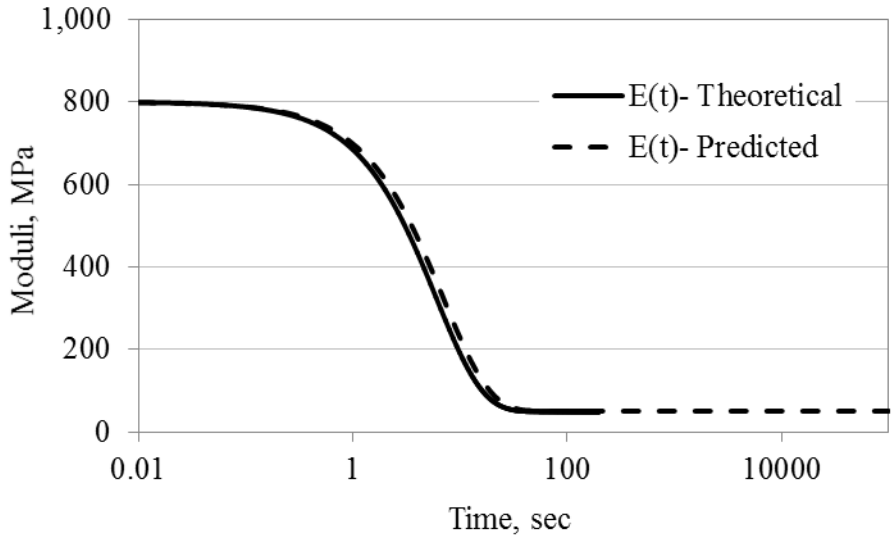

Figure 6.2. A comparison of input relaxation modulus and algorithm solution for smaller time intervals.

Further analysis indicated that amount of strain rate (slope of strain w.r.t. time) also had an effect on recovering the similar results. Higher slopes (0.1 strain/time interval) gave good match even at high time intervals (such as 0.1 sec or 1 sec), whereas, the smaller strain rates (3.12405E-07) needed time interval of about 0.001 sec to have a better fit.

In another simulation, a bi-linear strain data was simulated. The strain data was produced in such a way that the axial strain ε_{11} having a slope (strain rate) before a specific time followed by another, gentler, slope. This exercise was done to simulate an actual test data, where a ramp transient load is followed by a steady state load. A good stress fit was obtained using the fabricated data especially when constraints were not applied.

The code was then run on actual relaxation test data with different data acquisition rates. The fact that the stress in the actual data had kink, resulted in inability of achieving a good stress fit initially. Removing the constraints on instantaneous modulus values improved the fit tremendously.

6.4 Experimental Protocol

In this section, implementation of the alternative multi-axial linear viscoelastic characterization for asphalt concrete specimens is introduced. The SuperPave gyratory compactor (SGC) was used to prepare asphalt concrete cylindrical test specimens. The air voids for the SGC cylinders were kept at 7±0.5% which resulted in air voids of 4.5±0.5% for the cut-and-cored 150-mm tall and 100-mm thick test samples. Before testing the recycled mixtures prepared for this study, a more homogenous 9.5-mm NMAS surface mix was selected to conduct trial tests. The type and content of asphalt binder in the surface mixture were PG 70-22 and 6.1%, respectively.

Different loading configurations under which the surface mix samples were initially tested were compressive relaxation and creep, tensile relaxation and creep, monotonic strain/stress, and multiple creep-recovery. The on-specimen axial deformations were measured with three axial extensometers, whereas, two chain extensometers were used to measure transverse deformation. The actual test sample and the test schematic are shown in the Figure 6.3.

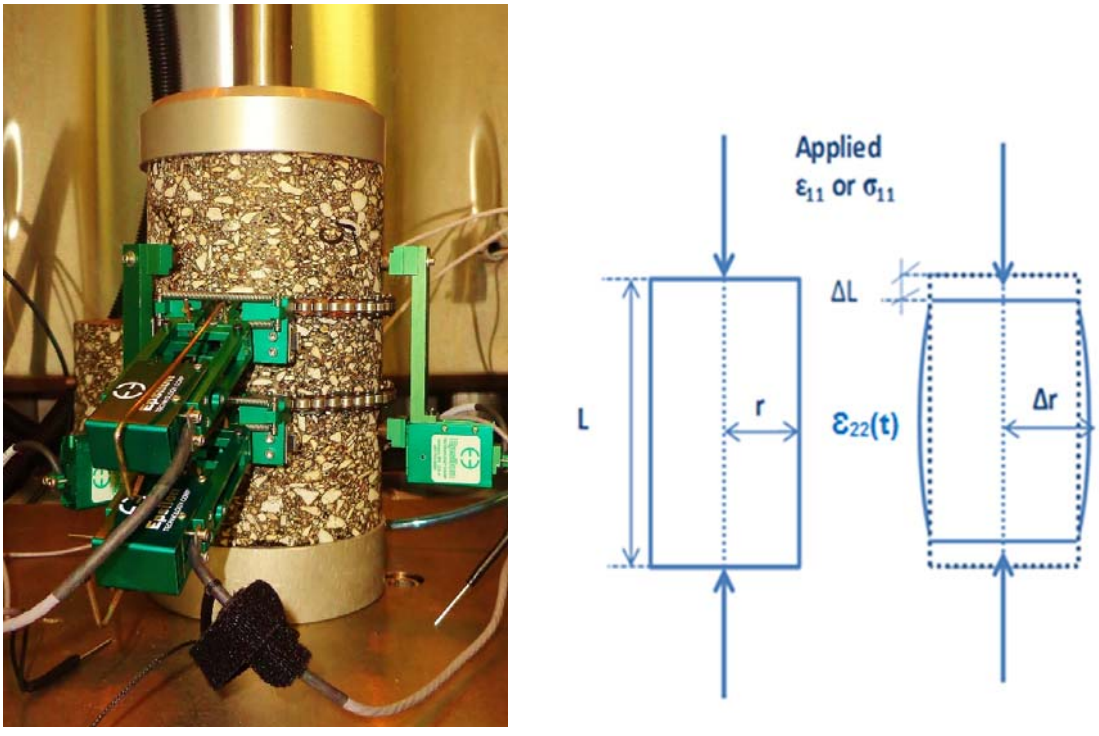

(a) *(b)*

Figure 6.3. (a) An instrumented sample and (b) test schematics.

Based on the preliminary tests, two downsides were observed with tensile tests. First, the inconvenience of preparing test sample using epoxy glues and second, and the more critical one, the reliability of measuring the lateral contraction using chain extensometers. Despite manufacturer assurances, chain extensometers were avoided to use for measuring lateral contraction.

Two testing modes, that is compressive relaxation (CR) and compressive Creep (CC) tests, were selected for testing the control and recycled mixtures. All relaxation tests are controlled based on actuator (cross-head) strains not on-specimen strains. The on-specimen strains continuously evolve during the test; it may not be a true relaxation test. The ratio of actuator deformation to on-specimen extensometer deformation largely depends on the testing temperature; lower the temperature higher is the ratio especially at the start of the test. At higher temperatures (38ºC or higher), the on-specimen strains can easily exceed the applied actuator strains. Table 6.1 shows the final test configuration adopted for this study.

Table 6.1. Final tests configuration.

Test Type	Loading Phase	Loading Type
Compressive Relaxation	Initial transient loading, $t \le t_1 = 0.25$ sec	Constant strain rate $\dot{\varepsilon}_{11}$ 1200 ms/sec[1] and 2400 ms/sec
	Steady state Loading, $t \ge t_1$	Constant ε_{11} 300 ms or 600 ms
Compressive Creep	Initial transient loading, $t \le t_1 = 0.25$ sec	Constant stress rate $\dot{\sigma}_{11}$ 1 kN/sec and 2 kN /sec
	Steady state Loading, $t \ge t_1$	Constant σ_{11} 0.25 kN or 0.5 kN

[1] 1200 ms/sec would reach the steady state target in time $t_1 = 0.25$ second. Similarly for other loading conditions.

AASHTO IDT Creep test (T 322) recommends keeping the strain levels between 50-750 microstrains (ms). Actuator strain levels of 300 ms and 600 ms made sure that on-specimen strains did not exceed the 500 ms for the tests conducted at 21 ºC. Any test exceeding the 500 ms limit was stopped before the total test time (1000 sec) to avoid any permanent strain accumulation. The initial transient loading rate was selected in such a way that the target loading in steady state conditions are achieved within time t_1. For

example, in a 300 ms CR test, initial transient load was applied at a rate of 1200 ms/sec reaching the target strain of 300 ms in 0.25 sec.

It is worth mentioning here that ideally the initial loading time t_1 should be selected in such a way that t_1 is equal to or less than the relaxation onset time t_0, the time at which creep or relaxation begins (Shtark 2013). If relaxation starts before the loading reaches to its constant value, the assumptions made to simplify viscoelastic characterization (simplification derived from constant stress or strain tests) are violated. Therefore, the target load or deformation in a creep or relaxation tests should be achieved before the time t_1 for accurate viscoelastic characterization. The stress-strain ratio σ/ε can provide relaxation or creep functions only if loading reached its constant target value before relaxation starts. It is difficult though, to attain such quick loading rate in available testing systems for asphalt concrete and becomes increasingly difficult with increase in temperatures because of decrease in t_0 as shown in Figure 6.4.

Initially, time t_1 = 1 sec and 4 sec were tried which proved to be too greater than t_0 as shown in Figure 6.5. Relaxation onset time t_0 could not be measured from the data but the loading time t_1=0.25 sec was eventually chosen to get as closer to t_0 as practically possible. The loading systems was able to achieve the target load in 0.25 sec for creep test; but for relaxation test it could not, as shown in Figure 6.6. The target actuator strain levels were achieved in 0.49 seconds for most of the relaxation tests. The impact of initial loading time on viscoelastic characterization of asphalt concrete materials is under looked. Significant errors can be introduced to relaxation or creep compliance functions when simply stress-strain ratio is used.

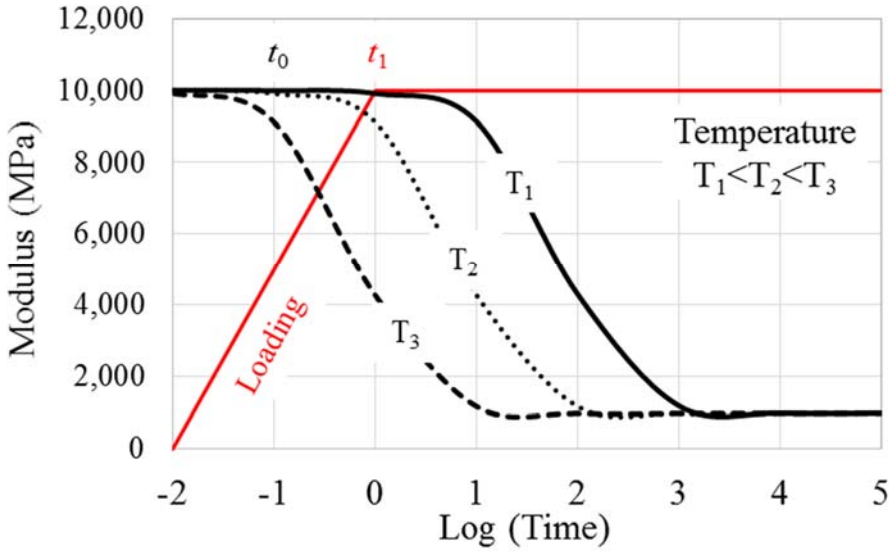

Figure 6.4. Modulus relaxation variation with temperature and loading phase.

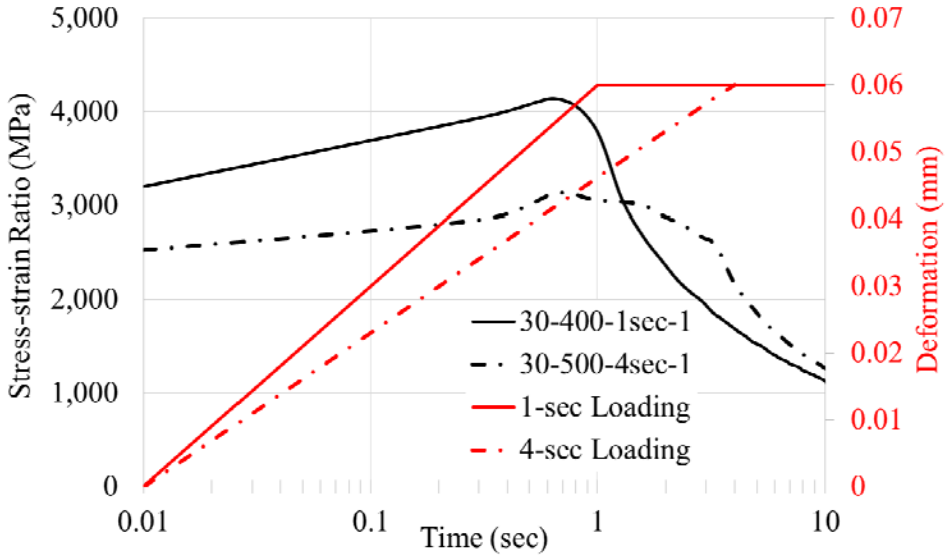

Figure 6.5. Relaxation tests conducted at t_1 = 1 sec and 4 sec illustrating the stress-strain ratio prior to reaching constant deformation in the loading head.

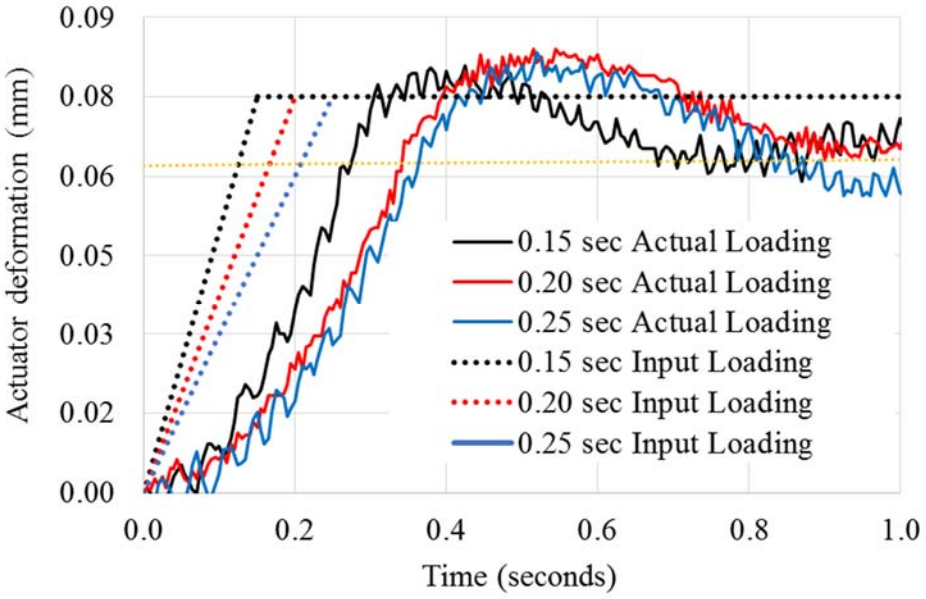

Figure 6.6. Input and actual loading for t_1 = 0.15, 0.20, and 0.25 sec.

Table 6.2 shows the adopted test matrix to test three District 5 mixtures, i.e. control mixture and recycled mixtures with 30% and 50% RAP. Six tests were conducted on each specimen in the same sequence as shown in the Table 6.2. Each sample was tested under all loading conditions in the same position without moving it. A rest period of at least 60 min was used between tests. To make sure that the testing suit did not cause any plastic deformation or damage to the sample, complex modulus test (E^*) was conducted on each sample before and after the testing suit.

Table 6.2. Experimental matrix for relaxation and creep tests.

Mix Type	E*-1	Relaxation		Creep		E*-2
		300 ms	600 ms	0.25 kN	0.5 kN	
Control	3	3	3	3	3	3
30% RAP	3	3	3	3	3	3
50% RAP	3	3	3	3	3	3

6.5 Results and Discussion

The output data was processed following the algorithm explained in section 6.3. The results of the complex modulus tests conducted before and after the relaxation and creep testing suit are shown in Figure 6.7. Though not intended to differentiate the recycled mixtures from each other, the increased in stiffness due to addition of RAP is clearly

visible in the plot. It can be concluded from the figures that the samples were tested without damaging them. There were few samples though (especially the control mix) which showed a slight increase in the E^* value after the testing suit; those samples were not taken into consideration in the analysis.

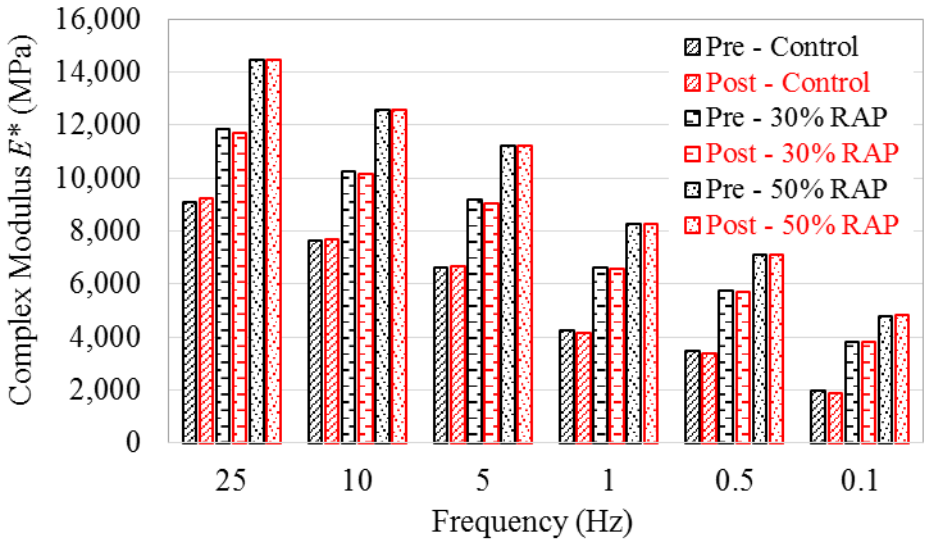

Figure 6.7. Complex modulus— pre- and post-testing values at 21ºC.

Both the compressive relaxation and creep test results were analyzed. It was found that the developed algorithm (code) did not result in some *"reasonable"* output data for the creep test. Apart from a few exceptions, the creep test results showed uncharacteristic moduli behavior, i.e. higher *G(t)* and *E(t)* than *K(t)*. In general, shear modulus *G(t)* is higher than its bulk counterpart *K(t)* only in auxetic materials which have negative elastic PRs and expand in lateral direction when stretched in axial direction. Figure 6.8 shows different moduli under different creep load magnitudes, when analyzed without applying constraints. This behavior, shown in Figure 6.8, exposed inability of the developed algorithm to tackle creep data. The algorithm defined by equations 6.10 to 6.12 is designed originally for derivation of relaxation functions with stresses measured on left hand side (target function) and strains applied (source function) on the right hand side along with the relaxation functions. Similar algorithms can be set up for calculation of compliance function with reversing target and source functions.

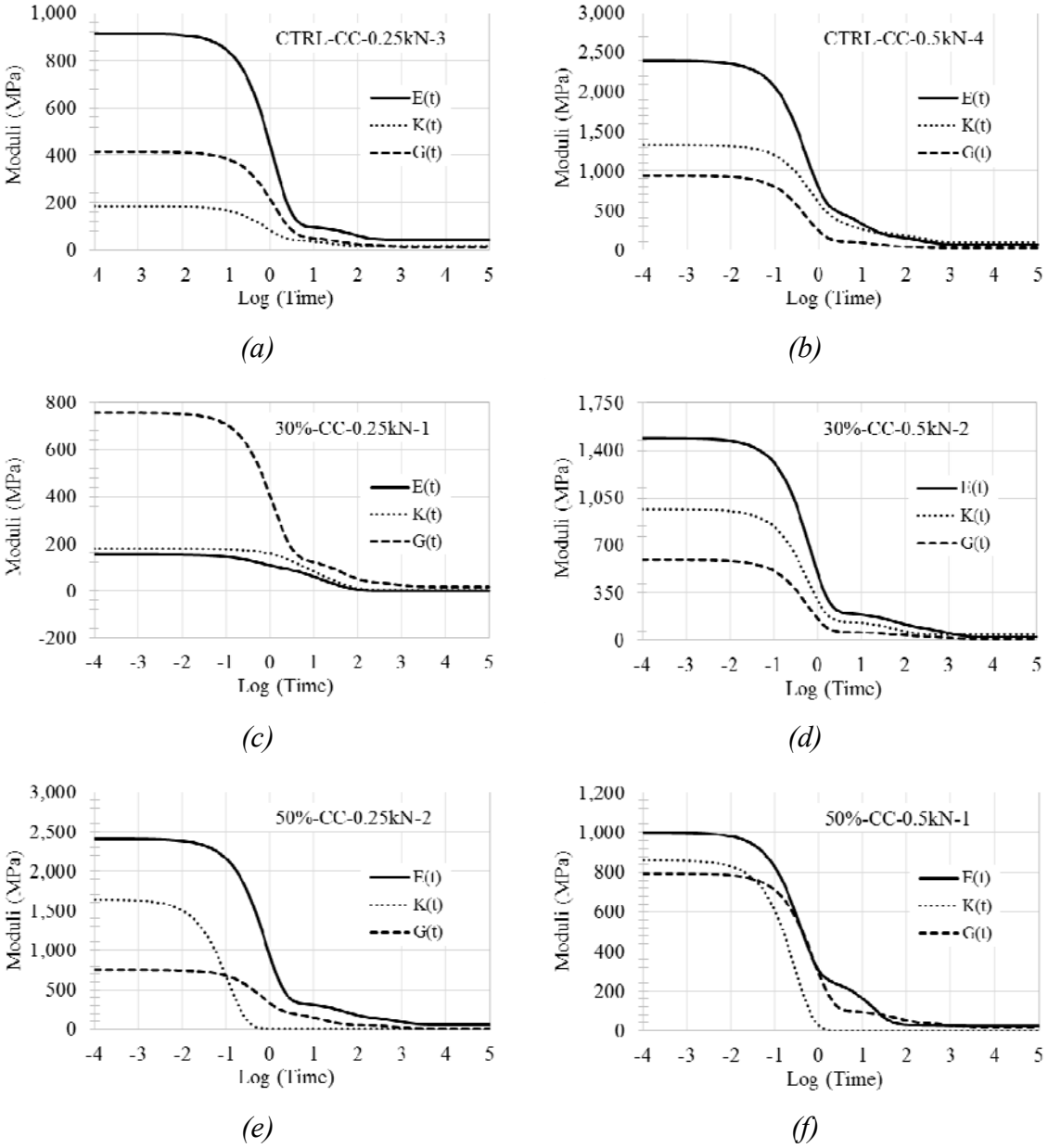

Figure 6.8. Creep test results for (a) control mix at 0.25 kN, (b) control mix at 0.5 kN, (c) 30% RAP mix at 0.25 kN, (d) 30% RAP mix at 0.5 kN, (e) 50% RAP mix at 0.25 kN, and (f) 30% RAP mix at 0.5 kN.

Due to inability of quasi-static tests to measure accurate instantaneous moduli, constrained non-linear optimization was also conducted to fit the measured stresses. The list of constraints is shown in Table 6.2; values of the constraints were estimated based on Prony series fitting on the master curves obtained from the E^* tests (refer section 4.2).

Table 6.3. Constraints for non-linear optimization.

Moduli (MPa)	D5-Control	D5-30% RAP	D5-50% RAP
E_0	22,577	22,838	21,705
E_∞	241	414	103
G_0	8,362[1]	8,458	8,039
G_∞	89	153	38
K_0	75,256[1]	76,126	72,351
K_∞	804	1,379	345

[1] obtained using ν = 0.35, where $G_0 = E_0/2(1+\nu)$ and $K_0 = E_0/(1-2\nu)$

The typical output, characterized by two plateaus and an intermediary hump, of the constrained optimization is shown in Figure 6.9. The lower plateau is most probably dictated by the actual test data whereas, the hump and upper plateau shows the effect of applied constraints. The applied instantaneous constraints seem to "*pull*" the curve upward because of inadequate data points in that region. The data was collected at intervals of 5 millisecond (200 data points per sec); higher data acquisition rates in the vicinity of time $t \approx 0$ could have improved the results significantly. When properly defined instantaneous modulus values are coupled with sufficient data points collected at early loading times, the accuracy of relaxation functions can be improved.

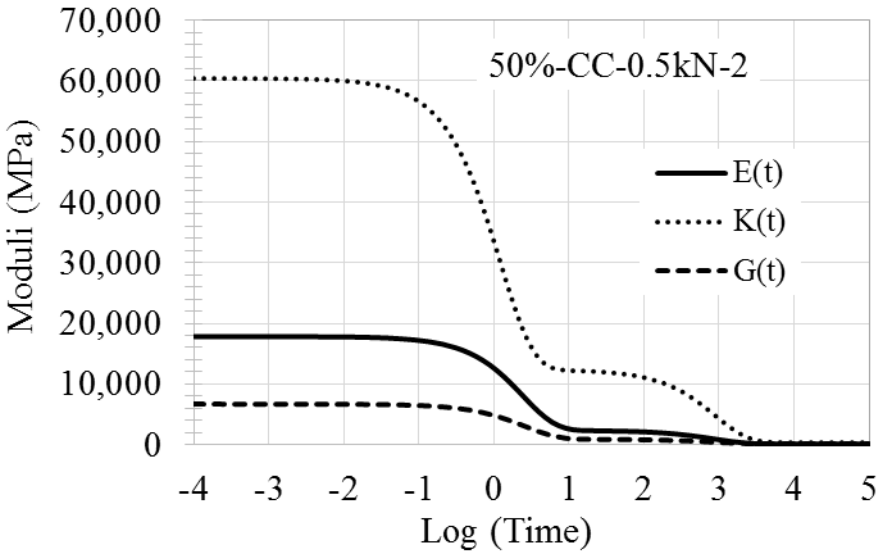

Figure 6.9. Moduli curves on constrained optimization on creep data.

Contrary to the creep tests, compressive relaxation tests resulted in some logical moduli trends, i.e. *K(t) > E(t) > G(t)* for asphalt mixtures as shown in Figure 6.10. These

results are obtained from unconstrained optimization. When initial estimates of instantaneous modulus values are not provided, modulus characterization at early loading times (times smaller than 0.1 sec) at intermediate temperatures becomes a challenge.

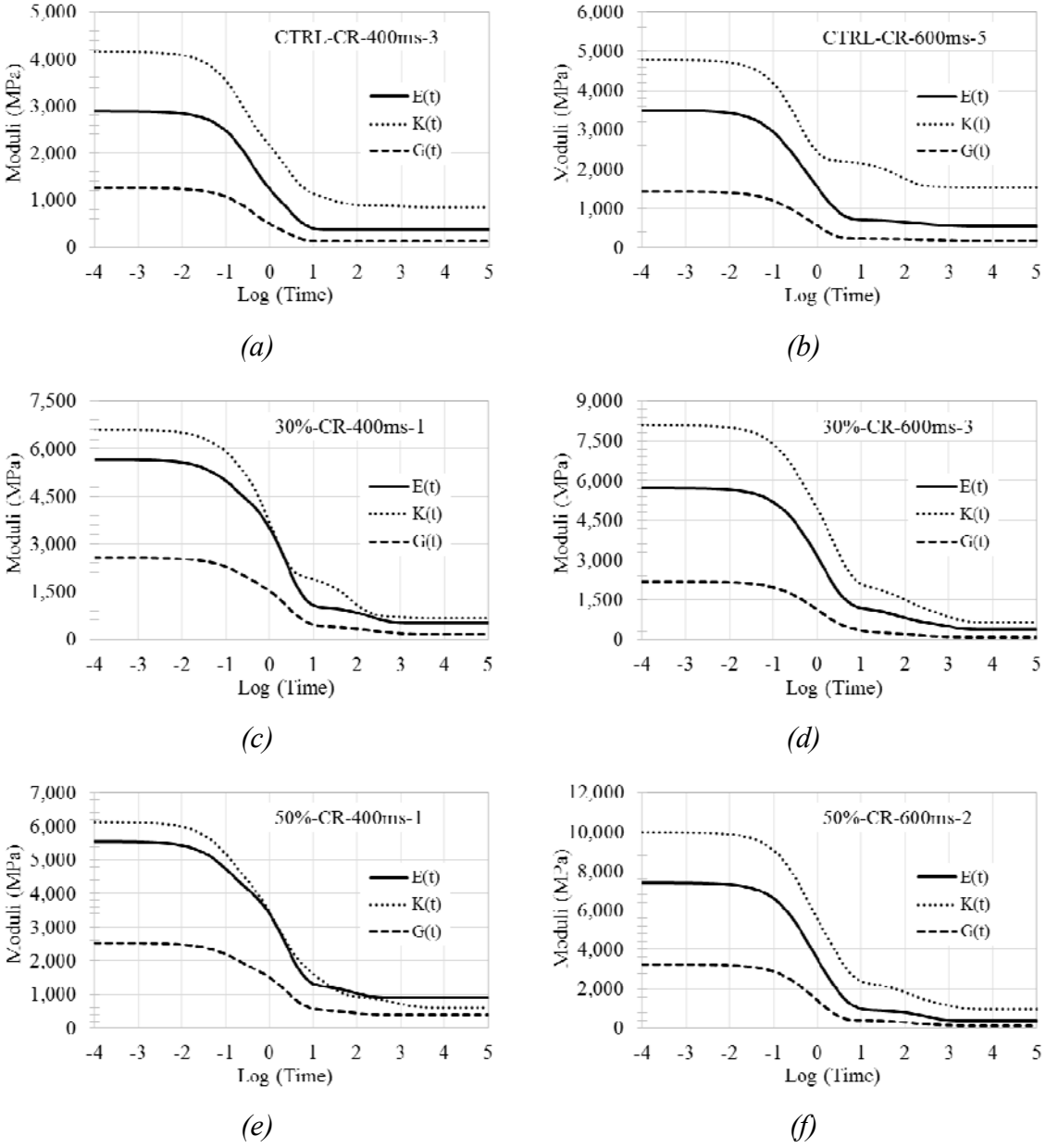

Figure 6.10. Relaxation test results for (a) control mix at 400 ms, (b) control mix at 600 ms, (c) 30% RAP mix at 400 ms, (d) 30% RAP mix at 600 ms, (e) 50% RAP mix at 400 ms, and (f) 30% RAP mix at 600 ms.

In order to improve modulus function at early loading times, instantaneous and infinity modulus constraints were also applied on relaxation data. Figure 6.11 shows the

results for a single 30% recycled mixture sample. Applying constraints on relaxation data resulted in slightly different moduli curves. It can be noted in the creep case (Figure 6.9) that even applying constraints could not make the curves reach to target instantaneous modulus values. For example, an equality constraint on bulk instantaneous modulus K_0 = 72,351 MPa resulted in a *K(t)* having its peak at 60,000 MPa only. On the contrary, constraints on the relaxation data optimization resulted in similar instantaneous moduli values.

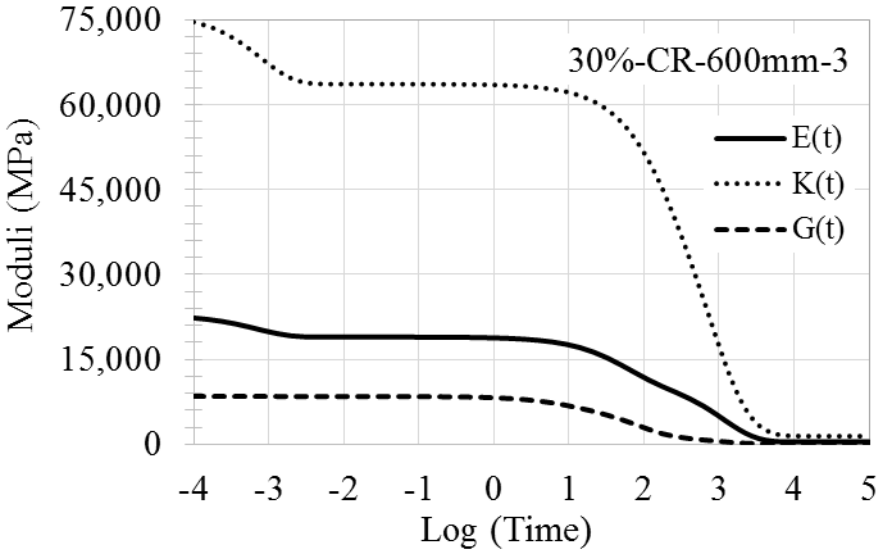

Figure 6.11. Moduli curves based on constrained optimization on relaxation data.

For viscoelastic materials, it is not uncommon to have bulk relaxation moduli several order of magnitude larger than the shear moduli and relax significantly slower than the shear and axial moduli (Hilton 2011). On the contrary, the normalized moduli plots, shown in Figure 6.12, narrates a slightly different story for asphalt concrete materials. There appears a consistent but very insignificant time shift of bulk relaxation moduli. This may be due to the fact that asphalt concrete is composed of 90-95% aggregates (elastic) and only 5-10% asphalt binder (viscoelastic), resulting in minor differences in relaxation times at 21ºC. At one hand, where this finding does make some justification for usual practice of considering similar relaxation times for asphalt concrete; on the other hand it strongly disapproves any assumption of considering constant bulk modulus. However, this finding, based on a relatively unconventional asphalt mixture with a high recycled content, may not be generalized. Additional testing

of different asphalt mixtures and improved means of measuring axial and radial deformations are critical for generalization.

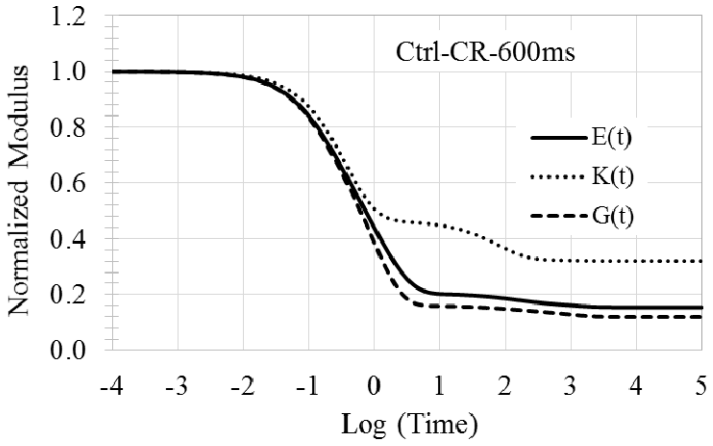

(a)

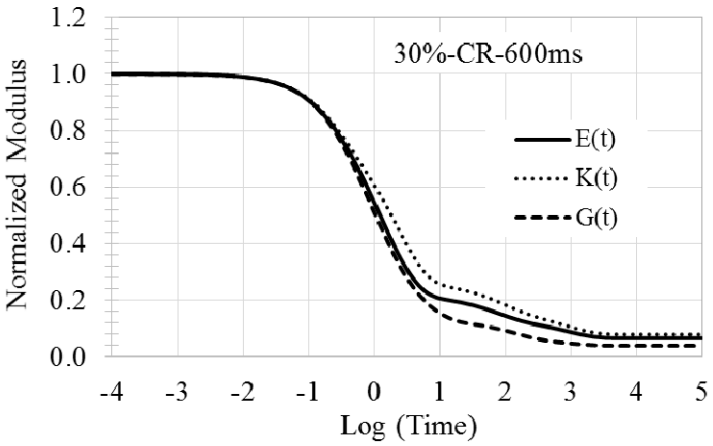

(b)

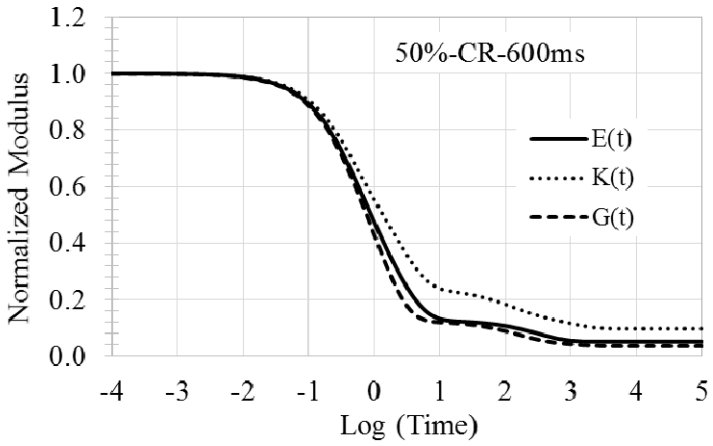

(c)

Figure 6.12. Normalized moduli obtained without constraints for (a) control mix at 600 ms, (b) 30% RAP mix at 600 ms, (c) 50% RAP mix at 600 ms

In order to explore effect of RAP, moduli *E(t)*, *G(t)*, and *K(t)* for the recycled mixtures were compared with virgin control mixture. The effect of RAP on mixtures' moduli is obvious; an increase in RAP content caused an increase in the moduli values, Figure 6.13.

As shown in Figure 6.14, moduli relaxation times were also compared for the control and recycled materials based on the unconstrained relaxation results. Being the softest, control mix has the highest relaxation rates followed by the recycled mix. Again, the difference between the relaxation rates is not that significant, though the results followed the expected trends.

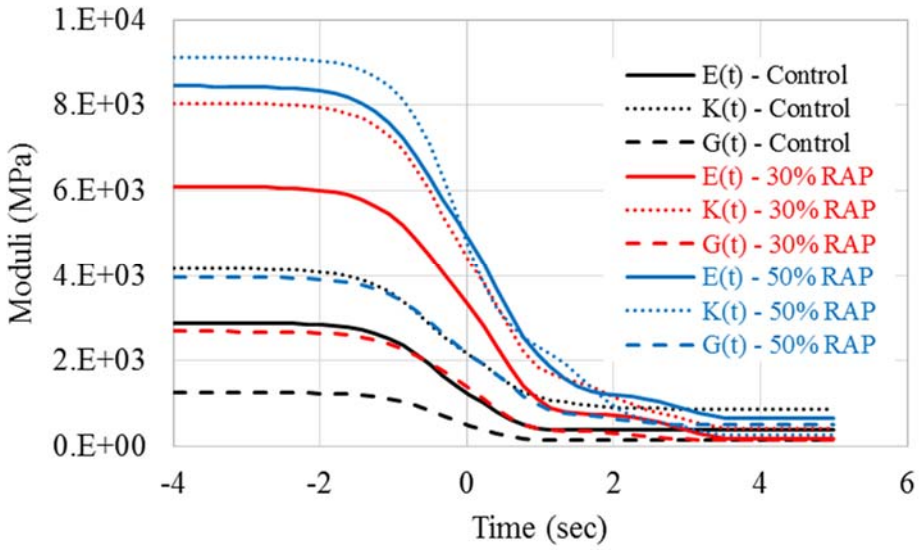

Figure 6.13. Comparison of relaxation moduli for different mixtures – unconstrained relaxation.

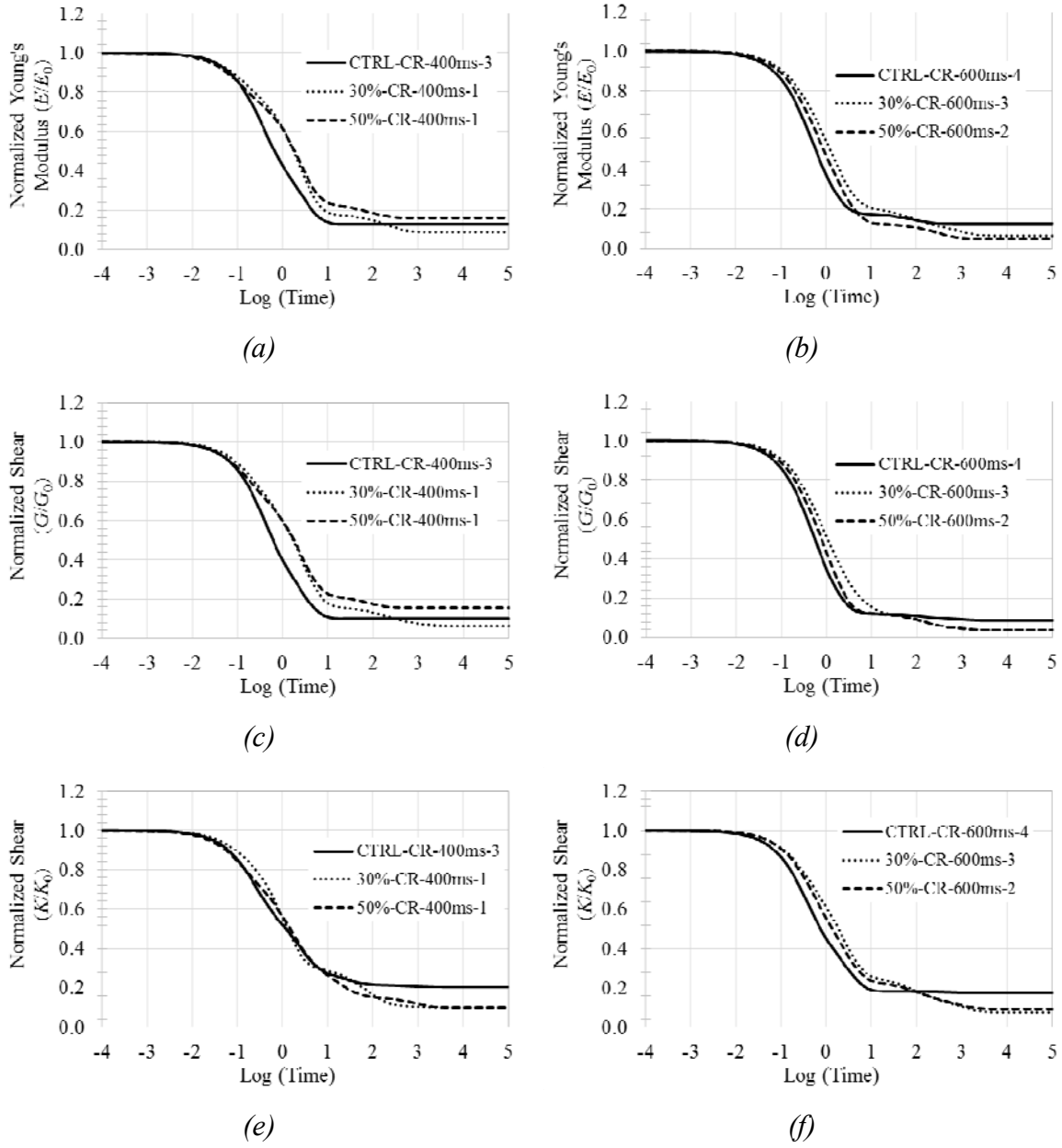

Figure 6.14. Mixture comparison (a) E/E_0 at 400 ms, (b) E/E_0 at 600 ms, (c) G/G_0 at 400 ms, (d) G/G_0 at 600 ms, (e) K/K_0 at 400 ms, and (f) K/K_0 at 600 ms.

6.6 Summary and Remarks

This chapter presents an alternative multi-axial viscoelastic characterization protocol and summarizes a laboratory experimental protocol to conduct multi-axial characterization of the virgin and recycled asphalt mixtures without the use of Poisson's ratios. The algorithm implemented has been described in details with its formulation and

implementation. A MATLAB code has been written and simulations have been run to verify the accuracy of the code. After preliminary experiments, two loading configurations, i.e. a uniaxial compressive creep test and compressive relaxation test were selected for further testing. The main premise of the multi-axial characterization is to obtain bulk, shear, and axial viscoelastic material functions (creep or relaxation) independently using a theoretically robust approach.

Importance of collecting the data at early loading times is recognized to capture complete relaxation or compliance functions. However, as shown in this study, it should be kept in mind that the capabilities of available loading machines may not be sufficient to apply load swiftly enough. Too many data points may therefore result in collecting noise rather than actual data. Therefore, master curve approach using temperature-frequency sweep adopted in the implementation of complex modulus test can be integrated into the algorithms to increase the accuracy at early loading times.

Based on the experimental investigation of some of the asphalt concrete materials designed in this study, the following conclusions can be drawn. Creep test data could not be appropriately utilized to determine the relaxation moduli by the developed algorithm. This can be expected because the formulation (Equations 6.10 to 6.12) are designed for calculation of relaxation functions. Relaxation test data, on the other hand, resulted in relatively suitable characterization of the control and recycled mixtures. It is observed that Young's, bulk, and shear moduli have similar relaxation pattern which is uncommon for viscoelastic materials reported in the literature. Control mix (without any RAP) showed lower moduli and slightly higher relaxation rates than its recycled counterparts.

The multi-axial algorithm presented in this chapter provides an opportunity for 3-D characterization of asphalt concrete materials and in general for all viscoelastic materials using a theoretically consistent approach. It only requires measurement of strains in the direction perpendicular to loading direction. The approach bypasses the need for Poisson's ratio for derivation of material functions needed for isotropic viscoelastic characterization. The presented approach offers a viable opportunity to bypass the need for PR; minor modifications of a simple and convenient test set up (uniaxial test) are needed.

However, it is important to say a few words about the challenges with viscoelastic

characterization using this approach or in general applicable to all other characterization procedures. Data collection at early loading times and determination of instantaneous modulus remain as a challenge. Accuracy of on-specimen radial and axial strain measurements, which is the backbone of the modulus determination, should also be improved. Image correlation (Michaeli et al. 2013, Shtark 2012) or laser measurement techniques are just some of the available techniques that can be exercised.

CHAPTER 7

ECONOMIC APPRAISAL OF USING HIGH RAP CONTENT IN ASPHALT MIXTURES

7.1 Introduction

Available funding is the key factor that drives a decision-making process in any transportation project. Pavement rehabilitation alternative selected solely on the basis of lowest initial cost may actually result in higher life-cycle cost relative to other alternatives. For pavement, LCCA is a decision tool that aids pavement designers and planners in identifying the most cost-effective pavement construction or rehabilitation strategies based on their life-cycle costs. For a highway pavement, apart from the initial cost, LCCA takes into account all the user and agency costs related to future activities, including periodic maintenance and rehabilitation.

There are a few studies related to LCCA of pavements in general (Pittenger et al. 2011, Chen and Flintsch 2007, Reigle and Zaniewski 2002, Ozbay et al. 2004) but very few compare costs associated with recycled and virgin mixtures. Visintine (2011) compared virgin mixtures with mixtures containing 30% and 40% RAP. She reported net savings of 19% when 30% RAP was used and savings ranging from 30% to 36% when 40% RAP was used in the asphalt mixtures. In another study, based on data from FHWA's LTPP SPS-5 experiment in Texas, Moya et al. (2011) compared the field performance of pavement sections with and without RAP. LCCA conducted on those pavement sections showed that, in the case of thick overlays, the long-term costs of using RAP in the mixture were similar to the costs of mixtures with no RAP. However, for thin pavement structures there was a clear economic benefit for not using RAP in the long run. It is important to note that RAP technology was not well-developed when the LTPP study was conducted. Better understanding of the RAP material, superior quality control, and practices like RAP fractionation have improved the quality of mixtures with RAP.

This Chapter takes on the task of presenting the economic perspective of using high RAP content (up to 50%) in asphalt mixtures. The economic analysis tool, LCCA, is

used to compare the difference alternatives based on life-cycle cost. Attempts are made to determine breakeven performance levels for mixtures based on varying the levels of probable field performance of the asphalt mixtures.

The economic impact of using high amount of RAP in binder course mixtures was assessed; the following tasks were conducted:

1. Conduct an LCCA for the mixtures involved in the study;
2. Compare the user and agency costs associated with different alternatives;
3. Determine the economic impact of the mixtures with RAP at varying performance levels of the mixtures;
4. Determine the breakeven performance level for each mixture with RAP;

FHWA's LCCA software, *RealCost* 2.5, was used to achieve the objectives of the study. *RealCost* calculates life-cycle values for both agency and user costs associated with new construction, as well as maintenance and rehabilitation. Both deterministic and probabilistic analysis were conducted for the life-cycle costs. In this study, LCCA was conducted for District 5 materials only.

7.2 Agency Cost

In a pavement project, agency cost comprises of preliminary engineering, contract administration, initial construction, maintenance and rehabilitation. For the LCCA conducted in this study, costs common to all alternatives canceled each other out and were therefore excluded from the LCCA.

RealCost requires undiscounted agency cost related to initial construction and maintenance activities as input. An analysis period of 45 years, as recommended by the Illinois Department of Transportation (IDOT), was selected. A 1.61-km (1-mile) lane of asphalt pavement section was selected near intersection of I-74 and Lincoln Avenue at Urbana, IL. Initial construction activities involved construction of a 254 mm (10 in.) binder course overlaid by a 5.1 mm (2 in) surface course. A shoulder 1.8 m (6 ft) wide and 305mm (12 in.) thick was also considered in the analysis. Binder course was the main variable in asphalt mixtures studied; mixtures with various amounts of RAP (0%, 30%, 40%, and 50%) were used in the binder course for each mixture. Asphalt mix

density used was 1422 kg/m^3 (2.05 T/yd^3), and 24 km (15 mi) was selected as the distance from the asphalt plant to the site. The project details are shown in Table 7.1.

Table 7.1. Project inputs to LCCA.

Project Length	1.61 km	1 mi
Pavement Thickness	254 mm	12 in
Lane Width	3.66 m	12 ft
Shoulder Width (inside)	1.83 m	6 ft
Shoulder Width (outside)	0 m	0 ft
Pavement Surface Area	6437 m^2	7040 yd^2
No of Lanes	1	1
No of Centerlines	1	1
No of Edges	1	1
No of Shoulders	1	1
Shoulder Surface Area	1609 m^2	1760yd^2
Discount Rate	4%	4%
Mixture mix density	1422 kg/m^3	2.05 tons/yd^3
Distance from Plant to Site	24 km	15 mi

Table 7.2 shows the schedule for maintenance and rehabilitation activities that was adopted from IDOT's Bureau of Design and Environment manual (IDOT 2013). The cost to conduct each activity was determined. While most of the unit prices for different construction materials and procedures were obtained from pay item reports available on IDOT's website, some information was also obtained from local asphalt plants. The remaining service life (RSL) at the end of the 45-yr period was also considered in the analysis. The value of a ton of RAP was determined by summing the costs of virgin binder and aggregates replaced by a ton of RAP minus the costs incurred to use a ton of RAP, such as stockpiling, processing (crushing and/or screening), and re-stockpiling.

Overheating the virgin aggregates before introducing the RAP to the drum is a common practice followed to avoid direct heating of RAP materials. It can cause extra fuel and energy use, which offsets the economic benefits of using RAP. Detailed production and energy consumption data were obtained from an asphalt plant using an automated tracking system energy monitoring. Although counterintuitive, the data showed no variation in energy consumption with respect to RAP content or RAP

moisture content. It may be hypothesized that the extra energy consumed during superheating might have been counterbalanced by the reduction in virgin aggregates to be heated. The plant data showed no difference in energy consumption with variation in RAP content; therefore, no extra cost was attributed to aggregates' superheating. Chapter 8 (Section 8.3.2) provides the detailed data analysis and discussion.

Table 7.2. IDOT maintenance and rehabilitation activity schedule (IDOT 2013).

Activity 1, Year 5
100% Longitudinal shoulder joint routing and sealing
100% Centerline joint routing and sealing (single-lane paving)
50% Random/thermal crack routing and sealing
0.10% Partial-depth pavement patching (mill and fill surface)
Activity 2, Year 10
100% Longitudinal shoulder joint routing and sealing
100% Centerline joint routing and sealing (single-lane paving)
50% Random/thermal crack routing and sealing
0.50% Partial-depth pavement patching (mill and fill surface)
Activity 3, Year 15
2.00 in. Milling, pavement and shoulder
1.0% Partial-depth pavement patching (mill and fill additional 2.00 in.)
2.00 in. Hot-mix asphalt overlay pavement
2.00 in. asphalt overlay shoulder
Activity 4, Year 20
Same as Activity 1
Activity 5, Year 25
Same as Activity 2
Activity 6, Year 30
2.00 in Milling, pavement only, standard design:
Pavement and shoulder, limiting strain criterion design
2.0% Partial-depth pavement patching (mill and fill additional 2.00 in, all designs)
1.0% Partial-depth shoulder patching (as follows):
Mill and fill surface, standard design
Mill and fill additional 2.00 in, limiting strain criterion design
Asphalt overlay, pavement (3.75 in, standard design; 2.00 in, limiting strain criterion design)
Asphalt overlay, shoulder (1.75 in, standard design; 2.00 in, limiting strain criterion design)
Activity 7, Year 35
Same as Activity 1
Activity 8, Year 40
Same as Activity 2

The cost associated with milling and transportation of RAP from a milling site to the asphalt plant was not considered in the analysis because the milling operation and transportation of RAP (either to a landfill or an asphalt plant) must occur, irrespective of its ultimate use. Moreover, transporting RAP to the asphalt plant also reduces the material being dumped, thereby reducing the burden on landfills and eliminating landfill tipping fees. Milling and transportation of milled material must be taken into account, however, when at-plant recycling is to be compared with in-place recycling.

Agency cost was measured. Table 7.3 shows net present values (NPV) obtained by discounting future costs using a discount rate of 4%. The basic NPV formula for discounting future amounts is the following:

$$NPV = \text{InitialCost} + \sum_{k=1}^{N} \text{RehabCost}_k \left[\frac{1}{(1+i)^n} \right] \qquad (7.1)$$

where i = discount rate and n = number of years.

Table 7.3. NPV calculations for agency cost for all alternatives.

	Control	Mix with 30% RAP	Mix with 40% RAP	Mix with 50% RAP
Initial construction cost/km	$360,595	$325,613	$313,953	$302,292
Maintenance cost/km	$127,501	$127,501	$127,501	$127,501
Total agency cost/km	$488,096	$453,114	$441,454	$429,793

The savings observed in Table 7.3 are attributed solely to the binder course in which mixtures with different RAP contents were used. Considering the cost of binder course only, mixtures with 30%, 40%, and 50% RAP saved approximately 17%, 22%, and 28%, respectively, relative to the virgin mixture. The first round of analysis was based on the assumption that all the recycled mixtures performed equally to the virgin mixtures; maintenance cost, therefore, remains constant for all the mixtures. Costs associated with the four mixtures under varying performance levels will be discussed later.

The undiscounted agency costs determined for initial construction and each maintenance activity were used as input to the *RealCost*. Since it was decided to conduct both deterministic and probabilistic calculations, a normalized distribution was chosen for agency costs with a standard deviation of 10%.

7.3 User Cost

User cost is the cost to highway users over the life of a project. It includes user delay costs, vehicle operating cost (VOC), and crash costs, which are attributed primarily to work zone operations during construction, maintenance, and rehabilitation. Most DOTs exclude user cost from their LCCAs, possibly because user costs are difficult to quantify, and the values associated with user costs are often disputed (Reigle and Zaniewski, 2002). Delwar and Papagiannakis (2001) showed that regardless of roadway facility, pavement type, and maintenance activities, the impact of most maintenance activities proved more expensive to the user than to the agency.

To calculate work zone user cost, *RealCost* uses traffic data as a key input. Traffic data such as annual average daily traffic (AADT) and truck volume were obtained from IDOT (2012). The AADT used was 49,500, with 2.2% single-unit trucks and 11.3% combination trucks. The traffic hourly distribution is the default given by the software. The speed limit was reduced from 105 km/h (65 mph) to a work zone speed limit of 72 km/h (45 mph). The annual traffic growth rate was assumed to be 4.0%. The free-flow capacity of 2061 vphpl (vehicles per hour per lane) was calculated by *RealCost* using input provided from traffic information. For the queue dissipation capacity, a normal distribution was used using 1818 vphpl as the mean value and 144 as the standard deviation (Walls and Smith, 1998). Two number of lanes were considered in each direction during normal conditions.

The values of user time per vehicle class were used in a triangular distribution and are presented in Table 7.4 (Walls and Smith, 1998). Because user time values were based on 1996 dollar value, an escalation factor based on the all-items consumer price index (CPI) was used to convert the values to 2011 dollars, as shown in Table 7.4. The CPI in the United States is defined by the Bureau of Labor Statistics (BLS 2013) as "a measure of the average change over time in the prices paid by urban consumers for a market

basket of consumer goods and services." According to BLS, the CPIs for 2011 and 1996 were 224.94 and 156.9, respectively. The ratio of the two CPI values provided the escalation factor of 1.43.

Table 7.4. User time value per vehicle class for 1996 and 2011.

	User Time Values					
	1996 (Walls & Smith 1998)			2011		
	Minimum	Likely	Maximum	Minimum	likely	Maximum
Passenger Vehicles	10.0	11.6	13.0	14.3	16.6	18.6
Single-unit Trucks	17.0	18.5	20.0	24.4	26.6	28.7
Combination Trucks	21.0	22.3	24.0	30.1	32.0	34.4

7.4 Deterministic Results

Based on deterministic calculations, the NPV of the user costs for all the mixtures are equal, as shown in Table 7.5. The reason they are equal is that construction activities in the initial construction phase and activities in the maintenance and rehabilitation phases were same for all the mixtures; it was assumed that all the mixtures performed equally well. The analysis showed net savings of $34,981 to $58,303 per km with the addition of 30% to 50% RAP.

Table 7.5. Life-cycle costs for all alternatives.

	Control	Mix with 30% RAP	Mix with 40% RAP	Mix with 50% RAP
Agency cost/km	$488,095	$453,114	$441,453	$429,792
User cost/km	$484,295	$484,295	$484,295	$484,295
Total life-cycle cost/km	$972,390	$937,408	$925,748	$914,087
Net savings/km compared with control	-	$34,981	$46,642	$58,303

Although most state DOTs ignore user cost in their LCCA, Figure 7.1 shows that, for the control mixture, the user cost is almost 50% of the total cost, indicating it is an indispensable part of the LCCA and a crucial decision-making criterion. For recycled mixtures, the percent user cost increased even more as the agency cost percent was reduced. Moreover, it can be observed that largest agency cost (74%) derives from the initial construction phase, whereas in case of user cost, maintenance activities affect the

total life-cycle user cost. User cost can vary, depending on traffic inputs as well as construction time of day (day or night) and the number of working days assigned to the initial construction and to each maintenance activity.

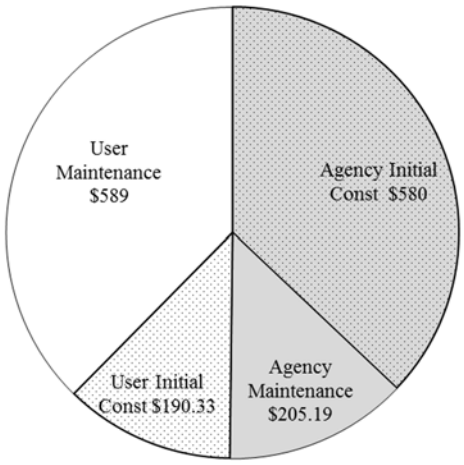

Figure 7.1. Breakdown of total cost in agency and user costs.

7.5 Breakeven Performance Levels

The LCCA results proved that recycled mixtures are more cost-effective than the control mix. The results are, though, based on an assumption that all the mixtures performed similarly to each other. However, it can be argued that recycled mixtures may perform worse than the virgin mixtures because of the high stiffness of aged RAP binder. Mixtures with RAP are considered more susceptible to thermal cracking relative to the virgin mixtures; the laboratory performance testing results also showed similar trends. The possible insufficient performance of recycled mixtures may necessitate more maintenance and rehabilitation activities, thereby offsetting the economic benefits of using RAP. The level of pavement performance at which the economic benefits of using RAP are balanced by the costs burden associated with maintenance activities may be termed as breakeven performance level. An effort has been made to determine the breakeven performance levels for the mixtures with different RAP contents.

Three performance scenarios (i.e., 90%, 80%, and 70%) were considered in addition to the base scenario of 100% performance. A 90% performance scenario would mean that the recycled mixtures performed equal to 90% of control mixture's

performance. Thus, if an activity were scheduled after an interval of 5 years in the base schedule, for the 90% performance scenario, the same activity would be planned after an interval of (90/100) × 5 = 4.5 years. Similarly, for 80% and 70% performance scenarios, the time interval between each activity would be 0.8 × 5 = 4 years and 0.7 × 5 = 3.5 years, respectively. This will increase the number of maintenance/rehabilitation activities during the analysis period of 45 years, as shown Table 7.6.

Table 7.6. Maintenance and rehabilitation activity schedule for all performance scenarios.

No of Activities	100% Performance		90% Performance		80% Performance		70% Performance	
	Activity #	Year	Activity #	Year	Activity #	Year	Activity #	Year
1	1	5.0	1	4.5	1	4.0	1	3.5
2	2	10.0	2	9.0	2	8.0	2	7.0
3	3	15.0	3	13.5	3	12.0	3	10.5
4	4	20.0	4	18.0	4	16.0	4	14.0
5	5	25.0	5	22.5	5	20.0	5	17.5
6	6	30.0	6	27.0	6	24.0	6	21.0
7	7	35.0	7	31.5	7	28.0	7	24.5
8	8	40.0	8	36.0	8	32.0	8	28.0
9	-	-	3-2	40.5	3-2	36.0	3-2	31.5
10	-	-	-	-	4-2	40.0	4-2	35.0
11	-	-	-	-	5-2	44.0	5-2	38.5
12	-	-	-	-	-	-	6-2	42.0

In each analysis performed, the control mixture was kept at 100% performance while the remaining mixtures were analyzed under various performance scenarios. The significance of RSL is highlighted here as the final activity for each performance level is conducted in a different year. Figures 7.2 and 7.3 show the net present values of the agency and total costs respectively under different scenarios.

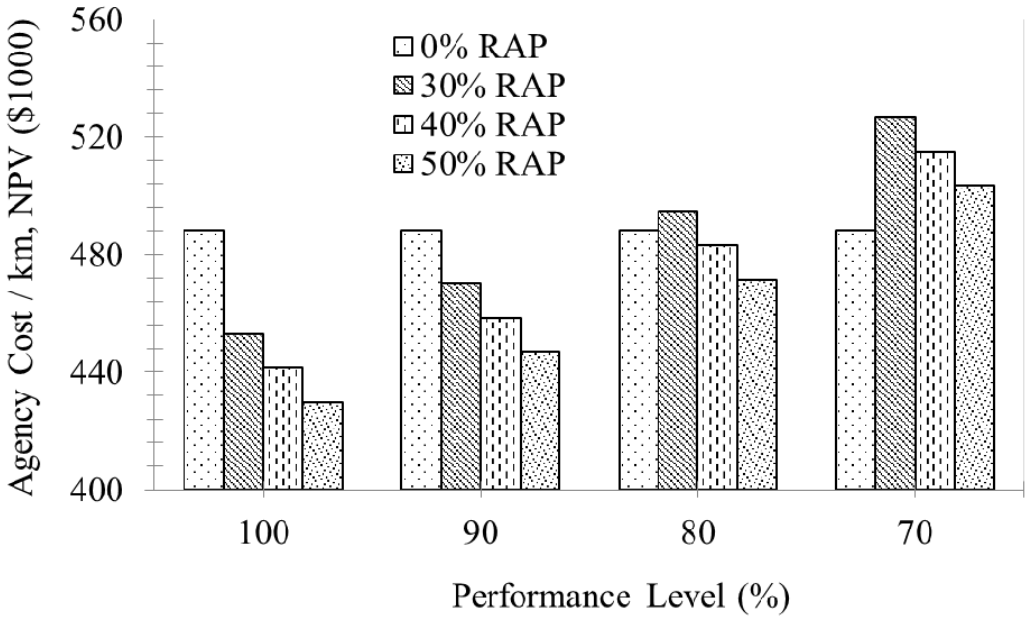

Figure 7.2. Net present value of agency costs under different performance scenarios.

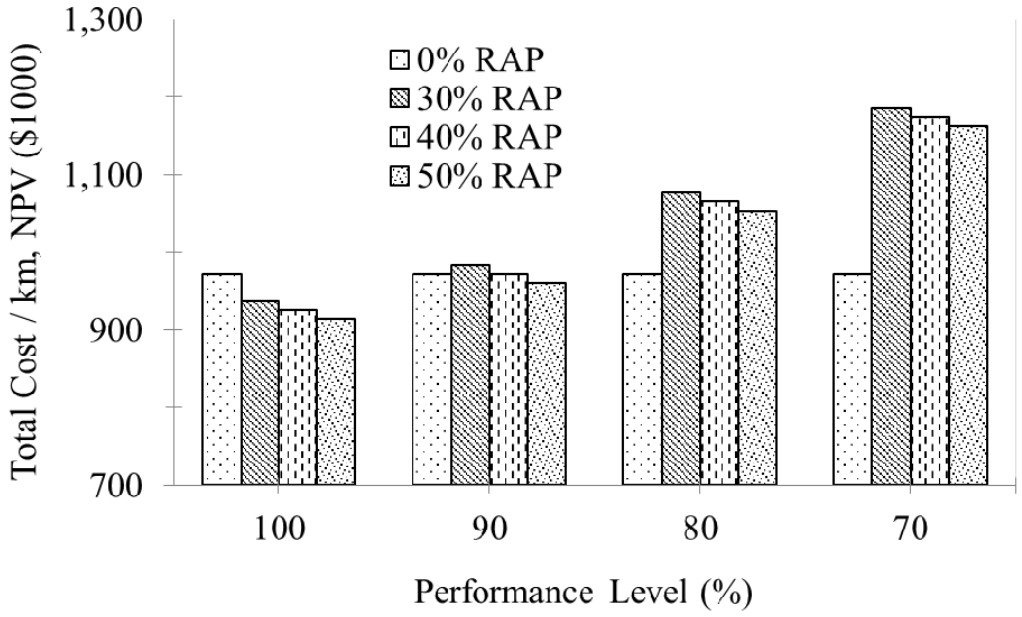

Figure 7.3. Net present value of total costs under different performance scenarios.

A significant effect of incorporating user cost is obvious from the results; an exponential increase in the total cost is observed with performance reduction of the mixtures. Figure 7.2 shows that, under 90% performance scenario, 30% recycled mix is

holding its economic advantage despite the compromised performance. But, at 80% performance scenario, it loses its economic advantage over the control mix. In case of total cost, this advantage diminishes even farther.

Figures 7.4 and 7.5 illustrate the same data in slightly different way. It can be seen from Figure 7.4 that as the performance of recycled mixtures further deteriorates, a crossover point is reached at which the economic benefits of using RAP are counterbalanced (breakeven) by the agency costs incurred from increased frequency of maintenance and rehabilitation activities. The advantage of using RAP is diminished significantly (95% compared with 82% for 30% recycled mix) when total costs instead of agency costs are taken in account, as shown in Figure 7.5, leaving the recycled mixtures with very little margin of underperformance. Being the most economical alternative, 50% recycled mix has the maximum margin (25%) of underperformance which sharply shrinks to 13% (100-87) when total cost is considered in lieu of agency cost. Table 7.7 shows the results in detail.

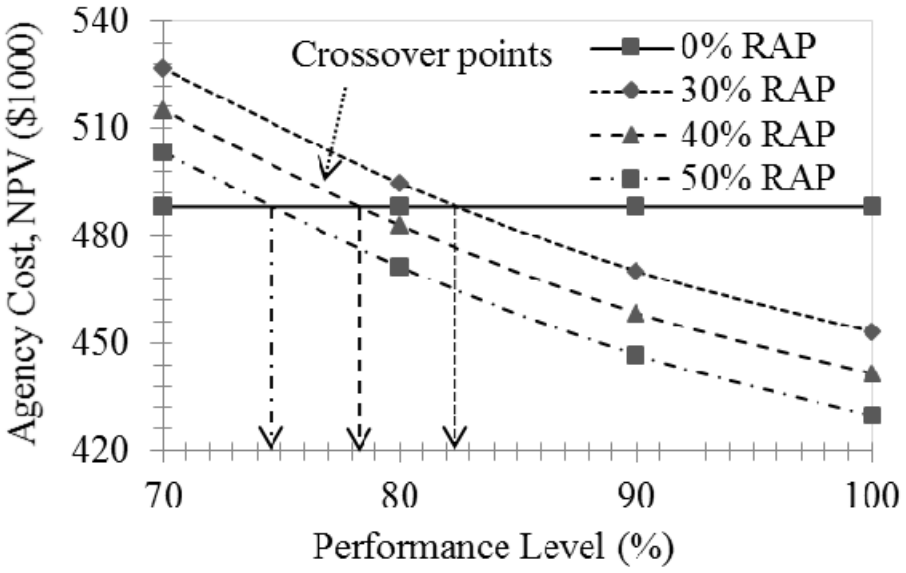

Figure 7.4. Breakeven performance levels based on agency cost.

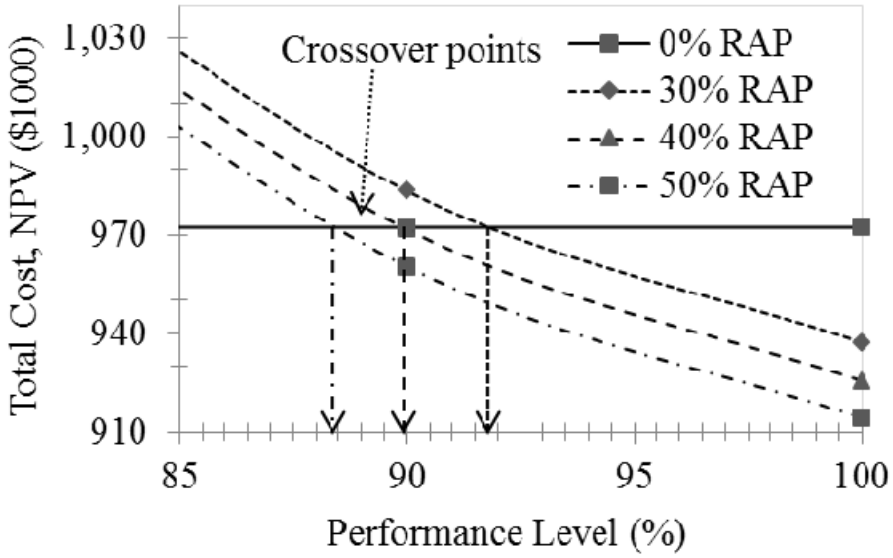

Figure 7.5. Breakeven performance levels based on total cost.

Table 7.7. LCCA results under different performance scenarios.

Mix Type	Performance (%)	LCCA		Breakeven Performance Levels	
		Agency Cost ($1000)	Total Cost ($1000)	Agency Cost	Total Cost
Control	100	786	1,565	--	--
Mix with 30% RAP	100	729	1,509	82	95
	90	757	1,583		
	80	796	1,733		
	70	848	1,908		
Mix with 40% RAP	100	710	1,490	78	90
	90	738	1,564		
	80	778	1,714		
	70	829	1,889		
Mix with 50% RAP	100	692	1,471	75	87
	90	719	1,545		
	80	759	1,696		
	70	810	1,871		

The LCCA analysis conducted in this study underscore the importance of achieving equivalent field performance for mixtures with RAP to that of the mixtures made with virgin materials. Well-directed organized research related to laboratory and field performance and improved construction practices will make sure that asphalt mixtures with RAP perform better than the breakeven performance levels calculated in this study.

7.6 Probabilistic Results

Probabilistic LCCA is conducted to account for variation or uncertainties associated with any individual input parameter. Probabilistic approach allows the individual analysis input to be defined by a frequency distribution (USDOT 2002). A completely different and separate LCCA was run for probabilistic approach. The main input variables and their distribution types used in the analysis are shown in Table 7.8.

Table 7.8. Probability distribution for different parameters.

Variable	Distribution Type
Initial Agency Cost	Normal (mean, std. dev.)
Maintenance and Rehabilitation Cost	Normal (mean, std. dev.)
Activity Service Life	Triangular (min., most likely, max.)
Activity Structural Life	Triangular (min., most likely, max.)
Discount Rate	Triangular (min., most likely, max.)

For an agency's initial and maintenance costs, normal distribution was selected with a of 10% (e.g., if the initial agency cost for Alternative 1—the control mix—is $360,595, its standard deviation is $36,059.50). Changes in asphalt binder prices can easily bring major changes in agency costs. Moreover, for the service life and structure life (in years) for different alternatives, triangular distributions (4.5, 5, 5.5), (4.5, 4.75, 5), (4, 4.5, 5), and (3.5, 4.25, 5), as presented in Table 7.8, were selected for the control and recycled mixtures with 30%, 40%, and 50% RAP, respectively. It is important to note that the *maximum value* for all the recycled mixtures was kept equal to the *most likely* value of the control mixture on the assumption that recycled mixtures will perform either

worse than or equal to the control mixture. The *minimum* values were selected based on the assumption that incorporation of RAP would reduce the performance. The *most likely* values for the mixtures were the average of the *minimum* and *maximum* values. Because the unpredictability of a mixture's performance is expected to increase with an increase in the RAP content, the larger range of values was selected for mixtures with higher RAP contents. A triangular distribution (3, 4, and 5) was selected for the discount rate. The distribution types and their values for traffic data related to user costs were discussed in Section 7.4.

The probability analysis results in Table 7.9 show the best and worst scenario for each alternative. It can be seen that, although the control mix has the least user cost, the minimum user cost for the mixture with 50% RAP is smaller than the average user cost of the control mix owing to the higher standard deviation for the mixture with 50% RAP. As seen earlier, the cost related to maintenance and rehabilitation activities was the main contributor to user cost. Because the primary difference between the alternatives is the maintenance activity schedule, user cost showed higher uncertainty than agency cost.

Table 7.9. Probabilistic results—total cost for all alternatives.

Stats	Total Cost, NPV ($1000) per km							
	Control		Mix with 30% RAP		Mix with 40% RAP		Mix with 50% RAP	
	Agency	User	Agency	User	Agency	User	Agency	User
Mean	488	486	461	507	460	526	460	555
Standard Deviation	36	36	35	37	34	39	34	44
Minimum	365	398	348	422	366	419	369	448
Maximum	591	613	569	641	559	672	572	720

RealCost uses Monte Carlo simulations that randomly draw samples from the inputs and produces output in the form of NPV cumulative distribution curves for each alternative, as shown in Figures 7.6 and 7.7. The larger range of the triangular distribution for recycled mixtures affected the user cost more than the agency cost. Agency costs for the recycled mixtures remained below those of the control throughout the probability levels, whereas the control mixture had the lowest user cost among the four alternatives. The two curves cannot be combined, according to the recommendation

in the LCCA Interim Technical Bulletin (Wills and Smith 1998) for keeping agency and user costs separate.

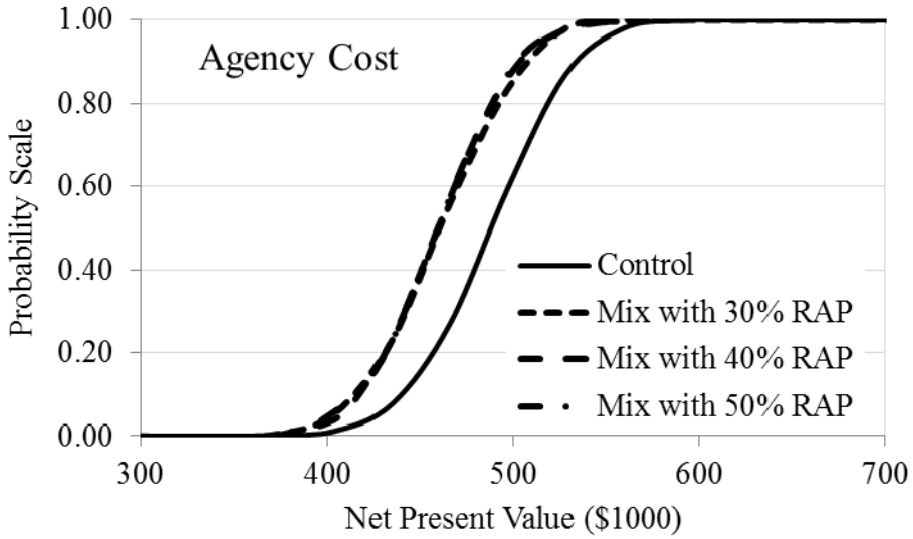

Figure 7.6. Commutative probability distribution of agency cost NPV for all alternatives.

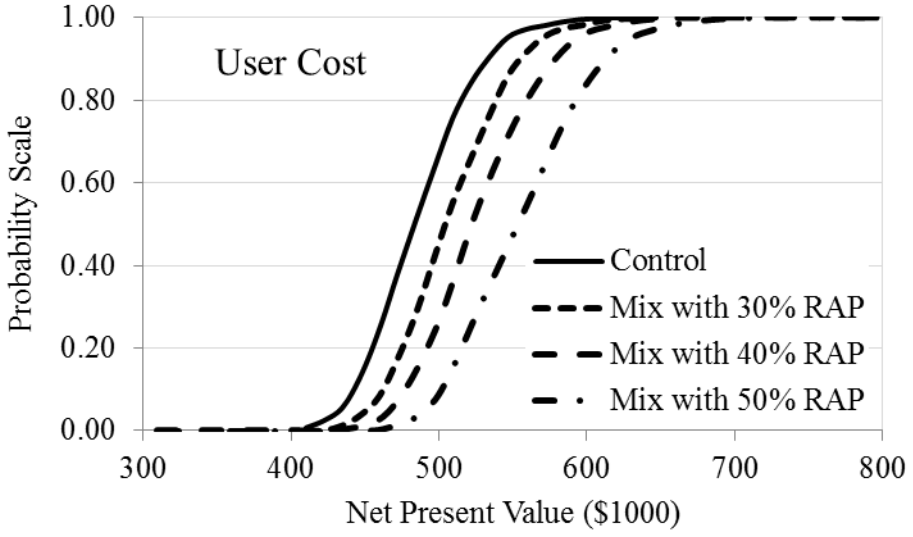

Figure 7.7. Commutative probability distribution of user cost NPV for all alternatives.

These figures also illustrate the probability that the project life-cycle cost of a particular alternative will be less than or equal to a specific value. For example, for a mixture with 30% RAP, there is 90% probability that its user cost will remain less than $530,000 per km. The agency life-cycle cost of recycled mixtures remained lower than that of the control mix, while the opposite is true for the user cost. Again, it is evident from Figures 7.6 and 7.7 that user cost is more sensitive than the agency cost to performance uncertainty.

RealCost also generates tornado plots that show the significance of model inputs on the life-cycle cost output distribution. Significance is measured by a correlation factor shown as the length of bars in a tornado graph, as depicted in Figures 7.8 and 7.9. A correlation coefficient of 1 indicates a complete positive correlation between variables, a value of 0 indicates no correlation, and a value of –1 indicates a complete inverse correlation. The correlation coefficient implies that if the input's mean is changed by 1 standard deviation of the input, the output mean will be changed by a correlation coefficient value times the standard deviation of the output. Hence, as shown in Figure 7.8, the most influential parameter is the Activity 1 Agency Cost. Because it is a positive correlation, if the mean value of the Activity 1 Agency Cost moves 1 standard deviation (in either direction), then the NPV for the control agency cost will move 0.94 times the standard deviation in same direction. Also, if the mean value of the second most influential parameter (discount rate) is increased by 1 standard deviation, then the NPV for the control agency cost will be decreased by 0.22 times the standard deviation life-cycle cost.

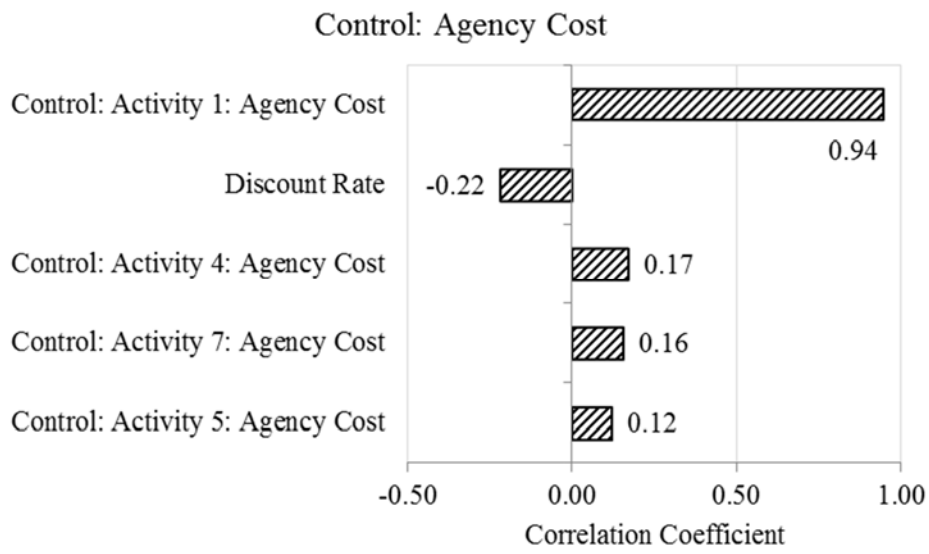

Figure 7.8. Tornado plots for control mix agency cost.

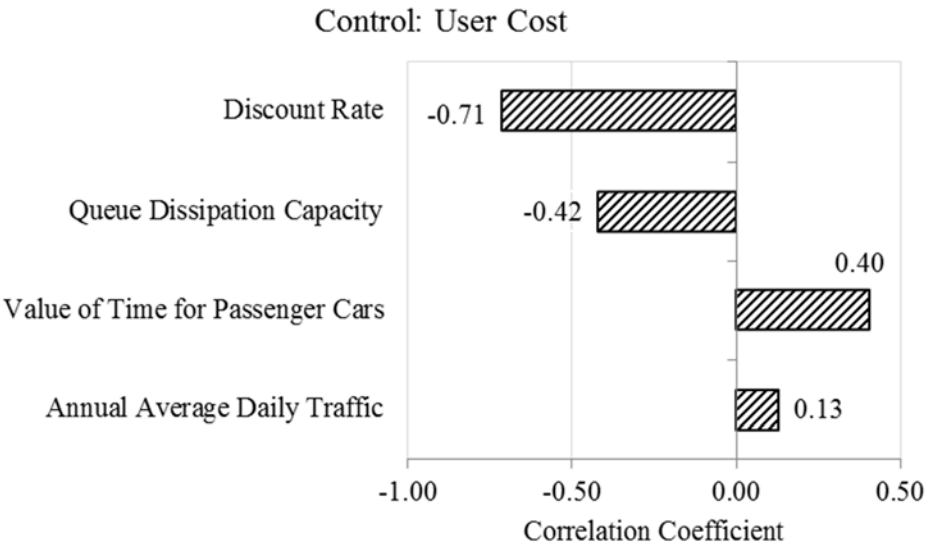

Figure 7.9. Tornado plots for control mix user cost.

It can be observed from the tornado plot in Figure 7.8 and detailed data in Table 7.10 that most influential factor for an alternative agency cost is initial construction of the alternative. The discount rate is in a distant second position; however, any correlation factor less than 0.6 is not considered significant. The discount rate is important because the bulk of the user cost originates from maintenance activities, which take place in future years. It is worth mentioning that user cost is also correlated to parameters such as

queue dissipation capacity and value of time for passenger cars. Researchers and agencies conducting LCCA should pay special consideration to such parameters and strive to improve the quality of traffic data.

7.7 Summary and Remarks

Using high RAP content is viable only if the recycled mixtures perform comparably to the mixtures made with virgin materials. The LCCA was conducted to assess the economic impact of incorporating a high amount of RAP in asphalt mixtures. The main economic benefits of using RAP are expected from savings in materials (i.e., aggregates and binder replacing virgin binders and aggregates). On the other hand, additional operations are needed to process RAP before its use in plants. Likewise, the superheating of virgin aggregates at asphalt plants may cause additional energy to be consumed during production of mixtures with RAP. Moreover, replacing the virgin binder grade with a softer binder may also cost more.

All of the aforementioned factors were taken into account when conducting the analysis. The detailed asphalt plant production and energy consumption data showed no variation in energy consumed during production of mixtures with different amounts of RAP.

The deterministic analysis over a period of 45 years showed a significant decrease in life-cycle cost with an increase in RAP content. Considering the cost of binder course only, mixtures with RAP saved up to 28% relative to the virgin mixture. These savings were observed based on an assumption that the performance of mixtures with RAP is similar to that of the virgin mixture. A methodology was followed to determine life-cycle costs associated with low-performing asphalt mixtures containing RAP. This process helped in determining a breakeven performance level for each mixture with RAP. The breakeven performance level is a crossover point at which the economic benefits of using RAP are balanced by the increased number of maintenance activities. The breakeven performance levels depend on material costs and traffic volume; hence, they may vary from one project to another.

Table 7.10. Correlation factors for all mix alternatives.

Agency Cost		User Cost	
		Control	
Input Variable		*Input Variable*	
Control: Activity 1: Agency Cost	0.94	Discount Rate	–0.71
Discount Rate	–0.22	Queue Dissipation Capacity	–0.42
Control: Activity 4: Agency Cost	0.17	Value of Time for Passenger Cars	0.40
Control: Activity 7: Agency Cost	0.16	Annual Average Daily Traffic	0.13
Control: Activity 5: Agency Cost	0.12		
		Mix with 30% RAP	
30% RAP: Activity 1: Agency Cost	0.93	Discount Rate	–0.71
Discount Rate	–0.25	Queue Dissipation Capacity	–0.42
30% RAP: Activity 4: Agency Cost	0.14	Value of Time for Passenger Cars	0.40
30% RAP: Activity 7: Agency Cost	0.11	Annual Average Daily Traffic	0.13
		Mix with 40% RAP	
40% RAP: Activity 1: Agency Cost	0.92	Discount Rate	–0.71
Discount Rate	–0.34	Queue Dissipation Capacity	–0.40
40% RAP: Activity 4: Agency Cost	0.11	Value of Time for Passenger Cars	0.38
40% RAP: Activity 7: Agency Cost	0.10	Annual Average Daily Traffic	0.17
		40% RAP: Activity 4: Service Life	–0.11
		Control: Activity 8: Structural Life	–0.10
		Mix with 50% RAP	
50% RAP: Activity 1: Agency Cost	0.89	Discount Rate	–0.68
Discount Rate	–0.33	Queue Dissipation Capacity	–0.39
50% RAP: Activity 4: Agency Cost	0.15	Value of Time for Passenger Cars	0.38
50% RAP: Activity 7: Agency Cost	0.13	Annual Average Daily Traffic	0.15
		50% RAP: Activity 2: Service Life	–0.15
		50% RAP: Activity 4: Service Life	–0.14
		50% RAP: Activity 1: Service Life	–0.14
		50% RAP: Activity 7: Service Life	–0.13
		50% RAP: Activity 5: Service Life	–0.12
		50% RAP: Activity 3: Service Life	–0.11

Probabilistic LCCA showed that agency cost is very sensitive to the initial construction cost of the alternatives, whereas user cost turned out to be most sensitive to the discount rate for the project.

Research related to RAP usually addresses issues such as the degree of blending between RAP binder and virgin binder, fractionation of RAP, determination of the binder PG grade to be used, the film thicknesses, and the laboratory performance of the mixtures. Although these issues are important, the ultimate issue is field performance of the recycled mixtures. In this study, the LCCA conducted under various performance scenarios underscored the importance of achieving field performance for recycled mixtures equivalent to that of control mixtures.

CHAPTER 8

ENVIRONMENTAL IMPACT OF USING HIGH RAP CONTENT IN ASPHALT MIXTURES

8.1 Introduction

The "Moving Ahead for Progress in the 21st Century Act" (MAP-21) became a law in the United States on July 6, 2012. MAP-21 is the first long-term highway authorization enacted since 2005 and will fund surface transportation programs at more than $105 billion for fiscal years 2013 and 2014 (FHWA, 2013b). MAP-21 established "environmental sustainability" as one of the national transportation goals; its purpose is "to enhance the performance of the transportation system while protecting and enhancing the natural environment." The US pavement industry, recognizing the need to move toward a sustainable pavement system, has also been promoting sustainable practices for many years.

Sustainable pavement systems may be defined as a network of high-quality, long-lasting pavements whose design, construction, and management take into account economic and social development, as well as environmental preservation. A few of the asphalt sustainability strategies include, but are not limited to, warm-mix asphalt (WMA), perpetual pavement thickness, in-place recycling, and use of reclaimed asphalt pavement (RAP) and recycled asphalt shingles (RAS).

Life-cycle assessment (LCA) makes an integral part of a sustainability triangle. Today's sustainability-driven systems require a product/process to be environmentally beneficial apart from being cost-effective. Last decade has seen pavement industry taking considerable strides towards the goal of sustainable pavement systems by looking into the carbon footprints of pavement products. LCA is gradually being introduced in the pavement industry as a decision-making tool along with more traditional life-cycle cost analysis.

Life-cycle assessment, for the first time, was used to analyze different pavements types in the late 1990s (e.g., Häkkinen and Mäkelä 1996, Horvath and Hendrickson

1998). Häkkinen and Mäkelä (1996) conducted a relatively regionalized LCA (data came from Nordic sources) to compare a stone-mastic asphalt with a doweled jointed plain concrete pavement (JPCP). The LCA included all phases of the pavement life cycle except end-of-life phase. Stripple (2001), a Swedish study, examined a JPCP and two asphalt pavements produced using hot and cold production techniques. Scope of Stripple's study included the entire roadway rather than just the pavement structure. The analysis includes the effects of road markings, signs, vegetation, and other issues not directly related to the pavement itself. The study did not precisely define the maintenance activities or which years they occur during the life cycle. Stripple concluded that without the feedstock energy, the JPCP consumes considerably more energy than do either of the asphalt pavements; the reverse is true when feedstock energy of the bitumen is considered.

At a few places in this chapter, the more general terminology, i.e. *bitumen,* will be used in lieu of asphalt binder. Treloar et al. (2004) used a hybrid LCA method to assess eight pavement types, including a CRCP, an undoweled JPCP, a composite pavement, and a variety of asphalt pavements. The construction phase was estimated using an Australian input-output model. The conclusions from the study are focused on highlighting the relatively small importance of the materials, construction, and maintenance phases relative to the roadway life cycle rather than choosing the best pavement type.

Although LCA of pavement recycling has been reported in a couple of studies (Carpenter et al. 2007, Chiu et al. 2008, and Kawakami et al. 2009), very few have addressed the use of RAP in asphalt pavement. A French study (Jullien et al. 2006) investigated four asphalt concretes made with different percentages of RAP (0%, 10%, 20%, and 30%) during road construction. The study focused on determining airborne emissions, odors, and pollutant release over time and odor production related to the asphalt-laying operation. The results showed an increase in gas emissions and a decrease in odors as the percentage of RAP increased. In an extension to this study, Ventura et al. (2008) compared binding courses of pavement sections made with various percentages of RAP (0%, 10%, 20%, and 30%) in a hot mix process.

In an extension to this study, Ventura et al. (2008) compared binding courses of

pavement sections made of RAP using various recycling rates (0%, 10%, 20%, and 30%) in a hot mix process. Except for the toxicity and eco-toxicity impact indicators, the entire set of computed indicators revealed a trend of decreasing potential environmental impacts with an increasing recycling rate. The study did not find any significant difference in the field performance of the four pavement sections (Jullien et al. 2006). To determine whether the binder courses required more frequent maintenance and to accurately estimate the environmental impact of different section, authors recommended regular assessment of pavement condition.

Brantley and Townsend (1999) addressed the important issue of leachate produced by RAP. They concluded that RAP samples in the study were not hazardous waste and did not leach chemical greater than allowed by typical groundwater standards. In Taiwan, Chiu et al. (2008) performed life cycle inventory (LCI) of three recycled materials by incorporating the database provided by Eco-indicator 99. The recycled materials used in the study were recycled asphalt concrete, asphalt rubber, and Glassphalt. The study showed that using recycled asphalt concrete can reduce the eco-burden by 23% relative to a virgin mixture. Using asphalt rubber increased the eco-burden by 16%, whereas, the eco-burden remained essentially the same when Glassphalt was used. The study did not go into detail of the mixtures composition and RAP content used. The researchers concluded that, although, reduction of the amount of asphalt and the consumption of heat are the keys to lower the eco-burden of rehabilitation work, the reduction in asphalt content may reduce the service life of pavement.

LCI is most important and challenging part of the LCA. For bitumen, LCI requires the data related to the energy consumed and GHG emissions through all the processes from cradle to grave. Data related to extraction of crude oil, its transportation to petroleum refinery, processing in petroleum refinery, bitumen blending and storage, and transportation to asphalt plant, are needed to make inventory for bitumen.

A few of the impediments to conducting a comprehensive LCA are time, availability and accuracy of data, and knowledge of the detailed processes involved. Because of these constraints, most environmental assessments limit their scope to the phases and processes that are feasible under their individual constraints (Santero 2009). The methodology and simplifications adopted in this study are explained in next sections.

The environmental impact of using high amount of RAP in asphalt binder mixtures was evaluated. This is accomplished through four primary tasks:

1. Conduct a comprehensive LCA for the mixtures involved in the study.
2. Compare the energy and carbon footprints of the asphalt mixtures with and without RAP.
3. Determine the environmental impact of the mixtures with RAP at varying performance levels of the mixtures.
4. Determine the breakeven performance levels of the mixtures with different RAP contents.

8.2 LCA Framework

8.2.1 Goal and Scope of LCA

The goal of conducting LCA in this study is to evaluate and compare the environmental impact of asphalt binder mixtures with and without RAP. Same project parameters (such as pavement section, functional unit, and the analysis period used in LCCA) were used for the LCA study and shown in Table 7.1. Binder course is the main variable in all the alternatives; mixtures with different amount of RAP are used in the binder course for each alternative. The LCA was conducted for District 5 material only. A hybrid LCA, a combination of process-based LCA and economic input-output LCA (*EIO-LCA*), was conducted to cover the material, construction, and maintenance and rehabilitation phases of a pavement's life cycle (Figure 8.1). Use-phase factors such as albedo, roadway lighting, and rolling resistance were not considered because the mixtures used in the study are asphalt binder mixtures, not surface mixtures. For the end-of-life phase, the "cut-off approach" (Nicholson et al. 2009) has been adopted. In the cut-off approach, the recycling burden associated with a product (i.e., the pavements under consideration at the end of 45 years) is ascribed to any other product (e.g., future pavement) which uses this recycling burden. This study's scope ends with the demolition of all pavement systems under consideration after the analysis period.

Benefits and burdens of using recycled product are only given to the downstream user, and the current pavement (under consideration) is not given credit for producing

recyclable materials. There exists other techniques to handle end-of-life phase such as the 50/50 method, closed-loop method, or substitution method, but the cut-off method is the most commonly used in pavement LCAs because of future uncertainties related to pavements. In this study, all alternate pavements are assumed to be treated similarly; therefore, demolition was not accounted for in the LCA. Material and transportation were considered for both initial construction and future maintenance and rehabilitation activities. Feedstock energy was calculated as well in compliance with ISO standard (ISO 2006b).

To maintain a reasonable scope, the LCA focused only on energy consumption and GHGs [carbon dioxide (CO_2), methane (CH_4), and nitrous oxide (N_2O)] in units of CO_2 equivalents. If it is assumed that pavement made with virgin material and pavement made with a specific RAP content have similar performance, the factors contributing to any differences between the two are: (1) materials extraction and production, (2) transportation, and (3) onsite equipment. The details of the maintenance and rehabilitation schedule (IDOT 2013) followed are shown in Table 7.2. Initial construction included construction of asphalt binder and surface courses, as well as the shoulder. As explained in Chapter 7, IDOT's 45-years maintenance and rehabilitation schedule was followed.

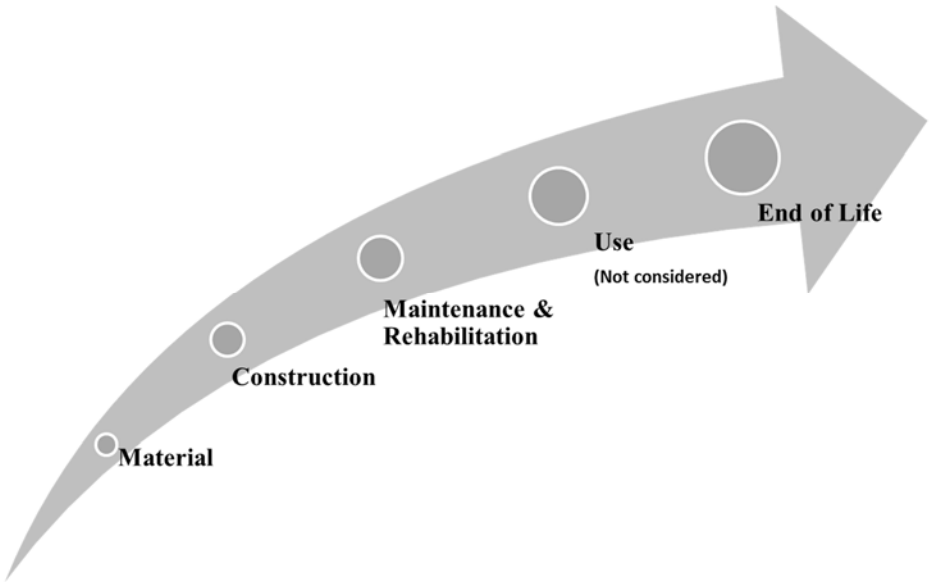

Figure 8.1 Life cycle of a highway pavement.

8.2.2 Life Cycle Inventory

Life-cycle inventory (LCI) is the most important and challenging phase of the LCA. For asphalt binder/bitumen, LCI requires the data related to energy consumed and GHG emissions through all the processes from cradle to grave. Data related to extraction of crude oil, transportation to the petroleum refinery, processing at the petroleum refinery, asphalt binder blending and storage, and transportation to the asphalt plant, are necessary to complete the LCI for asphalt binder.

At asphalt plants, RAP is not heated directly to avoid aging of RAP binder. Instead, virgin aggregates are overheated before introducing the RAP to the drum. However, this overheating of virgin aggregates can cause extra fuel and energy use, which may offset the economic benefits of using RAP. Exhaustive production and energy consumption data were obtained from an asphalt plant by using an energy monitoring and automated tracking system (MINDS 2012). Ten months of asphalt production data were collected at an interval of 5 sec. The key entities of the database were mix type, production, production rate, RAP content in the mix, aggregate and RAP moisture contents, and energy consumption during production of the mix. Figure 8.2 shows the effect of RAP and RAP moisture content on the electricity and gas consumption of the asphalt plant.

In order to measure any degree of linear dependence between RAP content and the energy consumption, Pearson correlation coefficients were determined. The Pearson correlation coefficient is a statistical measure of the linear correlation (dependence) between two variables. It can have a value between +1 and −1, where 1 is total positive correlation, 0 is no correlation, and −1 is total negative correlation. Table 8.1 shows the Pearson correlation coefficients for a part of the data acquired from the plant. The low values of coefficients as well as inconsistency between the signs (-ve or +ve) show the absence of any correlation between the RAP content and electrical ratio and/or total gas ratio.

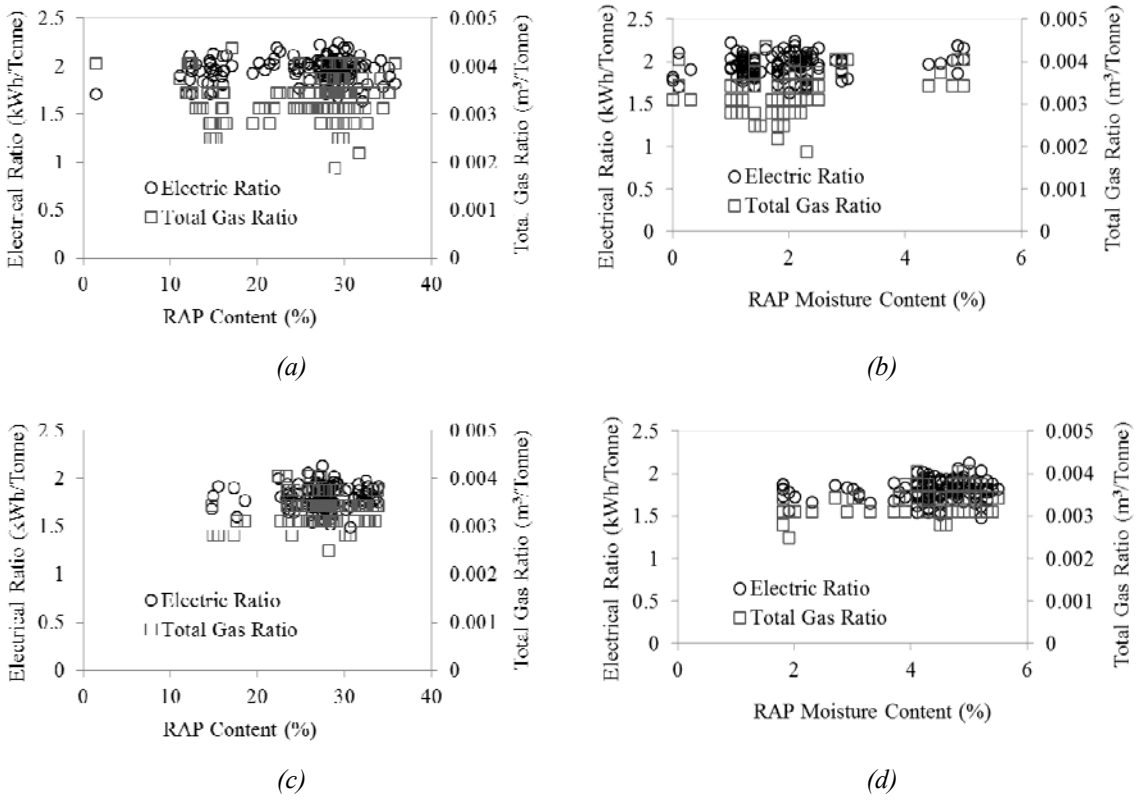

Figure 8.2. Effect of RAP content and moisture content on asphalt plant's energy consumption; (a) RAP effect – Sep 2011, (b) RAP moisture effect – Sep 2011, (c) RAP effect – Jun 2012, and (d) RAP moisture effect – Jun 2012.

Likewise, no energy variation was observed with respect to RAP's moisture content. This contradicts the finding of another study (Horton et al. 2011), which examined plant operating conditions while producing asphalt mixtures containing high RAP percentages (50%, 60%, and 70%). The study found that drum shell temperatures and virgin aggregate temperatures were too high to be sustainable when 60% and 70% RAP contents were used in mixtures. For 50% RAP, virgin aggregate temperature and drum shell temperature were found to be low enough to run for extended periods. The temperature of the drum shell is important, because operating at elevated temperatures for a prolonged period of time increases metal wear and fatigue on the plant.

Although the energy data were not documented, it can be inferred from the study's conclusions that more energy is required to produce mixtures with high RAP content if the discharge temperatures have to be kept constant. A possible reason for this inconsistency between Horton's study and the current study is that the former employed

small production runs for the study, whereas data in the current study have been taken from actual large production plant runs. The lack of energy variation due to RAP's inclusion may also be due to the fact that the final production mass is the same. The extra energy consumed due to superheating may be counterbalanced by the reduction in virgin aggregates to be heated. Figure 8.3 shows the discharge mix temperature for the same mixtures; uniform discharge mix temperatures data proved that there was no compromise on the temperature of the final product. Some of the lower discharge temperatures indicate the production of warm mix asphalt (WMA).

Table 8.1. Pearson correlation factors between different entities of asphalt plant's dataset.

Correlation between	Sep 2011	Oct 2011	Apr 2012	May 2012	Jun 2012	Aug 2012
RAP and Total Gas Ratio	0.02	0.15	-0.27	0.30	0.07	0.18
RAP and Electrical Ratio	0.07	-0.19	-0.11	0.17	-0.17	-0.22
RAP Moisture Content and Total Gas Ratio	0.32	0.20	0.20	0.21	0.29	0.17
RAP Moisture Content and Electrical Ratio	0.19	-0.16	0.04	-0.06	0.11	-0.02
RAP and Discharge Temperature	-0.21	-0.01	-0.28	0.01	-0.18	-0.15

Since the plant data did not show effect of RAP on production and energy consumption, asphalt production and related operations were included in the IO-LCA rather than the process-based LCA.

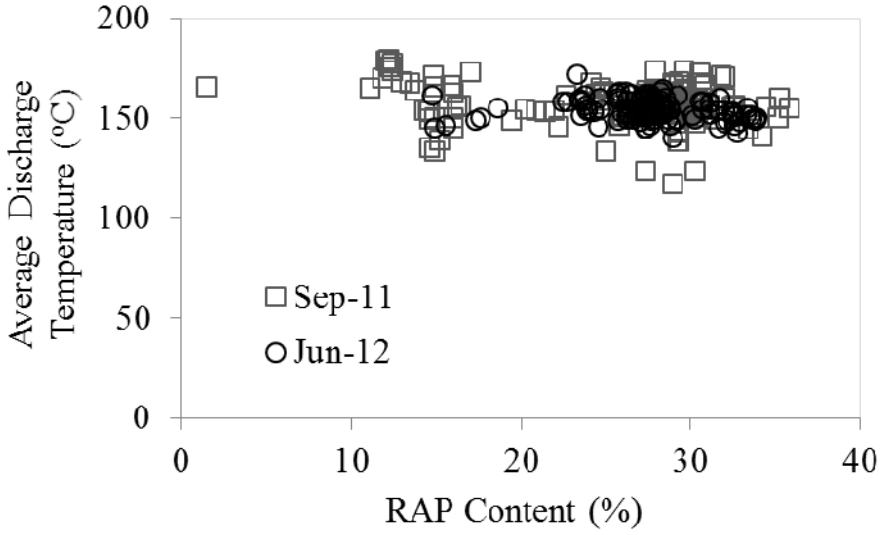

Figure 8.3. Asphalt concrete discharge temperatures for different months.

8.2.2.1 Economic Input-Output LCA

Economic Input-Output Life Cycle Assessment (*EIO-LCA*) uses information about purchases of materials by one industry from other industries as well as the information about direct environmental emissions by industries, to estimate the total emissions throughout the supply chain (CMU 2013). *EIO-LCA* "estimates the materials and energy resources required for, and the environmental emissions resulting from, activities in our economy (CMU 2013)." *EIO-LCA* can be used for initial screening to make an assessment of critical factors impacting the environment. The environmental impacts of asphalt binder production depend largely on crude extraction, transportation, and refining.

The online tool of *EIO-LCA* available at eiolca.net was used to find environmental factor for materials extraction and production phase. The first step in using *EIO-LCA* is choosing the model year and country for industry. The years for which the model exists are 1992, 1997, and 2002; for this study, the US 2002 National Producer Price models was used. In the next step, industry sector to analyze is selected. For the 2002 model, industry sectors divide the economy into 428 divisions grouping businesses that produce similar goods or services, or that use similar processes (CMU 2013).

The corresponding economic sector for asphalt binder refining in the *EIO-LCA* model is "#324110 Petroleum Refineries", which gives the energy consumption and emissions per unit of total refined products. The "Petroleum Refineries" sector was used for LCI of the asphalt binder used as emulsion in tack coat and polymer modified bitumen (PMB) used as crack sealant. The economic sector "asphalt paving mixtures and block manufacturing" was used for asphalt mixtures.

An allocation problem arises here: asphalt binder is a co-product rather than a by-product of the crude oil refining process. Since refining is a multi-output process that is aggregated in *EIO-LCA*, the energy and emissions attributed to its individual products must be allocated (ISO 2006a & 2006b). In this study, an economic allocation was used for the refining process. Thus, it was assumed that the economic contribution of a petroleum product is directly proportional to the energy and emissions attributed to refining that product. In order to calculate the economic allocation for asphalt binder, the

physical (by volume) and economic (dollar amount) percentages of asphalt product out of the total refined products are needed.

The percent yields by volume of each petroleum product were obtained by using averages of the 2003-2012 refinery yield data from the U.S. Energy Information Administration (EIA) (USEIA 2013a). The average US economic prices of each petroleum product for all sectors were taken from the EIA State Energy Data System for 2011(USEIA 2013b). These prices are given as dollars per energy unit, so prices were converted to dollars per volume using the approximate heat contents given by EIA. Using the percent volume yield and dollars per volume, the economic contributions or yields were calculated and are given in Table 8.2.

The economic allocation for any refined product can then be calculated by taking the ratio between the economic and volumetric yields. For asphalt, the volumetric yield is 2.79% while the economic yield is only 1.17%. The allocation is calculated to be 42.1% (economic yield divided by volumetic yield), which is fairly low compared to the other products; e.g., the allocation of 102.9% is achieved for motor gasoline by normalizing the economic yield by volumetric yield. This method is one-to-one comparison of different crude oil products to the crude oil, or in other words, the 42.1% means that $1 of asphalt binder has 42.1% of the impact of $1 of crude.

To apply the allocation, the energy and emission values given by the "Petroleum Refineries" sector in the *EIO-LCA* model are multiplied by 42.1%. It was found that the production of refined asphalt binder has an environmental impact of 13.3 MJ/$ and 1.2 kg CO_2e/$. Assuming a value of $500 (i.e., $326 in 2002 dollars; explained in next section) per ton of asphalt binder, the energy consumption is 4349 MJ/ton. Compared with 1842 MJ/ton from Eurobitume (2011), 3265 MJ/ton from Athena Institute (2006), and 12100 MJ/ton from US-Ecoinvent v.2, the energy obtained using the *EIO-LCA* model is somewhere in-between. A reason for these discrepancies could be the type of allocation used by each source. Eurobitume uses economic allocation while Athena Institute and US-Ecoinvent v.2 use mass allocation. In addition, each model assumes a different crude distribution, which heavily influences extraction and transportation processes. For example, depending on whether foreign or domestic crude oil is used, the greenhouse gases for diesel production in the U.S. can vary by 59% (NETL 2009).

Table 8.2. Volume and economic contributions of various refined petroleum products.

Refined Petroleum Product	Volume Yield (%)	Price ($/MJ)	Heat Content (MJ/bbl.)	Economic Yield (%)	Economic Allocation (%)
Motor Gasoline	45.7	0.0266	5482	47.05	102.9
Distillate Fuel Oil	26.4	0.0254	6140	29.14	110.2
Kerosene-Type Jet Fuel	9.46	0.0214	5976	8.57	90.6
Petroleum Coke	5.30	0.0034	6349	0.82	15.5
Still Gas	4.39	0.0000	6324	0.00	0.00
LPG	4.04	0.0219	4264	2.67	66.0
Residual Fuel Oil	3.89	0.0149	6626	2.71	69.7
Asphalt and Road Oil	2.79	0.0085	6994	1.17	42.1
Naphtha (Petrochemical Feedstock)	1.33	0.0227	6626	1.41	106.2
Lubricants	1.09	0.0660	6393	3.25	298.2
Other Oils (Petrochemical Feedstock)	1.02	0.0267	5835	1.12	110.1
Miscellaneous Petroleum Products	0.45	0.0674	6109	1.31	290.9
Special Naphthas	0.25	0.0283	5531	0.28	110.6
Kerosene	0.22	0.0265	5976	0.25	112.2
Aviation Gasoline	0.10	0.0300	5321	0.11	112.9
Waxes	0.10	0.0329	5836	0.14	135.8
Processing Gain(-) or Loss(+)	-6.54				

The adjusted environmental factors obtained from the *EIO-LCA* model per dollar of the economic activity are shown in Table 8.3.

Table 8.3. Environmental factors per dollar of economic activity.

	Asphalt paving mixtures and blocks	Petroleum refineries[1]
Energy (MJ/$)	22.900	13.314
CO_2, (kg/$)	1.3874	0.8579
CH_4-CO_2e (kg/$)	0.2631	0.3084
N_2O-CO_2e (kg/$)	0.0112	0.0027
GHG, CO_2e (kg/$)	1.6705	1.1721

[1] Only 42% of environmental factors for petroleum refinery are allocated to asphalt binder

The total life-cycle costs for asphalt mixture and asphalt binder (emulsion and PMB) used in the different alternatives throughout 45 years of the pavements' life cycle were determined and are shown in Table 8.4.

Table 8.4. Agency cost for all alternatives in 2002 dollars.

	Asphalt mixture cost to be used in *EIO-LCA*			
	Control	30% RAP	40% RAP	50% RAP
Initial construction cost per km	$235,194	$212,378	$204,772	$197,167
Maintenance cost per km	$44,125			
Total life-cycle cost per km	$279,319	$256,502	$248,897	$241,291
	Binder (sealant + emulsion) cost to be used in *EIO-LCA*			
	Control	30% RAP	40% RAP	50% RAP
Initial construction cost per km	$1,110			
Maintenance cost per km	$9,948			
Total life-cycle cost per km	$11,059			

It is worth mentioning here that all the prices included in the *EIO-LCA* model were from the year of the model. The cost of any alternative must therefore be adjusted to 2002 prices because the 2002 US producer price model was used in this study. One of the approaches to adjust producer price for a commodity is to use producer price index (PPI) for that commodity. The statistical abstract of the United States (BLS 2013) lists the PPI for all commodities in 2012 as 201 and in 2002 as 131. In this study, the maintenance and rehabilitation costs for 45 years were first discounted at a rate of 4% to year 2012. The net present value (NPV) for each alternative was then multiplied with 0.652, a ratio of PPIs from 2002 and 2012, to determine the costs in 2002 dollars. The energy and environmental factors (Table 8.3) were multiplied by the cost of asphalt mixture and asphalt binder (Table 8.4), resulting in the total amount of energy consumed and GHGs released for a particular alternative.

The *EIO-LCA* model took into account the energy consumption and GHG emissions associated with the material phase and initial construction and future maintenance activities. The asphalt paving mixtures and block manufacturing sector includes all the stages of asphalt concrete production (i.e., from extraction of the raw materials to the production of asphalt concrete at asphalt plant). Table 8.5 shows the energy consumption and GHGs emissions during initial construction and maintenance activities. It is important to note here that reductions in energy use and GHGs are attributed solely to the material phase, the only variable being the binder course. Processes involved in producing the control binder course consumed 3,110,090 MJ of

energy and released 226,870 kg of GHGs. Considering the binder course only, reduction of 17% to 28% were observed in both energy consumption and GHG emissions (i.e., production of an asphalt mix with 50% RAP requires only 72% of energy and GHGs compared to a virgin mix). This lower environmental and energy impact of recycled asphalt mixtures can be ascribed to the reduction in the asphalt binder needed to be extracted from crude oil as well as the subsequent reduction in processing, transportation, blending, and storage of asphalt binder.

Table 8.5. *EIO-LCA* - energy consumption and GHGs emissions per km.

	Energy (MJ)		GHG (kg CO_2e)	
Mixture type	Initial construction	Maintenance	Initial construction	Maintenance
Control	5,400,727	1,142,908	394,187	85,370
Mix with 30% RAP	4,878,232		356,072	
Mix with 40% RAP	4,704,067		343,368	
Mix with 50% RAP	4,529,902		330,663	

Assuming the same maintenance and rehabilitation activities for all the alternatives resulted in the same amount of energy consumption and GHG emissions during the maintenance phase for all the mixtures. This can be assumed because the study considers that all alternatives perform equally well.

8.2.2.2 Process-based LCA

Process-based LCA was used to determine environmental burdens related to construction activities during initial construction and maintenance activities. While transportation occurring in upstream supply chain processes is included in *EIO-LCA*, transportation activities after asphalt production need to be directly calculated. Moreover, the onsite equipment associated with asphalt placement must be taken into account. The typical equipment used for asphalt paving includes a paver, rollers, and a material-transfer vehicle (MTV).

Onsite equipment accounts for only a small fraction of the global warming potential (GWP) over the pavement life cycle. Zapata and Gambatese (2005) found that the placement phase of the asphalt concrete life cycle consumes less than 2% of total energy; whereas, the Athena Institute (2006) chose to neglect the impact of construction

equipment altogether. Minor maintenance activities such as crack and joint resealing and patch repairs to various depths of the pavement were also considered in analysis. Minor rehabilitation activities are usually ignored in LCA studies; in this study though, these activities held some importance when environmental impact of the recycled mixtures was considered under different performance scenarios.

The major activities considered for the LCI of virgin and recycled mixtures were (1) prime coat transport and spraying, (2) tack coat transport and spraying, (3) crack sealant application, (4) asphalt mix transport via dump truck, (5) asphalt mix transfer via MTV, (6) asphalt mix paving, (7) breakdown rolling, and (8) finish rolling. The type and model of equipment used in construction of an asphalt pavement varies based on type of pavement, contractor preferences, and agency requirements. The specific equipment used in this analysis for different construction and maintenance activities is listed in Table 8.6; the equipment selected was some of the typical equipment used in the US pavement industry.

Table 8.6. Equipment details used in initial construction and rehabilitation.

Equipment	Model	Productivity	Fuel consumption	Fuel type
Router	Crafco Model 30 (30 hp)[1]	—	11.4 L/hr	gasoline
Milling machine	Wirtgen W1900/75 (400 hp)	363 t/hr	87.3 L/hr	diesel
Dump trucks	GMC c8500 (275 hp)	20 t/trip	0.42 L/km	diesel
Jackhammers	90cc single cylinder 2-stroke	—	1.0 L/hr	gasoline
Self-propelled roller	95.4 hp	—	36.1 L/hr	diesel
Tanker truck	—	11924 L/tank	0.42 L/km	diesel
MTV	Cedarapids MS-1 (100 hp)	1,306 t/hr	21.0 L/hr	diesel
Asphalt paver	Dynapac F25C	1,542 t/hr	31.5 L/hr	diesel
Pneumatic rollers	Dynapac CP221	622 t/hr	25.0 L/hr	diesel
Tandem rollers	Ingersol rand DD90HF	358 t/hr	27.5 L/hr	diesel

[1] Data obtained from equipment manufacturers websites and PALATE software.

In an overlay activity, milling and transportation of RAP from site to landfill or asphalt plant must occur, regardless of its ultimate use. RAP milling and transportation is, therefore, not considered in the LCA analysis. Transporting RAP to the asphalt plant also reduces the material being dumped, thereby reducing the burden on landfills and eliminating landfill tipping fees. Milling and transportation of milled material must be

taken into account, however, when at-plant recycling is to be compared with in-place recycling. Additionally, since the cut-off method was followed for end-of-life phase, demolition/milling of the previous pavement (source of RAP for this study) should not be considered in this study. However, it is important to note that milling and hauling of material during different rehabilitation activities (Table 7.2) have been considered in the analysis.

The quantity of asphalt concrete used in initial construction and maintenance cycles was measured. Crack lengths and patching areas were determined based on IDOT's maintenance and rehabilitation schedule (Table 7.2) to calculate crack sealant and patching mix quantities. Once the material quantity was determined and the equipment to be used was identified, the amounts of CO_2, CH_4, and N_2O for material transportation from asphalt plant to site and for operating onsite equipment were calculated based on Equations 8.1 and 8.2.

For onsite equipment,

$$m(os)_{CO_2} = \sum_{i}^{Material} \sum_{j}^{Equipment} \left(\frac{m_i \times f_j \times EF_{ft}}{p_j} \right) \tag{8.1}$$

where,

$m(os)_{CO_2}$ = mass of CO_2 from on-site equipment (kg),
m_i = mass of material i (kg),
p_j = productivity of onsite equipment j (kg/hr),
f_j = fuel consumption of equipment j (L/hr), and
EF_{ft} = CO_2 emission factor for equipment j based on fuel type (kg/L).

For transportation,

$$m(t)_{CO_2} = \sum_{i}^{Material} \sum_{j}^{Equipment} \left(\frac{m_i \times f_j \times d_j \times EF_{ft}}{p_j} \right) \tag{8.2}$$

where,

$m(t)_{CO_2}$ = mass of CO_2 from material transportation (kg),
m_i = mass of material i (kg),
p_j = productivity/capacity of an equipment j (kg),
f_j = fuel consumption of equipment j (L/km),
d_j = distance travelled by equipment j (km), and
EF_{ft} = CO_2 emission factor for equipment j based on fuel type (kg/L).

Energy consumed during the process was also calculated using similar equations by replacing emission factors (EF) with the energy densities of the respective fuel types. Energy factors incorporated both process (upstream) and combustion (heating/calorific value) energies for the fuels and were obtained from USEPA (2008) and GREET (2013). The International Panel on Climate Change's 100-year time horizon factors were adopted as the basis for CO_2 equivalence for this study, as shown in Equation 8.3 for GWP.

$$GWP\ (kg) = GHG\ (kg\ CO_2e) = CO_2(kg) + CH_4(kg) \times 25 + N_2O(kg) \times 298 \quad (8.3)$$

Table 8.7 shows results from the process-based LCA, including onsite equipment and transportation to and from the asphalt plant. Assuming similar performance, and, consequently, similar maintenance activities, four different alternatives resulted in the same amounts of energy consumption and GHG emissions.

Table 8.7. Energy consumption and GHG emissions - construction phase.

Mix type	Activity	Energy (MJ)	CO_2 (kg)	CH_4 (kg)	N_2O (kg)	GHG (kg CO_2e)
All mixtures	Initial construction	320,737	18,758	0.0558	0.0525	18,775
	Maintenance	279,596	15,237	0.1112	0.0607	15,258
	Total	600,333	33,996	0.1670	0.1132	34,033

8.2.2.3 Hybrid LCA

Process-based LCAs, though detailed and thorough, are time consuming and can be costly to prepare. The *EIO-LCA*, though easy to conduct and reproducible, takes into account aggregate data and ignores process-specific details. In a hybrid LCA, the two LCAs complement each other and exploit each other's strengths. Hybrid analysis resulted in energy consumptions and GHG emission amounts during material and construction phases, as shown in Table 8.8.

The environmental burden associated with construction phase turned out to be the same for all the mixtures. There are two reasons for this: 1) the same equipment and construction techniques were used for paving the mixtures and 2) it was assumed that all the mixtures performed equally well in the field. Assumption of any underperformance of recycled mixtures would have triggered additional maintenance activities and, consequently, different construction costs.

Table 8.8. Hybrid LCA results for all alternatives.

	Life-cycle Phase	Control	Mix with 30% RAP	Mix with 40% RAP	Mix with 50% RAP
Energy (MJ)	Construction	600,333			
	Material	6,543,635	6,021,140	5,846,975	5,672,810
	Total	7,143,968	6,621,473	6,447,308	6,273,143
Carbon dioxide, CO_2 (kg)	Construction	33,996			
	Material	397,012	365,356	354,805	344,253
	Total	431,007	399,352	388,800	378,248
Methane, CH_4 (kg CO_2e)	Construction	4			
	Material	76,892	70,889	68,889	66,888
	Total	76,896	70,894	68,893	66,892
Nitrous oxide, N_2O (kg CO_2e)	Construction	34			
	Material	3,159	2,903	2,818	2,733
	Total	3,193	2,937	2,852	2,767
GHG (kg CO_2e)	Construction	34,033			
	Material	479,556	441,442	428,738	416,033
	Total	513,590	475,476	462,771	450,066

Increasing the RAP content in asphalt mixtures significantly decreased the energy consumption and reduced the emissions of GHGs. As described earlier, these savings are attributed solely to the material phase, the only variable being the binder course. The savings in energy ranged from 522,495 MJ to 870,825 MJ when 30% to 50% RAP was added. Similarly, a reduction in CO_2e emissions ranging from about 38,114 kg to 63,524 kg per km length of pavement was observed. A substantial difference was observed between the contributions from different life cycle phases to energy consumption and GHG. The construction phase was responsible for about 8.6% of total energy consumed and 6.8% of the total GHGs released, whereas the material phase proved to be a high energy, high-GWP-impact component.

The LCA results proved that incorporating RAP in asphalt mixtures is environmentally beneficial. It is important to remember, though, that these analyses were conducted based on the large assumption of equal performance. The questions therefore arise: What if the performance of the recycled mixtures were lesser than that of the virgin mixtures? Would we reap the same benefits? An attempt is made to answer these questions later in this study.

8.2.2.4 Feedstock Energy

According to the ISO 14044 standard (ISO, 2006b), feedstock energy is defined as "heat of combustion of a raw material input that is not used as an energy source to a product system, expressed in terms of higher heating value or lower heating value." To paraphrase, bitumen's feedstock energy is the portion of the resource input (crude oil) that ends up in asphalt binder rather than being used as fuel. The importance of feedstock energy is highlighted the most when asphalt pavement is compared with concrete pavement.

Santero (2009) gave a detailed overview of the issue of accounting for the feedstock energy in the energy inventory. He argued that although the ISO standard (ISO, 2006b) clearly states that feedstock energy should be included in a product's LCI, it never discusses a situation where the feedstock energy of a product is not easily released, as is the case with asphalt binder. Although asphalt binder cannot be simply labeled as a direct energy source, ignoring feedstock energy is difficult to justify in light of its properties as a residual product (Santero 2009). In the current study, feedstock energy was calculated to conform to ISO standards but was kept separate from process energy.

Feedstock energy was calculated by determining the asphalt binder used in the asphalt mixtures, emulsion used as a tack coat, and the sealants used in crack sealing. Asphalt binder's net calorific value of 40.2 MJ/kg (Garg et al. 2006), was used to calculate feedstock energies. There are two options to account for feedstock energy. First option is to consider feedstock for the total binder content i.e. aged asphalt binder contributed by RAP must also be included when determining the feedstock energy. Second option is to consider feedstock energy of virgin binder only. Binder in RAP might be ignored due to end of life assumptions i.e. feedstock energy of existing RAP should have already been considered when RAP was used as a virgin material in the previous pavement. Both of these options are debatable and no clear consensus exist on any of them. Both the options were exercised in this study.

The effect of feedstock energy is immense. In the first option, accounting for the feedstock energy resulted in a surge in the total energy from 7,143,968 MJ to 205,717,298 MJ. Since total binder content of control and mixtures with RAP was same (5.2%), regardless of the RAP content used (Chapter 3), feedstock energy did not affect

the ranking of the mixtures in this study. However, taking into consideration feedstock energy would have made a significant difference had the total binder content been different for each asphalt mix. For the second option, considering binder course only, feedstock energies for the control mix, and recycled mixtures with 30%, 40%, and 50% RAP were calculated to be 4,723,896 MJ, 3,490,959 MJ, 3,146,115 MJ, and 2,796,546 MJ, respectively. The total energy for recycled mixtures is significantly reduced if feedstock energy for RAP binder is not taken into account.

Though inconsequential in ranking the recycled mixtures in this study, feedstock energy in an LCA should be included only after addressing questions pertaining to the likelihood of using asphalt binder as direct fuel source, the refining processes of upgrading the asphalt binder to a globally acceptable combusting fuel, and the downstream effect of using an upgraded asphalt binder fuel (Santero 2009).

8.2.3 Breakeven Performance Levels

As discussed earlier in this chapter, the LCA was conducted based on the assumption that all mixtures performed equally well. Mixtures with RAP are considered more susceptible than virgin mixtures to thermal and fatigue cracking, if softer binder or rejuvenator was not used. Similar to economic benefits, if the recycled mixtures performance is insufficient, the environmental benefits of using RAP will be offset by the need for more frequent maintenance and rehabilitation activities. In chapter 7, methodology adopted to determine breakeven performance level for the mixtures with RAP is described in detail. In this chapter, breakeven performance levels for the mixtures are determined based on energy consumption and GHG emissions instead of project's economics (if hypothetically RAP mixes are assumed to perform less than control mixes). Table 7.6 shows different scenarios for which LCA was conducted.

The LCA conducted under different performance scenarios showed a reduction in the benefits of using RAP in the mixtures with decreased performance. Table 8.9 illustrates that, up to 80% performance, all the recycled mixtures maintained their advantage of less energy consumption and fewer GHG emissions despite lesser performance. But, as the performance levels declined further, a crossover point, as shown

in Figure 8.4, was reached at which all the benefits of using RAP were offset by the increased frequency of maintenance and rehabilitation activities.

Table 8.9. LCA results under different performance scenarios.

Mix type	Performance (%)	Impact categories		Breakeven performance level (%) based on	
		Energy (MJ)	GHG (kg CO_2e)	Energy	GHG
Control	100	7,143,968	513,590	—	—
Mix with 30% RAP	100	6,621,473	475,476	81.0	80.0
	90	7,003,956	500,959		
	80	7,171,745	513,119		
	70	7,749,850	553,531		
Mix with 40% RAP	100	6,447,308	462,771	77.0	76.0
	90	6,829,791	488,254		
	80	6,997,580	500,414		
	70	7,575,685	540,827		
Mix with 50% RAP	100	6,273,143	450,066	74.0	74.0
	90	6,655,626	475,550		
	80	6,823,415	487,710		
	70	7,401,520	528,122		

It can be observed that mixtures with higher RAP content have a greater margin for underperformance (e.g., 26% for 50% RAP) because of the higher reduction in GHG emissions and energy consumption. It is noteworthy that one would expect slightly different results had traffic delays in the construction work zone been considered in LCA. The breakeven performance levels determined in this study underscore the importance of achieving equivalent performance of the recycled mixtures in the field.

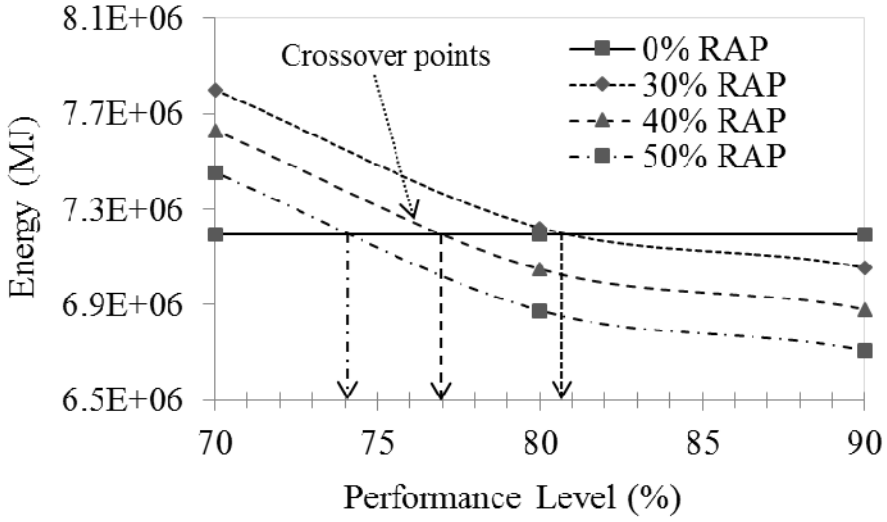

(a)

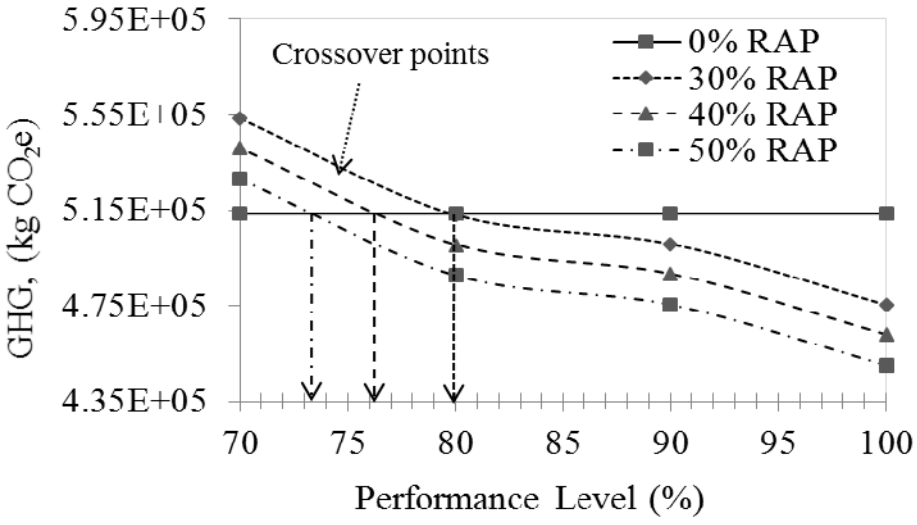

(b)

Figure 8.4. Breakeven performance levels based on (a) energy consumption and (b) GHG emissions.

8.3 Summary and Remarks

In the pavement industry, the purpose of conducting LCA is to better inform decision-makers by providing information about the environmental implications related to a certain construction/rehabilitation activity or a material/technology used in that activity. LCA does not take into account technical performance, cost comparison, and social

acceptance of a particular alternative. LCA alone does not guarantee success of an alternative; it is, therefore, recommended that LCA be used in conjunction with LCCA and other social parameters.

A hybrid LCA was conducted to evaluate the environmental impact of using a high RAP content in asphalt mixtures. The hybrid LCA was used to determine environmental footprints associated with material phase and construction phase of the pavement life-cycle. More production and energy data need to be collected from asphalt plants to validate the effect of RAP and RAP moisture on plants' energy usage. In future, *EIO-LCA* may be replaced by more detailed LCA provided that thorough process data related to extraction of crude oil, its transportation to a petroleum refinery, processing in a petroleum refinery, blending and storage of asphalt binder, and transportation to asphalt plant are collected. This would improve the confidence of users on LCA outcomes.

A significant reduction in energy consumption and GHGs was observed when RAP was introduced in the mixtures. Considering the binder course only, reduction of up to 28% was observed in both energy consumption and GHG emissions. It was also found that the construction phase contributed very little (about 6% to 8%) to the total energy and GHGs. A reduction of 26%, 33%, and 41% in feedstock energy was observed for the mixtures with 30%, 40%, and 50% RAP, respectively. LCA conducted under various performance scenarios highlighted the importance of achieving equivalent field performance for recycled mixtures to that of the virgin mixtures.

CHAPTER 9
SUMMARY, CONCLUSIONS, AND RECOMMENDATIONS

This main objective of this study is to evaluate the feasibility of using high amounts of RAP (up to 50%) in asphalt binder mixtures. A two-pronged approach was adopted to achieve the objective of the study: material characterization and economic and environmental analysis. Eight 3/4-in. (19-mm) NMAS binder mixtures (N_{des} = 90) were designed with the desired volumetrics; the mix designs included a control mix with 0% RAP and mixtures with 30%, 40%, and 50% RAP for each IDOT district. The effect of RAP on asphalt mixtures was analyzed through laboratory performance testing.

Laboratory experimental protocols were developed to conduct multiaxial characterization of the virgin and recycled asphalt mixtures. Young's, shear, and bulk moduli were determined directly in the time domain without the use of Poisson's ratios. Finally, the economic and environmental feasibility of the recycled mixtures were evaluated using life-cycle cost analysis (LCCA) and life-cycle assessment (LCA). Agency and user costs, as well as energy consumption and global warming potential of the recycled mixtures, were evaluated over the life cycle of a pavement. Breakeven performance levels of recycled mixtures were determined by conducting LCCA and LCA under different performance scenarios.

9.1 Findings

The key findings of this study are grouped into three categories and summarized as follows:

9.1.1 Asphalt Mix Design and Performance Testing

- Very similar and acceptable volumetrics were achieved for tested mix designs. The key reason behind achieving similar volumetrics is to gain control over gradation, which was accomplished by fractionating the RAP material similar to virgin aggregate.

- In general, tensile strength and tensile strength ratio (TSR) of the mixtures increased as RAP content increased. In addition, visual inspections conducted on failed split TSR specimen faces showed similar stripping behavior between the control and recycled mixtures.
- The complex modulus (E*) of the asphalt mixtures showed an increase in modulus as RAP content increased; however, the level of increase varied between mixes.
- The flow number data clearly showed a reduction in rutting potential as the RAP content increased for all asphalt mixtures.
- The wheel tracking test results for both asphalt mixture types were in agreement with the flow test data. The results suggested that increasing RAP content would reduce rutting potential.
- Based on the traditional fatigue curve slope analysis of beam fatigue test, fatigue life of the asphalt mixtures slightly improved with the addition of RAP for both materials. However, the behavior of mixes differed when energy based PV method for beam fatigue test and VECD theory on push-pull fatigue test were used.
- It was evident that RAP addition would increase the potential for thermal cracking (fracture energy was decreased). However, the current fracture tests may not quantitatively determine potential fracture due to loading rate and testing temperature combination.
- When single-bumped binder grade was used (compared to the same mix using PG 64-22), the following effects were observed:
    - The complex moduli (E*), at various loading frequencies and temperatures, were reduced for asphalt concrete, regardless of the RAP content, but they were still greater than those for the control mixture.
    - Rutting potential increased, as evident from flow and wheel tracking test results, but remained less than that for the control mixture.
    - Fatigue behavior improved.
    - In general, low-temperature fracture behavior marginally improved for the mixes (single bumping might not have an impact at low temperature).

Testing temperature is critical, and binder glassy transition temperature should be considered when analyzing data.

- When double-bumped binder grade was used, the following effects were observed:
    - In general, the complex moduli (E^*), at various loading frequencies and temperatures, were reduced compared to that for mixes base (PG 64-22) and single-bumped binder (PG 58-22).
    - The rutting potential increased with respect to single bumping, as indicated by both flow and wheel tracking test results.
    - Fatigue behavior did not show improvement with respect to asphalt mixtures with a single-bumped binder grade, but it did show improvement over the control mixture. It is important to note that, in general, all mixtures with RAP had K_2 values greater than IDOT's assumed typical design value of 0.35.
    - In general, low-temperature fracture behavior improved over no bumping and showed slight improvement with respect to asphalt mixtures using single-bumped binder grade.

9.1.2 Multiaxial Characterization of Asphalt Mixtures

- A brief literature review on the use of Poisson's ratios (PR) in the asphalt research community revealed that the majority of existing studies assumed an incorrect constant PR value of 0.35.
- The inapplicability of the correspondence principle to viscoelastic PRs was demonstrated. To determine the time dependence of viscoelastic PRs, a few simulations were conducted. The errors caused by incorrectly assuming constant PRs and the same moduli relaxation times for viscoelastic materials were quantified. The effect of varying moduli ratios on PRs was also studied. It is evident from the simulations that the assumptions of constant PRs and similar relaxation times can lead to serious errors in characterization of asphalt mixtures.
- A novel numerical technique to determine the viscoelastic properties of asphalt concrete by bypassing the PRs is implemented. The detailed analytical algorithm

was presented. A MATLAB code has been developed and simulations have been run to verify the accuracy of the code. A step-by-step procedure to obtain the Young's, shear, and bulk moduli directly in time domain was demonstrated.

- An experimental protocol was developed. After conducting various tests under different loading configuration, two tests were found to be suitable: (1) the compressive relaxation test and (2) the compressive creep test.
- Young's, shear, and bulk moduli were determined for the control and recycled mixtures. The relaxation test data, when analyzed using the developed algorithm, showed an increase in the mixtures' moduli with an increase in the RAP amount. Creep test data, however, could not be used to generate any reasonable trends.
- It was observed that Young's, bulk, and shear moduli had similar relaxation pattern which is uncommon for viscoelastic materials reported in the literature.
- Accurate determination of instantaneous moduli (K_0, G_0, and E_0) needs further exploration. The data collected near time zero were not sufficient to precisely determine instantaneous moduli.

9.1.3 Economic and Environmental Impact of Asphalt Mixtures with High RAP Content

- The LCCA deterministic analysis over a period of 45 years showed a significant decrease in life-cycle cost with an increase in RAP content. Considering the cost of binder course only, mixtures with RAP saved up to 28% relative to the virgin mixture.
- Probabilistic LCCA of various alternatives showed that agency cost is very sensitive to initial construction cost. However, user cost turned out to be most sensitive to the discount rate for the project. The user cost was almost 50% of the total cost for the control mixture.
- Exhaustive production and energy consumption data obtained from an asphalt plant using an energy monitoring and automated tracking system showed no energy variation with respect to RAP content and RAP's moisture content.
- A hybrid LCA was conducted to evaluate the environmental impact of using high RAP content in asphalt mixtures. Exhaustive production and energy consumption

data, obtained from an asphalt plant using an energy monitoring and automated tracking system, showed no relationship between RAP content and energy use. The LCA showed a significant reduction in energy consumption and greenhouse gas (GHG) emissions when RAP was introduced into the mixtures. It was found that the construction phase contributed very little (about 6% to 8%) to the total energy and GHGs. When feedstock energy was only considered for virgin binders, a predicted reduction of 26%, 33%, and 40% in feedstock energy was obtained for the mixtures with 30%, 40%, and 50% RAP, respectively.

- A methodology was followed to determine life-cycle costs and environmental burdens associated with possible low-performing recycled mixtures. The breakeven performance level of each recycled mixture was found, where breakeven performance level is a crossover point at which the economic/environmental benefits of using RAP are balanced by the increased number of maintenance activities due to poor performance. The net advantage of using RAP was diminished significantly when total costs instead of agency costs were taken in account, leaving the recycled mixtures with very little margin of underperformance.

9.2 Conclusions

The conclusions from this study are summarized below:

- It is possible to design high-quality asphalt mixtures with high RAP that meet the desired volumetrics and performance standards. The asphalt mixtures with RAP can perform equal to the mixtures produced with virgin aggregate, provided they are designed properly. The double-bumped asphalt binder grade was found effective in countering the RAP stiff residual asphalt binder and in helping to retain the original properties of the virgin mixture. Hence, proper asphalt grade or rejuvenator must be used in asphalt concrete mixes with RAP based on the RAP content and the environmental condition.
- Use of constant PRs for viscoelastic materials can lead to significant errors in estimating moduli values for asphalt mixtures.

- A multi-axial algorithm was introduced for asphalt concrete that provides an opportunity for 3-D characterization using a theoretically consistent approach. The approach is useful to determine bulk, shear, and Young's moduli directly in the time domain from relaxation test data.
- Economic and environmental analysis showed the viability of using high RAP content in asphalt mixtures provided that the resulting mixtures perform similarly to virgin mixtures. The LCCA and hybrid LCA conducted under various performance scenarios highlighted the importance of achieving field performance for recycled mixtures equivalent to that of virgin mixtures to realize the benefits.

9.3 Recommendations

- RAP fractionation should be recommended as a best practice for all asphalt mixtures that include RAP. A future study is recommended to evaluate the performance of asphalt mixtures with high RAP content in the field or under accelerated pavement loading tests. Such a study will help in comparing laboratory performance of these mixtures with their field performance.
- A quantified test should be developed to determine fracture properties of the mixtures with RAP. The tests conducted in this study did not differentiate 30% RAP mixtures from 50% RAP mixtures. It is recommended either to conduct the fracture tests at slightly higher temperatures or to develop a new fracture test that is sensitive to changes introduced by RAP to the mixtures.
- The viscoelastic characterization approach adopted in this study is promising. The proposed approach may prove to be a major milestone toward improvement of experimental characterization of asphalt concrete's linear viscoelastic behavior with multiaxial deformation measurements. Based on the knowledge gained in this study about viscoelastic characterization of asphalt mixtures, the potential areas for future research are as follows:
    - Photogrammetry techniques should be adopted; high-speed cameras can be used to capture the deformation during initial transition loading in the vicinity of zero time. This may help in providing better estimates of instantaneous moduli. Though not a significant issue in characterizing

asphalt concrete, it will also help obviate the use of metal wire strain extensometers for asphalt concrete. Laser measurement techniques can also be used to capture deformations.

  - The use of dynamic wave propagation experiments are suggested to be explored for determination of instantaneous moduli.
  - It is critical to eliminate the use of Poisson's ratio from viscoelastic characterization. Master curve approach using temperature-frequency sweep adopted in the implementation of complex modulus test can be integrated to the presented algorithms to increase the accuracy at early loading times.

- Field performances of in-service pavement with high RAP content should be closely monitored. It will help determine breakeven performance levels more accurately.
- It is recommended that an LCA be conducted at the local/regional level. Though difficult to collect, regionalized crude production, oil refinery, bitumen storage, and asphalt plant data can improve the reliability of the LCA. To confirm the findings of this study, more asphalt plants that use automated energy and production monitoring systems should be identified.

REFERENCES

Al-Qadi, I.L., Carpenter, S.H., Roberts, G.L., Ozer, H., and Aurangzeb, Q. (2009). Investigation of Working Binder in Hot-Mix Asphalt Containing Recycled Asphalt Pavements. Paper Number 09-1262, presented at 88th Annual Meeting of the Transportation Research Board, Washington D.C.

Ameri, M., Mansourian, A., Heidary Khavas, M., Aliha, M. R. M., & Ayatollahi, M. R. (2011). Cracked asphalt pavement under traffic loading – A 3D finite element analysis. *Engineering Fracture Mechanics*, 78(8), 1817–1826.

Anderson R. M. and Murphy, T. (2004). Laboratory Mix Design using RAP: Determining Aggregate Properties. Fall 2004 Magazine. http://www.asphaltmagazine. com /archives/2004/Fall/2004_Fall_Mag_Lab_Mix_Design_Using_RAP.pdf

ARRA. (2001). *Basic Asphalt Recycling Manual (BARM)*. Asphalt Recycling and Reclaiming Association.

Asphalt Institute (1989). *Hot-Mix Recycling*. The Asphalt Handbook MS-4.

Athena Institute (2006). *A Life Cycle Perspective on Concrete and Asphalt Roadways: Embodied Primary Energy and Global Warming Potential*. Prepared for the Cement Association of Canada.

Aurangzeb, Q., Al-Qadi, I.L., Abuawad, I., Pine, W., and Trepanier J. (2012). Achieving Desired Volumetrics and Performance for Mixtures with High Percentage of Reclaimed Asphalt Pavement. *Transportation Research Record: Journal of the Transportation Research Board*, Vol. 2294, pp. 34–42.

Benedetto, H. D., Delaporte, B., and Sauzéat, C. (2007). Three-Dimensional Linear Behavior of Bituminous Materials: Experiments and Modeling. *International Journal of Geomechanics.* ASCE/ 7:2, 149–157.

BLS. (2013). Bureau of labor statistics of the U.S. department of labor. http://www.bls.gov/data/#prices. Accessed on October 26, 2013.

Bukowski, J. (1997). Guideline for Design of Superpave Mixtures Containing Reclaimed Asphalt Pavement RAP. Memorandum, Expert Task Group, San Antonio.

CMU. (2013). Carnegie Mellon University Green Design Institute. Economic input-output life cycle assessment (*EIO-LCA*), US 1997 industry benchmark model, Available from: http://www.eiolca.net. Accessed 31 March, 2013.

Carpenter SH, Ghuzlan K, Shen S. (2003). Fatigue Endurance Limit for Highway and Airport Pavements. *Transportation Research Record: Journal of the Transportation Research Board,* Vol. 1832. p. 131–138.

Carpenter, S.H. (2006). *Fatigue Performance of IDOT Mixtures*. Publication FHWA-ICT-007-200, Illinois Center for Transportation (ICT), Rantoul, IL.

Chehab, G. R. Characterization of asphalt concrete in tension using a viscoelastoplastic model. PhD dissertation, North Carolina State University, Raleigh, NC, 2002.

Chen, C., & Flintsch, G. (2007). Fuzzy Logic Pavement Maintenance and Rehabilitation Triggering Approach for Probabilistic Life-Cycle Cost Analysis. *Transportation Research Record: Journal of the Transportation Research Board*, Vol. 1990, pp. 80–91.

Chiu, C.-T., Hsu, T.-H., & Yang, W.-F. (2008). Life cycle assessment on using recycled materials for rehabilitating asphalt pavements. *Resources, Conservation and Recycling*, *52*(3), 545–556. doi:10.1016/j.resconrec.2007.07.001

Collop, A. C., Scarpas, A. T., Kasbergen, C., and Bondt, A. D. (2003). Development and Finite Element Implementation of Stress-Dependent Elastoviscoplastic Constitutive Model with Damage for Asphalt. *Transportation Research Record: Journal of the Transportation Research Board*, Vol. 1832, 96-104.

Copeland, A. (2011). *Reclaimed Asphalt Pavement in Asphalt Mixtures: State of the Practice*. FHWA-HRT-11-021. McLean, VA.

Daniel, J. S. (2001). Development of a Simplified Fatigue Test and Analysis Procedure Using a Viscoelastic, Continuum Damage Model and its Implementation to Westrack Mixtures. Ph.D. Dissertation, North Carolina State University, Raleigh, NC.

Daniel, J.S. and Lachance, A. (2005). Mechanistic and Volumetric Properties of Asphalt Mixtures with RAP. *Transportation Research Record: Journal of the Transportation Research Board,* Vol. 1929, pp. 28-36.

Delwar, M. and Papagiannakins, A.T. (2001). Relative Importance of User and Agency Costs in Pavement LCCA. 5th International Conference on Managing Pavements.

Eurobitume. (2011). Life Cycle Inventory: Bitumen. European Bitumen Association, Brussels, Belgium.

FHWA. (2002). Federal Highway Administration. *Life-Cycle Cost Analysis Primer*. FHWA-IF-02-047, Washington, D.C.

FHWA. (2013a). Improving Transportation Investment Decisions Through Life-Cycle Cost Analysis Federal Highway Administration. http://www.fhwa.dot.gov/infrastructure/asstmgmt/lccafact.cfm

FHWA. (2013b). Moving Ahead for Progress in the 21st Century (MAP-21). US Department of Transportation, Federal Highway Administration. http://www.fhwa.dot.gov/map21/. Accessed 6/10/2013.

Gardiner, M.S. and Wagner, C. (1999). Use of Reclaimed Asphalt Pavement in Superpave Hot-Mix Asphalt Applications. *Transportation Research Record: Journal of the Transportation Research Board*, Vol. 1681, pp. 1-9.

Garg, A., Kazunari, K., Pulles, T. (2006) IPCC guidelines for national greenhouse gas inventories. Intergovernmental Panel on Climate Change.

Ghuzlan K, Carpenter S. H. (2000) Energy-Derived/Damage-Based Failure Criteria for fatigue testing, *Transportation Research Record: Journal of the Transportation Research Board,* Vol. 1723. Washington DC: National Research Council. p. 141–149.

Ghuzlan, K. (2001) Fatigue Damage Analysis in Asphalt Concrete Mixtures Based upon Dissipated Energy Concepts. Ph.D. Dissertation. University of Illinois at Urbana–Champaign.

González, J. M., Miquel Canet, J., Oller, S., & Miró, R. (2007). A viscoplastic constitutive model with strain rate variables for asphalt mixtures—numerical

simulation. *Computational Materials Science*, *38*(4), 543–560. doi:10.1016/j.commatsci.2006.03.013

Hajj, E.Y., Sebaaly, P. and Kandiah, P. (2008). *Use of Reclaimed Asphalt Pavements (RAP) in Airfields HMA Pavements*. Submitted to Airfield Asphalt Pavement Technology Program, Final Report, AAPTP Project No. 05-06.

Häkkinen, T., Mäkelä, K. (1996). *Environmental Impact of Concrete and Asphalt Pavements*. VTT, Finland: Technical Research Center of Finland. Research Notes 1752.

Heinicke, J.J. and Vinson, T. S. Effect of Test Condition Parameters on IRMr (1988). *Journal of Transportation Engineering*, Vol. 114, No. 2, pp. 153-172.

Hendrickson, C. T., Lave, L. B., and Matthews, H. S. (2006). Environmental Life *Cycle Assessment of Goods and Services: An Input-Output Approach*. Resources for the Future Press. Washington D.C.

Hilton, H. H. and Sung Y. (1998). The Significance of Anisotropic Viscoelastic Poisson Ratio Stress and Time Dependencies. *International Journal of Solids and Structure* 35:3081–3095.

Hilton, H. H. (2001). Implications and Constraints of Time Independent Poisson Ratios in Linear Isotropic and Anisotropic Viscoelasticity. *Journal of Elasticity* 63:221–251.

Hilton, H. H. and Fouly, A. R. A. E. (2007). Designer Auxetic Viscoelastic Sandwich Columns Tailored to Minimize Creep Buckling Failure Probabilities and Prolong Survival Times. Proceedings 48th AIAA/ASME/ASCE/AHS Structures, Structural Dynamics and Materials Conference, AIAA Paper 2700-2400.

Hilton, H. H. (2009). The Elusive and Fickle Viscoelastic Poisson's Ratio and its Relation to the Elastic-Viscoelastic Correspondence Principle. *Journal of Mechanics of Material and Structures*, *4*(September), 1341–1364.

Hilton, H. H. (2011). Clarifications of Certain Ambiguities and Failings of Poisson's Ratios in Linear Viscoelasticity." *Journal of Elasticity* 104:303–318.

Horton, A.R., Wielinski, J. C., Huber, G. A., Wissel, H. L., and McGaughey, M.A. (2011). Properties of High RAP Plant Mixtures. Canadian Technical Asphalt Association (CTAA) 56th Annual Conference Proceeding. Vol. LVI, pp. 328-349.

Horvath, A., Hendrickson, C. (1998). Comparison of Environmental Implications of Asphalt and Steel-Reinforced Concrete Pavements. *Transportation Research Record: Journal of the Transportation Research Board*, 1626:105–13.

Huang, B., Egan, B.K., Kingery, W.R., Zhang, Z., and Gang Z. (2004). Laboratory Study of Fatigue Characteristics of HMA Surface Mixtures Containing RAP. CD-ROM, Transportation Research Board of National Academies, Washington, D.C.

Huang, B., Li, G., Vukosavljevic, D., Shu, X., Egan, B.K. (2005). Laboratory Investigation of Mixing Hot-Mix Asphalt with Reclaimed Asphalt Pavement. *Transportation Research Record: Journal of the Transportation Research Board*, 1929:37–45.

Huang, B., Li, G., & Shu, X. (2006). Investigation into three-layered HMA mixtures. *Composites Part B: Engineering*, *37*(7-8), 679–690. doi:10.1016/j.compositesb.2005.08.005.

Huang, C.W., Masad, E., Muliana, A. H., & Bahia, H. (2007). Nonlinearly viscoelastic analysis of asphalt mixes subjected to shear loading. *Mechanics of Time-Dependent Materials*, *11*(2), 91–110. doi:10.1007/s11043-007-9034-5.

Huang, Y., R. Bird, and O. Heidrich. (2009). Development of a Life Cycle Assessment Tool for Construction and Maintenance of Asphalt Pavements. *Journal of Cleaner Production*, No. 17, pp. 283-296.

IDOT. (2012). Illinois Department of Transportation. Data and Maps. http://gettingaroundillinois.com. Accessed Nov. 25, 2012.

IDOT. (2013). Pavement Design, Chapter 54. *Bureau of Design and Environmental Manual*. Illinois Department of Transportation.

ISO. (2006a). Environmental management – life cycle assessment – principles and framework. Geneva: International Organization for Standardization. ISO

14040:2006(E).

ISO. (2006b). Environmental management – life cycle assessment – requirement and guidelines. Geneva: International Organization for Standardization. ISO 14044:2006(E).

Jullien, A., Monéron, P., Quaranta, G., & Gaillard, D. (2006). Air emissions from pavement layers composed of varying rates of reclaimed asphalt. *Resources, Conservation and Recycling*, *47*(4), 356–374. doi:10.1016/j.resconrec.2005.09.004.

Kai, L., & Fang, W. (2011). Computer Modeling Mechanical Analysis for Asphalt Overlay under Coupling Action of Temperature and Loads. *Procedia Engineering*, *15*, 5338–5342. doi:10.1016/j.proeng.2011.08.990.

Kandhal, P. S., Mallick, R. B. (1997). *Pavement Recycling Guidelines for State and Local Governments Participant's Reference Book*. Federal Highway Administration. Washington, D.C.

Karlsson, R. and Isacsson, U. (2006). Material-Related Aspects of Asphalt Recycling—State-of-the-Art", *Journal of Materials in Civil Engineering, ASCE*. Vol. 18, No. 1, ISSN 0899-1561/2006/1-81–92.

Kassem, E., Grasley, Z., & Masad, E. (2013). Viscoelastic Poisson's Ratio of Asphalt Mixtures. *International Journal of Geomechanics*, 13(2), 162–169. doi:10.1061/(ASCE)GM.1943-5622.0000199.

Khan, K. A., & Hilton, H. H. (2009). On Inconstant Poisson's Ratios in Non-Homogeneous Elastic Media. *Journal of Thermal Stresses*, *33*(1), 29–36. doi:10.1080/01495730903408773.

Khazanovich, L., Zofka, A., & Marasteanu, M. (2010). Parameter Identification Procedure for Heterogeneous Viscoelastic Composites using Iterative Functions. *Journal of Engineering Mechanics*, *136*(7), 849-857.

Kim Y. R., H. J. Lee, and D. N. Little. (1997). Fatigue Characterization of Asphalt Concrete Using Viscoelasticity and Continuum Damage Theory. *Journal of*

Association of Asphalt Paving Technologists, Vol. 66, pp. 520–569.

Kutay, M. E., N. Gibson, J. Youtcheff. (2008). Conventional and Viscoelastic Continuum Damage (VECD) Based Fatigue Analysis of Polymer Modified Asphalt Pavements. *Journal of the Association of Asphalt Paving Technologists*, Vol. 77. pp. 395–433.

Kutay, M. E., Gibson, N., Youtcheff, J., and Dongré, R. (2009) Use of Small Samples to Predict Fatigue Lives of Field Cores Newly Developed Formulation Based on Viscoelastic Continuum Damage Theory, *Transportation Research Record: Journal of the Transportation Research Board*, Vol. 2127, Transportation Research Board of the National Academies, Washington, D.C. pp. 90–97.

Kutay M. E. (2013). Software PP-VECD v0.1, Michigan State University. http://www.egr.msu.edu/~kutay/PPVECD/

Kim, R. Y., Guddati, M. N., Underwood, B. S., T.Y., Y., Subramanian, V., and Savadatti, S. (2009). *Development of a Multiaxial Viscoelastoplastic Continuum Damage Model for Asphalt Mixtures Technology*. FHWA-HRT-08-073.

Kim S., Sholar G.A., Byron T., and Kim J. (2009). Performance of Polymer Modified Asphalt Mixture with Reclaimed Asphalt Pavement. Presented at 88th Annual Meeting of the Transportation Research Board, Washington D.C, 2009.

Kim, J., Lee, H. S. and Kim, N. (2010). Determination of Shear and Bulk Moduli of Viscoelastic Solids from the Indirect Tension Creep Test. *Journal of Engineering Mechanics*, *136*(9), 1067-1075.

Lakes, R. S. and Wineman, A. (2006). On Poisson's Ratio in Linearly Viscoelastic Solids. *Journal of Elasticity* 85:45–63.

Lee, H. J., J. S. Daniel, and Y. R. Kim. (2000). Continuum Damage Mechanics–Based Fatigue Model of Asphalt Concrete. *Journal of Materials in Civil Engineering*, Vol. 12, No. 2, pp. 105–112.

Lee, H. S. and Kim, J. (2009). Determination of Viscoelastic Poisson's Ratio and Creep Compliance from the Indirect Tension Test. *Journal of Materials in Civil Engineering*, *21*(8), 416-425.

Li X., Marasteanu M.O., Williams R.C., and Clyne T.R. (2008). Effect of Reclaimed Asphalt Pavement (Proportion and Type) and Binder Grade on Asphalt Mixtures. *Journal of the Transportation Research Board*, No. 2051, pp. 90-97.

Lundstrom, R. and U. Isacsson. (2003). Asphalt Fatigue Modeling using Viscoelastic Continuum Damage Theory, *Road Materials and Pavement Design*, Vol. 4, No. 1, pp. 51–75.

Maher, A., and Bennert, T. (2008). *Evaluation of Poisson's Ratio for Use in the Mechanistic Empirical Pavement Design Guide*. *FHWA-NJ-2008-04*.

McDaniel, R. S., Soleymani, H., Anderson, R. M., Turner, P., and Peterson, R. (2008). *Recommended Use of Reclaimed Asphalt Pavement in the Superpave Mixture Design Method*. NCHRP Web Document 30 (Project D9-12), Transportation Research Board of National Academies, Washington D.C.

MEPDG (2004), *Guide for Mechanistic-Empirical Design of New and Rehabilitated Pavement Structures*. Final Report, NCHRP Project 1-37A. Transportation Research Board of the National Academies, Washington, D.C.

Michaeli, M., Shtark, A., Grosbein, H., Steevens, A. J., & Hilton, H. H. (2011). Analytical, Experimental and Computational Viscoelastic Material Characterizations absent Poisson' Ratios. Proceedings Fifty-Second AIAA/ASME/ASCE/AHS/ASC Structures, Structural Dynamics and Materials (SDM) Conference, AIAA Paper 2011-1809.

Michaeli, Michael, Abraham Shtark, Hagay Grosbein and Harry H. Hilton (2012) "Characterization of Isotropic Viscoelastic Moduli and Compliances from 1–D Tension Experiments," Proceedings Fifty-Third AIAA/ASME/ASCE/AHS/ASC Structures, Structural Dynamics and Materials (SDM) Conference, AIAA Paper 2012-1547.

Michaeli, M., Shtark, A., Grosbein, H., Altus, E., & Hilton, H. H. (2013). A Unified Real Time Approach to Characterizations of Isotropic Linear Viscoelastic Media from 1–D Experiments without Use of Poisson's Ratios. Proceedings Fifty-Fourth AIAA/ASME/ASCE/AHS/ASC Structures, Structural Dynamics and Materials

(SDM) Conference, AIAA Paper 2013-1692.

MINDS Inc. (2012). http://www.mindsinc.ca

Mogawer, W.S., Austerman, A.J., Engstrom, B., Bonaquist R. (2009). Incorporating High Percentages of Recycled Asphalt Pavement (RAP) and Warm Mix Asphalt (WMA) Technology into Thin Hot Mix Asphalt Overlays to be utilized as a Pavement Preservation Strategy. Presented at 88th Annual Meeting of the Transportation Research Board, Washington D.C.

Moya, J. P. A., Hong, F., and Prozzi, A. J. (2011). RAP: Save Today, Pay Later? Paper No. 11-1017, CD-ROM, Transportation Research Board of National Academies, Washington, D.C.

NETL. (2009). Consideration of Crude Oil Source in Evaluating Transportation Fuel GHG Emissions. Report DOE/NETL-2009/1360. National Energy Technology Laboratory, U.S. Department of Energy. 2009.

Nicholson, A. L., Olivetti, E. A., Gregory J. R., Field, F. R., Kirchain, R. E. (2009). End-of-Life LCA Allocation Methods: Open Loop Recycling Impacts on Robustness of Material Selection Decisions. Sustainable Systems and Technology. ISSST'09. IEEE International Symposium. 1-6.

Ott, R.L., and Longnecker, M. 2010. *An Introduction to Statistical Methods and Data Analysis. Belmont*, CA: Brooks/Cole, Cengage Learning.

Ozbay, K., Jawad, D., Parker, N. A., & Hussain, S. (2004). Life Cycle Cost Analysis : State-of-the-Practice vs State-of-the-Art. Paper 11-1017, Transportation Research Board Annual CD Room.

Ozer H, Al-Qadi IL, Carpenter SH, Aurangzeb Q, Roberts GL, Trepanier J. (2009) Evaluation of RAP impact on hot-mix asphalt design and performance. *Journal of the Association of Asphalt Paving Technologists*. 78: 317-351.

Pereira, P. A. A., Oliveira, J.R.M., and Picado-Santos, L.G. (2004) "Mechanical Characterization of Hot Mix Recycled Materials." *International Journal of Pavement Engineering* 5:211–220.

Pittenger, D., Gransberg, D. D., Zaman, M., & Riemer, C. (2011). Life-Cycle Cost-Based Pavement Preservation Treatment Design. *Transportation Research Record: Journal of the Transportation Research Board*, *2235*, pp. 28–35.

Read, W. T., (1950), Stress Analysis for Compressible Viscoelastic Materials. *Journal of Applied Physics*, 21, 671-674. doi: http://dx.doi.org/10.1063/1.1699729

Reigle, J. A., & Zaniewski, J. P. (2002). Risk-Based Life-Cycle Cost Analysis for Project-Level Pavement Management. *Transportation Research Record: Journal of the Transportation Research Board*, Vol. 1816, pp. 34–42.

SAIC (Scientific Applications International Corporation). (2006). *Life Cycle Assessment: Principles and Practice*. EPA/600/R-06/060, Cincinnati, Ohio.

Santero, N. J. (2009). Pavements and the environment: a life-cycle assessment approach. Berkeley: Doctoral Dissertation in the Civil and Environmental Engineering, University of California.

Santero, N., Masanet, E., and Horvath, A. (2010). Life-Cycle Assessment of Pavements: A Critical Review of Existing Literature and Research, SN3119a, Portland Cement Association, Skokie, Illinois, USA, 2010, 81 pages.

Santero, N., Masanet, E. and Horvath, A. (2011a). Life-Cycle Assessment of Pavements. Part I: Critical Review. Resources, Conservation, and Recycling. 55(9–10): 801–809.

Schapery, R. A. (1984). Correspondence principles and a generalized J-integral for large deformation and fracture analysis of viscoelastic media. *International Journal of Fracture*, Vol. 25, pp.195–223.

Shah, A., McDaniel, R.S., Huber, G.A., and Gallivan, V.L. (2007). Investigation of Properties of Plant-Produced Reclaimed Asphalt Pavement Mixtures. *Transportation Research Record: Journal of the Transportation Research Board*, Vol. 1998, pp. 103-111.

Shen S., Carpenter S. H. (2005) Application of Dissipated Energy Concept in Fatigue Endurance Limit Testing. *Transportation Research Record: Journal of the Transportation Research Board,* Vol. 1929. Washington DC: National Research

Council. p. 165–173.

Shen S. (2006). Dissipated Energy Concept for HMA Performance: Fatigue and Healing, Ph.D. Dissertation, University of Illinois at Urbana-Champaign.

Shtark, A., Grosbein, H., Sameach, G., & Hilton, H. H. (2012). An Alternate Protocol for Determining Viscoelastic Material Properties Based on Tensile Tests without the Use of Poisson's Ratios. Accepted for publication in ASME Journal of Applied Mechanics, JAM08-1361.

Shu, X., Huang, B., Vukosavljevic, D. (2008). Laboratory Evaluation of Fatigue Characteristics of Recycled Asphalt Mixture. *Journal of Construction and Building Materials 22*, Elsevier, pp. 1323-1330.

Sondag, M.S., Chadbourn, B. A., and Drescher. A. (2002). *Investigation of Recycled Asphalt Pavement (RAP) Mixtures*. Report No. MN/RC – 2002-15, Minnesota Department of Transportation, St. Paul, MN.

Stripple, H. (2001). *Life Cycle Assessment of Road: A Pilot Study for Inventory Analysis (Second Revised Edition)*. Swedish National Road Administration, IVL B 1210 E.

Treloar G, Love P, Crawford R. (2004). Hybrid life-cycle inventory for road construction and use. *Journal of Construction Engineering and Management* 2004; 130:43–49.

Tschoegl, N. W. (1989). *The phenomenological theory of linear viscoelastic behavior: An introduction*, Springer, New York.

Tschoegl, N. W., Knauss, W. G., and Emri, I. (2002). Poisson's ratio in linear viscoelasticity: a critical review. *Mech. Time-Depend. Mater.* 6:1 3–51.

USDOT. (2002). *Life-Cycle Cost Analysis Primer Life-Cycle Cost Analysis Primer*. United States Department of Transportation.

USEIA. (2013a). U.S. Energy information administration, U.S. Department of Energy. Petroleum supply annual 2005-2011. http://www.eia.gov/petroleum/supply/annual/volume1. Accessed November 6, 2013.

USEIA. (2013b). U.S. Energy information administration, U.S. Department of Energy. State energy data system (SEDS): 2011. http://www.eia.gov/state/seds/seds-data-fuel-prev.cfm?sid=US. Accessed November 7, 2013.

USEPA. (2008). Direct emissions from mobile combustion sources. US Environmental Protection Agency. EPA430-K-08-004.

Vavrik, W.R., Huber, G., Pine W.J., Carpenter, S.H., and Bailey, R. (2002). *Bailey Method for Gradation Selection in HMA Design*. Transportation Research E-Circular, E-C 044.

Ventura, A., & Monéron, P. (2011). Road Materials and Pavement Design Environmental Impact of a Binding Course Pavement Section , with Asphalt Recycled at Varying Rates Environmental Impact of a Binding Course Pavement Section , with Asphalt Recycled at Varying Rates. *Asphalt*. 37–41. doi:10.3166/RMPD.9HS.319-338.

Visintine, B. (2011). *An Investigation of Various Percentages of Reclaimed Asphalt Pavement on the Performance of Asphalt Pavements*. PhD Thesis, North Carolina State University.

West, R., Kvasnak, A., Tran, N., Powell, B., and Turner, P. (2009). Laboratory and Accelerated Field Performance Testing of Moderate and High RAP Content Mixes at the NCAT Test Track. Presented at 88th Annual Meeting of the Transportation Research Board, Washington D.C, 2009.

Widyatmoko, I. (2008). Mechanistic-Empirical Mixture Design for Hot Mix Asphalt Pavement Recycling. *Journal of Construction and Building Materials*. 22:77–87.

You, T., Abu Al-Rub, R. K., Darabi, M. K., Masad, E. a., & Little, D. N. (2012). Three-dimensional microstructural modeling of asphalt concrete using a unified viscoelastic–viscoplastic–viscodamage model. *Construction and Building Materials*, 28(1), 531–548. doi:10.1016/j.conbuildmat.2011.08.061

Zhang, H., Koeleian, G. A., and Lepech, M. D. (2008). An integrated life cycle assessment and life cycle analysis model for pavement overlay systems. First International Symposium on Life-Cycle Civil Engineering, Varenna, Lake Como, Italy: CRC Press/Balkema, pp. 907-912.

APPENDIX A ASPHALT MIXTURE DESIGN

Table A-1. Job mix formula for District 1 control (0% RAP) mix.

High RAP D1 N90 Control Mix	Design Target 4	1-point	Binder Opt. (–0.5%)	Binder Opt. (Optimum)	Binder Opt. (+0.5%)
Blend Percentages					
Adjusted for DCF?	No	Yes (0.4)	—	—	—
CM11	43.2	43.4	43.4	43.4	43.4
CM16	27.1	27.2	27.2	27.2	27.2
FM20	28.5	28.6	28.6	28.6	28.6
FM22	—	—	—	—	—
+3/8-in RAP	—	—	—	—	—
–3/8-in RAP	—	—	—	—	—
Mineral Filler	1.2	0.8	0.8	0.8	0.8
Total Aggregate	100.0	100.0	100.0	100.0	100.0
Percent Asphalt		4.8	4.5	5.0	5.5
Percent Aggregate	100.0	95.2	95.5	95.0	94.5
Bulk Specific Gravities					
CM11	2.711	2.711	2.711	2.711	2.711
CM16	2.659	2.659	2.659	2.659	2.659
FM20	2.697	2.697	2.697	2.697	2.697
FM22	—	—	—	—	—
+3/8-in RAP	—	—	—	—	—
–3/8-in RAP	—	—	—	—	—
Mineral Filler	2.900	2.900	2.900	2.900	2.900
Combined G_{sb}	2.695	2.695	2.695	2.695	2.695
Percent Passing from Washed Gradations					
1 in	100.0	100.0	100.0	100.0	100.0
3/4 in	96.1	96.1	96.1	96.1	96.1
1/2 in	75.6	76.2	76.1	76.1	76.1
3/8 in	64.5	65.3	65.4	65.4	65.4
No. 4	39.5	40.8	40.9	40.9	40.9
No. 8	27.5	28.0	28.2	28.2	28.2
No. 16	17.8	18.3	18.5	18.5	18.5
No. 30	12.3	12.8	13.1	13.1	13.1
No. 50	8.3	8.7	8.8	8.8	8.8
No. 100	6.2	6.2	6.2	6.2	6.2
No. 200	4.6	4.7	4.7	4.7	4.7

(continued, next page).

Table A-1 (continued). Job mix formula for District 1 control (0% RAP) mix.

Volumetrics					
G_{mb} 1 Dry Wt.	—	4912.1	4909.1	4931.3	4954.8
G_{mb} 1 Submerged Wt.	—	2888.4	2902.7	2926.8	2941.7
G_{mb} 1 SSD Wt.	—	4928.8	4922.2	4940.0	4960.3
G_{mb} 2 Dry Wt.	—	4916.2	4908.5	4931.6	4950.6
G_{mb} 2 Submerged Wt.	—	2896.7	2900.8	2923.5	2944.4
G_{mb} 2 SSD Wt.	—	4929.7	4920.8	4941.5	4958.2
G_{mb} 1	—	2.407	2.431	2.449	2.455
G_{mb} 2	—	2.418	2.430	2.444	2.458
Average G_{mb}	—	2.413	2.430	2.447	2.456
G_{mm} 1 Dry Wt.		2612.9	2605.5	2621.1	2632.0
G_{mm} 1 Pyc in Water Wt.		7657.3	7657.3	7657.3	7657.3
G_{mm} 1 Pyc + Sample in Water Wt.		9247.1	9245.9	9246.9	9247.0
G_{mm} 2 Dry Wt.		2611.2	2606.5	2622.6	2632.5
G_{mm} 2 Pyc in Water Wt.		7657.3	7657.3	7657.3	7657.3
G_{mm} 1 Pyc + Sample in Water Wt.		9244.4	9249.1	9247.5	9245.8
G_{mm} 1		2.554	2.562	2.541	2.525
G_{mm} 2		2.550	2.569	2.540	2.522
Average G_{mm}			2.565	2.541	2.524
G_b		1.03	1.03	1.03	1.03
G_{se}			2.759	2.754	2.757
Voids			5.2	3.7	2.7
VMA		14.8	13.9	13.7	13.9
VFA			62.2	73.0	80.7
Dust / Binder			1.0	0.9	0.9
P_{ba}			0.9	0.8	0.9
Effective Binder			3.7	4.2	4.7
Dust / Effective Binder			1.3	1.1	1.0
$N_{initial}$			8.0	8.0	8.0
N_{design}			90.0	90.0	90.0
Height 1 at $N_{initial}$					
Height 2 at $N_{initial}$					
Average Height at $N_{initial}$			—	—	—
Height 1 at N_{design}					
Height 2 at N_{design}					
Average Height at N_{design}			—	—	—
% of G_{mm} at $N_{initial}$			—	—	—

Table A-2. Volumetrics for District 1 control mix design.

D1-Control Mix Design Volumetrics Summary		
Volumetrics		IDOT Specifications
Binder (%)	4.9	—
Air Voids (%)	4.0	4
VMA (%)	13.7	13 (minimum)
VFA (%)	70.8	65–75
G_{mm}	2.546	—
G_{mb}		—
G_{se}	2.756	—

Table A-3. Job mix formula for District 1 30% RAP mix.

High RAP D1 N90 30% RAP Mix	Design Target	Binder Opt. (0.5%)	Binder Opt. (Optimum)	Binder Opt. (+0.5%)
Blend Percentages				
Adjusted for DCF?	Yes			
CM11	37.7	37.7	37.7	37.7
CM16	12.5	12.5	12.5	12.5
FM20	8.5	8.5	8.5	8.5
FM22	10.5	10.5	10.5	10.5
+3/8-in RAP	15.0	15.0	15.0	15.0
–3/8-in RAP	15.0	15.0	15.0	15.0
Mineral Filler	0.8	0.8	0.8	0.8
Total Aggregate	100.0	100.0	100.0	100.0
Percent Asphalt		4.3	4.8	5.3
Percent Aggregate	100.0	95.7	95.2	94.7
Bulk Specific Gravities				
CM11	2.711	2.632	2.632	2.632
CM16	2.659	2.620	2.620	2.620
FM20	2.697	2.635	2.635	2.635
FM22	2.669	2.669	2.669	2.669
+3/8-in RAP	2.687	2.627	2.627	2.627
–3/8-in RAP	2.671	2.641	2.641	2.641
Mineral Filler	2.900	2.900	2.900	2.900
Combined G_{sb}	2.691	2.691	2.691	2.691

(continued, next page)

Table A-3 (continued). Job mix formula for District 1 30% RAP mix.

1 in	100.0	99.5	99.5	99.5
3/4 in	96.1	95.9	95.9	95.9
1/2 in	75.9	76.3	76.3	76.3
3/8 in	63.7	64.8	64.8	64.8
No. 4	38.0	38.4	38.4	38.4
No. 8	23.2	23.4	23.4	23.4
No. 16	16.2	16.3	16.3	16.3
No. 30	12.4	12.6	12.6	12.6
No. 50	9.4	9.6	9.6	9.6
No. 100	6.8	7.0	7.0	7.0
No. 200	5.4	5.7	5.7	5.7
Volumetrics				
G_{mb} 1 Dry Wt.	—	4821.0	4840.2	4863.9
G_{mb} 1 Submerged Wt.	—	2853.3	2871.1	2882.9
G_{mb} 1 SSD Wt.	—	4836.2	4853.7	4873.8
G_{mb} 2 Dry Wt.	—	4819.9	4846.7	4868.8
G_{mb} 2 Submerged Wt.	—	2843.9	2873.0	2885.6
G_{mb} 2 SSD Wt.	—	4837.8	4856.4	4875.6
G_{mb} 1	—	2.431	2.441	2.443
G_{mb} 2	—	2.417	2.444	2.447
Average G_{mb}	—	2.424	2.442	2.445
G_{mm} 1 Dry Wt.		2560.2	2572.6	2586.2
G_{mm} 1 Pyc in Water Wt.		7657.3	7657.3	7657.3
G_{mm} 1 Pyc + Sample in Water Wt.		9219.8	9219.7	9223.4
G_{mm} 2 Dry Wt.		2567.1	2572.9	2589.4
G_{mm} 2 Pyc in Water Wt.		7657.3	7657.3	7657.3
G_{mm} 1 Pyc + Sample in Water Wt.		9221.3	9220.9	9223.5
G_{mm} 1	—	2.566	2.547	2.535
G_{mm} 2	—	2.559	2.549	2.531
Average G_{mm}	—	2.563	2.548	2.533
G_b	—	1.03	1.03	1.03
G_{se}	—	2.747	2.753	2.758
Voids	—	5.4	4.2	3.5
VMA	—	13.8	13.6	14.0
VFA	—	60.7	69.4	75.1
Dust / Binder	—	1.3	1.2	1.1
P_{ba}		0.78	0.86	0.94
Effective Binder		3.6	4.0	4.4

(continued, next page)

Table A-3 (continued). Job mix formula for District 1 30% RAP mix.

Dust / Effective Binder		1.6	1.4	1.3
$N_{initial}$		8.0	8.0	8.0
N_{design}		90.0	90.0	90.0
Height 1 at $N_{initial}$		130.98	131.12	132.09
Height 2 at $N_{initial}$		132.47	130.96	131.17
Average Height at $N_{initial}$		131.725	131.04	131.63
Height 1 at N_{design}		116.55	116.56	117.06
Height 2 at N_{design}		118.19	116.63	116.55
Average Height at N_{design}		117.37	116.595	116.81
% of G_{mm} at $N_{initial}$		84.3	85.3	85.7

Table A-4. Volumetrics for District 1 mix design with 30% RAP.

D1-30% RAP Mix Design Volumetrics Summary		
Volumetrics		IDOT Specifications
Binder (%)	4.9	—
Air Voids (%)	4.0	4
VMA (%)	13.6	13 (minimum)
VFA (%)	70.7	65–75
G_{mm}	2.545	—
G_{mb}	2.444	—
G_{se}	2.752	—

Table A-5. Job mix formula for District 1 40% RAP mix.

High RAP D1 N90 40% RAP Mix	Design Target 3	Binder Opt. (–0.5%)	Binder Opt. (Optimum)	Binder Opt. (+0.5%)
Blend Percentages				
Adjusted for DCF?	Yes	Yes	Yes	Yes
CM11	31.0	31.0	31.0	31.0
CM16	13.3	13.3	13.3	13.3
FM20	4.0	4.0	4.0	4.0
FM22	10.9	10.9	10.9	10.9
+3/8-in RAP	25.0	25.0	25.0	25.0
–3/8-in RAP	15.0	15.0	15.0	15.0
Mineral Filler	0.8	0.8	0.8	0.8
Total Aggregate	100.0	100.0	100.0	100.0
Percent Asphalt		4.5	5.0	5.5
Percent Aggregate	100.0	95.5	95.0	94.5
Bulk Specific Gravities				
CM11	2.711	2.632	2.632	2.632
CM16	2.659	2.620	2.620	2.620
FM20	2.697	2.635	2.635	2.635
FM22	2.669	2.669	2.669	2.669
+3/8-in. RAP	2.687	2.627	2.627	2.627
–3/8-in RAP	2.671	2.641	2.641	2.641
Mineral Filler	2.900	2.900	2.900	2.900
Combined G_{sb}	2.688	2.688	2.688	2.688
Percent Passing from Washed Gradations				
1 in	100.0	100.0	100.0	100.0
3/4 in	96.4	96.2	96.2	96.2
1/2 in	77.8	77.9	77.9	77.9
3/8 in	65.6	65.8	65.8	65.8
No. 4	37.9	38.4	38.4	38.4
No. 8	22.5	22.7	22.7	22.7
No. 16	16.3	16.5	16.5	16.5
No. 30	12.8	13.1	13.1	13.1
No. 50	9.9	10.1	10.1	10.1
No. 100	7.1	7.5	7.5	7.5
No. 200	5.7	6.0	6.0	6.0

(continued, next page).

Table A-5 (continued). Job mix formula for District 1 40% RAP mix.

Volumetrics				
G_{mb} 1 Dry Wt.		4814.2	4835.1	4859.1
G_{mb} 1 Submerged Wt.		2848.2	2864.3	2882.1
G_{mb} 1 SSD Wt.		4828.2	4846.0	4869.7
G_{mb} 2 Dry Wt.		4812.3	4837.7	4766.2
G_{mb} 2 Submerged Wt.		2844.7	2867.9	2826.1
G_{mb} 2 SSD Wt.		4826.3	4848.9	4775.8
G_{mb} 1	—	2.431	2.440	2.445
G_{mb} 2	—	2.428	2.442	2.445
Average G_{mb}	—	2.430	2.441	2.445
G_{mm} 1 Dry Wt.		2556.9	2570.8	2581.2
G_{mm} 1 Pyc in Water Wt.		7657.3	7657.3	7657.3
G_{mm} 1 Pyc + Sample in Water Wt.		9223.5	9218.6	9215.6
G_{mm} 2 Dry Wt.		2564.3	2554	2584.2
G_{mm} 2 Pyc in Water Wt.		7657.3	7657.3	7657.3
G_{mm} 1 Pyc + Sample in Water Wt.		9223.4	9208.2	9217.8
G_{mm} 1	—	2.581	2.547	2.523
G_{mm} 2	—	2.569	2.546	2.524
Average G_{mm}	—	2.575	2.546	2.524
G_b		1.03	1.03	1.03
G_{se}	—	2.771	2.760	2.757
Voids	—	5.6	4.1	3.1
VMA	—	13.7	13.7	14.0
VFA	—	58.8	70.0	77.7
Dust / Binder Content	—	1.3	1.1	1.0
P_{ba}		1.14	0.99	0.95
Effective Binder Content		3.4	4.1	4.6
Dust / Effective Binder Content		1.8	1.5	1.3
$N_{initial}$		8.0	8.0	8.0
N_{design}		90.0	90.0	90.0
Height 1 at $N_{initial}$		130.9	131.57	131.79
Height 2 at $N_{initial}$		130.74	130.68	128.51
Average Height at $N_{initial}$		130.82	131.125	130.15
Height 1 at N_{design}		116.12	116.43	117.19
Height 2 at N_{design}		116.27	116.05	114.5
Average Height at N_{design}		116.195	116.24	115.845
% of G_{mm} at $N_{initial}$		83.8	85.0	86.2

Table A-6. Volumetrics for District 1 mix design with 40% RAP.

D1-40% RAP Mix Design Volumetrics Summary		
Volumetrics		IDOT Specifications
Binder (%)	5.1	—
Air Voids (%)	4.0	4
VMA (%)	13.8	13 (minimum)
VFA (%)	70.9	65–75
G_{mm}	2.546	—
G_{mb}	2.442	—
G_{se}	2.762	—

Table A-7. Job mix formula for District 1 50% RAP mix.

High RAP D1 N90 50% RAP Mix	Design Target 3	Binder Opt. (–0.5%)	Binder Opt. (Optimum)	Binder Opt. (+0.5%)
Blend Percentages				
Adjusted for DCF?	Yes	Yes	Yes	Yes
CM11	25.5	25.5	25.5	25.5
CM16	14.0	14.0	14.0	14.0
FM20	0.0	0.0	0.0	0.0
FM22	10.3	10.3	10.3	10.3
+3/8-in RAP	35.0	35.0	35.0	35.0
–3/8-in RAP	15.0	15.0	15.0	15.0
Mineral Filler	0.2	0.2	0.2	0.2
Total Aggregate	100.0	100.0	100.0	100.0
Percent Asphalt		4.5	5.0	5.5
Percent Aggregate	100.0	95.5	95.0	94.5
Bulk Specific Gravities				
CM11	2.711	2.711	2.711	2.711
CM16	2.659	2.659	2.659	2.659
FM20	2.697	2.697	2.697	2.697
FM22	2.669	2.669	2.669	2.669
+3/8-in RAP	2.687	2.687	2.687	2.687
–3/8-in RAP	2.671	2.671	2.671	2.671
Mineral Filler	2.900	2.900	2.900	2.900
Combined G_{sb}	2.685	2.685	2.685	2.685

(continued, next page)

Table A-7 (continued). Job mix formula for District 1 50% RAP mix.

Percent Passing from Washed Gradations				
1 in	100.0	100.0	100.0	100.0
3/4 in	96.6	97.4	97.4	97.4
1/2 in	79.1	79.7	79.7	79.7
3/8 in	66.6	67.4	67.4	67.4
No. 4	37.2	37.8	37.8	37.8
No. 8	21.5	22.0	22.0	22.0
No. 16	16.0	16.3	16.3	16.3
No. 30	12.8	13.4	13.4	13.4
No. 50	9.8	10.5	10.5	10.5
No. 100	6.9	7.6	7.6	7.6
No. 200	5.5	6.2	6.2	6.2
Volumetrics				
G_{mb} 1 Dry Wt.	—	4788.1	4806.8	4802.0
G_{mb} 1 Submerged Wt.	—	2826.8	2842.9	2845.2
G_{mb} 1 SSD Wt.	—	4807.0	4817.2	4814.4
G_{mb} 2 Dry Wt.	—	4787.0	4808.8	4832.2
G_{mb} 2 Submerged Wt.	—	2820.1	2848.6	2863.4
G_{mb} 2 SSD Wt.	—	4808.4	4816.2	4842.6
G_{mb} 1	—	2.418	2.435	2.439
G_{mb} 2	—	2.408	2.444	2.441
Average G_{mb}	—	2.413	2.439	2.440
G_{mm} 1 Dry Wt.		2547.3	2562.6	2572.0
G_{mm} 1 Pyc in Water Wt.		7657.3	7657.3	7657.3
G_{mm} 1 Pyc + Sample in Water Wt.		9212.4	9210.0	9210.0
G_{mm} 2 Dry Wt.		2552.2	2563.0	2571.4
G_{mm} 2 Pyc in Water Wt.		7657.3	7657.3	7657.3
G_{mm} 2 Pyc + Sample in Water Wt.		9213.1	9212.3	9211.2
G_{mm} 1		2.567	2.537	2.523
G_{mm} 2		2.561	2.543	2.527
Average G_{mm}		2.564	2.540	2.525
G_b		1.03	1.03	1.03
G_{se}		2.758	2.752	2.758
Voids		5.9	4.0	3.4
VMA		14.2	13.7	14.1
VFA		58.4	71.1	76.2
Dust / Binder Content		1.4	1.2	1.1
P_{ba}		1.0	0.9	1.0
Effective Binder Content		3.5	4.1	4.5

(continued, next page)

Table A-7 (continued). Job mix formula for District 1 50% RAP mix.

Dust / Effective Binder Content		1.7	1.5	1.4
$N_{initial}$		8.0	8.0	8.0
N_{design}		90.0	90.0	90.0
Height 1 at $N_{initial}$		131.7	131.0	130.8
Height 2 at $N_{initial}$		132.0	130.6	130.7
Average Height at $N_{initial}$		131.9	130.8	130.7
Height 1 at N_{design}		117.1	116.3	116.0
Height 2 at N_{design}		117.2	116.1	116.3
Average Height at N_{design}		117.1	116.2	116.2
% of G_{mm} at $N_{initial}$		83.6	85.3	85.9

Table A-8. Volumetrics for District 1 mix design with 50% RAP.

D1-50% RAP Mix Design Volumetrics Summary		
Volumetrics		IDOT Specifications
Binder (%)	5.0	—
Air Voids (%)	4.0	4
VMA (%)	13.7	13 (minimum)
VFA (%)	71.0	65–75
G_{mm}	2.543	—
G_{mb}	2.440	—
G_{se}	2.756	—

Table A-9. Job mix formula for District 5 control (0%) RAP mix.

High RAP D5 N90 Control Mix	Open Road's Target Blend (85BIT2893 - 19532)	Open Road's Actual Blend (85BIT2893 - 19532)	Design Target 2	Verification
Blend Percentages				
Adjusted for DCF?	—	—	No	Yes (0.6)
CM11	42.0	42.0	38.5	38.7
CM16	37.3	37.3	37.9	38.2
FM20	19.5	19.5	21.6	21.8
FM22	—	—	—	—
Mineral Filler	1.2	1.2	2.0	1.3
Total Aggregate	100.0	100.0	100.0	100.0
Percent Asphalt	5.4	5.4	—	5.2
Percent Aggregate	94.6	94.6	—	94.8
Bulk Specific Gravities				
CM11	2.636	—	2.632	2.632
CM16	2.627	—	2.620	2.620
FM20	2.617	—	2.635	2.635
FM22			2.551	2.551
Mineral Filler	2.800	—	2.900	2.900
Combined G_{sb}	2.631	2.631	2.633	2.633
Percent Passing from Washed Gradations				
1 in	100.0	100.0	100.0	100.0
3/4 in	95.0	96.0	93.1	93.1
1/2 in	76.9	78.0	76.6	76.6
3/8 in	67.1	68.0	67.8	67.8
1/4 in	—	—	—	—
No. 4	40.0	42.0	38.7	38.7
No. 8	21.4	22.0	21.7	21.7
No. 16	12.7	13.0	13.6	13.6
No. 30	8.3	9.0	9.0	9.0
No. 50	6.3	7.0	6.8	6.8
No. 100	5.4	6.0	5.6	5.6
No. 200	4.9	5.3	4.9	4.9

(continued, next page)

Table A-9 (continued). Job mix formula for District 5 control (0%) RAP mix.

Volumetrics				
G_{mb} 1 Dry Wt.	—	—		4709.2
G_{mb} 1 Submerged Wt.	—	—		2754.8
G_{mb} 1 SSD Wt.	—	—		4722.1
G_{mb} 2 Dry Wt.	—	—		4708.7
G_{mb} 2 Submerged Wt.	—	—		2756.6
G_{mb} 2 SSD Wt.	—	—		4718.7
G_{mb} 1	—	—		2.394
G_{mb} 2	—	—		2.400
Average G_{mb}	2.398	2.398	—	2.397
G_{mm} 1 Dry Wt.	—	—		2625.1
G_{mm} 1 Pyc in Water Wt.	—	—		1383.8
G_{mm} 1 Pyc + Sample in Water Wt.	—	—		2957.8
G_{mm} 2 Dry Wt.	—	—		2624.0
G_{mm} 2 Pyc in Water Wt.	—	—		1383.8
G_{mm} 1 Pyc + Sample in Water Wt.	—	—		2957.4
G_{mm} 1	—	—		2.497
G_{mm} 2	—	—		2.498
Average G_{mm}	2.497	2.497	—	2.498
Gb	1.037	—		1.030
G_{se}	2.717	—	—	2.710
Voids	4.0	4.0	—	4.0
VMA	13.8	13.8	—	13.7
VFA	71.0	71.0	—	70.5
Dust / Binder Content	0.91	—	—	0.9
P_{ba}	—	—		1.1
Effective Binder Content	—	—		1.0
Dust / Effective Binder Content	—	—	—	0.9
$N_{initial}$	10.0	—	—	1.1
N_{design}	90.0	90.0	—	5.1
Height 1 at $N_{initial}$	—	—	—	1.0
Height 2 at $N_{initial}$	—	—	—	8.0
Average Height at $N_{initial}$	—	—	—	90.0
Height 1 at N_{design}	—	—	—	—
Height 2 at N_{design}	—	—	—	—
Average Height at N_{design}	—	—	—	—
% of G_{mm} at $N_{initial}$	—	—	—	—

Table A-10. Volumetrics for District 5 control mix design.

D5-Control Mix Design Volumetrics Summary		
Volumetrics		IDOT Specifications
Binder (%)	5.2	—
Air Voids (%)	4.0	4
VMA (%)	13.8	13 (minimum)
VFA (%)	71.0	65–75
G_{mm}	2.497	—
G_{se}	2.710	—

Table A-11. Job mix formula for District 5 mixture with 30% RAP.

High RAP D5 N90 30% RAP Mix	Design Target 2	1-point	Binder Opt. (–0.5%)	Binder Opt. (Optimum)	Binder Opt. (+0.5%)
Blend Percentages					
Adjusted for DCF?	No	Yes (0.6)			
CM11	34.5	34.7	34.7	34.7	34.7
CM16	15.5	15.6	15.6	15.6	15.6
FM20	9.0	9.1	9.1	9.1	9.1
FM22	10.0	10.1	10.1	10.1	10.1
+3/8-in RAP	15.0	15.0	15.0	15.0	15.0
–3/8-in RAP	15.0	15.0	15.0	15.0	15.0
Mineral Filler	1.0	0.5	0.5	0.5	0.5
Total Aggregate	100.0	100.0	100.0	100.0	100.0
Percent Asphalt		5.1	4.8	5.3	5.8
Percent Aggregate	100.0	94.9	95.2	94.7	94.2
Bulk Specific Gravities					
CM11	2.632	2.632	2.632	2.632	2.632
CM16	2.620	2.620	2.620	2.620	2.620
FM20	2.635	2.635	2.635	2.635	2.635
FM22	2.669	2.669	2.669	2.669	2.669
+3/8-in RAP	2.627	2.627	2.627	2.627	2.627
–3/8-in RAP	2.641	2.641	2.641	2.641	2.641
Mineral Filler	2.900	2.900	2.900	2.900	2.900
Combined G_{sb}		2.637	2.637	2.637	2.637

(continued, next page)

Table A-11 (continued). Job mix formula for District 5 mixture with 30% RAP.

Percent Passing from Washed Gradations					
1 in	100.0	100.0	100.0	100.0	100.0
3/4 in	93.7	94.7	94.9	94.9	94.9
1/2 in	77.6	77.8	78.4	78.4	78.4
3/8 in	68.3	68.8	68.0	68.0	68.0
No. 4	39.5	39.5	39.4	39.4	39.4
No. 8	22.4	22.4	22.2	22.2	22.2
No. 16	14.6	15.1	15.1	15.1	15.1
No. 30	10.6	10.6	10.5	10.5	10.5
No. 50	7.9	7.9	7.7	7.7	7.7
No. 100	6.3	6.4	6.3	6.3	6.3
No. 200	5.3	5.5	5.3	5.3	5.3
Volumetrics					
G_{mb} 1 Dry Wt.	—	4630.6	4618.8	4641.2	4659.7
G_{mb} 1 Submerged Wt.	—	2706.5	2696.1	2718.0	2738.1
G_{mb} 1 SSD Wt.	—	4642.3	4637.4	4652.3	4667
G_{mb} 2 Dry Wt.	—	4636.2	4621.2	4643.0	4662.7
G_{mb} 2 Submerged Wt.	—	2714.0	2698.1	2717.4	2730.1
G_{mb} 2 SSD Wt.	—	4648.8	4633.5	4651.3	4670.8
G_{mb} 1	—	2.392	2.379	2.399	2.416
G_{mb} 2	—	2.396	2.388	2.401	2.403
Average G_{mb}	—	2.394	2.383	2.400	2.409
G_{mm} 1 Dry Wt.		2585.8	2579.1	2595.9	2604.9
G_{mm} 1 Pyc in Water Wt.		1563.1	1563.1	1563.1	1563.1
G_{mm} 1 Pyc + Sample in Water Wt.		3117.4	3119.1	3118.8	3115.2
G_{mm} 2 Dry Wt.		2587.2	2584.2	2594.8	2606.4
G_{mm} 2 Pyc in Water Wt.		1563.1	1563.1	1563.1	1563.1
G_{mm} 1 Pyc + Sample in Water Wt.		3117.6	3120.9	3118.2	3117.2
G_{mm} 1	—	2.507	2.521	2.496	2.474
G_{mm} 2	—	2.505	2.518	2.496	2.477
Average G_{mm}	—	2.506	2.519	2.496	2.476
G_b	—	1.03	1.03	1.03	1.03
G_{se}	—	2.715	2.717	2.712	2.710
Voids	—	4.5	5.4	3.8	2.7
VMA	—	13.8	14.0	13.8	13.9
VFA	—	67.7	61.4	72.2	80.6
Dust / Binder	—	1.0	1.1	1.0	0.9
P_{ba}		1.12	1.15	1.08	1.05
Effective Binder		4.0	3.7	4.3	4.8

(continued, next page)

Table A-11 (continued). Job mix formula for District 5 mixture with 30% RAP.

Dust / Effective Binder		1.4	1.4	1.2	1.1
$N_{initial}$			8.0	8.0	8.0
N_{design}			90.0	90.0	90.0
Height 1 at $N_{initial}$			128.15	127.15	126.06
Height 2 at $N_{initial}$			127.69	126.68	127.21
Average Height at $N_{initial}$			127.92	126.915	126.635
Height 1 at N_{design}			113.51	112.99	112.77
Height 2 at N_{design}			113.09	112.83	112.9
Average Height at N_{design}			113.3	112.91	112.835
% of G_{mm} at $N_{initial}$			83.8	85.5	86.7

Table A-12. Volumetrics for District 5 mixture with 30% RAP.

D5-30% RAP Mix Design Volumetrics Summary		
Volumetrics		IDOT Specifications
Binder (%)	5.2	—
Air Voids (%)	4.0	4
VMA (%)	13.8	13 (minimum)
VFA (%)	71.0	65–75
G_{mm}	2.501	—
G_{se}	2.713	—

Table A-13. Job mix formula for District 5 40% RAP mix.

High RAP D5 N90 40% RAP Mix	Design Target 3	1-point	Binder Opt. (–0.5%)	Binder Opt. (Optimum)	Binder Opt. (+0.5%)
Blend Percentages					
Adjusted for DCF?	No	Yes (0.67)			
CM11	31.2	31.4	31.4	31.4	31.4
CM16	12.5	12.6	12.6	12.6	12.6
FM20	6.5	6.6	6.6	6.6	6.6
FM22	9.0	9.1	9.1	9.1	9.1
+3/8-in RAP	25.0	25.0	25.0	25.0	25.0
–3/8-in RAP	15.0	15.0	15.0	15.0	15.0
Mineral Filler	0.8	0.4	0.4	0.4	0.4
Total Aggregate	100.0	100.0	100.0	100.0	100.0
Percent Asphalt		5.2	4.8	5.3	5.8
Percent Aggregate	100.0	94.8	95.2	94.7	94.2
Bulk Specific Gravities					
CM11	2.632		2.632	2.632	2.632
CM16	2.620		2.620	2.620	2.620
FM20	2.635		2.635	2.635	2.635
FM22	2.669		2.669	2.669	2.669
+3/8-in RAP	2.627		2.627	2.627	2.627
–3/8-in RAP	2.641		2.641	2.641	2.641
Mineral Filler	2.900		2.900	2.900	2.900
Combined G_{sb}	2.636	2.636	2.636	2.636	2.636
Percent Passing from Washed Gradations					
1 in	100.0	100.0	100.0	100.0	100.0
3/4 in	94.4	94.3	93.8	93.8	93.8
1/2 in	79.3	79.4	78.4	78.4	78.4
3/8 in	69.7	69.7	69.1	69.1	69.1
1/4 in	—	—	—	—	—
No. 4	39.3	39.2	39.2	39.2	39.2
No. 8	22.3	22.7	22.4	22.4	22.4
No. 16	14.8	15.1	14.8	14.8	14.8
No. 30	11.0	11.2	11.0	11.0	11.0
No. 50	8.2	8.1	7.9	7.9	7.9
No. 100	6.4	6.5	6.3	6.3	6.3
No. 200	5.4	5.5	5.3	5.3	5.3

(continued, next page)

Table A-13 (continued). Job mix formula for District 5 40% RAP mix.

Volumetrics					
G_{mb} 1 Dry Wt.		4623.2	4609.8	4626.2	4641.5
G_{mb} 1 Submerged Wt.		2708.9	2695.2	2710.5	2727.9
G_{mb} 1 SSD Wt.		4635.8	4626.6	4635.9	4650.8
G_{mb} 2 Dry Wt.		4623.6	4611.2	4627.9	4639.2
G_{mb} 2 Submerged Wt.		2705.8	2696.0	2714.9	2726.2
G_{mb} 2 SSD Wt.		4638.9	4629.2	4639.7	4648.5
G_{mb} 1	—	2.399	2.387	2.403	2.414
G_{mb} 2	—	2.392	2.385	2.404	2.413
Average G_{mb}	—	2.396	2.386	2.404	2.414
G_{mm} 1 Dry Wt.		2581.7	2575.7	2582.1	2596.8
G_{mm} 1 Pyc in Water Wt.		1563.1	1563.1	1563.1	1563.1
G_{mm} 1 Pyc + Sample in Water Wt.		3113.1	3115.0	3110.9	3109.8
G_{mm} 2 Dry Wt.		2583.3	2571.8	2585.2	2591.7
G_{mm} 2 Pyc in Water Wt.		1563.1	1563.1	1563.1	1563.1
G_{mm} 1 Pyc + Sample in Water Wt.		3113.9	3114.1	3110.8	3108.4
G_{mm} 1	—	2.502	2.516	2.496	2.473
G_{mm} 2	—	2.502	2.519	2.492	2.477
Average G_{mm}	—	2.502	2.518	2.494	2.475
G_b		1.03	1.03	1.03	1.03
G_{se}	—	2.715	2.716	2.710	2.709
Voids	—	4.2	5.2	3.6	2.5
VMA	—	13.8	13.8	13.6	13.7
VFA	—	69.4	62.1	73.5	82.1
Dust / Binder	—	1.0	1.1	1.0	0.9
P_{ba}			1.15	1.06	1.05
Effective Binder			3.7	4.3	4.8
Dust / Effective Binder			1.4	1.2	1.1
$N_{initial}$			8.0	8.0	8.0
N_{design}			90.0	90.0	90.0
Height 1 at $N_{initial}$			127.5	126.78	127.01
Height 2 at $N_{initial}$			127.93	127.04	126.82
Average Height at $N_{initial}$			127.715	126.91	126.915
Height 1 at N_{design}			113.37	112.45	112.45
Height 2 at N_{design}			113.69	112.59	112.45
Average Height at N_{design}			113.53	112.52	112.45
% of G_{mm} at $N_{initial}$			84.2	85.5	86.4

Table A-14. Volumetrics for District 5 mix design with 40% RAP.

D5-40% RAP Mix Design Volumetrics Summary		
Volumetrics		IDOT Specifications
Binder (%)	5.2	—
Air Voids (%)	4.0	4
VMA (%)	13.6	13 (minimum)
VFA (%)	70.8	65–75
G_{mm}	2.500	—
G_{se}	2.711	—

Table A-15. Job mix formula for District 5 50% RAP mix.

High RAP D5 N90 50% RAP Mix	Design Target 4	1-point	Binder Opt. (–0.5%)	Binder Opt. (Optimum)	Binder Opt. (+0.5%)	1-point
Blend Percentages						
Adjusted for DCF?	No	Yes (0.5)				
CM11	25.6	25.8	25.8	25.8	25.8	25.8
CM16	9.5	9.6	9.6	9.6	9.6	9.6
FM20	4.8	4.8	4.8	4.8	4.8	4.8
FM22	9.6	9.7	9.7	9.7	9.7	9.7
+3/ 8in. RAP	35.0	35.0	35.0	35.0	35.0	35.0
–3/8-in RAP	15.0	15.0	15.0	15.0	15.0	15.0
Mineral Filler	0.5	0.2	0.2	0.2	0.2	0.2
Total Aggregate	100.0	100.0	100.0	100.0	100.0	100.0
Percent Asphalt		5.3	4.7	5.2	5.7	5.2
Percent Aggregate	100.0	94.7	95.3	94.8	94.3	94.8
Bulk Specific Gravities						
CM11	2.632					
CM16	2.620					
FM20	2.635					
FM22	2.669					
+3/8-in RAP	2.627					
–3/8-in RAP	2.641					
Mineral Filler	2.900					
Combined G_{sb}	2.635	2.635	2.635	2.635	2.635	2.635

(continued, next page)

Table A-15 (continued). Job mix formula for District 5 50% RAP mix.

Percent Passing from Washed Gradations						
1 in	100.0	100.0	100.0	100.0	100.0	100.0
3/4 in	95.2	95.6	95.2	95.2	95.2	95.5
1/2 in	81.2	81.8	81.8	81.8	81.8	80.9
3/8 in	71.4	71.6	72.1	72.1	72.1	71.5
1/4 in	—	—	—	—	—	—
No. 4	39.9	40.3	40.5	40.5	40.5	40.1
No. 8	23.3	23.3	23.4	23.4	23.4	23.2
No. 16	15.6	15.7	15.9	15.9	15.9	15.4
No. 30	11.7	11.9	11.8	11.8	11.8	11.7
No. 50	8.6	8.7	8.5	8.5	8.5	8.6
No. 100	6.6	6.8	6.7	6.7	6.7	6.7
No. 200	5.4	5.7	5.6	5.6	5.6	5.6
Volumetrics						
G_{mb} 1 Dry Wt.	—	4613.0	4590.0	4605.3	4625.0	4605.6
G_{mb} 1 Submerged Wt.	—	2708.5	2689.6	2701.8	2716.4	2694.4
G_{mb} 1 SSD Wt.	—	4628.2	4615.2	4615.4	4635.1	4617.9
G_{mb} 2 Dry Wt.	—	4613.1	4588.3	4612.5	4624.2	4606.6
G_{mb} 2 Submerged Wt.	—	2704.0	2687.1	2706.5	2714.7	2701.3
G_{mb} 2 SSD Wt.	—	4625.2	4613.6	4622.2	4632.8	4616.2
G_{mb} 1	—	2.403	2.384	2.407	2.410	2.394
G_{mb} 2	—	2.401	2.382	2.408	2.411	2.406
Average G_{mb}	—	2.402	2.383	2.404	2.411	2.400
G_{mm} 1 Dry Wt.		—	2563.5	2575.0	2585.5	2570.4
G_{mm} 1 Pyc in Water Wt.		—	1563.1	1563.1	1563.1	1563.1
G_{mm} 1 Pyc + Sample in Water Wt.		—	3108.8	3109.3	3106.6	3105.9
G_{mm} 2 Dry Wt.		—	2561.6	2572.8	2587.5	2571.8
G_{mm} 2 Pyc in Water Wt.		—	1563.1	1563.1	1563.1	1563.1
G_{mm} 1 Pyc + Sample in Water Wt.		—	3107.9	3106.4	3107.7	3106.2
G_{mm} 1			2.519	2.503	2.481	2.501
G_{mm} 2			2.519	2.499	2.481	2.500
Average G_{mm}			2.519	2.501	2.481	2.501
G_b		1.03	1.03	1.03	1.03	1.03
G_{se}			2.712	2.714	2.712	2.714
Voids			5.4	3.9	2.8	4.0
VMA		13.7	13.8	13.5	13.7	13.7

(continued, next page)

Table A-15 (continued). Job mix formula for District 5 50% RAP mix.

VFA			60.9	71.3	79.4	70.5
Dust/Binder			1.2	1.1	1.0	1.1
P_{ba}			1.1	1.1	1.1	1.1
Effective Binder			3.6	4.1	4.7	4.1
Dust / Effective Binder			1.5	1.3	1.2	1.4
$N_{initial}$			8.0	8.0	8.0	8.0
N_{design}			90.0	90.0	90.0	90.0
Height 1 at $N_{initial}$			126.1	126.4	125.8	126.3
Height 2 at $N_{initial}$			126.6	126.8	125.9	126.1
Average Height at $N_{initial}$			126.4	126.4	125.8	126.2
Height 1 at N_{design}			112.4	112.1	111.9	112.2
Height 2 at N_{design}			112.9	111.5	112.0	111.9
Average Height at N_{design}			112.6	111.9	111.9	112.1
% of G_{mm} at $N_{initial}$			84.3	85.1	86.4	85.2

Table A-16. Volumetrics for District 5 mix design with 50% RAP.

D5-50% RAP Mix Design Volumetrics Summary		
Volumetrics		IDOT Specifications
Binder (%)	5.2	—
Air Voids (%)	4.0	4
VMA (%)	13.5	13 (minimum)
VFA (%)	70.4	65–75
G_{mm}	2.505	—
G_{se}	2.713	—

APPENDIX B PERFORMANCE TEST RESULTS

Table B-1. Semi-Circular Bending (SCB) test results at –24ºC for District 1.

	Mix-Binder Type	Fracture Energy (J/m^2)	Avg.	Std Dev	COV	Peak Load	Avg.	Std dev	COV
1	0-6422-1	410	425	28	7	5.6	5.7	0.2	3.2
2	0-6422-2	407				5.9			
3	0-6422-3	457				5.5			
4	30-6422-1	408	459	49	11	5.1	5.3	0.2	4.3
5	30-6422-2	505				5.1			
6	30-6422-3	463				5.5			
7	40-6422-1	385	513	112	22	6.2	6.1	0.4	6.9
8	40-6422-2	590				6.4			
9	40-6422-3	565				5.6			
10	50-6422-1	419	496	109	22	5.9	6.2	0.3	5.0
11	50-6422-2	572				6.3			
12	50-6422-3	1196*				6.5			
1	30-5822-1	520	595	159	27	7.3	6.4	1.0	15.9
2	30-5822-2	488				5.3			
3	30-5822-3	778				6.6			
4	40-5822-1	403	456	49	11	5.3	5.6	0.3	5.8
5	40-5822-2	463				5.9			
6	40-5822-3	500				5.8			
7	50-5822-1	624	564	170	30	4.9	5.6	0.6	10.2
8	50-5822-2	373				5.8			
9	50-5822-3	696				5.9			
1	30-5828-1	510	542	109	20	5.6	6.2	0.6	10.2
2	30-5828-2	663				6.9			
3	30-5828-3	453				6.3			
4	40-5828-1	630	581	85	15	6.6	6.8	0.9	12.8
5	40-5828-2	629				7.8			
6	40-5828-3	483				6.1			
7	50-5828-1	434	606	162	27	5.0	5.8	0.7	12.3
8	50-5828-2	754				6.4			
9	50-5828-3	631				6.1			

* Outlier

Table B-2. Semi-Circular Bending (SCB) test results at –12ºC for District 1.

	Mix-Binder Type	Fracture Energy (J/m^2)	Avg.	Std Dev	COV	Peak Load	Avg.	Std Dev	COV
1	0-6422-1	617	950	312	33	5.3	5.3	0.2	2.9
2	0-6422-2	1233				5.5			
3	0-6422-3	1001				5.2			
4	30-6422-1	532	610	72	12	5.3	5.4	0.7	12.2
5	30-6422-2	675				6.1			
6	30-6422-3	622				4.8			
7	40-6422-1	747	741	157	21	6.0	5.6	0.6	9.9
8	40-6422-2	582				5.0			
9	40-6422-3	894				5.9			
10	50-6422-1	755	713	60	8	5.9	6.2	0.5	7.8
11	50-6422-2	671				6.0			
12	50-6422-3	1080*				6.8			
1	30-5822-1	713	718	6	1	5.3	5.5	0.2	4.3
2	30-5822-2	717				5.5			
3	30-5822-3	724				5.8			
4	40-5822-1	695	753	180	24	5.8	5.9	0.1	2.0
5	40-5822-2	955				6.0			
6	40-5822-3	610				6.0			
7	50-5822-1	514	581	66	11	5.7	5.8	0.2	3.6
8	50-5822-2	582				6.1			
9	50-5822-3	646				5.7			
1	30-5828-1	572	728	184	25	5.5	5.5	0.3	5.8
2	30-5828-2	681				5.9			
3	30-5828-3	932				5.2			
4	40-5828-1	655	783	168	21	6.1	6.2	0.4	6.4
5	40-5828-2	974				6.7			
6	40-5828-3	720				5.9			
7	50-5828-1	695	842	204	24	5.6	5.9	0.3	5.1
8	50-5828-2	756				5.9			
9	50-5828-3	1075				6.2			

* Outlier

Table B-3. Semi-Circular Bending (SCB) test results at –11.2ºF (–24ºC) for District 5.

	Mix-Binder Type	Fracture Energy (J/m^2)	Avg.	Std Dev	COV	Peak Load	Avg.	Std Dev	COV
1	0-6422-1	456	531	146	27	6.6	6.3	0.7	11.0
2	0-6422-2	699				6.8			
3	0-6422-3	439				5.5			
4	30-6422-1	601	602	63	11	6.7	6.2	0.4	7.2
5	30-6422-2	539				5.9			
6	30-6422-3	666				6.0			
7	40-6422-1	427	465	38	8	6.4	5.7	0.6	11.1
8	40-6422-2	503				5.6			
9	40-6422-3	465				5.1			
10	50-6422-1	410	541	120	22	4.8	6.0	1.1	18.6
11	50-6422-2	567				7.0			
12	50-6422-3	646				6.3			
1	30-5822-1	372	479	99	21	5.4	6.0	0.5	8.8
2	30-5822-2	567				6.2			
3	30-5822-3	499				6.4			
4	40-5822-1	514	550	33	6	5.9	6.3	0.4	7.2
5	40-5822-2	558				6.1			
6	40-5822-3	579				6.8			
7	50-5822-1	560	509	50	10	7.9	6.5	1.2	18.7
8	50-5822-2	461				5.9			
9	50-5822-3	506				5.8			
1	30-5828-1	489	491	31	6	5.0	5.7	0.7	12.2
2	30-5828-2	462				6.4			
3	30-5828-3	523				5.8			
4	40-5828-1	617	656	138	21	6.7	6.3	0.4	6.0
5	40-5828-2	694				5.9			
6	40-5828-3	427				6.2			
7	50-5828-1	631	662	148	22	8.0	6.9	1.2	17.1
8	50-5828-2	823				7.1			
9	50-5828-3	532				5.7			

Table B-4. Semi-Circular Bending (SCB) test results at –12ºC for District 5.

	Mix-Binder Type	Fracture Energy (J/m^2)	Avg.	Std Dev	COV	Peak Load	Avg.	Std Dev	COV
1	0-6422-1	651	617	30	5	4.8	5.1	0.4	7.4
2	0-6422-2	591				5.0			
3	0-6422-3	609				5.5			
4	30-6422-1	417	542	156	29	5.6	5.2	0.3	6.2
5	30-6422-2	717				5.1			
6	30-6422-3	492				4.9			
7	40-6422-1	530	514	15	3	5.8	6.1	0.4	6.1
8	40-6422-2	510				6.5			
9	40-6422-3	501				5.9			
10	50-6422-1	566	501	56	11	6.1	5.6	0.4	7.2
11	50-6422-2	466				5.3			
12	50-6422-3	472				5.4			
1	30-5822-1	458	534	106	20	4.0	4.4	0.5	10.9
2	30-5822-2	609				4.7			
3	30-5822-3	0				0.0			
4	40-5822-1	819	657	144	22	5.8	6.0	0.6	10.1
5	40-5822-2	544				5.5			
6	40-5822-3	608				6.7			
7	50-5822-1	451	585	128	22	5.0	4.8	0.4	8.5
8	50-5822-2	601				5.1			
9	50-5822-3	705				4.4			
1	30-5828-1	896	754	125	17	5.1	5.3	0.3	5.7
2	30-5828-2	661				5.7			
3	30-5828-3	705				5.3			
4	40-5828-1	697	583	119	20	5.4	5.3	0.2	4.2
5	40-5828-2	460				5.0			
6	40-5828-3	592				5.5			
7	50-5828-1	551	567	127	22	4.8	5.6	0.9	15.4
8	50-5828-2	785				6.5			
9	50-5828-3	583				5.6			

Table B-5. Four-point beam fatigue test data for District 1.

Sample ID	Strain (μ Strain)	Initial Stiffness (S)	Nf
0-6422-1000	1000	3262	2870
0-6422-800	800	3339	8490
0-6422-700	700	3172	11820
0-6422-500	500	3483	31320
0-6422-400	400	3650	47290
0-6422-300	300	4094	279580
30-6422-1000	1000	3724	3350
30-6422-800	800	4238	7290
30-6422-700	700	4120	13890
30-6422-500	500	4120	67000
30-6422-400	400	4586	124840
30-6422-300	300	5044	380740
30-5822-1000	1000	3424	3060
30-5822-800	800	3641	9270
30-5822-700	700	3534	19190
30-5822-500	500	4417	47650
30-5822-400	400	4286	115670
30-5822-300	300	4948	979310
30-5828-1000	1000	2472	11790
30-5828-800	800	2927	8810
30-5828-700	700	1870	35230
30-5828-500	500	3192	176050
30-5828-400	400	3422	329740
30- 5828-300	300	3468	1465230

(continued, next page)

Table B-5 (continued). Four-point beam fatigue test data for District 1.

Sample ID	Strain (μ Strain)	Initial Stiffness (S)	Nf
40-6422-1000	1000	2954	6290
40-6422-800	800	4053	6780
40-6422-700	700	4181	11540
40-6422-500	500	3670	121030
40-6422-400	400	4483	250930
40-6422-300	300	3164	207150
40-5822-1000	1000	3659	4480
40-5822-800	800	4122	5570
40-5822-700	700	3780	13720
40-5822-500	500	4641	81450
40-5822-400	400	4940	197060
40-5822-300	300	4565	243870
40-5828-1000	1000	2875	10510
40-5828-800	800	3534	13330
40-5828-700	700	3444	19740
40-5828-500	500	4387	80850
40-5828-400	400	4093	302670
40-5828-300	300	3765	471380
50-6422-1000	1000	3565	2680
50-6422-800	800	3575	6460
50-6422-700	700	3641	9940
50-6422-500	500	4998	100800
50-6422-400	400	4744	102480
50-6422-300	300	5015	423130
50-5822-1000	1000	3786	2220
50-5822-800	800	4062	9560
50-5822-700	700	4335	7010
50-5822-500	500	4767	34930
50-5822-400	400	5328	142460
50-5822-300	300	4689	1261060
50-5828-1000	1000	3244	5820
50-5828-800	800	3307	23280
50-5828-700	700	3894	19050
50-5828-400	400	4133	274430
50-5828-300	300	4295	645180

Table B-6. Four-point beam fatigue test data for District 5.

Sample ID	Strain (μ Strain)	Initial Stiffness (S)	Nf
0-6422-1000	1000	2409	6450
0-6422-800	800	2882	15740
0-6422-700	700	3369	22880
0-6422-500	500	3664	66370
0-6422-400	400	3450	184140
0-6422-300	300	4108	544630
30-6422-1000	1000	3794	5250
30-6422-800	800	4134	10930
30-6422-700	700	4178	15730
30-6422-500	500	4182	53350
30-6422-400	400	4403	278540
30-6422-300	300	5269	404420
30-5822-1000	1000	3115	10400
30-5822-800	800	3111	15150
30-5822-700	700	3273	31060
30-5822-500	500	3700	220180
30-5822-400	400	4054	345440
30-5822-300	300	4220	654210
30-5828-1000	1000	2778	9950
30-5828-800	800	2966	11730
30-5828-700	700	3120	45440
30-5828-500	500	3400	78630
30-5828-400	400	3626	322460
30-5828-300	300	4041	361260

(continued, next page)

Table B-6 (continued). Four-point beam fatigue test data for District 5.

Sample ID	Strain (μ Strain)	Initial Stiffness (S)	Nf
40-6422-1000	1000	4108	3450
40-6422-800	800	4657	9030
40-6422-700	700	4394	8560
40-6422-500	500	5022	59850
40-6422-400	400	5181	129160
40-6422-300	300	5820	916710
40-5822-1000	1000	3311	7640
40-5822-800	800	3933	10330
40-5822-700	700	3928	28440
40-5822-500	500	4209	77050
40-5822-400	400	4585	746830
40-5822-300	300	4981	863570
40-5828-1000	1000	2924	7930
40-5828-800	800	3259	6990
40-5828-700	700	3750	49340
40-5828-500	500	3585	47740
40-5828-400	400	4298	421300
40-5828-300	300	4352	974050
50-6422-1000	1000	4487	4100
50-6422-800	800	4820	5140
50-6422-700	700	4672	8940
50-6422-500	500	5271	29990
50-6422-400	400	5537	229440
50-6422-300	300	5745	266420
50-5822-1000	1000	3215	5700
50-5822-800	800	3833	7730
50-5822-700	700	3548	15820
50-5822-500	500	4529	161940
50-5822-400	400	5159	193350
50-5822-300	300	4767	1521430
50-5828-1000	1000	3547	3240
50-5828-800	800	3543	14090
50-5828-700	700	4139	19510
50-5828-500	500	4734	51930
50-5828-400	400	4796	337190
50-5828-300	300	4587	797990

Table B-7. Moisture Susceptibility test data for District 1.

Mix Type	Sample No.	Unconditioned Samples		Conditioned Samples		TSR
		Tensile Strength (psi)	Air Voids	Tensile Strength (psi)	Air Voids	
Control	1	68.6	6.8	71.5	6.5	90.2
	2	84.6	6.9	71.2	7.5	
	3	90.7	6.5	77.3	6.5	
	Average	81.3	6.7	73.3	6.8	
30% RAP	1	105.3	6.5	93.7	6.5	93.4
	2	94.0	7.3	92.8	6.8	
	3	98.1	6.5	91.3	6.8	
	Average	99.1	6.8	92.6	6.7	
40% RAP	1	110.9	6.8	92.5	6.9	89.7
	2	111.4	7.4	104.8	7.1	
	3	99.0	6.6	90.7	6.7	
	Average	107.1	6.9	96.0	6.9	
50% RAP	1	86.8	7.1	104.1	6.6	99.9
	2	116.0	7.4	102.5	7.0	
	3	122.8	6.6	118.6	7.1	
	Average	108.5	7.0	108.4	6.9	

Table B-8. Moisture susceptibility test data for District 5.

Mix Type	Sample No.	Unconditioned Samples		Conditioned Samples		TSR
		Tensile Strength (psi)	Air Voids	Tensile Strength (psi)	Air Voids	
Control	1	50.6	6.8	51.5	6.7	89.5
	2	53.3	7.2	48.1	7.2	
	3	55.1	6.8	48.9	7.1	
	Average	54.2	6.9	48.5	7.0	
30% RAP	1	90.0	7.0	76.0	6.9	85.7
	2	100.8	6.5	82.8	6.8	
	3	91.9	6.9	83.6	6.6	
	Average	94.2	6.8	80.8	6.8	
40% RAP	1	92.4	6.9	81.1	7.1	83.7
	2	92.8	7.2	74.9	7.1	
	3	89.4	7.1	74.0	7.0	
	Average	91.6	7.1	76.7	7.1	
50% RAP	1	118.8	7.2	99.9	6.9	87.3
	2	113.6	6.8	102.8	7.1	
	3	121.1	7.0	106.0	6.9	
	Average	117.8	7.0	102.9	7.0	

A typical SAS output file.

```
The SAS System                                                          1

The GLM Procedure

               Class Level Information

Class         Levels    Values

Mixtures           4    0-6422 40-5822 40-5828 40-6422


Number of Observations Read          12
Number of Observations Used          12

The SAS System                                                          2

The GLM Procedure

Dependent Variable: values

                                   Sum of
Source                     DF       Squares   Mean Square  F Value  Pr > F

Model                       3   32508386803   10836128934     5.54  0.0236

Error                       8   15644177931    1955522241

Corrected Total            11   48152564734


R-Square     Coeff Var      Root MSE    values Mean

0.675112      22.39153      44221.29       197491.2


Source                     DF     Type I SS   Mean Square  F Value  Pr > F

Mixtures                    3   32508386803   10836128934     5.54  0.0236


Source                     DF   Type III SS   Mean Square  F Value  Pr > F

Mixtures                    3   32508386803   10836128934     5.54  0.0236
```

(continued, next page)

The GLM Procedure

Tukey's Studentized Range (HSD) Test for values

NOTE: This test controls the Type I experimentwise error rate, but it generally has a higher Type II error rate than REGWQ.

Alpha	0.05
Error Degrees of Freedom	8
Error Mean Square	1.9555E9
Critical Value of Studentized Range	4.52881
Minimum Significant Difference	115626

Means with the same letter are not significantly different.

Tukey Grouping	Mean	N	Mixtures
A	268163	3	40-6422
A			
B A	203012	3	40-5822
B A			
B A	197528	3	40-5828
B			
B	121261	3	0-6422

The GLM Procedure
Least Squares Means
Adjustment for Multiple Comparisons: Tukey

Mixtures	values LSMEAN	LSMEAN Number
0-6422	121260.667	1
40-5822	203012.333	2
40-5828	197528.333	3
40-6422	268163.333	4

Least Squares Means for effect Mixtures
Pr > |t| for H0: LSMean(i)=LSMean(j)

Dependent Variable: values

i/j	1	2	3	4
1		0.1859	0.2280	0.0152
2	0.1859		0.9986	0.3379
3	0.2280	0.9986		0.2793
4	0.0152	0.3379	0.2793	